Biodiversity Analysis of Endophytic Fungi and Chemical Investigation of their Secondary Metabolites

(Analyse der Biodiversität endophytischer Pilze und die chemische Untersuchung ihrer Sekundärmetabolite)

Inaugural-Dissertation
zur
Erlangung des Doktorgrades
der Mathematisch-Naturwissenschaftlichen Fakultät
der Heinrich-Heine-Universität Düsseldorf

vorgelegt von
Mustapha El Amrani
Aus Boudnib-Marokko

Düsseldorf, 27 April 2016

Aus dem Institut für Pharmazeutische Biologie und Biotechnologie
der Heinrich-Heine Universität Düsseldorf

Gedruckt mit der Genehmigung der
Mathematisch-Naturwissenschaftlichen Fakultät der
Heinrich-Heine-Universität Düsseldorf

Referent: Prof. Dr. Peter Proksch
Koreferent: Prof. Dr. Matthias U. Kassack
Tag der mündlichen Prüfung: 27 Januar 2016

Erklärung

Hiermit erkläre ich ehrenwörtlich, dass ich die vorliegende Dissertation mit dem Titel „Analyse der Biodiversität endophytischer Pilze und die chemische Untersuchung ihrer Sekundärmetabolite“ selbst angefertigt habe. Außer den angegebenen Quellen und Hilfsmitteln wurden keine weiteren verwendet. Diese Dissertation wurde weder in gleicher noch in abgewandelter Form in einem anderen Prüfungsverfahren vorgelegt. Weiterhin erkläre ich, dass ich früher weder akademische Grade erworben habe, noch dies versucht habe.

Düsseldorf, den 20 Januar 2016

Mustapha El Amrani

Acknowledgements

First of all, I would like to express my cordial thank and gratitude to Prof. Dr. Peter Proksch for providing me this valuable opportunity to purse the doctoral research and for the excellent work facilities in the Institute of Pharmaceutical Biology and Biotechnology, Heinrich-Heine University, Düsseldorf. I would also like to express my heartfelt gratitude and deep thanks for his genial supervision, admirable guidance, fruitful discussions, generous considerations and unforgettable support for my study in Düsseldorf.

My special thanks are to Dr. Sherif Elsayed for his valuable suggestions, constructive discussions and continuous encouragement.

I am deeply indebted to Dr. Daowan Lai for all his precious help, patient guidance and scientific advices.

I would like to express my appreciation to Dr. Victor Wray (Helmholtz Centre for Infection Research) for the distinguished NMR measurements and his significant opinion on the structure elucidation of compounds, Prof. W. E. G. Müller (University of Mainz) for conducting the cytotoxicity assays. I am also thankful to Dr. Peters and his colleagues (HHU-Düsseldorf) for 500 MHz ^{1}H-NMR and 125 MHz ^{13}C-NMR measurement as well as Dr. Keck and Dr. Tommes (HHU-Düsseldorf) for EI-mass spectra measurements.

My thankfulness is also to to Prof. Dr. Wenhan Lin (National Research Laboratories of Natural and Biomimetic Drugs, Peking University, Health Science Center) and to Prof. Dr. Bingui Wang (Laboratory of Experimental Marine Biology, Institute of Oceanology, Chinese Academy of Science) and Dr. RuAngelie Edrada-Ebel (Strathclyde Institute of Pharmacy and Biomedical Sciences, University of Strathclyde) for their fruitful discussions, constructive advices and measurements of NMR and HRMS spectra.

I would like to acknowledge Prof. Dr. Matthias U. Kassack for conducting cytotoxicity assays and estimating my PhD study as second referee. I am grateful to Dr. Julia Kjer for instructing me when I started my study at the institute. I would like to deeply thank the PBIII team as well as the Dionex team and to my laborpartner H. Niemann.

I am indebted to Mrs. Claudia Eckelskemper for her kind and generous help of administration, and the technical staff Mrs. Waltraud Schlag, Mrs. Simone Miljanovic and Mrs. Katja Friedrich for their geniality, friendliness and for supplying laboratory materials. My thanks are also to, Mr. Klaus Dieter Jansen, Mrs. Eva Müller and Mrs. Heike Goldbach-Gecke for their help.

I would like to extend my sincere thanks to my past and present colleagues Dr. M. Bayer, Dr. A. Putz, Dr. J. Xu, C. Pham, Dr. B. Lipowicz, D. Rönsberg, Andreas Marmann, L. Hammerschmidt, A. Ola, Dr. R. Bara, G. Daletos, Dr. Y. Zhou, Dr. W. Ebrahim, F. Z. Kabbaj, F. Okoye, M. A. Tarabeen, M. Elnekity, and all the others for the nice multicultural time I spent with them, for their help and assistance whenever I needed it.

At the end, I would like to express my deepest thanks and gratitude to my family for encouraging and supporting me always in good and bad times to finish this study.

To all of you, thank you very much!

Zusammenfassung

Endophytische Pilze, isoliert aus erdgebundenen oder mangroven Pflanzen, produzieren Naturprodukte mit einer weiten chemischen und strukturellen Diversität. Einige von diesen eignen sich zur spezifischen medizinischen Anwendung, besonders diese, welche biologische Aktivitäten in pharmazeutisch relevanten Bioassay-Systemen zeigen. Letztere repräsentieren potentielle Leitstrukturen und können optimiert werden, um therapeutisch-effektive und bioaktive Mittel hervorzubringen.

Vier endophytische Pilze wurden als biologische Quelle für die Arbeit untersucht, Epicoccum nigrum, Stemphylium globuliferum, Aureobasidium pullulans und das nicht indentifizierte Isolat AMO 3-2, mit dem Ziel, sekundäre Metabolite aus endophytischen Pilzen zu isolieren, gefolgt von Strukturaufklärung und Prüfung des pharmakologischen Potentials. Die Pilze wuchsen in festem Reismedium, in einer Zeitspanne von drei bis vier Wochen, heran. Die erhaltenen Extrakte wurden mit Hilfe von verschiedenen chromatographischen Trennverfahren getrennt bis sekundäre Metabolite in reiner Form isoliert wurden.

Strukturaufklärung der isolierten Sekundärmetabolite wurde mittels modernster analytischer Verfahren, einschließlich Versuche der Massenspektrometrie (MS) und Kernspinresonanzspektroskopie (NMR), betrieben. Schließlich unterlagen die isolierten Substanzen verschiedenen Bioassays, um deren antimikrobielle, antimykotische und zytotoxische Aktivität, wie auch inhibitorische Profile gegenüber ausgewählten Proteinkinasen, zu untersuchen.

1. AMO 3-2.

Fünf Farinomalein-Derivate, einschließlich vier neue Substanzen, Farinomaleine B-E, und einem neuen Isoindolin-Kongener ((R)-5,7-dihydroxy-3-methylisoindolin-1-on), wie auch der bekannte Sekundärmetabolit p-Hydroxyphenylacetylsäure, isolierte man von dem nicht identifizierten endophytischen Pilz AMO 3-2, erhalten aus dem inneren Gewebe gesunder Blätter der mangroven Pflanze Avicenna marina, aus Oman. Die Strukturen der neuen Substanzen wurden eindeutig gelöst, auf Basis derer Molekularmasse, wie auch ein- und zweidimensonaler NMR-spektroskopischer Daten. Bei Auswertung der Zytotoxizität gegen

die Maus-Lymphomzellline L5178Y, zeigte nur Farinomalein B eine mäßige Aktivität.

2. *Epicoccum nigrum*.

Der Pilzstamm *Epicoccum nigrum* wurde isoliert aus *Mentha suaveolens*, welches in Marokko heranwuchs. Fünf neue Substanzen wurden aus diesem Pilzstamm gewonnen: Epicoccon C, Epicoccon D, 2,3,4-Trihydroxy-5-(methoxymethyl)-5-methylbenzaldehyd, 5,6,7,9a-Tetrahydroxy-2,3,3a,8-tetramethyl-3a,4-dihydro-1H-cyclo-penta[b]naphthalin-1,9(9aH)-dion und 3,4,8,9,10-Pentahydroxy-2,7-dimethyl-11-oxo-11,12-dihydro-6H-6,12-epoxydibenzo[b,f]-oxozin-1-carbaldehyd und die fünf bekannten Substanzen Epicoccin, 5-Methoxy-7-methyl-1,3-dihydroisobenzofuran-4,6-diol, Epicoccon A, Epicoccon B und 2-(2-Formyl-3,4,5-trihydroxy-6-methylphenyl)-6,7-dihydroxy-5-methylbenzofuran-4-carbaldehyd.

Diese Substanzen zeigten verschiedene Aktivitäten, beginnend bei zytotoxischer Aktivität gegen L5178Y-Zellen oder gegen die sensible menschliche Ovarienkrebszelllinie A2780 und gegen Methicillin-resistenten *Staphylococcus aureus* (MRSA), zwei Substanzen zeigten eine hohe inhibitorische Aktivität gegen eine Rheie von Proteinkinase, die bei verschiedenen Krebs-Arten sowie bei Metastasen-Bildung eine wichtige Rolle spielen.

3. *Aureobasidium pullulans*.

Aureobasidium pullulans wurde isoliert aus Aloe vera. Aus diesem Pilz wurden zwei Indolderivate, Iso-Ochracinsäure, 6-Hydroxyisoskleron und dessen Derivate, sowie das neue Naturprodukt (Z)-4-(5-Acetoxy-3-methylpent-2-enamido) butansäure isoliert. Keines dieser Substanzen zeigte signifikante Aktivität im Zytotoxizitätsassay (MTT) gegen die L5178Y-Zelllinie.

4. *Stemphylium globuliferum*.

Der Extrakt des Pilzstammes *Stemphylium globuliferum*, isoliert aus *Mentha pullegium*, erbrachte zwei bekannte Anthrachinonderivate, genannt Tetrahydroaltersolanol B und Alterporriol O. Diese Substanzen zeigten keine Aktivität in Zytotoxizitätsassays oder gegen multiresistente Bakterienstämme.

Eine Gesamtmenge von funfundzwanzig Substanzen wurden in dieser Arbeit isoliert, von denen man elf als neue Naturprodukte identifizierte. Beide, bekannte und unbekannte Substanzen, wurden bezüglich ihrer biologischen Aktivität mittels verschiedener Bioassay-Systemen getestet.

Im zweiten Teil dieser Arbeit wurde die mykotische Diversität in der mangroven Pflanze *A. marina* durch Kultur-unabhängigen Methoden mittels Polymerase-Kettenreaktion (PCR), gekoppelt mit Denaturing Gradient Gel Electrophoresis (DGGE), sowie einer Kultur-basierten Methode, welche daraus bestand, den endophytischen Pilz zu isolieren und separat zu identifizieren. Bei Beiden Methoden wurden ITS-Bereichen genutzt, um die Isolate zu identifizieren.

Eine phylogenetische Analyse wurde durchgeführt und Referenzsequenzen von GenBank dienten als Referenzen, um OTUs zu klassifizieren, welche beim Blast Vergleich mit GenBank-Sequenzen identifiziert werden konnten.

Während beide Methoden verschiedene Pilzs-Populationen lieferten, folgten die Ergebnisse von DGGE oder die Kultur-abhängige Methode derselben Tendenz und bestätigten, dass die mykotisch-endophytische Population variiert, in Anpassung an die geographische Situation und Zeitperiode.

Table of content

1. Introduction

1.1. Natural products approach to drug discovery

Beside essential compounds such as sugars and proteins that are known as primary metabolites and are common to all organisms, every biological organism produces a different kind of metabolites, the so called secondary metabolites. The biosynthesis of these latter is often a response to infections, competition for nutrients or other external stimuli such as environmental changes; they can serve also as communication tools, sensory devices, or may help by defense mechanisms. Biologically active natural products produced by plants, animals, insects, fungi, bacteria and protozoans have been isolated to be used in pharmaceutical drug discovery and design (Rollinger *et al*., 2006).

Natural products were since early human history utilized to alleviate disease, and they are still a rich source of chemical diversity for drug discovery. Numerous therapeutics for humans, are small molecules, isolated from plants, fungi or bacteria. With 60% of anticancer compounds and 75% of drugs for infectious diseases that are either natural products or natural product derivatives (Newman *et al.,* 2003 and Cragg *et al.,* 2005), natural products continued to prove, their dominant role as significant sources of drugs and leads.

In the past decades the field of natural product research registered a significant decline due to the emergence of new strategies in drug discovery, starting by target validation, combinatorial chemistry and high-throughput screening as a new paradigm for drug discovery (Drews, 1998). The difficulties in isolating pure compounds from crude extracts, identifying their high complex structures and elucidating their mechanism of action or synthesizing them were also problems that supported this trend.

Pharmaceutical companies cut back on their natural product screening efforts in the late 1980s and early 1990s, because the paradigm followed was not compatible with the new high-throughput screening approach, which promises if associated with combinatorial chemistry to give results in a short time line, which was known as ‘blitz’ screen (start to finish in three months) (Lam, 2007).

From its introduction and untill recently, the use of combinatorial chemistry yielded only one compound, which can be classified as *de novo* new chemical entity (NCE) and which was reported in the public domain and approved for drug use anywhere. This is the antitumor

compound known as sorafenib (Nexavar, 1) from Bayer, approved by the FDA in 2005. It was known during development as BAY- 43-9006 and is a multikinase inhibitor, targeting several serine/ threonine and receptor tyrosine kinases (RAF kinase, VEGFR-2, VEGFR-3, PDGFR-beta, KIT, and FLT-3) and is in multiple clinical trials as both combination and single-agent therapies at the present time (Newman and Cragg, 2007).

Pharmaceutical companies are nowadays renewing the interest in natural products, despite the increasing interest to rapid screening approaches, hit identification and hit-to-lead development and all these emerging trends and also because of the unrealized expectations from the mentioned rapid strategies. (Koehen *et al.,* 2005)

1.2. Biodiversity and natural products

Newman and Cragg (2007) confirmed the decreasing interest of pharmaceutical companies in natural products, which is due to economic reasons rather than scientific, but also indicated that almost 50% of new drugs introduced from 1981–2006 had a natural product origin or are inspired from natural product. It is known, that in order to find a hit, thousands of chemicals must be evaluated.

Only natural products, due to their richness in different structural types can guaranty such a huge pipeline of new interesting compounds. The immense variety of organisms and their interaction with the environment and with their neighbors is the evolution of diverse complex natural products, which enhance survival and competitiveness of the producing organisms (Waterman, 1992).

Novel chemicals, with potential as drug leads, can be discovered if the biodiversity of organisms in many areas of the world with their different habitats can be accessed (Harvey, 2000).

1.3. The potential of fungal natural products in drug discovery

Fungi are capable to synthesize a plethora of secondary metabolites, with a wide range of chemical diversity and promising pharmaceutical applications, they drew the interest of scientists because of their various ecological functions and their mycotoxins (Bergmann *et al*., 2007).

Fungi are eukaryotic, non-photosynthetic microorganisms, but the definition of this group of

organisms is not a simple task. The fungal kingdom gathers an ubiquitous and a broad range of heterotrophic organisms with diverse cellular structures, reproduction, biochemistry, physiology, and secondary metabolism. Fungi are found in every conceivable organic substrate examined in the world (Hawkesworth *et al*., 1983). Fungi can be saprotrophic, mutualistic symbionts, including mycangial associates of insects, mycorrhizae, lichens, and endophytes but also pathogenic and parasitic, the can be harmful effectively against all groups of organisms, including bacteria, plants, other fungi, and animals, including humans (Debbab *et al.,* 2011).

It was the discovery of penicillin in 1928 by Alexander Fleming, which drew the interest to fungi as source of potential bioactive secondary metabolites. The interest was strengthened, when other antimicrobial substances such as griseofulvin (Grove *et al*., 1952) or cephalosporin C (Newton *et al.,* 1955) (Fig. 1) had been discovered from fungi or other therapeutic agents. The list of interesting substances from fungi ranges from antibiotic agents to cholesterol lowering substances, represented by lovastatin, the first in its group from fungi (Endo, 1979) and extends to cyclosporine which was isolated from the fungus *Tolypocladium inflatum* (Traber *et al*., 1982; 1987), as an immunosuppressant or to the potent anticancer agent taxol as fungal secondary metabolite (Strobel *et al.,* 1996)

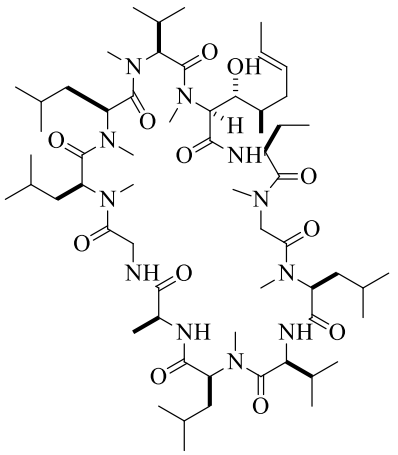

Cyclosporine A

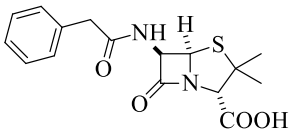

Penicillin G

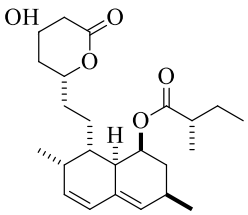

Lovastatin

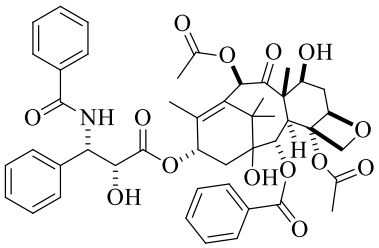

Taxol

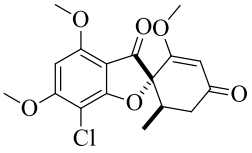

Griseofulvin

Fig. 1: Examples of fungal products used as drugs.

1.4. Endophytic fungi

Bacon and White (2000) defined endophytes as all microbes that colonize living, internal tissues of plants without causing any immediate, overt negative effects. Endophytes have been found in virtually every organ of every plant species examined, although their distribution between individual plants is heterogeneous (Bacon *et al*., 2000). The majority of them find their way to the host plant through a horizontal transmission, but inconspicuous infections through airborne spores are not the only way of infection, endophytes may also be vertically transmitted to the next plant generations via seeds (Hartley *et al.,* 2009). Endophytes live within tissues of healthy plants for all or nearly all their life cycle, but when the host plant is stressed or weakened, they may become parasitic after many years of

symptomless cohabitation (Firáková *et al.,* 2007; Limsuwan *et al.,* 2009).

Fungal endophytes are mainly members of the phylum Ascomycota, whereas Basidiomycetes, Deuteromycetes and Oomycetes are rarely represented (Saikonnen *et al.,* 1998; Arnold, 2007). In surveys done before the year 2000, Stone estimated the average number of endophytes per plant to be around 50 species (Stone *et al.,* 2004).

1.5. Endophytic fungi as sources of bioactive products

Endophytes are ubiquitous and show a rich biodiversity; they are capable of synthesizing a variety of bioactive compounds, hundreds of natural products were reported from endophytes, including alkaloids (El Amrani *et al.,* 2012), terpenoids (De Souza *et al.,* 2011), flavonoids (Qiu *et al.,* 2010) and steroids (Zhang *et al.,* 2009). Most of the natural products from endophytes are antibiotics, anticancer agents or biological control agents.

The most famous example of successful drugs derived from endophytic fungi is the one-billion-dollar drug paclitaxel (Taxol®). This highly functionalized diterpenoid was first isolated from the inner bark of *Taxus brevifolia* in1969. It is used since 1992 as a cytostatic agent against breast cancer and ovarian carcinoma (Wani *et al.,* 1971; Strobel *et al.,* 2004). Endophytic fungi gained more interest when Strobel (1993) reported that *Taxomyces andreanae,* an endophytic fungus of *Taxus brevifolia*, also produces paclitaxel (Strobel *et al.,* 1993). Extracting paclitaxel from the bark of *Taxus* species with traditional methods is inefficient and environmentally costly or not feasible in the long term. To treat just five hundred patients, 1 kg paclitaxel is needed, but the production of this amount requires 10 tons of barks or 300 trees.

New ways of producing paclitaxel were the solution to protect this limited resource and reducing the cost of drug therapy. Fungi have the advantage of being easy to culture with reasonable costs. A recent study reported a potentially industrial yield of paclitaxel of 1124.34 µg/L via optimized fermentation, using a paclitaxel producing endophytic isolate of *Chaetomium sp*. (Jin *et al.,* 2011). Screening of the diverse group of fungi that may produce valuable medicinal plant products is a promising approach for producing drugs on a commercial scale using microbes (Strobel, 2003; Strobel and Daisy, 2003).

1.6. Analyzing fungal diversity in the host plant

Fungal life within the tissues of a host plant is a fascinating phenomenon and the composition of a fungal community inside of a plant is getting more interesting. Recently the analysis of fungal communities populating plants or living in soil caught the attention of microbiologists. Fungi maintain important symbiotic relationships with plants and bacteria (Garrett, 1981; Parkinson, 1983; Yu *et al.,* 2005) but many are pathogenic (Jaworski *et al.,* 1978; Cahill *et al.,* 2004). Furthermore, some fungi influence or stop the growth of others, this group is known as biological control agents (Mejía *et al.,* 2008). Plants in natural ecosystems are known to build symbiotic relationships with mycorrhizal fungi and/or fungal endophytes (Petrini, 1986). Plant ecology, fitness, and evolution is deeply influenced by these fungal symbionts or endophytes (Brundrett, 2006). Neverthless, the fungal group and their constitution is involved in shaping plant communities (Clay & Holah, 1999) and manifesting strong effects on the community structure and diversity of associated organisms e.g. bacteria, nematodes and insects (Omacini *et al.,* 2001).

Obviously, understanding endophyte-host interaction is only possible if we can understand the role of endophytes in a certain community and if we can understand interactions between members of a fungal endophyte population. Hence, the need of screening fungal endophytic populations inside of plants has emerged to provide insights to fungal diversity, and conventional and molecular techniques have been used.

1.6.1 Microscopy and culture-based methods

To assess fungal diversity, cultural methods were the earliest techniques used and they were coupled with morphological details from microscopy to allow identification and to detect exactly which taxon is present. It is because of their simplicity, low cost and the fact that they are easy to conduct, that these techniques commonly used.

Endophytic fungi have previously been isolated and cultured on artificial media and identified based on morphological characters (Guo *et al.,* 1998; 2003; Taylor *et al.,* 1999; Nambiar *et al.,* 2009). The fungi that do not sporulate on media have been termed *Mycelia sterilia* and often been grouped as morphospecies (Guo *et al.,* 2000; 2003; Promputtha *et al.,* 2005).

Methods to promote sporulation in *Mycelia sterilia* have been developed (Fröhlich *et al*., 2000; Guo *et al*., 1998; Taylor *et al*., 1999) and proportions of non-sporulating fungi among isolated endophytes are increasing (Guo *et al.,* 2000; Kumar *et al.,* 2004).

DNA sequence-based methodologies have been successfully used for the phylogenetic placement and classification of morphospecies obtained as endophytes, which resolve the problem of identifying non-sporulating fungi (Guo *et al.,* 2003; Promputtha *et al.,* 2005; Wang *et al*., 2005).

These methodologies have the advantage of being easy, fast and reliable in finding dominant culturable fungal taxa, but they are limited by the fact, that not all fungi are easy to cultivate and it is difficult to find an artificial medium, which is suitable for the whole fungal community of a host plant. Moreover, fungi do not grow with the same rhythm; fast growing fungi can crowd out slow growing isolates which will not reflect a proper diversity assessment. Dormant spores can represent numerically dominant populations in their natural environment but may never grow in culture and will escape normal culture-based sreening and hence, provide biased data regarding fungal diversity. Even for fungi that sporulate and can be cultured, it is not always easy to correctly identify them with certainty.

1.6.2. Molecular-based or culture-independent methods

Due to the different advantages of culture-based method in reflecting a correct image of a fungal population in natural environment; alternative methods, which largely circumvent cultivation of target organisms undergoes intensive and prompt development. Hybrid methods, which combine PCR amplification of rDNA genes and other DNA fingerprinting techniques, were born. They include terminal restriction fragment length polymorphism (T-RFLP), amplified rDNA restriction analysis (ARDRA), amplified random intergeneric spacer analysis (ARISA), denaturing gradient gel electrophoresis (DGGE), temperature gradient gel electrophoresis (TGGE) and oligonucleotide fingerprinting of rRNA genes or single-stranded conformation polymorphism (SSCP) (Sun *et al.,* 2012; Rezaei-Matehkolaei *et al.,* 2012).

They have been not only frequently used to analyze endophytic communities inside plants, but more to screen soil microbial populations in combination with traditional techniques (Lowell *et al.,* 2001; Maarit-Niemi *et al.,* 2001; Ranjard *et al.,* 2001; Kirk *et al.,* 2004). The list of such methods includes also fluorescence *in situ* oligonucleotide hybridization (FISH) (Baschien *et al.,* 2001) as well as oligonucleotide fingerprinting of ribosomal RNA genes (ORFG).

A new method consists of providing $^{13}CO_2$ to plants, microbes depending on a carbon flux from their host plant become rapidly labeled. RNA based stable isotope probing (SIP–RNA) based on the fractionation of heavily labeled [^{13}C] RNAs from a mixture led to identify a wide variety of microbes occurring in roots and that were mostly previously unknown (Vandenkoornhuyse *et al*., 2007).

1.6.3. Estimation of fungal diversity in the host by DGGE method

The use of rDNA fragment, a highly variable region as a molecular indicator for complex microbial populations, based on total DNA extracts of environmental samples in combination with DGGE was developed by Muyzer (Muyzer *et al*., 1993). Originally, individual PCR segments of rDNA, which have almost the same size in different individuals of the microbial community, were cloned prior to sequencing. Denaturing gradient gel electrophoresis (DGGE) separation allows separating these sequences with similar size by electrophoretic techniques (O'Callaghan *et al.,* 2003).

DGGE has also disadvantages, it gives generally better resolution between bands in a profile by shorter fragments of DNA (<500 bp), this is limiting the taxonomic information that can be obtained by sequencing excised bands. In addition, even the most sensitive staining methods are often not sensitive enough to detect all the diversity present within a sample, particularly for the less dominant members of the community. Furthermore, in some cases, single bands on a gel have been shown to comprise more than a single sequence type (Schmalenberger and Tebbe, 2003). This method is based on PCR and therefore, has all disadvantages of PCR, starting from ITS universal primers. It is known, that all primer sets have a range of biases, and an appropriate solution will be to use more than one primer combination (Bellemain *et al.,* 2010).

1.7. Aim and scopes of the study

The aim of this study was the purification of endophytic fungal strains from mangrove and terrestrial plants, the cultivation of these fungal strains and extraction followed by bioactivity guided isolation, characterization and structural elucidation of their biologically active secondary metabolites in order to preliminarily evaluate their pharmaceutical potential. Four endophytic fungi were investigated as biological sources of the study, namely *Epicoccum nigrum*, *Stemphylium globuliferum*, *Aureobasidium pullulans* and the unidentified isolate AMO 3-2.

The fungi were grown on solid rice medium at 21 °C for 3-4 weeks, followed by harvesting and subsequent extraction with ethyl acetate. The obtained crude extracts were then fractionated and separated using various chromatographic techniques and their fractions were analyzed by HPLC-DAD for their purity and by ESI-LC/MS for their molecular weight and fragmentation patterns. The pure compounds were submitted to state-of-the-art one- and two-dimensional NMR techniques for structural elucidation. In addition, selected compounds were derivatized in order to determine their absolute stereochemistry.

Furthermore, fractions and pure compounds were subjected to selected bioassays to determine their pharmaceutical potential. Thus, antimicrobial activity was studied using the agar diffusion assay, whereas cytotoxicity was studied *in vitro* using mouse lymphoma (L5178Y), A2780 and A2780 CisR cell lines. Moreover, some pure compounds were also tested for their protein kinase inhibitory activity. The latter three assays were conducted in

cooperation with Prof. W. E. G. Müller (Mainz), Prof. M. U. Kassack (Düsseldorf), and ProQinase GmbH (Freiburg), respectively.

In the second part, biodiversity of endophytic fungi was estimated using culture- and culture-independent methods. Healthy leaves of *Avicennia marina* were collected from two different geographic regions; namely Hainan in China and Muscat in Oman, with the purpose to compare their fungal endophytic populations. Furthermore, two samples from the same plant collected in Sept 2009 and Aug 2011 at the same region (Hainan in China) were analyzed, with the aim of answering the question “Did the fungal endophytic populations of a certain plant change with time?”

2. Materials and methods

2.1. Isolation and structural elucidation of bioactive secondary metabolites from endophytic fungi

2.1.1. Materials

2.1.1.1. Biological materials

i. Plant material

Plant samples were collected from Düsseldorf (Germany), Morocco, Oman and P.R. China. The identification was done based on the morphological characters and ribosomal DNA comparison.

Small pieces from healthy stems, leaves and flowers were cut and placed in plastic bags after any excess moisture was removed. Every attempt was made to store the materials at 4° C and the isolation was made within 24 hours after sampling.

ii. Pure fungal strains isolated from the collected plants

A list of the endophytic fungal strains isolated from different organs of the collected plant samples and their corresponding botanical sources is shown in Table 2.1.

Table 2.1: Pure fungal strains and their botanical sources

Fungal code	Plant Part	Identity	Source
AMO 3-2	Leaves	Unidentified	*Avicennia marina* (Acanthaceae)
MB	Leaves	*Aureobasidium pullulans*	*Aloe vera* (Xanthorrhoeaceae)
BSL1W	Leaves	*Epicoccum nigrum*	*Mentha suaveolens Ehr.* (Lamiaceae)
Stemphylium globuliferum	Stems	*Stemphylium globuliferum*	*Mentha pulegium* (Lamiaceae)

iii. Taxonomy

Aureobasidium pullulans

Kingdom: Fungi

Phylum: Ascomycota

Class: Dothideomycetes

Subclass: Dothideomycetidae

Order: Dothideales

Family: Dothioraceae

Genus: *Aureobasidium*

Epicoccum nigrum

Kingdom: Fungi

Phylum: Ascomycota

Class: Dothideomycetes

Subclass: Pleosporomycetidae

Order: Pleosporales

*Family:*Pleosporaceae

Genus: *Epicoccum*

Stemphylium globuliferum

Kingdom: Fungi

Phylum: Ascomycota

Class: Dothideomycetes

Subclass: Pleosporomycetidae

Order: Pleosporales

Family: Pleosporaceae

Genus: *Stemphylium*

2.1.1.2. Media

2.1.1.2.1. Composition of malt agar (MA) medium

This medium is suitable for short term storage of fungal cultures, purification or fresh seeding for preparation of liquid cultures.

Agar-agar	15.0 g
Malt extract	15.0 g
Distilled water	to 1000 mL
pH	7.4 -7.8 (adjusted with NaOH/HCl)

To suppress bacterial growth during the isolation of endophytic fungi from plant tissues, 0.2 or 0.1 g of chloramphenicol or streptomycin were added to the medium, respectively.

2.1.1.2.2. Composition of Wickerham medium for liquid cultures

Yeast extract	3.0 g
Malt extract	3.0 g
Peptone	5.0 g
Glucose	10.0 g
Distilled water	to 1000 mL
pH	7.2 -7.4 (adjusted with NaOH/HCl)

2.1.1.2.3. Composition of rice medium for solid cultures

Rice	100.0 g
Distilled water	110.0 g

Water was added to the rice and kept overnight before autoclaving.

2.1.1.2.4. Composition of Luria Bertani (LB) medium

Peptone	10.0 g
Malt extract	5.0 g
NaCl	10.0 g
Distilled water	to 1000 mL
pH	7.0 (adjusted with NaOH/HCl)

To prepare the agar plates, 15.0 g agar were added to 1 L broth media.

2.1.1.3. Chemicals

2.1.1.3.1. General laboratory chemicals

Anisaldehyde	Merck
(4-methoxybenzaldehyde)	Merck
(-)-2-Butanol	Merck
Dimethylsulfoxide	Merck
Formaldehyde	Merck
L-(+)-Ascorbic acid	Merck
Hydrochloric acid	Merck
Potassium hydroxide	Merck
Pyridine	Merck

Concentrated sulphuric acid	Merck
Trifloroacetic acid (TFA)	Merck
Concentrated ammonia solution	Fluka
Acetic anhydride	Merck
Ortho-phosphoric acid 85% (p.a.)	Merck
Sodium hydrogen carbonate	Sigma

2.1.1.3.2. Chemicals for culture media

Agar-agar	Galke
Chloramphenicol	Sigma
Glucose	Caelo
Malt extract	Merck
NaCl	Merck
Peptone	BD
Streptomycin	Sigma
Yeast extract	Sigma

2.1.1.3.3. Chemicals for agarose gel electrophoresis

Agarose	Biozym
TBE-buffer	Sigma
SYBR Safe	Invitrogen
DNA Ladder	NEB

2.1.1.3.4. Chemicals for chromatography

Stationary phases

Pre-coated TLC plates, Silica Gel 60 F_{254}, layer thickness 0.2 mm	Merck
Silica Gel 60, 0.04 - 0.063 mm mesh size	Merck
Pre-coated TLC plates, RP-18, F_{254} S, layer thickness 0.25 mm	Merck
RP-18, 0.04 - 0.063 mm mesh size	Merck

Sephadex LH 20, 0.25 - 0.1 mm mesh size	Merck
Diaion HP20	Supelco

2.1.1.4. Solvents

2.1.1.4.1. General solvents

Acetone, acetonitrile, dichloromethane, ethanol, ethyl acetate, n-hexane and methanol were used. The solvents were purchased from the Institute of Chemistry, University of Duesseldorf. Some of them were distilled before using and special grades were used for spectroscopic measurements.

2.1.1.4.2. Solvents for HPLC

Acetonitrile	LiChroSolv HPLC grade (Merck)
Methanol	LiChroSolv HPLC grade (Merck)
Nanopure water	distilled and heavy metals free water obtained by passing distilled water through nano- and ion-exchange filter cells (Barnstead, France)

2.1.1.4.3. Solvents for optical rotation

Chloroform	Spectral grade (Sigma)
Methanol	Spectral grade (Sigma)
Water	Spectral grade (Fluka)

2.1.1.4.4. Solvents for NMR

Acetone-d_6	Uvasol, Merck
Chloroform-d_3	Uvasol, Merck
DMF-d_7	Uvasol, Merck
DMSO-d_6	Uvasol, Merck
Methanol-d_4	Uvasol, Merck
Pyridine-d_5	Uvasol, Merck

2.1.1.5. Methods

2.1.1.5.1. Fermentation of fungi

Fermentation of the fungi for the isolation of new metabolites was carried out on rice

medium at 21°C under static conditions for 4-6 weeks. 5-15 Erlenmeyer flasks (1 L) with 100 g commercially available rice and 110 mL of distilled water were kept overnight prior to autoclaving and inoculation with the pure isolate.

2.1.1.5.2. Extraction of fungal culture

The cultures were extracted three times with EtOAc and partitioned by liquid-liquid fractionation between *n*-hexane, H_2O and 90% aqueous methanol. The latter was fractionated by vacuum liquid chromatography (VLC) on a silica gel column using a step gradient of *n*-hexane-dichloromethane-methanol. The resulting fractions were analysed by HPLC. Promising fractions were subjected to further chromatographic separation.

Isolation of natural products was carried out from three endophytic fungi isolated from terrestrial plants: *Aureobasidium pullulans* (from *Aloe vera*), *Stemphylium globuliferum* (from *Mentha pulegium*), *Epicoccum nigrum* (from *Mentha suaveolens* Ehr.) and the marine-derived AMO 3-2 from the mangrove plant *Avicennia marina*.

It is because their bioactivity and chemical patterns of their extracts in HPLC chromatograms, that these fungi were chosen for natural products isolation. The procedures were described in figures 2.1 to 2.4.

Figur 2-1: Secondary metabolites isolated from the extract of AMO 3-2.

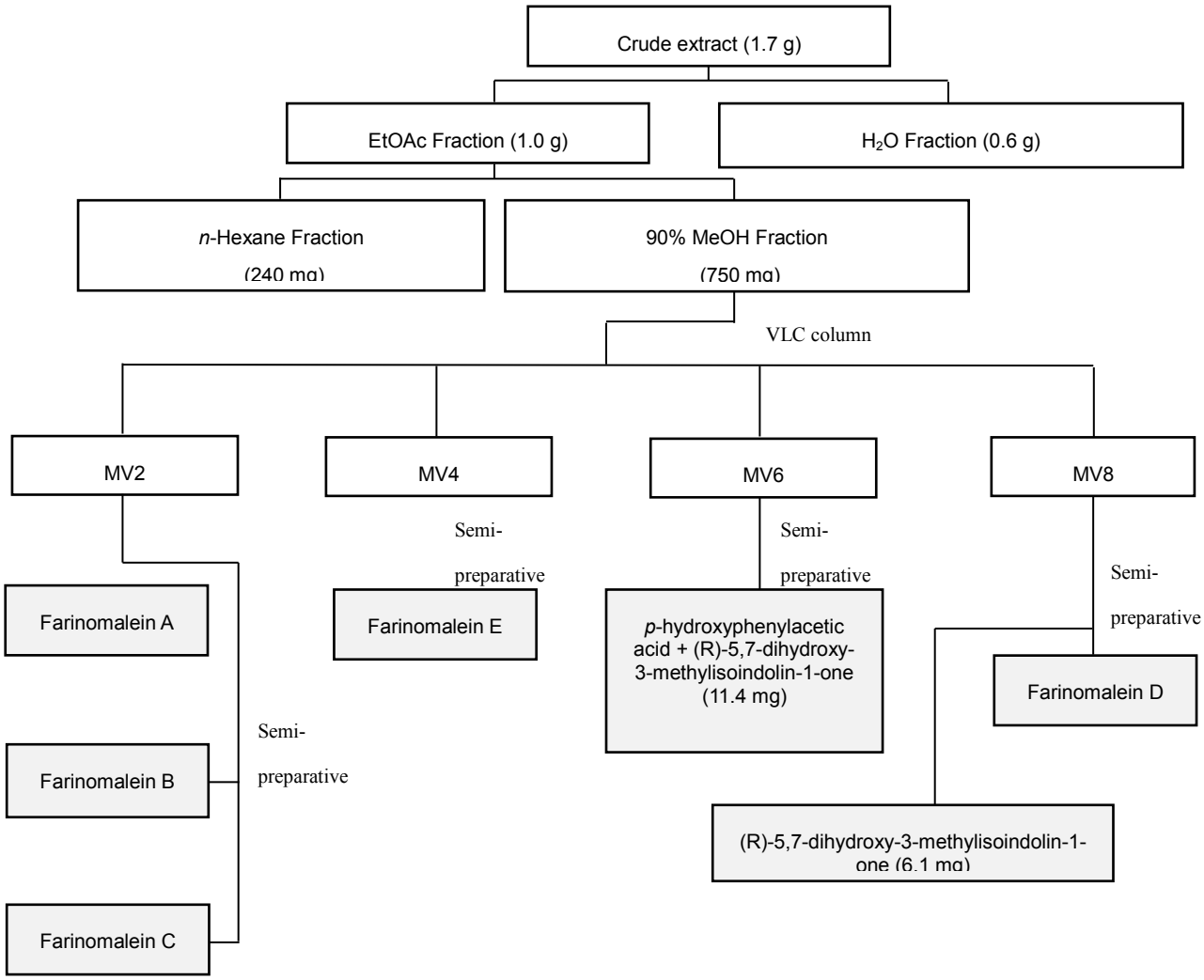

Figure 2-2: Secondary metabolites isolated from the extract of *Epicoccum nigrum*.

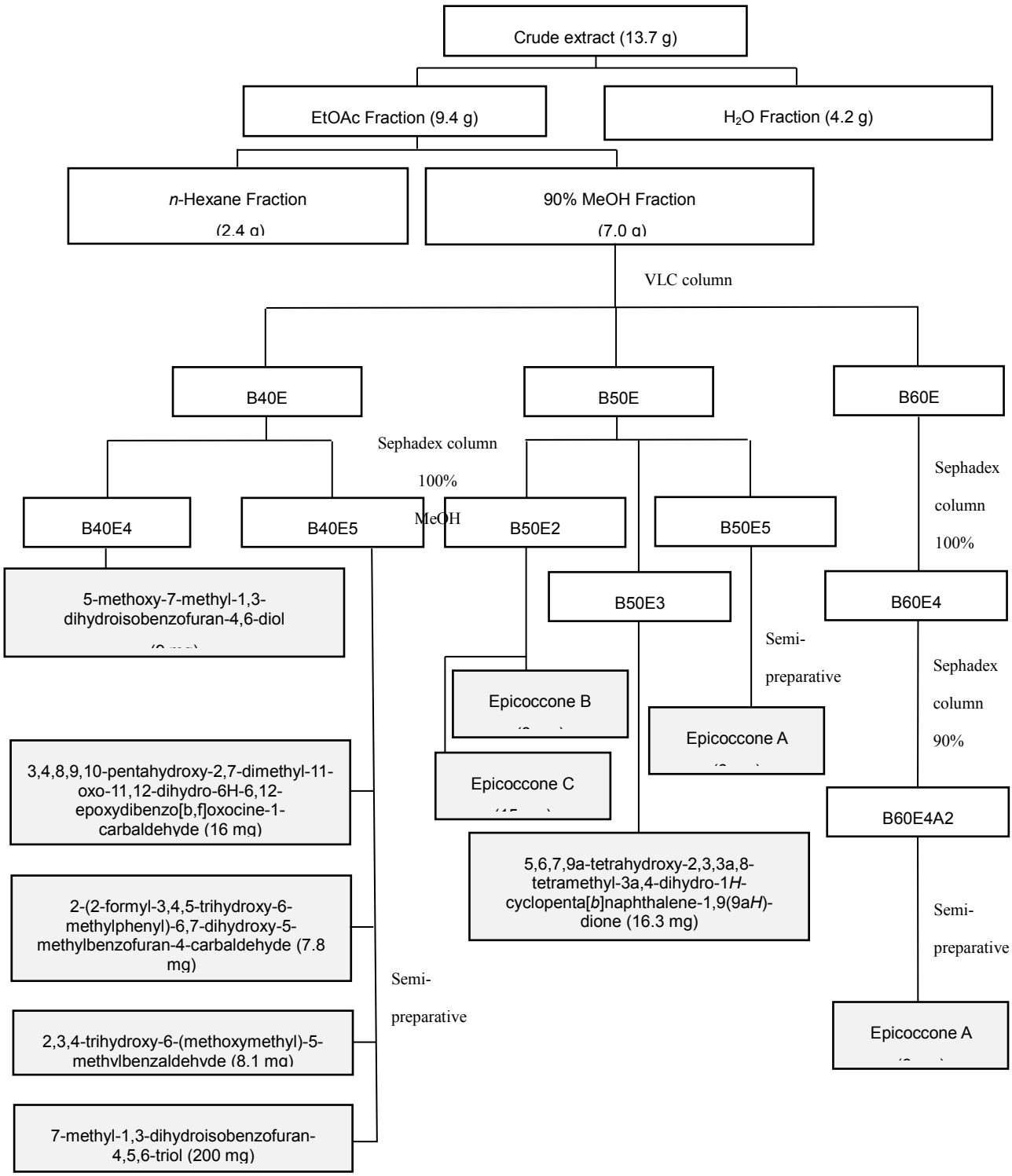

Figure 2-3 Secondary metabolites isolated from the extract of *Aureobasidium pullulans*.

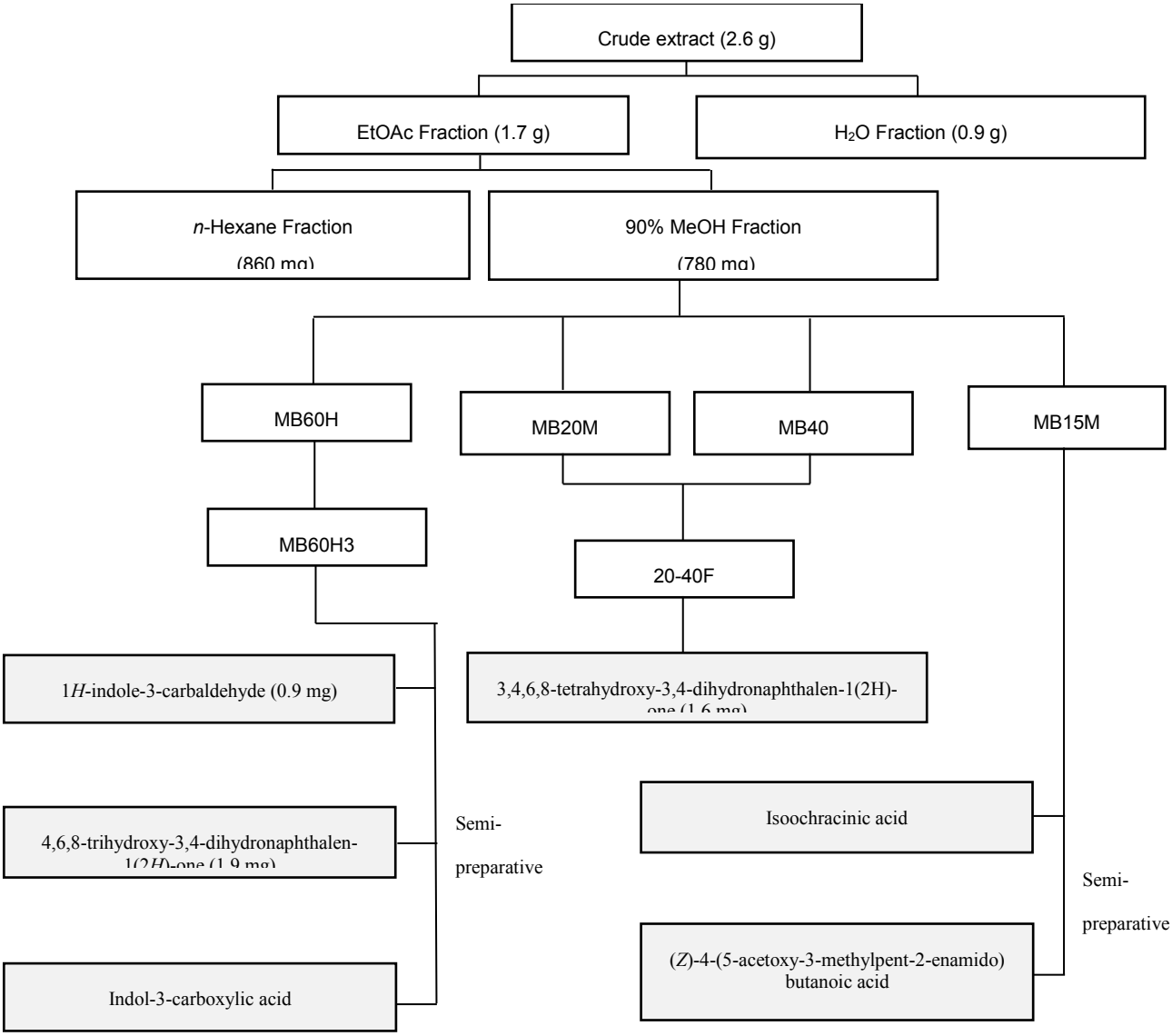

Figure 2.4 Secondary metabolites isolated from the extract of *Stemphylium globuliferum*

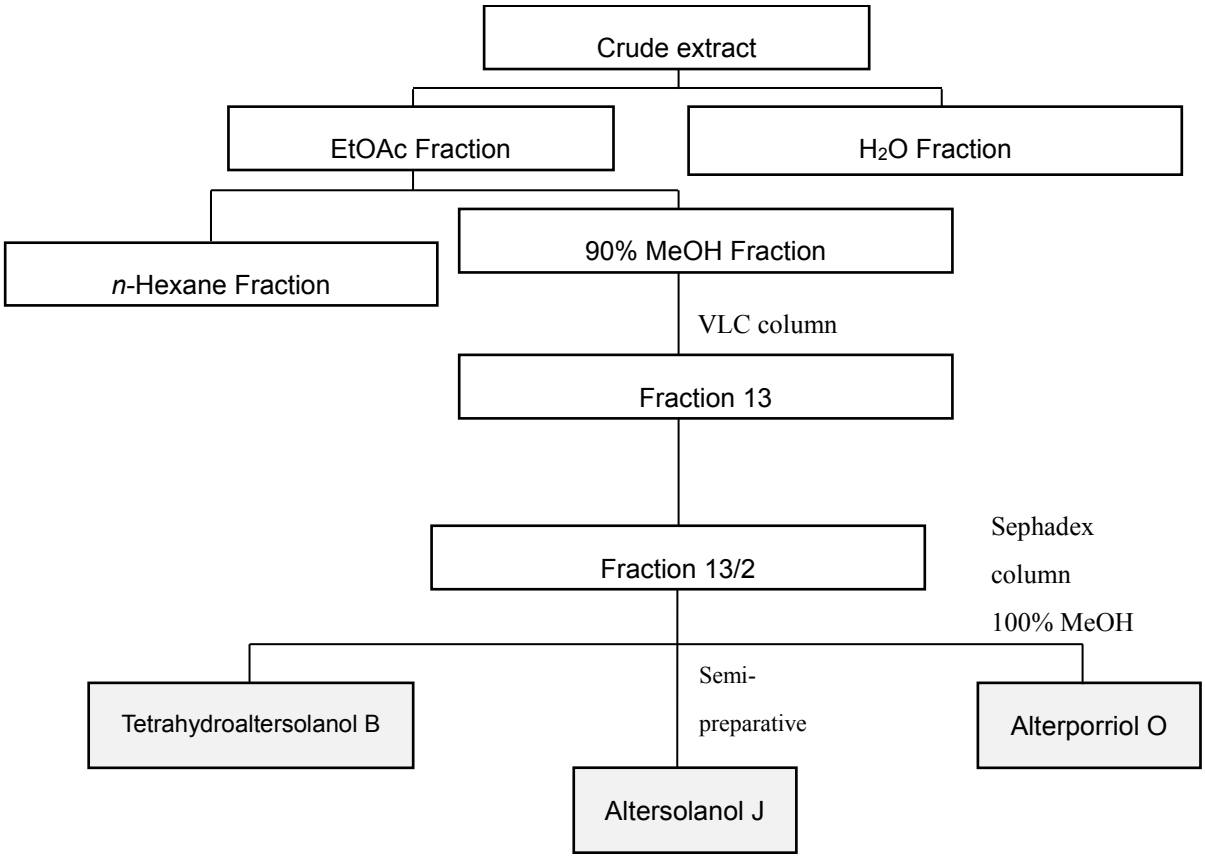

2.1.1.5.3. Chromatographic methods

i. Thin layer chromatography (TLC)

Like other chromatography methods, TLC is a separation method in which the components are distributed between two different phases, stationary phase and mobile phase. The difference in affinities for the two Phases let different compound move at different rates. A pre-coated TLC plate with silica gel 60 F_{254} (layer thickness 0.2 mm, E. Merck, Darmstadt, Germany) was used in combination with the following eluents:

For polar compounds	EtOAc:MeOH:H_2O (30:5:4 and 30:7:6)
For semi-polar compounds	DCM:MeOH (95:5, 90:10, 85:15, 80:20, and 70:30)
	DCM:MeOH:EtOAc (90:10:5, and 80:20:10)

For non-polar compounds *n*-Hexane:EtOAc (95:5, 90:10, 85:15, 80:20, and 70:30)

n-Hexane:MeOH (95:5, and 90:10)

For polar substances a TLC on reversed phase RP18 F_{254} was used (layer thickness 0.25 mm, Merk, Darmstadt, Germany) as well as different solvent systems of MeOH:H_2O (90:10, 80:20, 70:30, and 60:40). The band separation on TLC was detected under UV lamp at 254 and 366 nm, followed by spraying TLC plates with anisaldehyde/H_2SO_4 reagent and they were heated subsequently at 110°C.

Anisaldehyde/H_2SO_4 Spray Reagent (Per 100 mL)

Methanol:	85 mL
Glacial Acetic Acid:	10 mL
Conc. H_2SO_4:	5 mL (added slowly)
Anisaldehyde:	0.5 mL

Vanillin/H_2SO_4 Spray Reagent

Methanol	85 mL
Conc. H_2SO_4	15 mL (added slowly)
Vanillin	1 g

ii. Vacuum liquid chromatography (VLC)

Usually used as an initial isolation step for samples having relatively large weights. The silica gel 60 was packed into a sintered glass filter funnel under applied vacuum. The sample used was adsorbed onto a small amount of silica gel using volatile solvents. The resulting sample mixture was then packed onto the top of the column. Using step gradient elution with non-polar solvent (e.g. *n*-Hexane or DCM) and increasing amounts of polar solvents (e.g. EtOAc or MeOH) successive fractions were collected. The flow was produced by vacuum and the column was allowed to run dry after each fraction collected.

iii. Column chromatography

Fractions derived from VLC were subjected to repeated separation through column chromatography using appropriate stationary and mobile phase solvent systems previously determined by TLC. The following separation systems were used:

a. Normal phase chromatography using a polar stationary phase, typically silica gel, in conjunction with a non-polar mobile phase (e.g. *n*-Hexane or DCM) with gradually increasing amount of a polar solvent (e.g. EtOAc or MeOH). Thus, hydrophobic compounds elute quicker than hydrophilic compounds.

b. Reversed phase (RP) chromatography using a non-polar stationary phase and a polar mobile phase (e.g. H2O, MeOH). The stationary phase consists of silica packed with n-alkyl chains covalently bound. For instance, C-8 signifies an octanyl chain and C-18 an octadecyl ligand in the matrix. The more hydrophobic the matrix on each ligand, the greater the tendency of the column to retain hydrophobic moieties. Thus, hydrophilic compounds elute more quickly than do hydrophobic compounds. Elution was performed using H2O with gradually increasing amount of MeOH.

c. Size exclusion chromatography involves separations based on molecular size of compounds being analysed. The stationary phase consists of porous beads (Sephadex LH-20). Compounds having larger molecular size will be excluded from the interior of the bead and thus will firstly elute, while compounds with smaller molecular size will enter the beads and elute according to their ability to exit from the small sized pores where they were trapped. Elution was performed using MeOH or MeOH:DCM (1:1).

d. Ion exclusion chromatography uses ion exchange resin beds (Diaion HP-20) that acts as a charged solid separation medium. The components of the processed sample have different electrical affinities to his medium and consequently they differently retained by the resin according to their different affinities.

e.

The conditions of analytical HPLC:

Flow rate: 1 mL/min

Injection volume: 20-30 μL

Sample concentration: ca. 0.1- 0.5 mg/mL

Column temperature: 20°C

UV detection wavelengths: 235, 254, 280, and 340 nm

HPLC system specifications:

Pump Dionex P580A LPG

Detector Dionex Photodiode Array Detector UVD 340S

Column thermostat STH 585

Autosampler ASI-100T

HPLC Program Chromeleon (V. 6.3)

Column Knauer (125 × 4 mm, ID), pre-packed with Eurosphere 100–5 C18, with pre-column

Standard gradient for analytical HPLC

Time (min)	Acidic water (%)	MeOH (%)
0	90	10
5	90	10
35	0	100
45	0	100
50	0	10
60	0	10

2.1.1.5.4. Structure elucidation of the isolated secondary metabolites

i. Mass spectrometry (MS)

Mass spectroscopy (MS) is an analytical technique used to determine the elemental composition of a molecule, it is essential for structure elucidation of molecules. A mass spectrometer allows generally through ionization of molecules and separation of those ions according to their mass-to-charge ratios (*m/z*) to determine their molecular weight. The needed amount can be in nanogram. Mass spectrometers include usually three parts: ion source, mass analyzer, and detector, which should be maintained under high vacuum conditions so as to maintain the ions travel through the instrument without any hindrance from air molecules. The sample undergoes vaporization and is then ionized from the ion source before the separation in electromagnetic fields according to their mass (m) to charge (z) ratio (*m/z*) in the mass analyzer. The ionization occurs in both negative and positive charges. The detector transmits the signals to the data system where the mass spectrum is recorded. Molecules have distinctive fragmentation patterns which provide structural information of the compound.

ii. Electrospray ionization mass spectrometry (ESIMS)

After loading it in ESI, the liquid containing our sample undergoes vaporization, it is sprayed through a capillary into a chamber, where the resulting droplets get charged due to an applied potential of a few kV. When solvent evaporate after heating and reducing the pressure, the droplets disappear leaving highly charged molecules, those are driven by the electric field to move into the analyzer region. ESI is suitable for polar and higher molecular weight, because it overcomes their propensity to fragment when ionized.

iii. Liquid chromatography mass spectrometry (LC/MS)

High pressure liquid chromatography is coupled with mass spectrometer to separate and analyze complex mixtures. In on-line analyzes, the eluted liquids coming out of the LC column, are directly injected to MS and a mass spectrum of each component of the mixture can be recorded separately. The samples can be first collected than later injected to the MS, when an off-line analysis is conducted.

HPLC/ESI-MS was carried out using a Finnigan LCQ-DECA mass spectrometer connected to a UV detector. The samples were dissolved in water/MeOH mixtures and injected to HPLC/ESI-MS set-up. For standard MS/MS measurements, the same solvent gradient like that of the HPLC was used.

iv. **LC/MS system specifications**

HPLC system	Agilent 1100 series (pump, detector and autosampler)
	Finnigan LC Q-DECA
MS spectrometer	Knauer, (250 × 2 mm, ID), prepacked with Eurosphere 100-5
Column	C18, with integrated pre-column

v. Electron impact mass spectrometry (EI-MS)

The sample is ionized by bombarding with beam of electrons. The sample is vaporized and directly injected into a high vacuum chamber, where the ionization by bombarding with electrons occurs, neutral molecules are introduced to the ion source in a perpendicular direction to the electron beam, which have been accelerated by an electric field. This induces ionization and fragmentation of these molecules. The ionization process follows a predictable pattern and leads to the formation of molecular ion M^+ or radical cation. EI-MS is suitable for molecules with low molecular weight of 600 Da or less, the samples must be volatile and thermally stable. All analysis using this method were conducted by Dr. Keck and Dr. Tommes at the Institute of Inorganic Chemistry, University of Düsseldorf. The EI mass spectrometer type is Finnegan MAT 8200.

vi. High resolution mass spectrometry (HR-MS)

By passing the ion beam through an electrostatic analyzer before it enters the magnetic sector, the accuracy is widely improved. Ion masses can be measured with an accuracy of about 1 ppm. This kind of measurement gives also the atomic composition of the molecular ions.

HRESI-MS was measured on a Micromass Qtof 2 mass spectrometer at Helmholtz Centre for Infection Research, Braunschweig. The time-to-flight analyzer separates ions according to their mass-to-charge ratios (*m/z)* by measuring the time it takes for ions to travel through a field free region known as the flight.

vii. Nuclear magnetic resonance spectroscopy (NMR)

First observed in 1946, nuclear magnetic resonance leads to the development of a technic, called NMR spectroscopy, which is now almost indispensable for structure elucidation. NMR spectroscopy allows determining chemical and physical proprieties of those nuclei of atoms having magnetic properties. Some nuclei experience this phenomenon, and others do not, depending upon whether they possess a property called spin. NMR spectroscopy is nowadays routinely used to study chemical structure by giving not only the constituent of a molecule but also its relative stereochemistry.

Widely used are ^{1}H and ^{13}C, both having a spin of 1⁄2, a proton having a spin when placed in an external magnet field aligns itself with the external field and takes a low energy orientation aligned with the applied field or a high energy orientation opposed to the applied magnetic field, but also changing from one position to the other by absorbing or losing a photon.

By registration of resonance signals from a sample, which is dissolved in a deuterated solvent and undergoing a varying magnetic field over a small range, we can get a NMR spectrum. The latter can include information about the nature and number of adjacent atoms, the chemical linkage, molecular conformation and interatomic distances. Depending on the environment of each proton they obtain different shielding and deshielding effects appearing in different parts of the resulting NMR spectrum. The resulting frequency where the nuclei resonate, the so-called chemical shift, is given in ppm and the coupling constants between adjacent nuclei in Hertz (Hz).

NMR spectra were carried out on a Bruker ARX-500, Institute for Inorganic and Structural Chemistry, Heinrich-Heine University, Duesseldorf. Some measurements were also performed

at the Helmholtz Centre for Infection Research, Braunschweig, by Dr. Victor Wray using an AVANCE DMX-600 NMR spectrometer. All 1D and 2D spectra were obtained using the standard Bruker software. The samples were dissolved in suitable deuterated solvents and the solvent signals were used as internal standards (reference signal).

viii. Optical activity

Optical rotation or optical activity is a phenomenon observed in the 1811 in quartz by the French physicist Dominique F.J. Arago. Polarized light changes its polarization after passing through a chiral molecule; this can be measured with a polarimeter. This equipment consists of a light source, two polarizing filters and a cell that contains a solution of the analyzed compound.

Optical activity is a macroscopic property of a molecule and differs between enantiomers. Samples containing two enantiomers in the same ratio are optically inactive. In a solution the measured optical rotation depends on concentration (c) and light path length (l) of the sample. The specific rotation, [α], expresses the optical rotation degree after correction of concentration and path length. Thus the specific rotation is a specific quantity for a chiral molecule at certain temperature (T) and at certain wavelength (λ).

$$[\alpha]_{\lambda}^{T} = 100\ \alpha\ /c.l$$

where:

$[\alpha]_{\lambda}^{T}$ is specific rotation at certain temperature T and wavelength λ

a = the angle of rotation (^{o}),

l = optical path length in (dm)

λ = wavelength

T = temperature

c = concentration (g/100 mL)

The measurement of optical rotation presented in this study, was recorded on Perkin-Elmer 241 MC polarimeter and using a 0.5 mL cuvette with 1 dm length.

$[\alpha]_D^{20}$ is the specific optical rotation of Sodium-D-line at the wavelength, 589 nm and at a temperature of 20 °C.

ix. Determination of absolute stereochemistry by Mosher reaction

The reaction was performed based on a modified Mosher ester procedure described by Su et al. (Ohtani *et al*., 1991; Su *et al*., 2002).

A similar quantity of the analyzed compound (1 mg each) was dried under vacuum and transferred into two NMR tubes after dissolving each in 0.5 mL deuterated pyridine and (*R*)-MTPA chloride [(*R*)-(-)- *α*-(trifluoromethyl) phenylacetyl chloride] for the first tube and (*S*)-MTPA ester [(*S*)-(-)- *α*-(trifluoromethyl) phenylacetyl chloride] for the second (under a N_2 gas stream). The reagent was added in the ratio of 0.14 mM reagent to 0.10 mM of the compound (Dale and Mosher, 1973). The NMR tubes were shaken carefully and incubated for several hours at room temperature before measuring ^{1}H-NMR and ^{1}H–^{1}H COSY spectra, which can confirm the assignment of the signals.

2.1.1.5.5. Biological activity assays

A bioassay-guided separation can lead to the discovery of compounds with interesting activity. Samples from crude extracts and from different fractions, resulting of different separation were submitted to biological activity tests.

i. Antimicrobial and antifungal assay

Primary screening assay was carried out using extracts and pure compounds. In 96 well plates the compounds were tested for their inhibitory activity against the resistant pathogens: *Escherichia coli*, *Enterococcus faecium*, *Staphylococcus aureus*, *Streptococcus pneumonia*, *Pseudomonas aeruginosa*, *Klebsiella pneumonia*, *Candida albicans*, *Candida krusei*, *Aspergillus fumigatus*, *Aspergillus faecius*.

Pure compounds were diluted from 250 to 62.5 µg/mL and extracts from 1250 to 312 µg/mL in Müller Hinton Bouillon (Merck, Germany) for bacterial screening and in RPMI (PAA, Austria), enriched with 2% glucose (PAA, Austria), for fungal screening. Afterwards the substance/extract solution was overlaid with the microbes (105 CFU/mL) and cultivated for

bacteria 24 h for fungi 48h at 35°C. As negative control an antibiotic/antimycotic mix (PAA, Austria) was used in addition to a non-treated infected control (positive). The result was analysed by checking the microbial growth with the eye and by measurement of the turbidity at 650 nm. All procedures were done under aseptic conditions in a sterile laminar air flow according to good laboratory practice.

Substances which show inhibitory activity by a concentration of 125 µg/ml (625 µg/ml for extracts) were considered as possible candidates for MIC assay (minimal inhibition concentration). This latter was performed to identify the minimal concentration inhibiting the growth of the microorganisms. Therefore, the substances/extracts were diluted from 250 g/mL to 0.24 g/mL and screened in the same manner as in the primary screening.

ii. Cytotoxicity test

a) Microculture tetrazolium (MTT) assay

Cytotoxicity assays were performed by Prof. Dr. W. E. G. Müller, Institute for Physiological Chemistry and Pathobiochemistry, University of Mainz, Mainz. Cytotoxicity was evaluated against L5178Y mouse lymphoma cells using microculture tetrazolium (MTT) assay, and compared to that of untreated controls (Carmichael *et al*., 1987).

Cell cultures

L5178Y mouse lymphoma cells were grown in Eagle's minimal essential medium supplemented with 10% horse serum in roller tube culture. The medium contained 100 Units/mL penicillin and 100 µg/mL streptomycin. The cells were maintained in a humified atmosphere at 37°C with 5% CO_2.

MTT colorimetric assay

Stock solutions of the test samples were prepared in ethanol 96% (v/v). Exponentially, growing cells were harvested, counted and diluted appropriately. Of the cell suspension, 50 µL containing 3750 cells were pipetted into 96-well microtiter plates. Subsequently, 50 µL of a solution of the test samples containing the appropriate concentration was added to each

well. The concentration range was 3 and 10 µg/mL. The small amount of ethanol present in the wells did not affect the experiments. The test plates were incubated at 37° C with 5% CO_2 for 72 h. A solution of 3-(4,5-dimethylthiazol-2-yl)-2,5-diphenyltetrazolium bromide (MTT) was prepared at 5 mg/mL in phosphate buffered saline (PBS; 1.5 mM KH_2PO_4, 6.5 mM Na_2HPO_4, 137 mM NaCl, 2.7 mM KCl; pH 7.4) and from this solution, 20 μL was pipetted into each well. The yellow MTT penetrates the healthy living cells and in the presence of mitochondrial dehydrogenases, MTT is transformed to its blue formazan complex. After an incubation period of 3h 45 min at 37° C in a humidified incubator with 5% CO_2, the medium was centrifuged (15 min, 20 °C, 210 x g) with 200 μL DMSO, the cells were lysed to liberate the formed formazan product. After thorough mixing, the absorbance was measured at 520 nm using a scanning microliter-well spectrophotometer. The color intensity is correlated with the number of healthy living cells. Cell survival was calculated using the formula:

$$\text{Survival \%} = 100 \times \frac{\text{Absorbance of treated cells} - \text{absorbance of culture medium}}{\text{Absorbance of untreated cells} - \text{absorbance of culture medium}}$$

All experiments were carried out in triplicates and repeated three times. As controls, media with 0.1% EGMME/DMSO were included in the experiments.

MTT cell viability assays

Cytotoxicity tests were carried out by Prof. Dr. M. U. Kassack (Institut für Pharmazeutische und Medizinische Chemie, Heinrich-Heine University, Düsseldorf) using the cell lines A2780 (A2780 sens), A2780 CisR and K562.

Materials, cell lines and cell culture

The human ovarian carcinoma cell line A2780 (A2780 sens) was obtained from European Collection of Cell Cultures (ECACC, Salisbury, UK). A2780 cells were exposed to weekly cycles of 2 µmol/L cisplatin over a period of 24 weeks. Cisplatin-resistant cells were denoted A2780 CisR. The human chronic myelogenous leukemia cell line K562 was obtained from the German Collection of Microorganisms and Cell Cultures (DSMZ, Germany). All other reagents were

supplied by Sigma Chemicals unless otherwise stated.

All cell lines were grown at 37 °C under humidified air supplemented with 5% CO_2 in RPMI 1640 (PAN Biotech, Germany) containing 10% fetal calf serum (PAN Biotech, Germany), 100 IU/mL penicillin and 100 µg/mL streptomycin. The cells were grown to 80% confluency before using them for the MTT cell viability assay.

b) Protein kinase assay

Protein kinase assays were carried out by Dr. Michael Kubbutat (ProQinase GmbH, Freiburg, Germany).

Protein kinase enzymes are integral components of numerous signal transduction pathways involved in the regulation of cell growth, differentiation, and response to changes in the extracellular environment. Consequently, kinases are major targets for potentially developing novel drugs to treat diseases such as cancer and various inflammatory disorders.

The inhibitory potency of the samples was determined using 16 protein kinases (see Table 2.2). The IC_{50} profile of compounds/fractions showing an inhibitory potency of ≥ 40% with at least one of the 16 kinases at an assay concentration of 1×10^{-06} g/mL was determined. IC_{50} values were measured by testing 10 concentrations of each sample in singlicate (n=1).

Sample preparation

The compounds/fractions were provided as 1×10^{-03} g/mL stock solutions in 100% DMSO (1000 or 500 µL) in micronic boxes. The boxes were stored at -20°C. Prior to the assays, 100 µL of the stock solutions were transferred into separate microtiter plates. Subsequently, they were subjected to serial, semi-logarithmic dilution using 100% DMSO as a solvent resulting in 10 different concentrations. 100% DMSO was used as control. Subsequently, 7 × 5 µL of each concentration were aliquoted and diluted with 45 µL H_2O only a few minutes before the transfer into the assay plate to minimize precipitation. The plates were shaken thoroughly and then used for the transfer of 5 µL compound solution into the assay plates.

Recombinant protein kinases

All protein kinases were expressed in Sf9 insect cells as human recombinant GST-fusion proteins or His-tagged proteins by means of the baculovirus expression system. Kinases

were purified by affinity chromatography using either GSH-agarose (Sigma) or NiNTH-agarose (Qiagen). Purity was checked by SDS-PAGE/silver staining and the identity of each kinase was verified by western blot analysis with kinase specific antibodies or by mass spectrometry.

Protein kinase assay

A proprietary protein kinase assay (33PanQinase® Activity Assay) was used for measuring the kinase activity of the protein kinases. All kinase assays were performed in 96- well Flash Plates™ from Perkin Elmer/NEN (Boston, MA, USA) in a 50 µL reaction volume. The reaction mixture was pipetted in the following order: 20 µL assay buffer, 5 µL ATP solution in H_2O, 5 µL test compound in 10% DMSO and 10 µL substrate/10 µL enzyme solution (premixed). The assay for all enzymes contained 60 mM HEPES-NaOH (pH 7.5), 3 mM $MgCl_2$, 3mM $MnCl_2$, 3 pM Na-orthovanadate, 1.2 mM DTT, 50 pg/mL PEG20000, 1 pM [y-33P]-ATP. The reaction mixtures were incubated at 30°C for 80 minutes and stopped with 50 µL 2% (v/v) H_3PO_4. The plates were aspirated and washed two times with 200 µL of 0.9% (w/v) NaCl or 200 pL H_2O. Incorporation of ^{33}Pi was determined with a microplate scintillation counter (Microbeta Trilux, Wallac). All assays were performed with a Beckman Coulter/Sagian robotic system.

Table 2.2: List of Protein kinases and their substrates

Family	Kinase	Substrate	Oncologically relevant mechanism	Disease
Serine/threonine kinases	AKT1/PKB Alpha	GSC3 (14-27)	Apoptosis	Gastric cancer (Staal, 1987)
	ARK5	Autophos.	Apoptosis	Colorectal cancer (Kusakai *et al.*, 2004)
	Aurora B	Tetra(LRRWSLG)	Proliferation	Breast cancer (Keen and Tylor 2004)
	PLK-1	Casein	Proliferation	Prostate cancer (Weichert *et al.*, 2004)

	MEK1 wt	ERK2-KR	Apoptosis	Multiple cancers (Ryan *et al*., 2000)
	NEK2	RB-CTF	Apoptosis	Ewing's tumors & B cell lymphoma (Schultz *et al.*, 1994)
	NEK6	GSK3(14-27)	Apoptosis	Multiple cancers (Li *et al.*, 2003)
	PIM1	GSK3(14-27)	Apoptosis	prostate cancer (Dhanasekaran *et al.*, 2001)
	PRK1	RBER-CHKtide	Proliferation	Prostate cancer (Manser *et al.*, 1994)

Family	Kinase	Substrate	Oncologically relevant mechanism	Disease
Receptor tyrosine kinase	IGF1-R	Poly(glu,Tyr)$_{4:1}$	Apoptosis	Braest cancer (Zhang and Yee 2000)
	MET wt	Poly(Ala,glu,Lys,Tyr) $_{6:2:4:1}$	Metastasis	Lung cancer (Qiao *et al.*, 2002)
	VEGF-R2	Poly(glu,Tyr)$_{4:1}$	Angiogenesis	Pancreatic cancer (Li *et al.*, 2003)
	ALK	poly(Glu,Tyr)$_{4:1}$	Apoptosis	anaplastic large-cell lymphoma (Morris *et al.*, 1994)
	AXL	poly(Glu,Tyr)$_{4:1}$	Proliferation	Ovarian, gastric and breast cancer (*Liu et al.*, 1988)
Soluble tyrosine kinase	FAK	Poly(glu,Tyr)$_{4:1}$	Metastasis	Breast cancer (Schmitz *et al.*, 2005)
	SRC	Poly(glu,Tyr)$_{4:1}$	Metastasis	Colon cancer (Dehm *et al.*, 2001)

2.2. Biodiversity-screening of endophytic fungi

Endophytic fungi dwelling asymptomatically within plant tissues have been found in all studied plants. Endophyte communities can be analysed using culture- and culture-independent methods.

2.2.1 Culture dependent screening method

i. Isolation of endophytic fungi

Healthy plant materials were washed with sterilized demineralized water, then sterilized with 70% ethanol for 1-2 minutes in order to eliminate surface contaminating microbes and ultimately re-washed with sterilized demineralized water to stop the sterilization. The inner tissues were carefully dissected under sterile conditions and placed onto malt agar plates containing antibiotic (see section 2.1.2.1). After 2-3 Days, hyphae growing from the plant material were immediately transferred to fresh plates in order to get pure strains, incubated again for several days, and periodically checked for culture purity.

ii. Cultivation for screening and isolation of secondary metabolites

Pure fungi strains were transferred into Erlenmeyer flasks (1L each) containing 100g rice and 110 ml water for solid cultures or 300 mL of Wickerham medium for liquid cultures. The cultures were then incubated at 21°C in darkness (no shaking) for 3 or 4 weeks. While 1 Flask was enough to carry out small scales cultures, large scale cultivation needed 30 and 10 1L Erlenmeyer flasks for liquid and solid rice cultures, respectively.

iii. DNA Isolation and Fungi Identification

DNA isolation was carried out with ZR Fungal/Bacterial DNA Kit™ (ZYMO RESEARCH, D6005), following the manufacturer Protocol:

1. Add 50-200 mg of fungal cells to a ZR BashingBead™ Lysis Tube. Add 750 µl Lysis Solution to the tube.

2. Vortex for 5 minutes.

Processing times may be as little as 40 seconds when using high-speed cell disrupters.

3. Centrifuge the ZR BashingBead™ Lysis Tube in a microcentrifuge at 10,000 x g for 1 minute.

4. Transfer up to 400 µl supernatant to a Zymo-Spin™ IV Spin Filter (orange top) in a Collection Tube and centrifuge at 7,000 rpm (~7,000 x g) for 1 minute. (Snap off the base of the Zymo-Spin IV™ Spin Filter prior to use).

5. Add 1,200 µl of Fungal/Bacterial DNA Binding Buffer to the filtrate in the Collection Tube from Step 4.

6. Transfer 800 µl of the mixture from Step 5 to a Zymo-Spin™ IIC Column in a Collection Tube and centrifuge at 10,000 x g for 1 minute.

7. Discard the flow through from the Collection Tube and repeat Step 6.

8. Add 200 µl DNA Pre-Wash Buffer to the Zymo-Spin™ IIC Column in a newcollection Tube and centrifuge at 10,000 x g for 1 minute.

9. Add 500 µl Fungal/Bacterial DNA Wash Buffer to the Zymo-Spin™ IIC Column and centrifuge at 10,000 x g for 1 minute.

10. Transfer the Zymo-Spin™ IIC Column to a clean 1.5 ml microcentrifuge tube and add 100 µl (25 µl minimum) DNA Elution Buffer directly to the column matrix or steril watter.

Centrifuge at 10,000 x g for 30 seconds to elute the DNA.

After isolation of the genomic DNA, quantification was done after agarose Gel Electrophoresis for DNA with the Software GelQuant.NET, where the fluorescent of the samples, were compared to that of a known amount of the ladder.

iv. DNA amplification

DNA amplification by PCR was performed using Hot StarTaq Master Mix Taq polymerase (Qiagen) and the primers (Invitrogen):

ITS1	5’-TCCGTAGGTGAACCTGCGG-3’	White *et al.* 1990
ITS4	5’-TCCTCCGCTTATTGATATGC-3’	White *et al.* 1990
NS1	5’-GTAGTCATATGCTTGTCTC-3’	White *et al*. 1990
Fung	5’-ATTCCCCGTTACCCGTTG-3’	May *et al.* 2001

PCR program:

ITS1\ITS4:

Initial denaturation	95,0 °C	15:00	min.	
Denaturation	95,0 °C	1:00	min.	35 times
Annealing	56,0 °C	0:30	sec.	
Extension	72,0 °C	1:00	min.	
Final extension	72,0 °C	10:00	min.	

v. Purification of PCR products

DNA Purification from Agarose Gel was carried out with QiaQuick Gel Extraction Kit (Quiagen) following the manufacturer instractions:

1. Excise the DNA fragment from the agarose gel with a clean, sharp scalpel. Minimize the size of the gel slice by removing extra agarose.

2. Weigh the gel slice in a colorless tube. Add 3 volumes of Buffer QG to 1 volume of gel (100 mg ~ 100 µl).

For example, add 300 µl of Buffer QG to each 100 mg of gel. For >2% agarose gels, add 6 volumes of Buffer QG. The maximum amount of gel slice per QIAquick column is 400 mg; for gel slices >400 mg use more than one QIAquick column.

3. Incubate at 50°C for 10 min (or until the gel slice has completely dissolved). To help dissolve gel, mix by vortexing the tube every 2–3 min during the incubation.

IMPORTANT: Solubilize agarose completely. For >2% gels, increase incubation time.

4. After the gel slice has dissolved completely, check that the color of the mixture is yellow (similar to Buffer QG without dissolved agarose). If the color of the mixture is orange or violet, add 10 µl of 3 M sodium acetate, pH 5.0, and mix. The color of the mixture will turn to yellow. The adsorption of DNA to the QIAquick membrane is efficient only at pH ≤7.5. Buffer QG contains a pH indicator which is yellow at pH ≤7.5 and orange or violet at higher pH, allowing easy determination of the optimal pH for DNA binding.

5. Add 1 gel volume of isopropanol to the sample and mix. For example, if the agarose gel slice is 100 mg, add 100 µl isopropanol. This step increases the yield of DNA fragments <500 bp and >4 kb. For DNA fragments between 500 bp and 4 kb, addition of isopropanol has no effect on yield. Do not centrifuge the sample at this stage.

6. Place a QIAquick spin column in a provided 2 ml collection tube.

7. To bind DNA, apply the sample to the QIAquick column, and centrifuge for 1 min. The maximum volume of the column reservoir is 800 µl. For sample volumes of more than 800 µl, simply load and spin again.

8. Discard flow-through and place QIAquick column back in the same collection tube. Collection tubes are re-used to reduce plastic waste.

9. (Optional): Add 0.5 ml of Buffer QG to QIAquick column and centrifuge for 1 min. This step will remove all traces of agarose. It is only required when the DNA will subsequently be used for direct sequencing, in vitro transcription or microinjection.

10. To wash, add 0.75 ml of Buffer PE to QIAquick column and centrifuge for 1 min.

Note: If the DNA will be used for salt sensitive applications, such as blunt-end ligation and direct sequencing, let the column stand 2–5 min after addition of Buffer PE, before centrifuging.

11. Discard the flow-through and centrifuge the QIAquick column for an additional 1 min at ≥10,000 x g (~13,000 rpm).

IMPORTANT: Residual ethanol from Buffer PE will not be completely removed unless the flow-through is discarded before this additional centrifugation.

12. Place QIAquick column into a clean 1.5 ml microcentrifuge tube.

13. To elute DNA, add 50 µl of Buffer EB (10 mM Tris•Cl, pH 8.5) or H2O to the center of the QIAquick membrane and centrifuge the column for 1 min at maximum speed. Alternatively, for increased DNA concentration, add 30 µl elution buffer to the center of the QIAquick membrane, let the column stand for 1 min, and then centrifuge for 1 min.

The purified PCR products can be stored at -20 °C before sequencing.

vi. Fungi Identification:

DNA sequencing was performed using primers ITS1 or NS1 and performed by BMBF, Heinrich Heine Universität Düsseldorf or GATC Biotech AG. Nucleotide sequences of ITS rDNA of each taxon were compared using a Blast search in the nucleotide database in GenBank.

2.2.2 Culture independent screening method

Denaturing gradient gel electrophoresis (DGGE)

This electrophoretic method is usually used to identify single base changes in a segment of DNA. Double-stranded DNA faces an increasing denaturant environment and begins to melt. The melting temperature of certain domains is sequence-specific.

DNA starts to melt when the Tm of the lowest domain is reached, this reduces its mobility in a polyacrylamide gel with a denaturing gradient. While temperature is kept steady at 60°C a linear denaturing gradient formed with urea and formamide, is applied perpendicular or parallel to the direction of electrophoresis. The combination of both, temperature and denaturant gradient is required for DNA separation.

2.3. Materials

2.3.1 Biological materials

The mangrove plant *Avicennia marina* was collected from different locations and in different times, from Oman and P.R. China. The identification was done based on the morphological characters and ribosomal DNA comparison.

The samples were treated in the same way as those collect for isolation of endophytic fungi (see **2.b.1.1.**).

Table 2.1: Plant material used for DGGE

Plant	Collection site	Collection date	Plant Part
Avicennia marina	Dongzhai mangrove garden Haikou (Hainan) China	Sept 2009	Leaves Stems
	Dongzhai mangrove garden Haikou (Hainan) China	Aug 2011	Leaves Stems
	Qurum beach (Muscat) Oman	Sept 2008	Leaves Stems

2.3.2 Chemicals for DGGE

Acrylamide	Serva
Bis-acrylamid	Serva
Formamide (deionized)	Applichem
Urea	Serva
TAE Buffer	Sigma
SYBR Gold	NEB

2.3.3 Amplification of ITS region using primer with GC Clamp

The surface of healthy leaves was first repetitively washed with sterile water, before total DNA isolated isolation. This latter was conducted using Phenol-Chloroform method (Duong et al. 2006). The resulting total DNA was used as template for PCR. A GC clamp was added to the reverse-primer pair to avoid total melting of the DNA strands during electrophorese.

The following primers were used:

ITS1	5'-TCCGTAGGTGAACCTGCGG-3'	White *et al.* 1990
ITS4	5'-CGCCCGCCGCGCCCCGCGCCCGGCCGCC GCCCCCGCCCCTCCTCCGCTTATTGATATGC-3'	White *et al.* 1990
NS1	5'-GTAGTCATATGCTTGTCTC-3'	White *et al*. 1990
GCfung	5'-CGCCCGCCGCGCCCCGCGCCCGGCCGCC GCCCCCGCCCCATTCCCCGTTACCCGTTG-3'	May *et al.* 2001
EF4	GGAAGGG[G/A]TGTATTTATTAG	SMIT et al. 1999

NS1\GC-fung:

Initial denaturation	95,0 °C	15:00	min.	
Denaturation	95,0 °C	1:00	min.	
Annealing	55,0 °C	1:10	min	35 times
Extension	72,0 °C	1:00	min.	
Final extension	72,0 °C	10:00	min.	

ITS1\GC-ITS4:

Initial denaturation	95,0 °C	15:00	min.	
Denaturation	95,0 °C	1:00	min.	
Annealing	56,0 °C	0:30	sec.	35 times
Extension	72,0 °C	1:00	min.	
Final extension	72,0 °C	10:00	min.	

2.3.4 Nested PCR

Nested PCR is a technique allowing increasing the PCR yield from weak reactions or generating more specific DNA fragments, which are more suitable for DGGE or more specific for the targeted organisms. This technique requires two successive PCR reactions with different Primer pairs. The product resulting from the first amplification is subject to a second PCR with other primers that target a region within the region targeted by the first PCR primers.

There are a number of reasons to employ nested PCR:

1. Increase PCR yield from weak reactions
2. Avoid detrimental effects of PCR amplification with primers that have a GC-clamp
3. Generate specific DNA fragments suitable for DGGE analysis from DNA fragments that are not suitable for DGGE analysis
4. Allow direct DGGE comparisons of general and specific population analyses
5. Recover additional sequence information than that provided in DGGE-appropriate

fragments.

6. Avoid having to develop and optimize new DGGE conditions for a new primer set.

2.3.5 Preparation of DGGE gel

By mixing two gel stock solutions 0% and 100%, different denaturing gel solutions (15%, 20%, 30%, 60% and 70%) were prepared. In order to start the polymerasation of the polyacrylamide gel, Ammonium persulfate and TEMED (final concentration of each was 0.09%) were added immediately before pouring the Gel.

After cleaning the Slices with ethanol and assembling the sandwich following the instructions of the manufacturer, prepare 10 ml from both, lower and higher denaturing concentration in sterile 12 ml Falcon tubes. Add 9 µl TEMED and 90 µl APS (10%) to each one of the solutions and mix. The polymerization will start immediately (solid gel after ~ 6 min).

Put the solutions into two 10 ml syringes and integrate them to a delivery system (Biorad, Model 475 gradient delivery system) low denaturing concentration solution in the right syringe and in the left the higher denaturing containing solution. Finally rotate the cam wheel slowly and steadily to deliver the gel solution into the assembled vertical sandwish in order to cast the gel vertically, with parallel gradually from lower concentration of denaturant (upper position of the gel) to higher concentration (lower position of the gel). Let polymerase for 60 min.

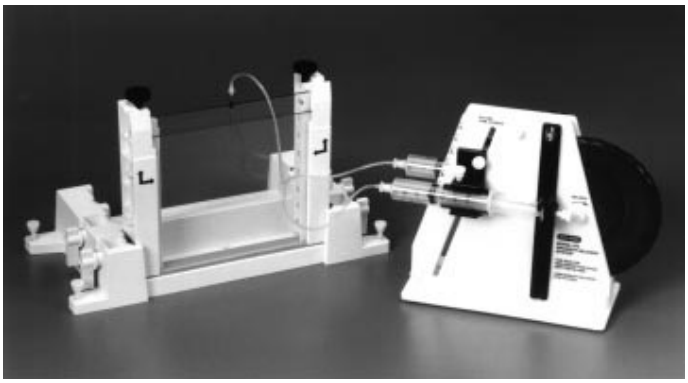

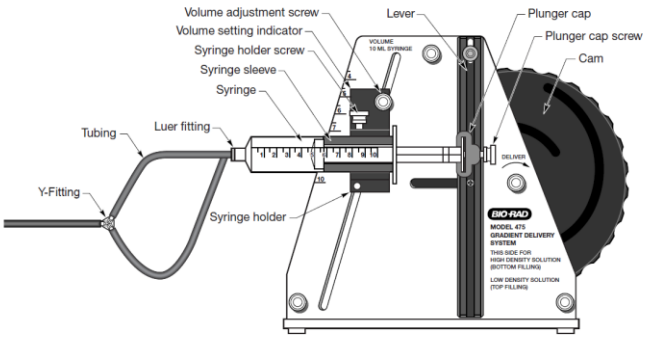

Fig. 2.3.5: Casting a parallel gradient gel (DCode™, source BIO-RAD).

2.3.6 Carrying out DGGE

1. The electrophoresis tank should contain 7 L of TAE buffer.
2. When the temperature of running buffer has reached 60°C, turn the system off.
3. Remove and place the temperature control module on the DCode lid stand. Place the core and the attached gel assemblies into the buffer chamber. Place the temperature control module on top of the electrophoresis tank.
4. Connect the power cord and turn the power, pump, and heater on. wash the wells with running buffer to remove any unpolymerized gel material/leached denaturants from the wells. If necessary, add more buffer to the “max” line on the electrophoresis tank. Place the clear loading lid back onto the temperature control module.
5. Allow the system to reach the set initial temperature before loading samples. This may take 10–15 minutes.
6. Apply power (130 V) to the DCode system and begin electrophoresis.

2.3.7 Purification of bands

The bands excised from the polyacrylamide gel were incubated by night in 4°C in 30 µl sterile water. From the incubation solution, 5 µl was used to amplify the separated DNA using the primers NS 1 and Fung (or ITS1/ITS4). PCR products were then purified and submitted for direct sequencing to GATC-Biotech AG or BMBF, Heinrich Heine Universität Düsseldorf with

the primer ITS1 or NS1. The sequences obtained from each single band, represent each a different fungus and were identified by comparison with the GenBank using BLAST search (www.ncbi.nlm.nih.gov/blast).

3. Results

3.1. Farinomalein A (compound 1, known)

Farinomalein A	
Synonym(s)	3-(3-isopropyl-2,5-dioxo-2,5-dihydro-1*H*-pyrrol-1-yl)propanoic acid
Biological Source	AMO3-2 (unidentified fungus)
Sample Code	AMO 3-2/3-2
Sample Amount	40 mg
Molecular Formula	$C_{10}H_{13}NO_4$
Molecular Weight	211 g/mol
Solubility	MeOH
Physical Description	white powder
HPLC Retention Time	19.11 min (standard gradient)

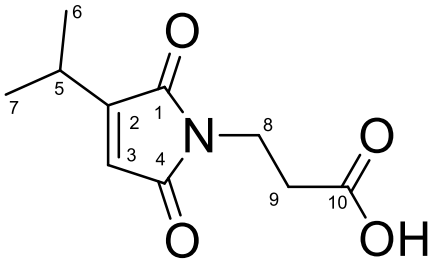

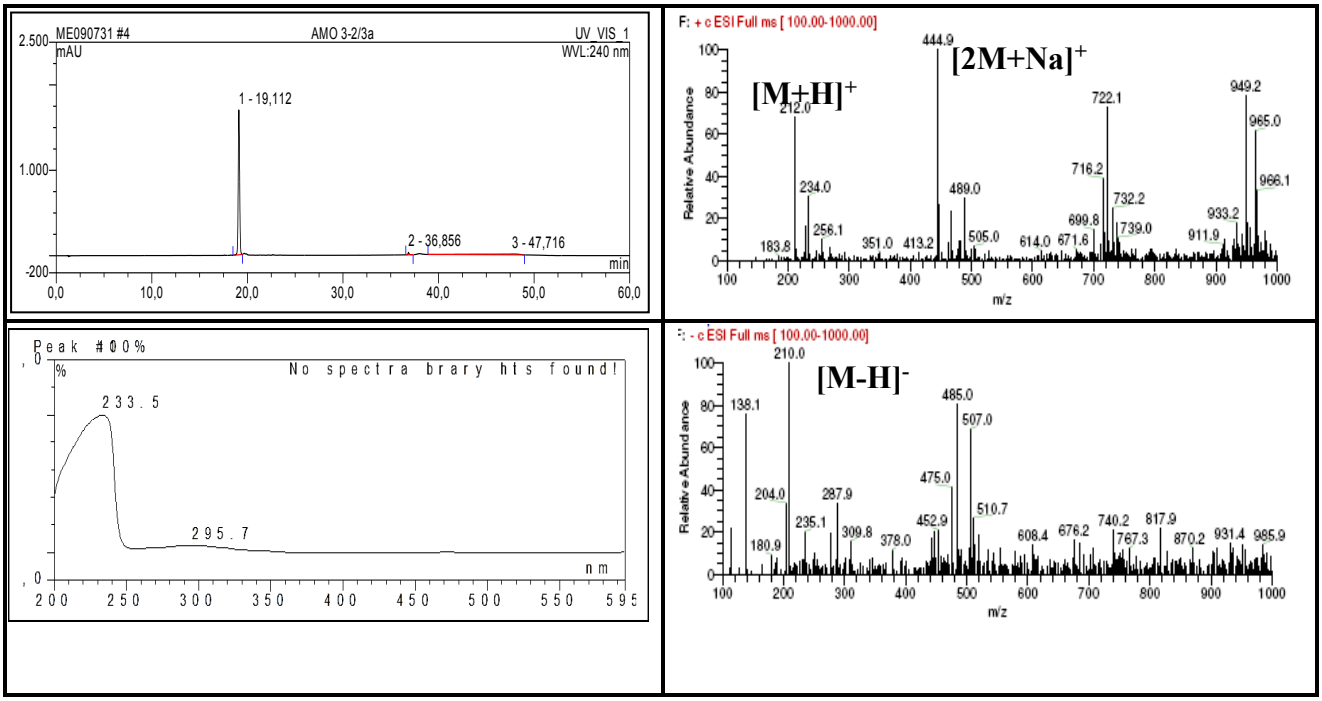

Farinomalein A (**1**) was isolated as a white amorphous powder (40 mg), which showed UV absorbance at λ_{max} (MeOH) 233.5 nm. Positive and negative ESI-MS showed pseudo molecular ion peaks at *m/z* 212 $[M+H]^+$ and at *m/z* 210 $[M-H]^-$, respectively, indicating a molecular weight of 211 g/mol. HRESIMS established a molecular formula of $C_{10}H_{13}NO_4$ indicating five degrees of unsaturation in the molecule. ^1H NMR spectrum (Table 3.1.) revealed two equivalent methyl groups (CH_3-6 and CH_3-7) at δ_H 1.12 (d, 6.9 Hz) which were coupled to a proton (H-5) at δ_H 2.69 (m) which in turn showed a long range correlation to olefinic proton H-3 at δ_H 6.57 (d, 1.3 Hz) in ^1H-^1H COSY spectrum, this spectrum indicated further correlations between two aliphatic methylene groups at δ_H 3.58 (CH_2-8) and δ_H 2.47 (CH_2-9), respectively.

Analysis of ^{13}C and DEPT spectra revealed the presence of four sp^2-hybridized carbons, whose positions in the molecule were clarified with the help of a 2D HMBC spectrum. This indicated correlations of the methylene protons H_2-9 with a carboxyl carbon C-10 (δ_C 172.0) and to the vicinal methylene carbon CH_2-8. The latter methylene protons showed a two-bond correlation to carbon C-1 (δ_C 170.4) whereas the proton H-3 (δ_H 6.57) showed correlations to C-4, C-2 and to C-5. The HMBC spectrum finally indicated the isopropyl group was connected to C-2 (δ_C 154.9) based on the correlations of H-5 with C-3, C-2, CH_3-6, C1 and CH_3-7, respectively. All this and the presence of two almost equivalent carbonyl groups indicate that structure contain a maleimide ring.

To confirm the structure of the maleimide ring, 2D ^1H-^{15}N HMBC spectrum was recorded (Fig. 3.1.1). This showed long-range correlations between H-3 and a single nitrogen resonance at 123.8 ppm. The protons H-8 and H-9 showed also correlations to the nitrogen atom. The structure of **1** was confirmed by comparison of its spectral data with those of the literature

(Putri et al., 2009) which supported the identification of **1** as farinomalein.

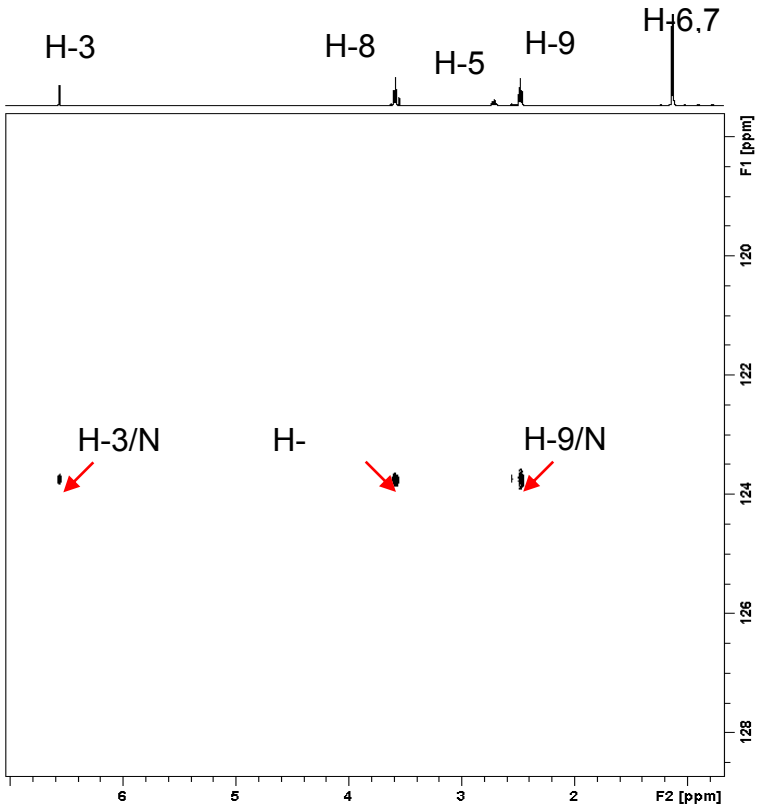

Fig. 3.1.: ^{1}H-^{15}N HMBC spectrum of compound **1**.

		1*	Farinomalein A§	
Position	δ_H (mult.; *J* in Hz)	δ_C	δ_H (mult.; *J* in Hz)	*δ_C
1		170.6 (C)		172.6 (C)
2		154.9 (C)		157.3 (C)
3	6.57 (d; 1.5)	125.0 (CH)	6.37 (d, 1.6)	126.0 (CH)
4		170.4 (C)		172.3 (C)
5	2.69 (m)	25.2 (CH)	2.80 (dh, 1.6, 6.9)	27.2 (CH)
6-Me	1.12 (d; 6.9)	20.5 (CH_3)	1.21 (d, 6.9)	21.3 (CH_3)
7-Me	1.12 (d; 6.9)	20.5 (CH_3)	1.21 (d, 6.9)	20.1.3 (CH_3)

	7	3.58 (t; 7.3)	33.3 (CH_2)	3.74 (t, 7.2)	34.9 (CH_2)	
	8	2.47 (t; 7.3)	32.5 (CH_2)	2.58 (t, 7.2)	34.0 (CH_2)	
	10		172.0 (C)		175.0 (C)	
	10-OH	12.39				

Table 3.1.: ^{1}H, ^{13}C NMR spectrum of compound **1** in DMSO-d_6 and farinomalein A in MeOH-d_4.

*****Measured in (DMSO-d_6) at 600 MHz (^{1}H) and 150 MHz (^{13}C).

$^{\$}$Measured in (MeOH-$d_4$) at 500 MHz ($^{1}H$) and 100 MHz ($^{13}C$).

3.2. Farinomalein B (compound 2, new)

Farinomalein B	
Synonym(s)	Methyl 3-(3-isopropyl-2,5-dioxo-2,5-dihydro-1H-pyrrol-1-yl)propanoic acid
Biological Source	AMO3-2 (unidentifiable fungus)
Sample Code	AMO 3-2/4
Sample Amount	9 mg
Molecular Formula	$C_{11}H_{15}NO_4$
Molecular Weight	225 g/mol
Solubility	MeOH
Physical Description	white powder
HPLC Retention Time	22.16 min (standard gradient)

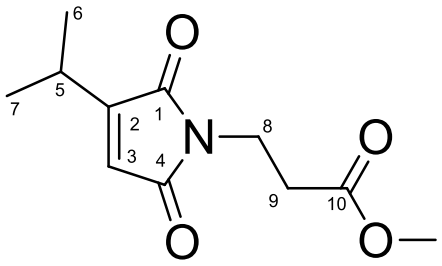

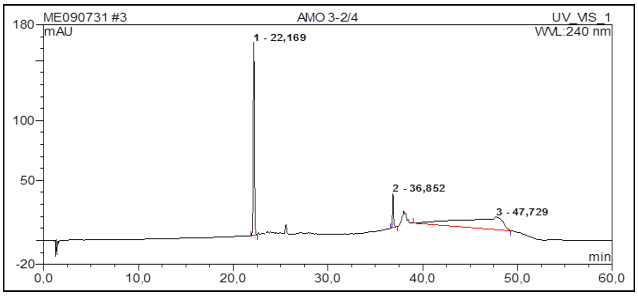

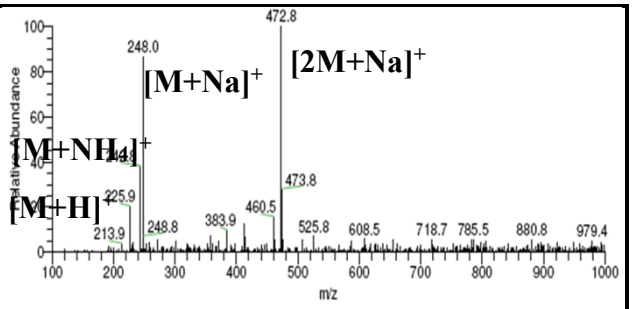

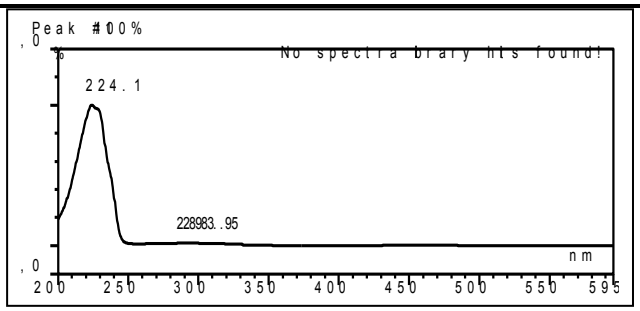

(-)-ESI-MS: no ionization

Compound **2** was isolated from the EtOAc extract of rice cultures of the strain AMO 3-2 in the form of a white powder (9 mg). The UV spectrum showed λ_{max} (MeOH) at 224.1 nm, which is characteristic for the maleimide ring. Positive ESI-MS showed a pseudo molecular ion peak at *m/z* 225.9 $[M+H]^+$ (base peak) indicating a molecular weight of 225 g/mol. Compound **2** was found to have the molecular formula of $C_{11}H_{15}NO_4$ by HRESIMS measurment. The NMR data of **2** (Table 3.2.) were very similar to those of **1** except for the presence of an additional three proton singlet at δ_H 3.65 attributed to the OCH_3-10 (δ_C 52.2). HMBC correlation of OCH_3-10 to C-10 (δ_C 173.1) indicates that **2** is the methyl ester of **1**. This was confirmed after comparison of the NMR data of **2** with the synthetic farinomalein methyl ester (Putri et al., 2009).

Compound **2** was unambiguously identified as methyl 3-(3-isopropyl-2,5-dioxo-2,5-dihydro-1*H*-pyrrol-1-yl) propanoate to which the name farinomalein B was proposed. The presence of **2** already in the crude extract excludes the possibility that **2** could be an artifact arising from methylation of **1** during the purification of the extract. Compound **1** was also incubated in MeOH for several days and analyzed by HPLC, however no building of **2** or any other compounds were detected.

Table 3.2.: NMR spectroscopic data of **Farinomalein-methyl** and **2** at 500 MHz (^{1}H) and 125 MHz (^{13}C) in MeOH-d_4.

	Methylfarinomalein B		**2**		
Position	δ_H (mult.; *J* in Hz)	δ_C	δ_H (mult.; *J* in Hz)	δ_C	**HMBC** correlations (H→C)
1		170.8		172.3	
2		156.0		157.1	
3	6.39 (d; 1.5)	126.0	6.39 (d; 1.5)	125.9	C4; C6; C7
4		170.8		172.4	
5	2.81 (d×sep[c]; 1.5, 6.9)	27.2	2.81 (d×sep; 1.5, 6.9)	27.0	C8;C9; C6; C5
6-Me	1.23 (d; 6.8)	21.3	1.23 (d; 6.8)	21.1	C9; C7; C6
7-Me	1.23 (d; 6.8)	21.3	1.23 (d; 6.8)	21.1	C8; C7; C6
8	3.76 (t; 7.1)	34.9	3.76 (t; 7.1)	34.6	C11; C4
9	2.61 (t; 7.1)	34.0	2.61 (t; 7.1)	33.8	C10; C12
10		72.0		173.1	
O-Me	3.65 (s)	52.5	3.65 (s)	52.2	C12

[c]sep.: septet

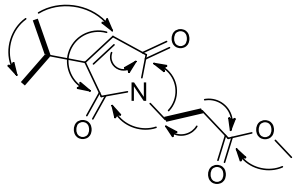

2

Fig. 3.2. Key ^{1}H-^{1}H-COSY and HMBC correlations of **2**.

3.3. Farinomalein C (compound 3, new)

Farinomalein C	
Synonym(s)	Butyl 3-(3-isopropyl-2,5-dioxo-2,5-dihydro-1*H*-pyrrol-1-yl)propanoate
Biological Source	AMO3-2 (unidentifiable fungus)
Sample Code	MV2E3
Sample Amount	5.1 mg
Molecular Formula	$C_{14}H_{21}NO_4$
Molecular Weight	267 g/mol
Solubility	MeOH
Physical Description	white powder
HPLC Retention Time	28.31 min (standard gradient)

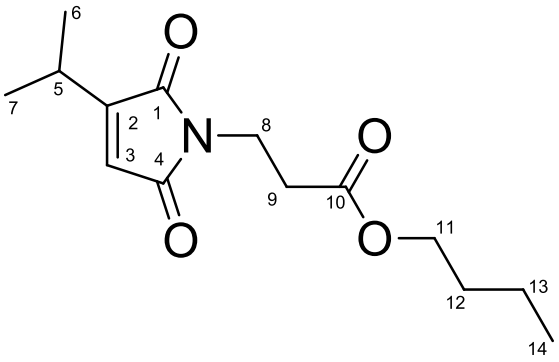

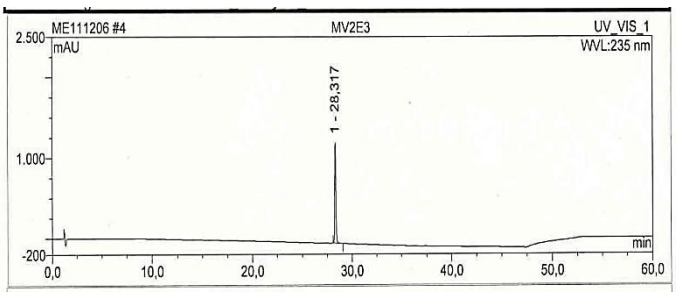

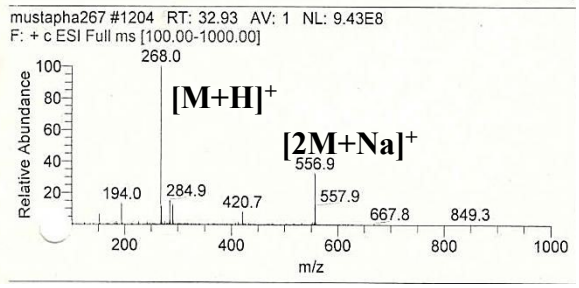

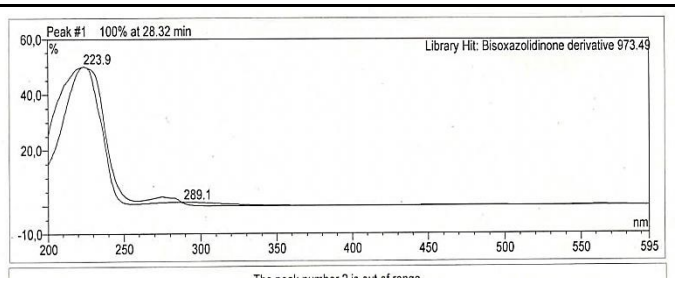

(-)-ESI-MS: no ionization

Farinomalein C (**3**) was obtained as a white amorphous solid (5 mg) with UV maxima at λ_{max} 223.9 nm similar to **1**. Compound **3** displayed similar spectroscopic data to those of **1**, suggesting that both compounds have the same basic molecular framework.

HRESIMS of **3** helped to establish the molecular formula as $C_{14}H_{21}NO_4$ indicating the same degrees of unsaturation in **1**. The molecular weight of **3** differs from that of **1** by 57 amu (C_4H_9) higher. ^{1}H NMR and ^{1}H-^{1}H COSY spectra (Table 3.3. & Fig. 3.3.) revealed four new signals comparing to that of **1**, all involved in a spin system extending from H-11 at δ_H 4.05 (t, *J*= 6.6 Hz) to H_3-14 at δ_H 0.95 (t, *J*= 7.3 Hz) to form a *n*-butyl group. Compound **3** was identified as butyl 3-(3-isopropyl-2,5-dioxo-2,5-dihydro-1*H*-pyrrol-1-yl) propanoate and was named farinomalein C.

Table 3.3.: NMR spectroscopic data of **3** at 500MHz (^{1}H) and 125 MHz (^{13}C) in MeOH-d_4.

Position	**3**		
	δ_H (mult.; *J* in Hz)	δ_C	**HMBC** correlations (H→C)
1		172.0 C	
2		157.1 C	
3	6.38 (d; 1.6)	125.9 CH	C4; C6; C7
4		172.8 C	
5	2.80(d×sep.; 1.0, 6.9)	27.0 CH	C8; C9; C6; C5
6	1.22 (d; 6.9)	21.1 CH_3	C9; C7; C6
7	1.22 (d; 6.9)	21.1 CH_3	C8; C7; C6
8	3.74 (t; 7.0)	34.7 CH_2	C11; C4
9	2.60 (t; 7.0)	34.0 CH_2	C10; C12
10		172.3 C	
11	4.05 (t; 6.6)	65.7 CH_2	C10; C12; C13;
12	1.59 (m)	31.7 CH_2	C11; C14
13	1.38 (m)	20.2 CH_2	C11
14	0.95 (t; 7.3)	14.0 CH_3	C12

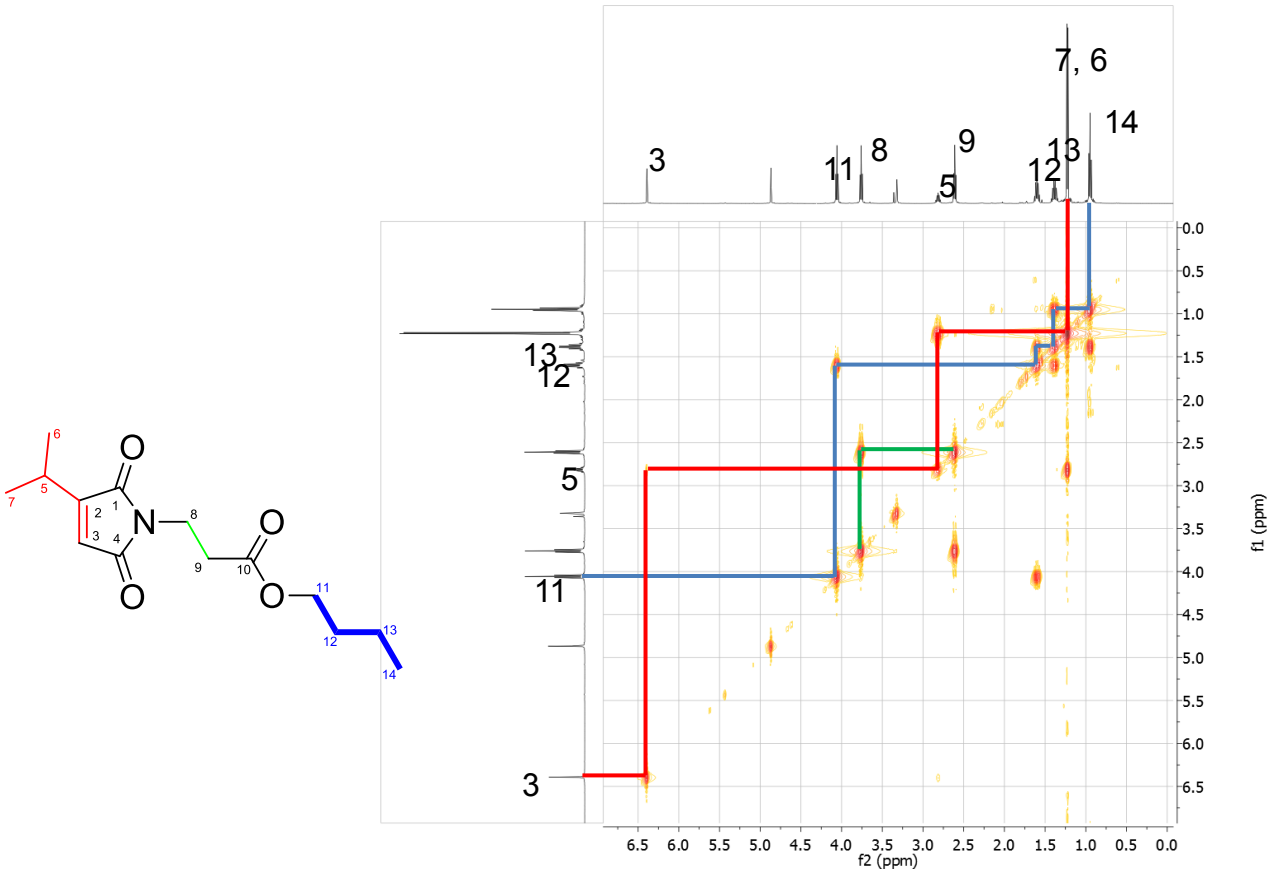

Fig. 3.3.: ^{1}H-^{1}H COSY spectrum of compound **3.**

3.4. Farinomalein D (compound 4, new)

Farinomalein D	
Synonym(s)	2,3-Dihydroxypropyl 3-(3-isopropyl-2,5-dioxo-2,5-dihydro-1*H*-pyrrol-1-yl)propanoate
Biological Source	AMO3-2 (unidentifiable fungus)
Sample Code	MV8E3
Sample Amount	6.0 mg
Molecular Formula	$C_{13}H_{19}NO_4$
Molecular Weight	285 g/mol
Solubility	MeOH
Physical Description	white powder
$[\alpha]^{20}_D$	+ 4.0 (*c* 0.1, MeOH)
HPLC Retention Time	16.74 min (standard gradient)

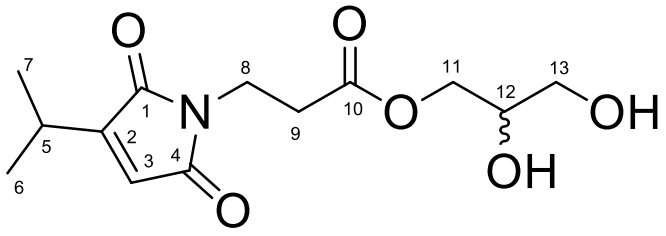

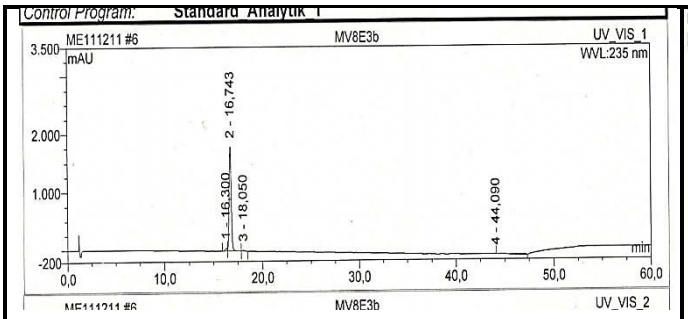

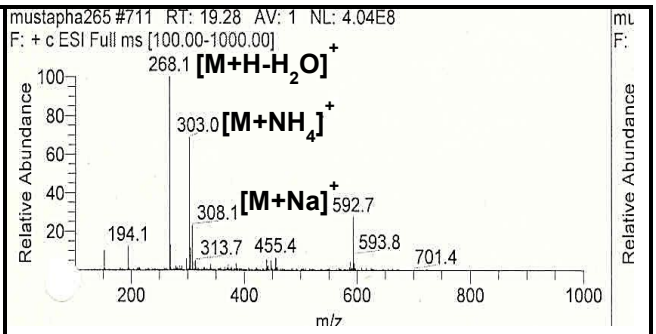

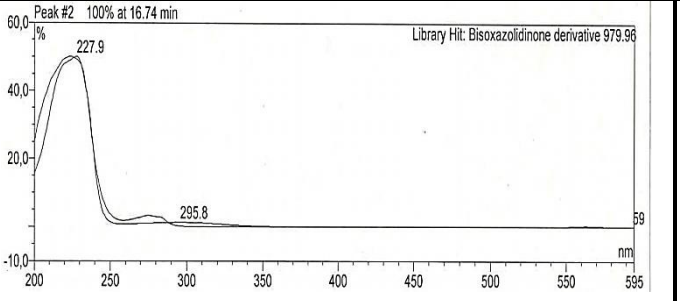

(-)-ESI-MS: no ionization

Compound **4** was isolated from the EtOAc extract of rice cultures of AMO 3-2 as a white solid (3 mg). It showed UV absorbance maximum at λ_{max} (MeOH) 227.9 nm. Positive ESI-MS showed pseudo molecular ion peaks at *m/z* 268 $[M+H-H_2O]^+$, at *m/z* 303 $[M+NH_4]^+$ and *m/z* 308 $[M+Na]^+$ indicating a molecular weight of 285 g/mol. HRESI-MS exhibited a strong peak at *m/z* 308.1104 $[M+Na]^+$ indicating the molecular formula $C_{13}H_{19}NO_6$ (calculated 308.1110), which contain three more carbons and two more oxygen atoms than **1**.

^{1}H NMR and ^{1}H-^{1}H COSY spectra showed four new signals which are not present in **1** and building a new spin-system (Figure 3.4). These latter include doublet of doublets at δ_H 4.05 (1H), at δ_H 4.14 (1H) and δ_H 3.54 (2H) in addition to a multiplet at δ_H 3.82 ppm (1H), referring to propane-1,2-diol residue, which is confirmed by the difference in the molecular weight of 74 amu higher than **1**. Compound **4** was identified as 2,3-dihydroxypropyl 3-(3-isopropyl-2,5-dioxo-2,5-dihydro-1*H*-pyrrol-1-yl) propanoate and was given the name farinomalein D.

The absolute configuration of the hydoxymethine group was not assigned, since anomalous $\Delta\delta$ values were found after derivatization with MTPA-Cl using Mosher's method (Dale & Mosher 1973).

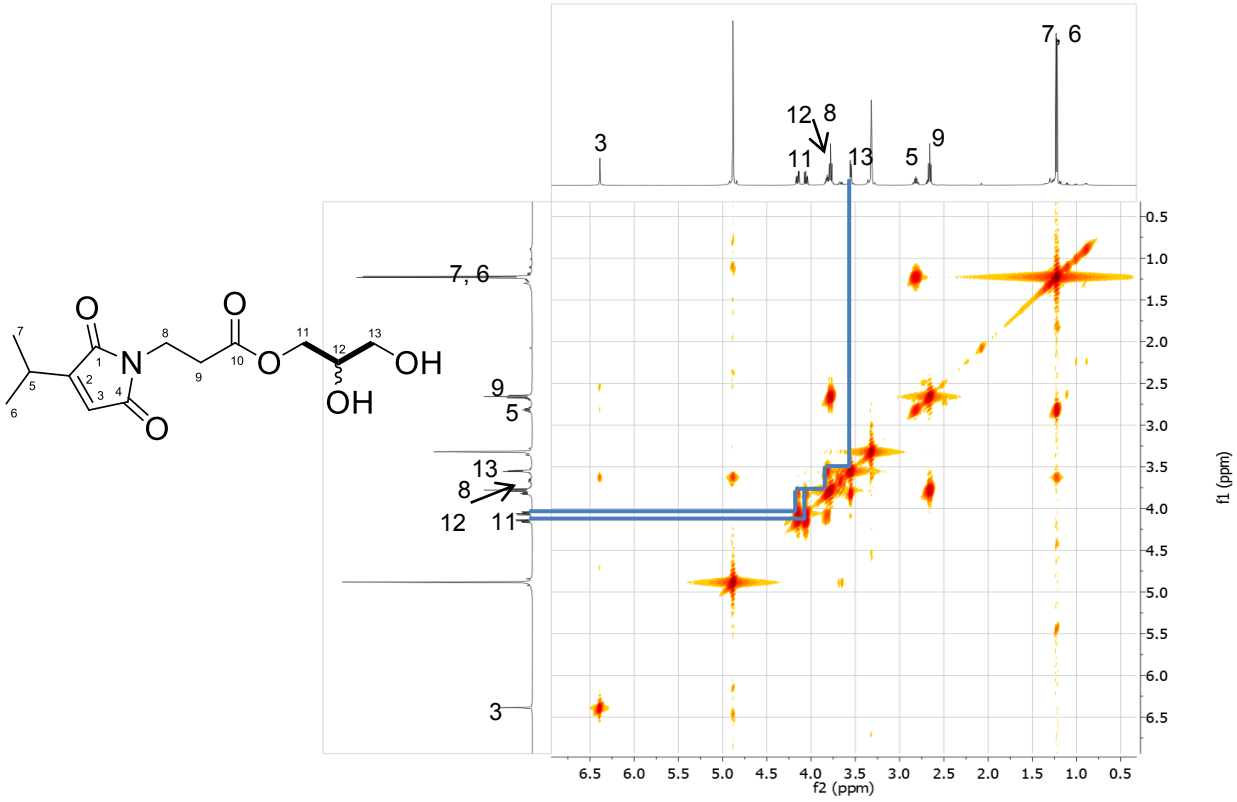

Fig. 3.4.: ^{1}H-^{1}H COSY of compound **4.**

Table 3.4: NMR spectroscopic data of **4** at 500MHz (^{1}H) and 125 MHz (^{13}C) in MeOH-d_4.

Position	**4**		
	δ_H (mult.; *J* in Hz)	δ_C	**HMBC** correlations (H→C)
1		172.1 C	
2		157.1 C	
3	6.38 (d; 1.6)	125.9 CH	C4; C6; C7
4		172.6 C	
5	2.81(d×sep.; 1.6, 6.8)	27.0 CH	C8; C9; C6; C5
6	1.22 (d; 6.9)	21.1 CH_3	C9; C7; C6
7	1.22 (d; 6.9)	21.1 CH_3	C8; C7; C6
8	3.76 (t; 7.0)	34.6 CH_2	C11; C4
9	2.65 (t; 7.0)	33.8 CH_2	C10; C12
10		172.3 C	
11	4.05 (dd; 11.3, 6.4) 4.14 (dd; 11.3, 4.3)	66.9 CH_2	C10; C12; C13
12	3.82 (m)	71.0 CH	C11
13	3.54 (d; 5.8)	64.0 CH_2	C11

3.5. Farinomalein E (compound 5, new)

Farinomalein E	
Synonym(s)	(*E*)-5-((3-(3-isopropyl-2,5-dioxo-2,5-dihydro-1*H*-pyrrol-1-yl)propanoyl)oxy)-3-methylpent-2-enoic acid
Biological Source	AMO3-2 (unidentifiable fungus)
Sample Code	MV4E43
Sample Amount	3.3 mg
Molecular Formula	$C_{16}H_{21}NO_6$
Molecular Weight	323 g/mol
Solubility	MeOH
Physical Description	white powder
HPLC Retention Time	23.56 min (standard gradient)

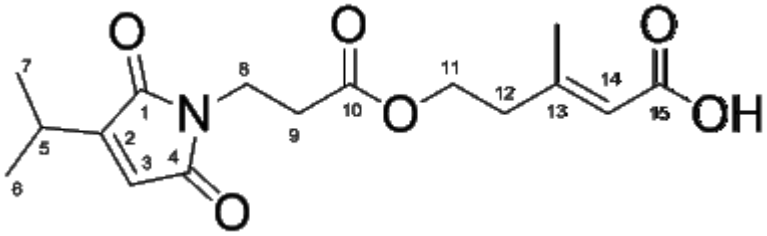

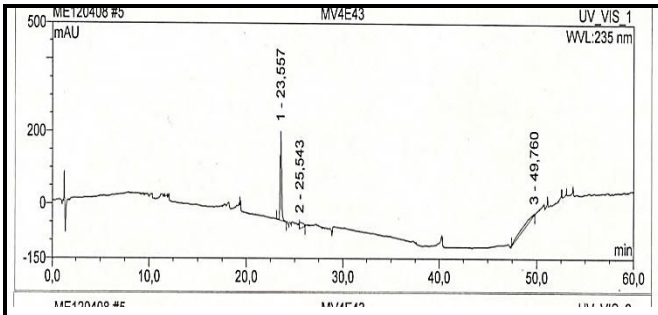

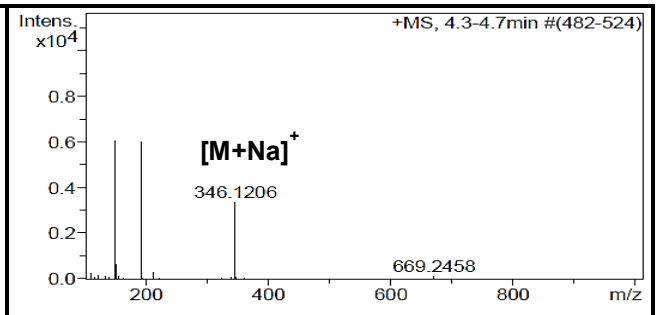

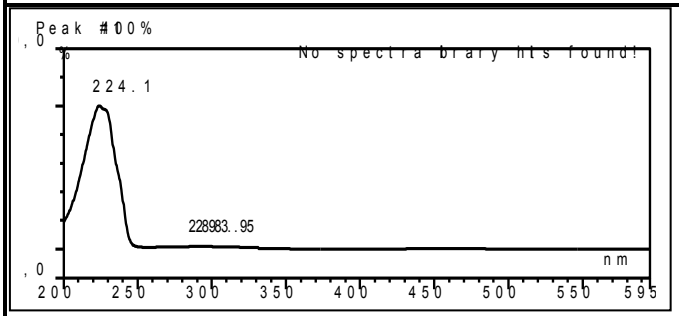

(-)-ESI-MS: no ionization

Farinomalein E (**5**) was obtained as a white solid (3.3 mg) with an UV spectrum similar to that of **1-4.** This compound showed a maximum absorption at λ_{max} (MeOH) 224.1 nm, which indicated the presence of maleimide ring in the molecule. Its molecular weight was established as 323 g/mol according to the molecular ion peak observed at *m/z* 346.12 $[M+Na]^+$ upon positive ionization by ESI-MS analysis. The molecular formula of **5** was determined as $C_{16}H_{21}O_6$ based on the prominent signal at *m/z* 346.1260 $[M+Na]^+$ (calc. for $C_{16}H_{21}NO_6Na$ 346.1261) in the HRESIMS, indicating 112 amu higher than **1** in the molecular weight. The molecular formula of **5** indicates seven degrees of unsaturation (two more than in **1**).

Comparison of NMR data and molecular weight with **1** indicate the presence of an additional residue, namely 3-methylpent-2-enoic acid.

^{1}H NMR spectrum showed four new signals not present in that of **1**, a triplet corresponding to H-11 at δ_H 4.23 (2H, ^3J =6.5 Hz) as well as a doublet of triplet integrated as two protons H-12 at δ_H 2.48 (^3J =6.5 and ^4J = 0.6 Hz) and a methyl group building a doublet at δ_H 2.16 (J =1.3Hz) in addition to a broad doublet at δ_H 5.70 (1H; J =1.1Hz). The latter two signals correspond respectively to a methyl-group (CH_3-13) and H-14, both setting on double-bond and showing a mutual correlation in the ^{1}H-^{1}H COSY spectrum. The second spin-system connects H-11 to H-12.

HMBC correlations (Fig. 3.1.5.1) from H-11 (δ_H 4.23) to C-10 (δ_C 63.2) and to C-12 (δ_C 40.5) show that the 3-methylhex-2-enoic acid residue is connected to the rest of the molecule through an ester bond. The relative stereochemistry of the double bond was deduced as *E* from the observation of NOE correlation between H-12/H-14 present in the ROESY spectrum (Fig. 3.5. Compound **5** is a new natural product to which the trivial name farinomalein E was given.

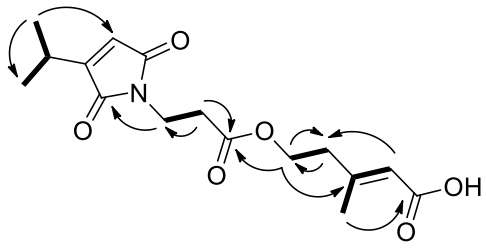

Fig. 3.5.: ^{1}H-^{1}H COSY and HMBC key correlations of compound **5.**

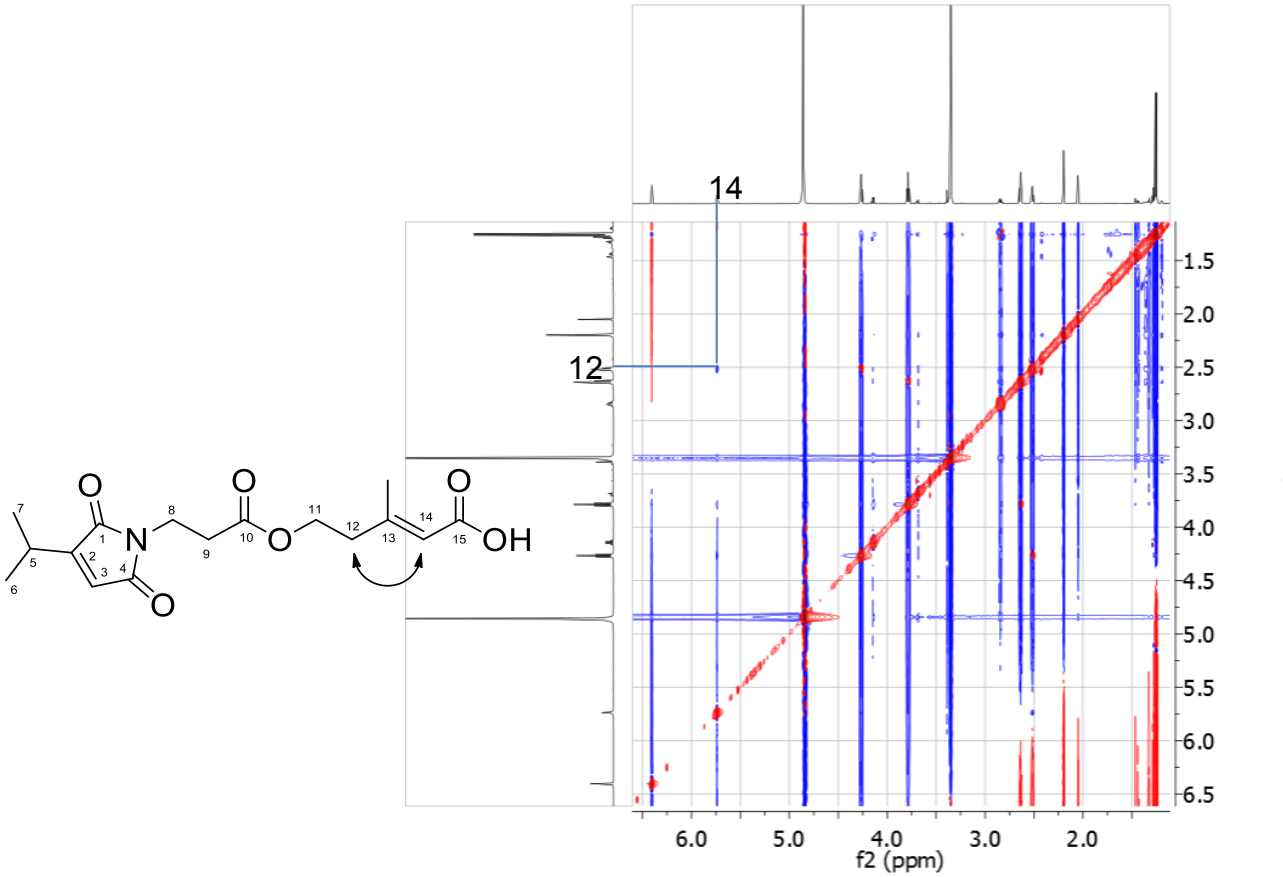

Fig. 3.5.: 2D ROESY spectrum and key correlations of compound **5**.

Table 3.5.: NMR spectroscopic data of **5** at 500MHz (^{1}H) and 125 MHz (^{13}C) in MeOH-d_4.

Position	5	
	δ_H (mult.; *J* in Hz)	δ_C
1		172.2 C
2		156.7 C
3	6.26 (d; 1.6)	125.9 CH
4		172.6 C
5	2.80 (d×sep.; 1.6, 6.8)	27.0 CH
6	1.21 (d; 6.9)	21.1 CH_3
7	1.21 (d; 6.9)	21.1 CH_3
8	3.75 (t; 6.9)	34.7 CH_2
9	2.60 (t; 6.8)	34.0 CH_2
10		172.2 C
11	4.23 (t; 6.5)	63.2 CH_2
12	2.48 (t; 6,5)	40.5 CH_2
13		156.9 C
14	5.70 (d; 1.1)	118.9 CH
		169.7 C
13-Me	2.16 (d; 1.3)	18.7 CH_3

3.6. 5,7-Dihydroxy-3-methylisoindolin-1-one (compound 6, new)

(*R*)-5,7-Dihydroxy-3-methylisoindolin-1-one	
Synonym(s)	
Biological Source	AMO3-2 (unidentifiable fungus)
Sample Code	MV8E1
Sample Amount	6.1 mg
Molecular Formula	$C_9H_9NO_3$
Molecular Weight	179 g/mol
Solubility	MeOH
Physical Description	Pale red oil
$[\alpha]^{20}_D$	+18.1 (*c* 0.1, MeOH)
HPLC Retention Time	9.80 min (standard gradient)

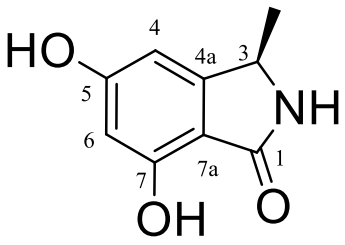

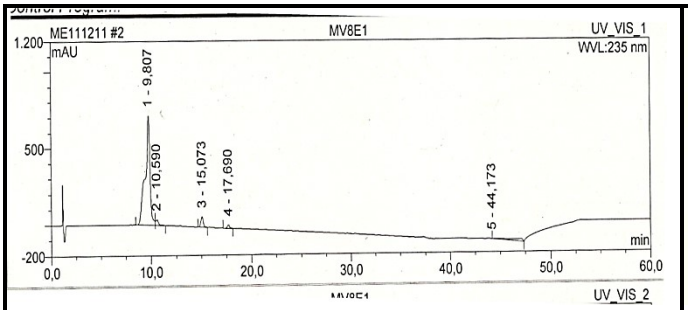

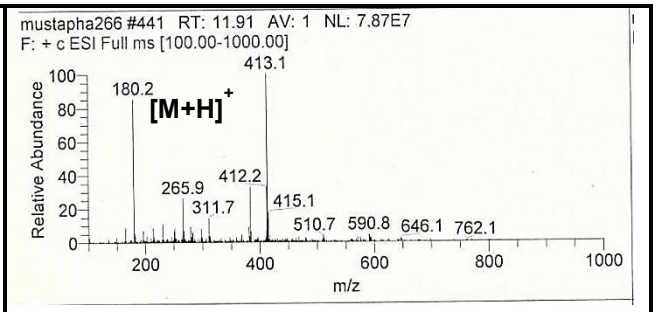

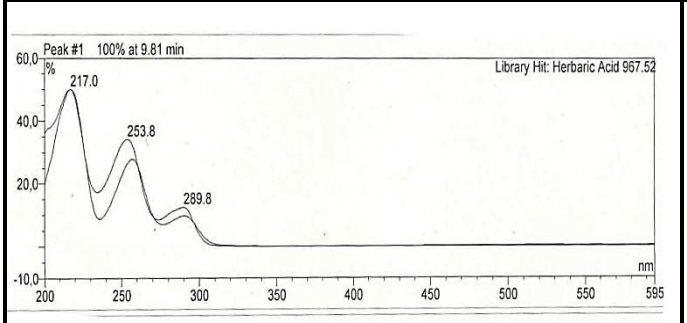

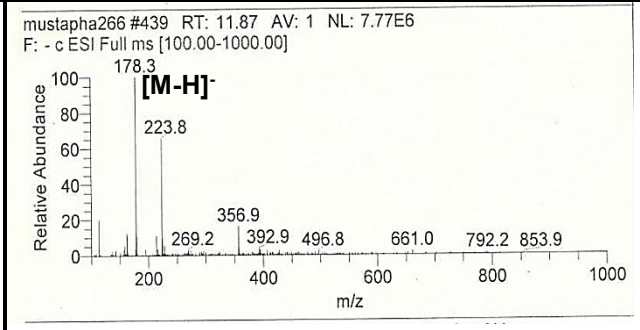

Compound **6** was obtained from the EtOAc extract of the unidentifiable strain AMO 3-2. It was obtained as pale red oil (6 mg), its UV spectrum showed maximum absorption at 217.0, 253.8 and 289.8 nm. The molecular weight of **6** was established as 179 g/mol. This was deduced from ESI-MS analysis, where a molecular ion peak at *m*/*z* 180.2 $[M+H]^+$ upon positive ionization and a molecular ion peak at *m*/*z* 178.3 $[M-H]^-$ upon negative ionization was observed. The molecular formula of **6** was determined by HRESIMS as $C_9H_9NO_3$ based on the prominent signal at *m*/*z* 202.0477 $[M+Na]^+$ (calc. for $C_9H_9NO_3Na$ 202.0475) indicating six degrees of unsaturation.

^1H NMR data (Table 3.1.6) showed four signals: two broad singlets corresponding to two aromatic protons setting in meta position (H-6 and H-4) at δ_H 6.22 and δ_H 6.37, the other two signals correspond to a methyl group (CH_3-3) at δ_H 1.39 (d, *J* = 6.7 Hz) and their vicinal proton H-3 at δ_H 4.53 (q, *J* = 6.7 Hz). When measuring in DMSO-d_6 three exchangeable protons were observed at δ_H 8.10 (NH-2), 9.24 (OH-5) and 10.01 (OH-7). ^1H-^1H COSY spectrum showed a correlation between H-4 and H-6 as well as between CH_3-3 and H-3.

The ^{13}C NMR spectrum of **6** exhibited nine signals, which were assigned from a DEPT-135 experiment to five quaternary carbons (including one carbonyl δ_C 173.2, and four olefinic carbons), three methine carbons (two of which are olefinic carbons) and one methyl carbon. These signals were indicative of the presence of a tetrasubstituted benzene ring. This substructure in addition to the carbonyl group accounts for five degrees of unsaturation in the molecule, thus the remaining one could only result from a ring. The above moieties were linked together by analysis of ^1H-^1H COSY, and HMBC correlations (Fig.3.6). The absolute stereochemistry of **6** was deduced by comparison of the specific optical rotation value with that of the similar compound (Chen, 2004) [**6**: $[\alpha]^{20}_D$ +18.1 (*c* 0.1, MeOH); (*R*)-methyl-2,3-dihydro-1*H*-isoindolin-1-one: $[\alpha]^{20}_D$ +39.1 (*c* 1.0, MeOH)]. Therefore, compound **6** was identified as (*R*)-5,7-dihydroxy-3-methylisoindolin-1-one.

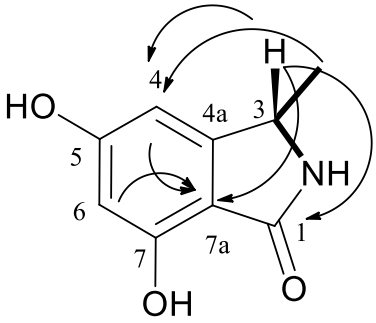

Fig. 3.6.: Key ^{1}H-^{1}H COSY and HMBC (H→C) correlations of compound **6.**

Table 3.6.: NMR spectroscopic data of **6** at 600 MHz (^{1}H) and 150 (^{13}C) MHz

Position	$\delta_H{}^a$ (mult.; *J* in Hz)	$\delta_H{}^b$ (mult.; *J* in Hz)	$\delta_C{}^b$	HMBC^a
1			173.2 C	
2	8.10 (s)			3, 4a, 7a
3	4.42 (q; 6.7)	4.53 (q, 6.7)	54.2 CH	3-CH_3, 4a
4	6.32 (br. s)	6.37 (br. s)	102.2 CH	3, 6, 7a
4a			154.1 C	
5	9.24 (br. s)		158.2 C	
6	6.18 (br. s)	6.22 (br. s)	102.4 CH	4, 5, 7a, 7
7	10.01 (br. s)		164.8 C	
7a			109.6 C	
3-CH_3	1.27 (d; 6.7)	1.39 (d, 6.7)	20.6 CH_3	3, 4a

[a] measured in DMSO-d_6

[b] measured in MeOH-d_4

3.7. *p*-hydroxyphenylacetic acid (compound 7, known)

2-(4-hydroxyphenyl)acetic acid	
Synonym(s)	*p*-hydroxyphenylacetic acid
Biological Source	AMO3-2 (unidentifiable fungus)
Sample Code	MV6E91
Sample Amount	9 mg
Molecular Formula	$C_8H_8NO_3$
Molecular Weight	152 g/mol
Solubility	MeOH
Physical Description	Pale brown oil
HPLC Retention Time	9.14 min (standard gradient)

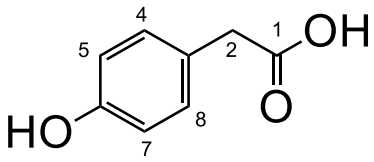

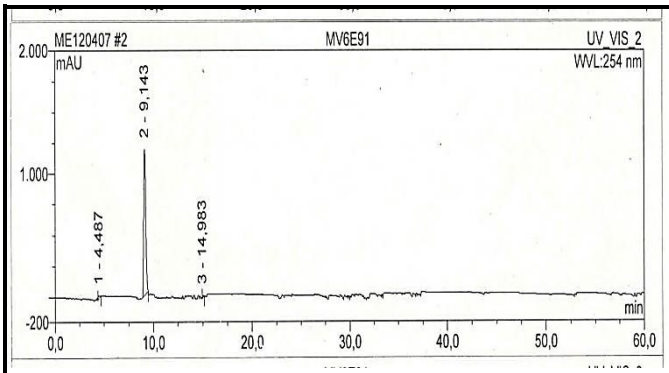

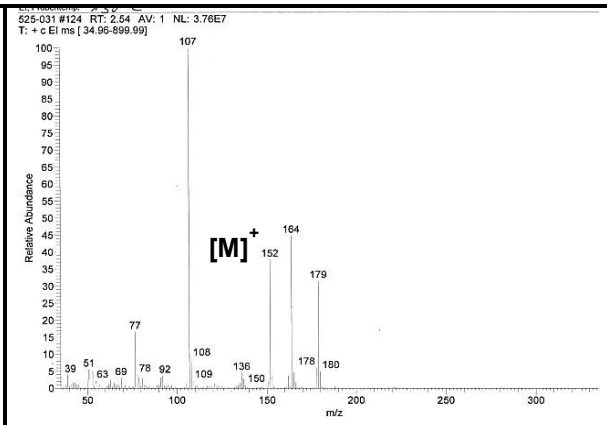

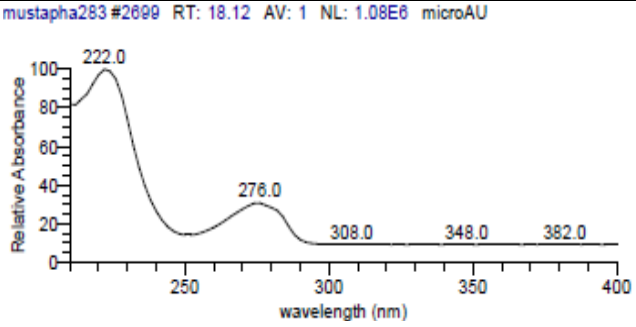

Compound **7** was isolated from the EtOAc extract of rice cultures of the isolate AMO 3-2 together with compound **6** as pale red oil in inseparable mixture (9 mg together with **6**). EI-MS showed molecular ion peak at *m/z* 152 $[M]^+$ (base peak), indicating a molecular weight of 152 g/mol.

The ^{1}H NMR-spectrum (in MeOH-d_4) showed, in addition to the signals of compound **6**, other signals attributed to: two pairs of equivalent aromatic protons as doublet signals, corresponding to H-5/H-7 at δ_H 6.72 (d, J = 8.4 Hz) and H-4/H-8 at δ_H 7.08 (d, J = 8.4 Hz). A singlet at 3.48ppm, which corresponds to CH_2-2, was also observed. The COSY spectrum showed correlations from H-4 to H-5 and from H-7 to H-8 as well as a long correlation from H-2 to H-4 and H-8.

The ^{13}C spectrum exhibited six signals (in addition to those of compound **6**), including a CH_2-2 at δ_C 41.3, two equivalent carbons at δ_C 116.4 (CH-5 and CH-7) and two others at δ_C 131.5 (CH-4 and CH-8), as well as carbonyl carbon at δ_C 176.5 and the two quaternary carbons C-3 and C-6 at δ_C 127.0 and 165.0, respectively. The structure of **7** was confirmed by HMBC experiment. *p*-hydroxyphenylacetic acid was reported to enhance the growth of red alga *Porphyra tenera conchocelis.* (Fries & Iwasaki 1977)

Table 3.7.: NMR spectroscopic data of **7** at 600MHz (^{1}H) and 150 MHz (^{13}C) in MeOH-d_4

Position	**MV6E91**		
	δ_H	δ_C	HMBC
1		176.5 C	
2	3.48	41.3 CH_2	C1; C3; C4
3		127.0 C	
4	7.08 (d, 8.4)	131.5 CH	C1; C2; C6; C7; C8
5	6.72 (d, 8.4)	116.4 CH	C3; C4
6		165.0 C	
7	6.72 (d, 8.4)	116.4 CH	C3; C8
8	7.08 (d, 8.4)	131.5 CH	C1; C2; C4; C6; C7

3.8. 7-Methyl-1,3-dihydroisobenzofuran-4,5,6-triol (compound 8, known)

7-Methyl-1,3-dihydroisobenzofuran-4,5,6-triol	
Synonym(s)	Epicoccine
Biological Source	*Epicoccum nigrum* (BSL1W)
Sample Code	B40E5-3
Sample Amount	200 mg
Molecular Formula	$C_9H_{10}O_4$
Molecular Weight	182 g/mol
Solubility	MeOH
Physical Description	Pale yellow powder
HPLC Retention Time	13.41 min (standard gradient)

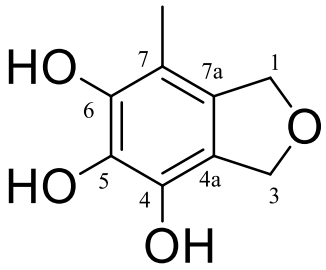

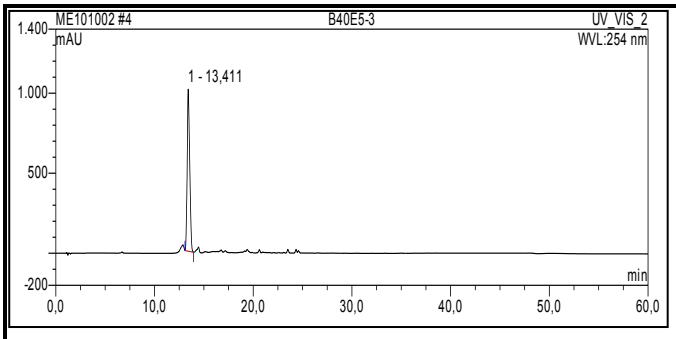

(+)-ESI-MS: no ionization

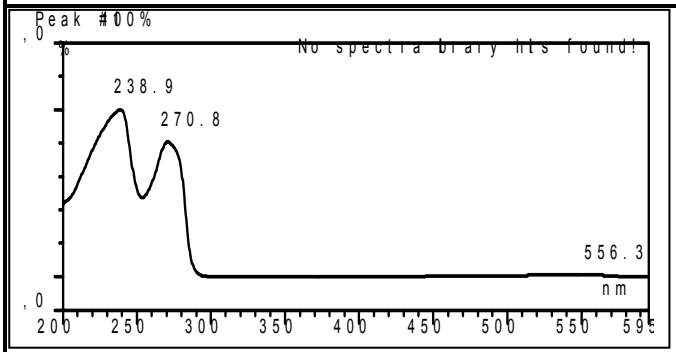

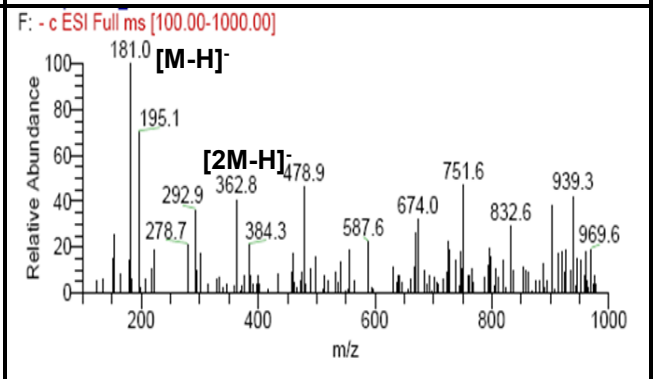

Compound **8** was isolated as a pale yellow powder (200 mg). It revealed UV absorption at λ_{max} (MeOH) 238.9 and 270.8 nm. According to the pseudo molecular ion peaks observed at *m/z* 181.0 $[M-H]^-$ (base peak) and 362.8 $[2M-H]^-$ in the negative ionization mode ESI-MS, compound **8** should have a molecular weight of 182 g/mol. The ^{13}C NMR spectrum of **8** showed nine carbons, divided by DEPT 135 into: six quarternary, two methylene and a methyl groups (Table 3.8).

Furthermore, ^1H-NMR spectrum (DMSO-d_6) of **8** displayed three aromatic hydroxyl groups at δ_H 8.06 (OH-6), δ_H 8.09 (OH-5) and δ_H 8.49 ppm (OH-4) in addition to an aromatic methyl group at δ_H 1.91 (CH_3-7) and two CH_2 signals attributed to the oxymethylene protons at δ_H 4.84 (H-1) and δ_H 4.88 (H-3).

Detailed analysis of ^1H-^1H COSY and HMBC spectra and comparison of the NMR data with the literature (Ishikawa et *al*. 1996) led to a conclusion that **8** is the known compound 7-methyl-1,3-dihydroisobenzofuran-4,5,6-triol, which was isolated from *Apergillus terreus* (Ishikawa et *al*. 1996) and has been reported also as secondary metabolite of *Epicoccum nigrum* (Hilaire et *al.*2008).

Table. 3.8.: Comparison of the ^1H NMR data of **8** (in DMSO-d_6) with literature.

position	δ_H (*J* Hz) *B40E5-3*	δ_H (*J*Hz) Literature*
1	4.84 (2H)	4.83 (2H)
3	4.88 (2H)	4.87 (2H)
4(OH)	8.49 (1H)	8.45 (1H)
5(OH)	8.09 (1H)	8.06 (1H)
6(OH)	8.06 (1H)	8.02 (1H)
7-Me	1.91 (3H)	1.91 (3H)

*Ishikawa et *al*. 1996

3.9. 5-Methoxy-7-methyl-1,3-dihydroisobenzofuran-4,6-diol (compound 9, known)

5-Methoxy-7-methyl-1,3-dihydroisobenzofuran-4,6-diol	
Synonym(s)	
Biological Source	*Epicoccum nigrum* (BSL1W)
Sample Code	B40E4-6
Sample Amount	9 mg
Molecular Formula	$C_{10}H_{12}O_4$
Molecular Weight	196 g/mol
Solubility	MeOH
Physical Description	Pale yellow powder
HPLC Retention Time	17.81 min (standard gradient)

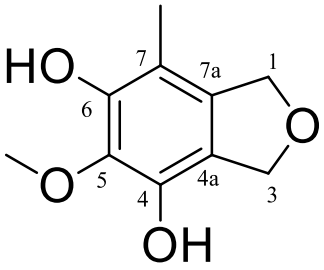

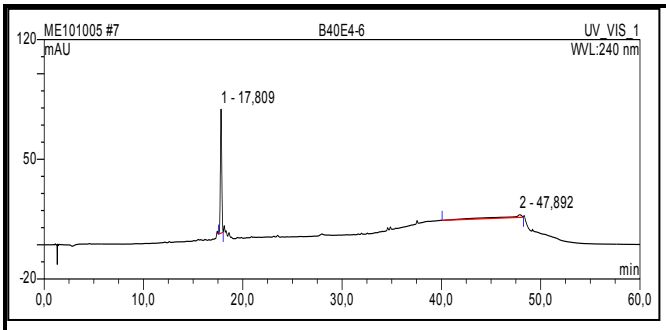

(+)-ESI-MS: no ionization

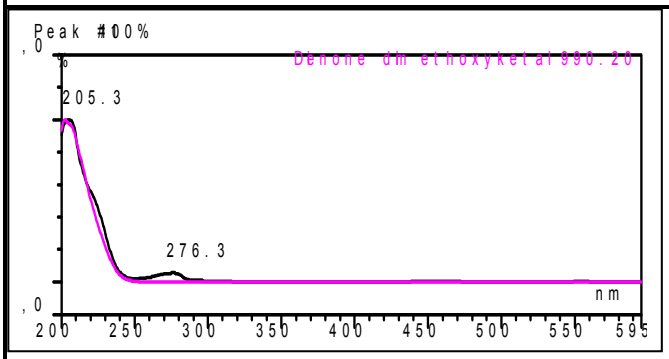

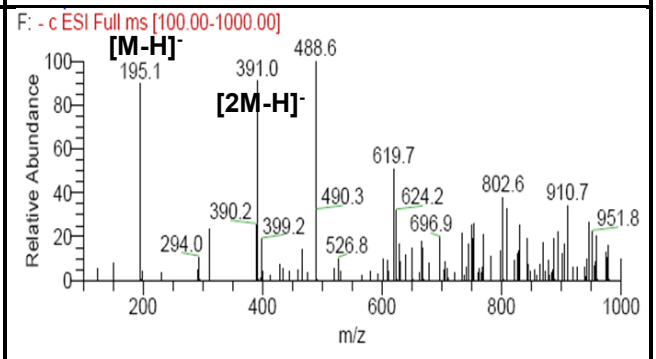

Compound **9** was isolated from the EtOAc extract of the rice culture of *Epicoccum nigrum* as pale yellow powder (9 mg). It exhibited UV absorption at λ_{max} (MeOH) 205.3nm. Only negative ESI-MS showed ionization, pseudo molecular ion peaks at *m/z* 195.1 $[M-H]^-$ (base peak) and *m/z* 391.0 $[2M-H]^-$ indicate a molecular weight of 196 g/mol.

^1H NMR and ^{13}C NMR data of **9** (Table 3.1.9) were closely similar to those of **8**. It revealed a new signal attributable to a methoxy group at δ_H 3.63 / δ_C 60.1 (OCH_3-5), while a hydroxyl group signal is not present. From the difference in the molecular weight to **8** (14 amu) and comparison of the NMR data, we came to the conclusion that **9** is a methylated derivative of **8**. The compound was thus identified as the known 5-methoxy-7-methyl-1,3-dihydroisobenzofuran-4,6-diol, which was confirmed by comparison of UV, ^1H NMR and mass spectral data with those published by Lee *et al*. (2007).

Table. 3.9.: Comparison of the ^1H-NMR data of **8** with literature.

Position	δ_C **9**[§]	δ_C Literature*
1	72.6	73.5
3	71.7	72.1
4	141.8	140.8
4a	115.5	116.1
5	135.3	134.6
5-OMe	60.1	61.0
6	147.8	146.7
7	108.3	109.2
7a	133.5	134.1
7-Me	12.0	11.7

[§]Measured in DMSO-d_6 at 100 MHz

*Measured in 10:1 $CDCl_3$-CD_3OD at 100 MHz (Lee *et al*. 2007)

3.10. Epicoccone A (compound 10, known)

4,5,6-Trihydroxy-7-methylisobenzofuran-1(3H)-one	
Synonym(s)	Epicoccone A
Biological Source	*Epicoccum nigrum* (BSL1W)
Sample Code	B50-5-3II
Sample Amount	6 mg
Molecular Formula	$C_9H_{10}O_5$
Molecular Weight	196 g/mol
Solubility	MeOH
Physical Description	Brawn-yellow powder
HPLC Retention Time	14.46 min (standard gradient)

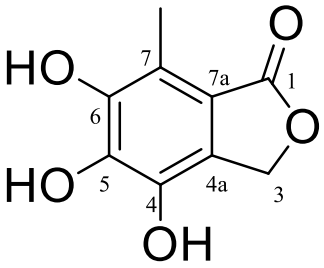

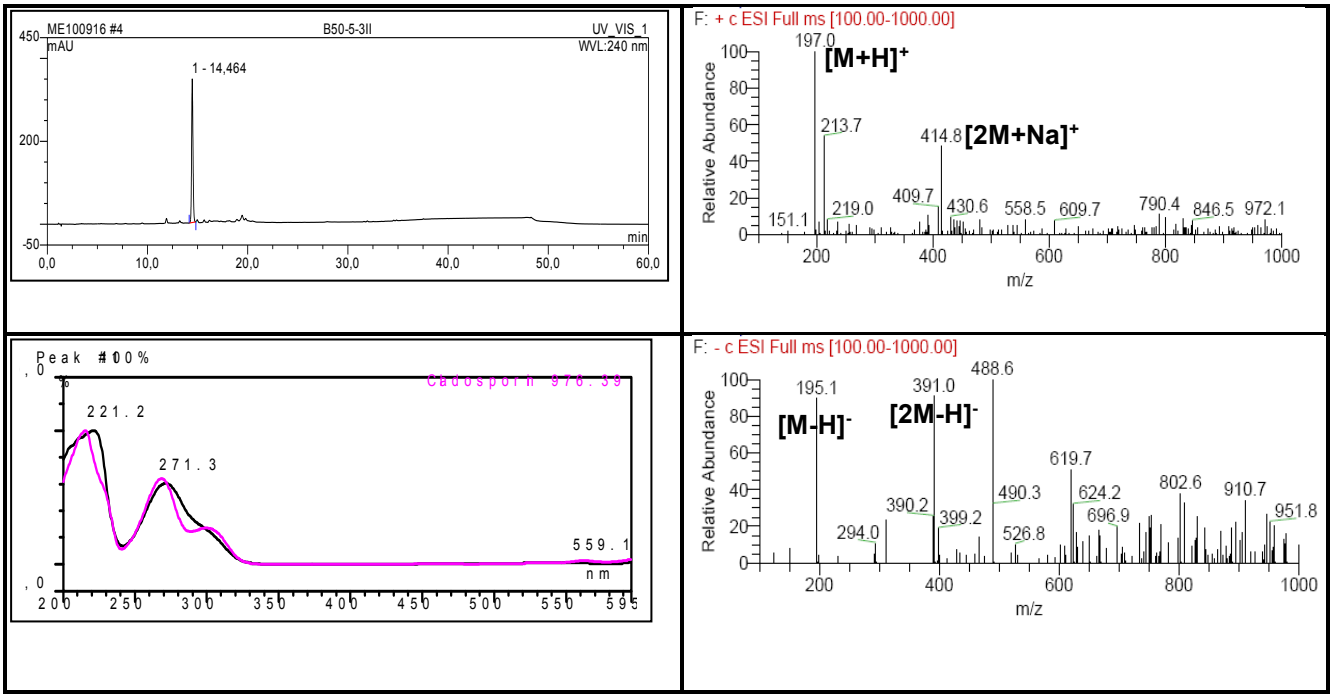

Epicoccone A (**10**) was isolated from the EtOAc extract of rice cultures of *Epicoccum nigrum* as a brown-yellow powder (6 mg). It showed UV absorption at λ_{max} (MeOH) 221.2 and 271.3 nm and its positive molecular ion peaks at *m/z* 197.0 $[M+H]^+$ and 414.8 $[2M+Na]^+$, when the negative ESI-MS exhibited the molecular ion peaks at *m/z* 195.1 $[M-H]^-$ and *m/z* 391.0 $[M-H]^-$, all of this indicate a molecular weight of 196 g/mol, with an increase of 14 amu compared to **8**. ^{1}H NMR spectrum of **10** (Table 3.10) was quite similar to that of **8**, indicating a structural resemblance between both compounds. Like compound **8**, the ^{1}H-NMR spectrum of **10** exhibited a methyl group at δ_H 2.31, three exchangeable hydroxyl groups at δ_H 8.70, 9.32 and 9.42 but only one methylene group at δ_H 5.07. In ^{13}C spectrum a new signal referring to a carbonyl group at δ_C 170.3 replaced one of the two oxymethylene signals present in **8**. Position of the carbonyl group (C-1) was confirmed by HMBC since the correlation between H-3 and C-7a (δ_C 111.3) is stronger than correlation with C-4a (δ_C 125.1) and there is no correlation between H-3 and C-7 The structure of **10** was determined as 4,5,6-trihydroxy-7-methylisobenzofuran-1(3*H*)-one on the basis of HMBC correlations and by comparison with the reported data (Abdel-Lateff *et al*. 2003).

Table. 3.10.: Comparison of the ^{13}C NMR data of **10** with literature.

	δ_c	
Position	***Literature**[a]*	**10**[b]
1	174.6	170.3
3	68.0	65.3
4	138.1	135.7
4a	127.9	125.1
5	141.5	138.7
6	146.3	143.8
7	118.3	114.8
7a	113.9	111.3
7-Me	9.7	8.4

[a] measured in MeOH-d_4 at 75.5 MHz

[b] measured in DMSO-d_6 at 125 MHz

*Abdel-Lateff & al. 2003

3.11. Epicoccone B (compound 11, known)

5,6,7-Trihydroxy-4-methylisobenzofuran-1(3*H*)-one	
Synonym(s)	Epicoccone B
Biological Source	*Epicoccum nigrum* (BSL1W)
Sample Code	50E215-2
Sample Amount	8 mg
Molecular Formula	$C_9H_8O_5$
Molecular Weight	196 g/mol
Solubility	MeOH
Physical Description	Brawn-yellow powder
HPLC Retention Time	16.67 min (standard gradient)

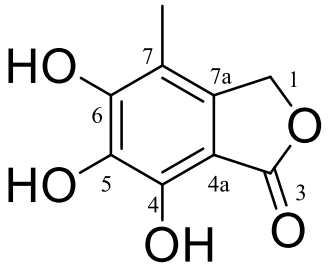

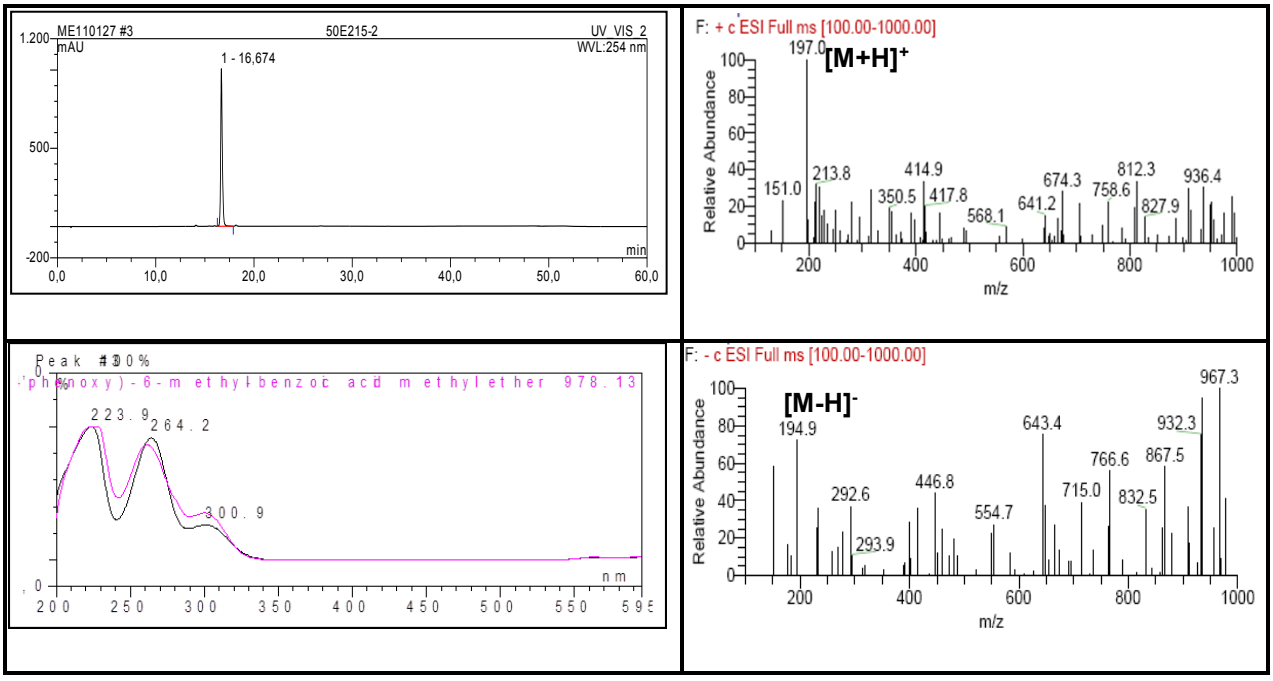

Epicoccone B (**11**) was isolated from the EtOAc extract of rice cultures of *Epicoccum nigrum* as a brown powder (8 mg). It showed UV absorbances at λ_{max} (MeOH) 223.9 and 264.2 nm and its positive and negative ESI-MS showed pseudo molecular ion peaks at *m/z* 197.0 $[M+H]^+$ and at *m/z* 195.1 $[M-H]^-$ indicating a molecular weight of 196 g/mol. ^{1}H NMR spectrum of **11** (Table 3.11.) was quite similar to that of **10**, indicating that both compounds might be isomers.

Like compound **10**, ^{1}H-NMR spectrum exhibited a methyl group at δ_H 2.31 ppm, three hydroxyl groups at δ_H 8.70, 9.32 and 9.42 but only one methylene group at δ_H 5.07. In the ^{13}C NMR spectrum of **11** a new signal referring to a carbonyl group at δ_C 170.3 replaced one of the two oxymethylene signals presented in **8**. The position of the carbonyl group (C-1) was confirmed by HMBC spectrum since the correlation between the protons H-1 and C-7 (δ_C 109.1) is stronger than correlation with C-4(δ_C 143.0), which is very weak. The structure of **11** was determined as 5,6,7-trihydroxy-4-methylisobenzofuran-1(3*H*)-one on the basis of HMBC correlations and confirmed by comparison with the reported data (Hilair *et al*. 2008).

Table. 3.11.: Comparison of the ^{13}C NMR data of **11** with literature.

	δ_C	
Position	***Literature**[a]*	**10**[b]
1	67.6	67.7
3	169.8	169.8
4	143.0	143.1
4a	102.7	102.7
5	132.8	132.8
6	151.1	151.2
7	109.1	109.1
7a	138.0	138.1
7-Me	10.7	10.7

[a] measured in MeOH-d_4 at 75.5 MHz

[b] measured in MeOH-d_4 at 125 MHz

* Hilair et al. 2008

3.12. Epicoccone C (compound 12, new)

5,6,7-Trihydroxy-3-methoxy-4-methylisobenzofuran-1(3*H*)-one	
Synonym(s)	Epicoccone C
Biological Source	*Epicoccum nigrum* (BSL1W)
Sample Code	50E215-3
Sample Amount	15 mg
Molecular Formula	$C_{10}H_{10}NO_6$
Molecular Weight	226 g/mol
Solubility	MeOH
Physical Description	black amorphous solid
$[\alpha]^{20}_D$	+ 1.0 (*c* 0.1, MeOH)
HPLC Retention Time	18.13 min (standard gradient)

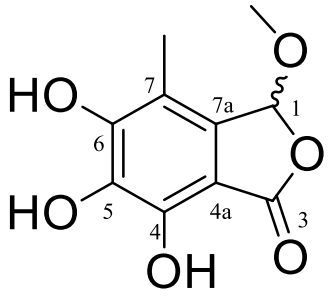

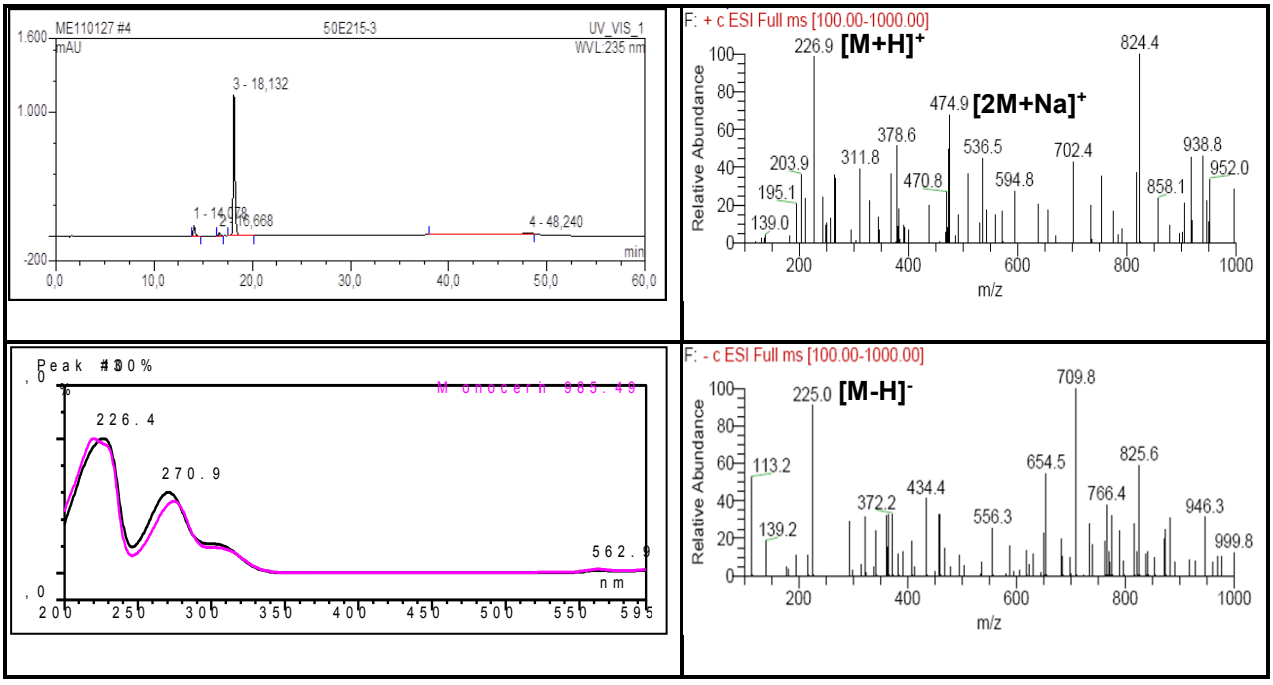

Compound **12** was isolated as a black amorphous solid. A molecular formula of $C_{10}H_{10}O_6$ was established based on HRESIMS, corresponding to 6 degrees of unsaturation. ^{1}H NMR spectrum of this compound showed three signals (in MeOH) attributable to a methyl group at δ_H 2.13 (CH_3-7), a methoxy group at δ_H 3.49 (OCH_3-1) and an oxymethine proton at δ_H 6.27 (H-1). Analysis of the ^{13}C and DEPT spectra revealed the presence of seven sp^2-hybridized carbons, including a carbonyl group at δ_C 167.3 and six carbons belonging to a fully substituted benzene ring, in which three of them bounded to the hydroxyl group at δ_C 151.2, 142.9 and 134.5 and one at δ_C 112.2 bounded to a methyl group. The NMR data of **12** showed big similarity to epicoccone B. The only difference is the methoxy group setting in position 1, which is in accordance with the difference in the molecular weight (30 amu). The position of the methoxy group was confirmed by the HMBC correlation between the methoxy group to C-1. The $[\alpha]^{20}_D$ + 1.0 (*c* 0.1, MeOH) value indicate this compound to be racemate. Compound **12** was determined as the new secondary metabolite: 5,6,7-trihydroxy-3-methoxy-4-methylisobenzofuran-1(3*H*)-one and was given the trivial name epicoccone C.

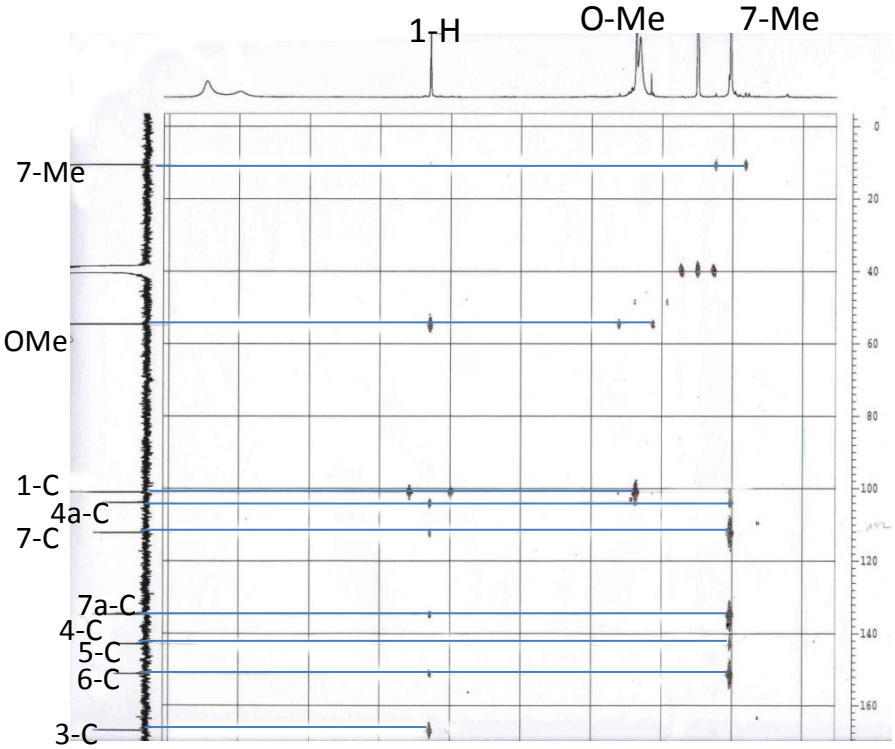

Fig. 3.12.: HMBC spectrum correlations of compound **12** (in DMSO-d_6 at 600MHz).

Table. 3.12: NMR spectroscopic data of **12** at 600 MHz (^{1}H) and 150 MHz (^{13}C) in MeOH-d_4.

Position	**12**			
	δ_H	δ_C	^{1}H-^{1}H COSY	HMBC Correlations (H → C #)
1	6.27	101.0 (CH)	CH_3-7	OCH_3-1, 4a, 7, 7a, 6 (w), 3
3		167.3 (C)		
4		134.5 (C)		
4a		103.9 (C)		
5		142.9 (C)		
6		151.2 (C)		
7		112.2 (C)		
7a		134.8 (C)		
OCH_3-1	3.49	54.6 (CH_3)		1
CH_3-7	2.13	10.6 (CH_3)	1	4a (w), 7, 4(w), 7a, 5 (w), 6

(w) Weak correlation

3.13. Epicoccone D (compound 13, new)

5,6,7-Trihydroxy-3-methoxy-4-methylisobenzofuran-1(3H)-one	
Synonym(s)	Epicoccone D
Biological Source	*Epicoccum nigrum* (BSL1W)
Sample Code	60E4A233
Sample Amount	9 mg
Molecular Formula	$C_{10}H_{10}NO_6$
Molecular Weight	226 g/mol
Solubility	MeOH
Physical Description	Yellow amorphous solid
$[\alpha]^{20}_D$	+ 0.8 (*c* 0.1, MeOH)
HPLC Retention Time	15.63 min (standard gradient)

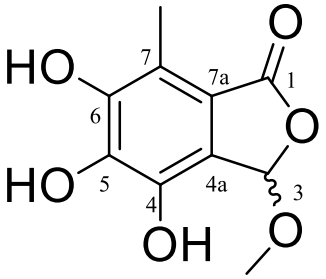

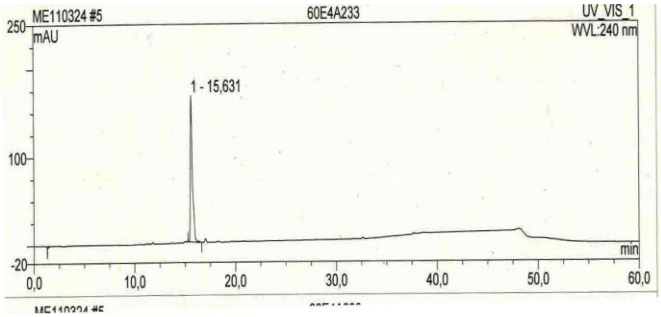

(+)-ESI-MS: no ionization

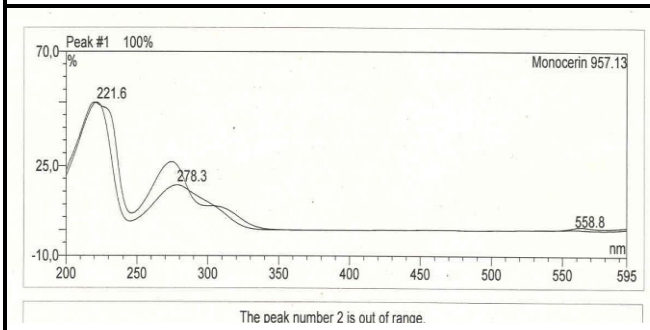

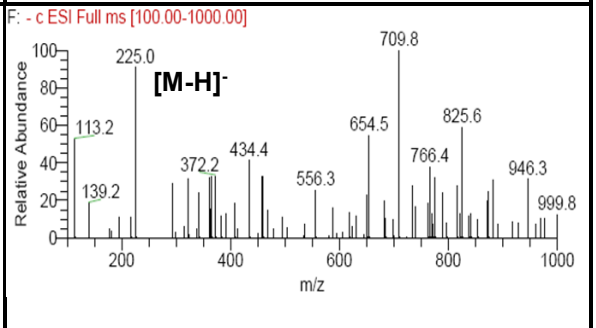

Compound **13** was isolated as yellow amorphous solid. It showed the same molecular formula as compound **12**, namely $C_{10}H_{10}O_6$, which was established based on HRESIMS. ^{1}H NMR spectrum of this compound showed three signals (in MeOH-d_4) attributable to a methyl group at δ_H 2.40 (CH_3-7), a methoxy group at δ_H 3.47 (OCH_3-3) and an oxymethine proton at δ_H 6.26 (H-3). Its great similarity to **12**, indicate that both compound could be isomers.

Analysis of ^{13}C, DEPT and HMBC spectra revealed that **13** is the isomer of **12.** This explains why CH_3-7 is now more downfield in **13** (near to the keto group). HMBC correlations from CH_3-7 to the carbon (C-7a) and from H-3 to C-4 confirm the position of both of them. The $[\alpha]^{20}_D$ + 0.8 (*c* 0.1, MeOH) value indicate this compound to be racemate. Compound **13** was determined as the new secondary metabolite 4,5,6-trihydroxy-3-methoxy-7-methylisobenzofuran-1(3*H*)-one and was given the trivial name epicoccone D.

Table. 3.13.: Comparison of NMR spectroscopic data of **13** and **12**.

Position	**13**[§]		**12***	
	δ_H	δ_C	δ_H	δ_C
1		176.5	6.27	101.0 (CH_2)
3	6.26	102.2		167.3 (C)
4		141.6		134.5 (C)
4a		124.7		103.9 (C)
5		140.1		142.9 (C)
6		147.8		151.2 (C)
7		118.8		112.2 (C)
7a		115.7		134.8 (C)
OCH_3-1	3.47	55.6	3.49	54.6 (CH_3)
CH_3-7	2.40	10.0	2.13	10.6 (CH_3)

[§]At 500 MHz (^{1}H) and 100 MHz (^{13}C) in MeOH-d_4.

*At 600 MHz (^{1}H) and 150 MHz (^{13}C) in MeOH-d_4.

3.14. 2,3,4-Trihydroxy-6-(methoxymethyl)-5-methylbenzaldehyde (compound 14, new)

2,3,4-Trihydroxy-6-(methoxymethyl)-5-methylbenzaldehyde	
Synonym(s)	
Biological Source	*Epicoccum nigrum* (BSL1W)
Sample Code	40E49-1
Sample Amount	8.1 mg
Molecular Formula	$C_{10}H_{12}O_5$
Molecular Weight	212 g/mol
Solubility	MeOH
Physical Description	Brown solid
HPLC Retention Time	18.62 min (standard gradient)

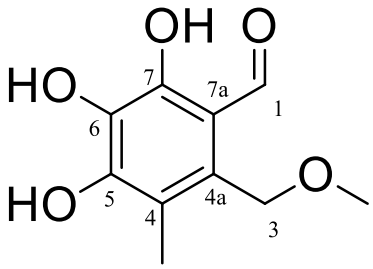

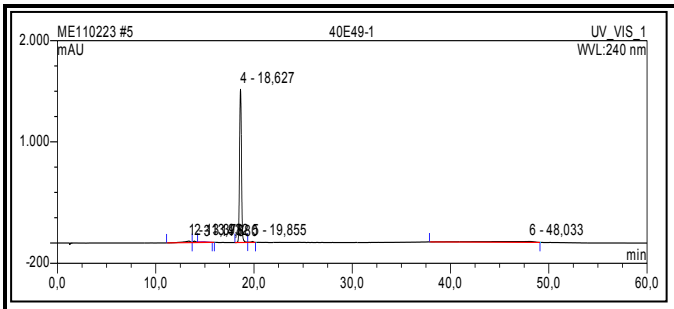

(+)-ESI-MS: no ionization

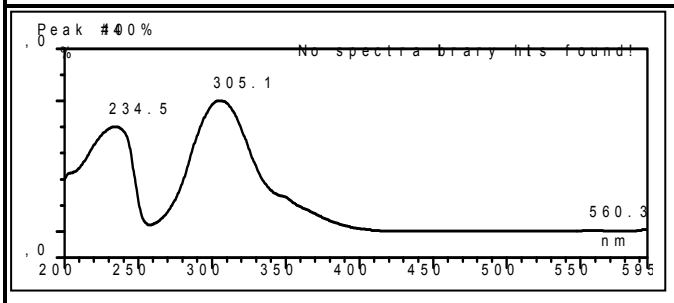

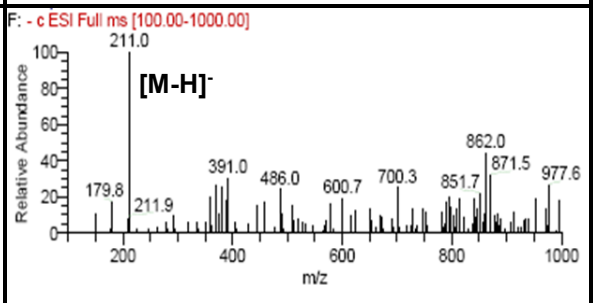

Compound **14** was isolated from the EtOAc extract of rice cultures of *Epicoccum nigrum* as a brown powder (8 mg). It showed UV absorption at 234.5 and 305.1 nm. Its molecular weight of 212 g/mol was obtained on the basis of the negative molecular ion peak at *m/z* 211.0 $[M-H]^-$. The molecular formula $C_{10}H_{12}O_5$ was deduced from HRESIMS measurement. The ^{13}C and DEPT 135 data, which showed 10 carbon signals including an aldehyde-group at δ_C 196.4, a methyl group at δ_C 10.9 (CH_3-4), a methoxy group at δ_C 58.2 (CH_3-3) , a methylene at δ_C 67.0 (CH_2-3) and 6 sp^2-hybridized carbons. HMBC correlations from OCH_3-3 to C-3 and from H-1 to C-7, C-7a and C-4a confirmed the positions of the methoxy group and aldehyde group, respectively. Compound **14** was determined as 2,3,4-trihydroxy-6-(methoxymethyl)-5-methylbenzaldehyde.

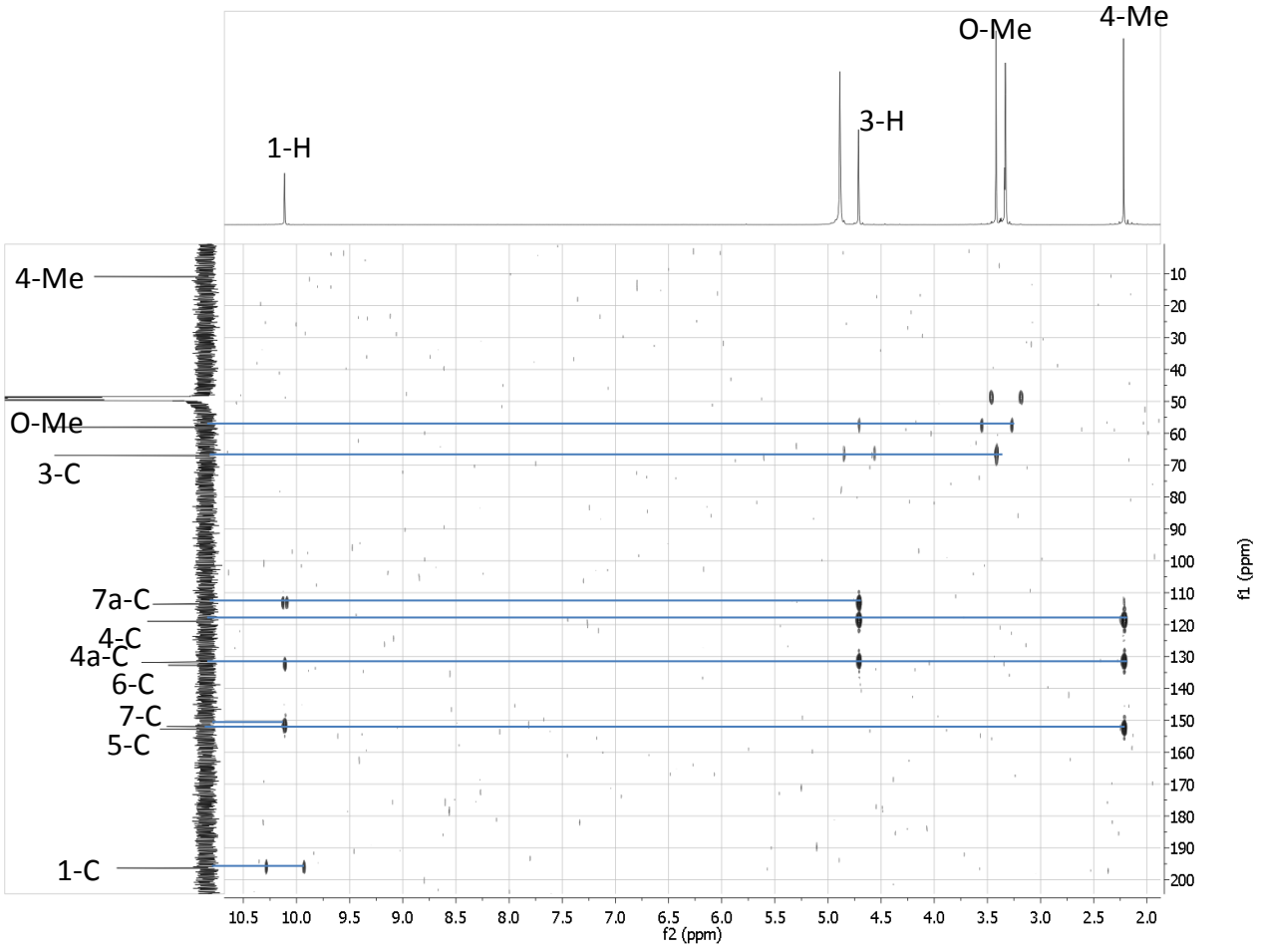

Fig. 3.14.: HMBC spectrum of compound **14** (in MeOH-d_4 at 500MHz).

Table. 3.14.: NMR spectroscopic data of **14** at 500 MHz (^{1}H) and 125 MHz (^{13}C) in MeOH-d_4.

Position	**13**		
	δ_H	δ_C	HMBC correlations (H → C)
1	10.10 (1H, s)	196.4 (CH)	7a, 4a, 7
3	4.70 (2H, s)	67.0 (CH_2)	7a, 4, 4a, 3-OMe
3-OMe	3.40 (3H, s)	58.2 (CH_3)	3
4		119.0 (C)	
4a		113.6 (C)	
5		152.8 (C)	
6		152.0 (C)	
7		132.8 (C)	
7a		131.9 (C)	
4-Me	2.20 (3H, s)	10.9 (CH_3)	4, 4a, 5

3.15. 5,6,7,9a-Tetrahydroxy-2,3,3a,8-tetramethyl-3a,4-dihydro-1H-cyclopenta[b]-naphthalene-1,9(9aH)-dione (compound 15, new)

5,6,7,9a-Tetrahydroxy-2,3,3a,8-tetramethyl-3a,4-dihydro-1*H*-cyclopenta[*b*]naphthalene-1,9(9a*H*)-dione	
Biological Source	*Epicoccum nigrum* (BSL1W)
Sample Code	50E31-4
Sample Amount	16.3 mg
Molecular Formula	$C_{17}H_{18}O_6$
Molecular Weight	318 g/mol
Solubility	MeOH
Physical Description	Brown- yellow solid
$[\alpha]^{20}_D$	+ 0.2 (*c* 0.1, MeOH)
HPLC Retention Time	17.37 min (standard gradient)

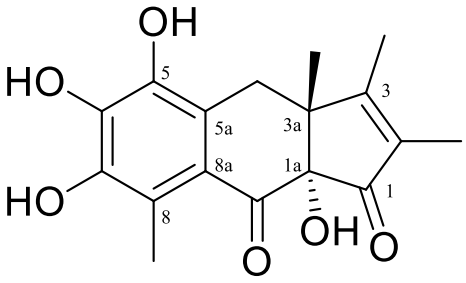

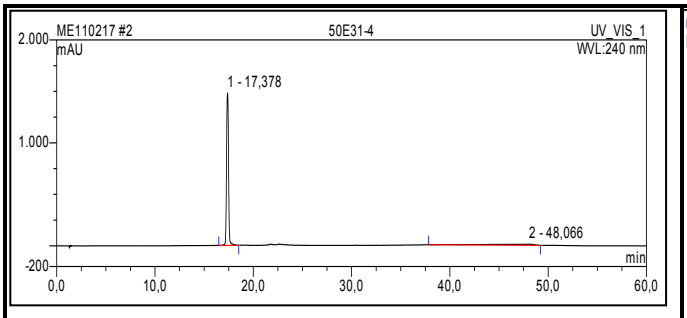

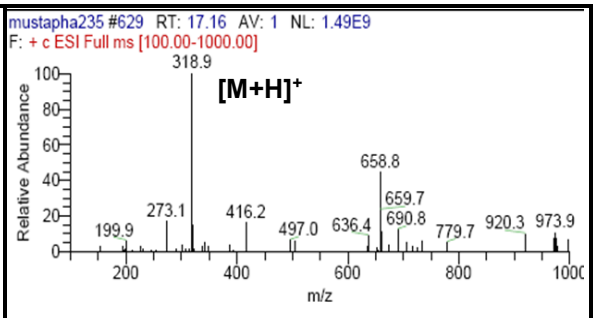

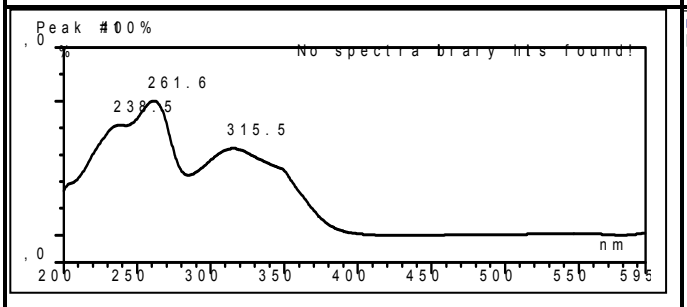

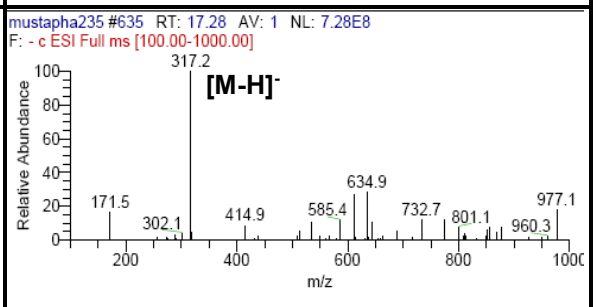

Compound (**15**) was isolated as a brown yellow solid (16 mg). This compound revealed UV absorbances at λ_{max} (MeOH) 238.5, 261.6 and 315 nm. Positive and negative ESI-MS showed pseudo molecular ion peaks at *m/z* 318.9 $[M+H]^+$ and 317.2 $[M-H]^-$ respectively, indicating a molecular weight of 318 g/mol. HRESIMS established a molecular formula of $C_{17}H_{18}O_6$ indicating nine degrees of unsaturation. ^{1}H NMR (MeOH-d_4) spectrum showed six signals attributable to four methyl groups, including two singlets at δ_H 1.29 (CH_3-3a) and at δ_H 2.08, two doublets at δ_H 1.52 (*J*= 0.7 Hz) and at δ_H 1.97 (*J*= 0.7 Hz), corresponding respectively to CH_3-2 and CH_3-3. In addition, ^{1}H NMR spectrum exhibited two doublets at δ_H 2.42 (*J*= 15.5 Hz) and at δ_H 3.43 (*J*= 15.5 Hz) referring to the two germinal protons at position 4. Analysis of ^{13}C NMR and DEPT 135 spectra confirmed the presence of one secondary and four primary carbons as well as twelve quaternary carbons, two of them can be attributed to keto groups (δ_C 197.2 and 204.7). Key HMBC correlations from the protons CH_3-8 (δ_H 2.08 ppm) to the keto C-9 (δ_C 197.2) as well as from H-4 to C-5 (δ_C 140.8) and to C-3 (δ_C 179.9) lead to identify Compound **15** as (3a*S*,9a*S*)-5,6,7,9a-tetrahydroxy-2,3,3a,8-tetramethyl-3a,4-dihydro-1*H*-cyclopenta[*b*]naphthalene-1,9(9a*H*)-dione. This was confirmed by 2D ROESY result while unambiguous 1D NOE spectra helped to establish the relative stereochemistry.

Table. 3.15.: NMR spectroscopic data of **15** at 600 MHz (^{1}H) and 150 MHz (^{13}C) in MeOH-d_4.

Position	δ_H mult. (*J* Hz)	δ_C	COSY	HMBC (H→C)	ROESY
1		204.7 (C)			
1a		89.2 (C)			
2		136.0 (C)			
2-Me	1.52 (3H,d, 0.7)	8.2 (CH_3)	3-Me	2-Me	2, 1, 3, 3a
3		179.9 (C)			
3a-Me	1.28	22.5 (CH_3)		3a-Me	3a, 4, 3, 1a, 5a
3a		39.1			
3-Me	1.97 (3H,d, 0.7)	12.2 (CH_3)	2-Me	3-Me	3, 3a, 2, 1
4a	2.42 (1H,d,15.5)	29.5 (CH_2)	4b	4	3a-Me, 3a, 1a, 5a, 5, 3
4b	3.43 (1H,d, 15.5)	29.2 (CH_2)	4a	4	3a-Me, 3a, 1a, 5a, 5, 3
5		140.8 (C)			
5a		121.5 (C)			
6		140.6 (C)			
7		143.9 (C)			
8		119.1 (C)			
8-Me	2.08	12.1 (CH_3)		8-Me	8, 8a, 7, 9
8a		123.3 (C)			
9		197.2 (C)			

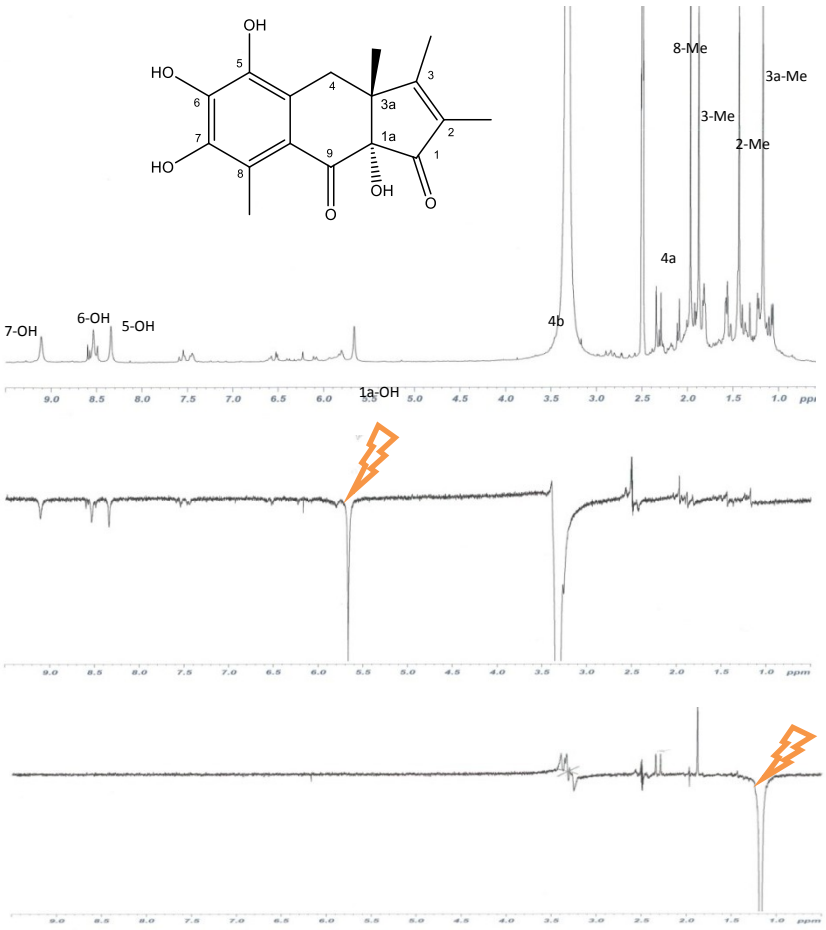

Fig. 3.15.: 1D NOE experiment for compound **15** (in DMSO-d_6 at 600MHz).

3.16. 3,4,8,9,10-Pentahydroxy-2,7-dimethyl-11-oxo-11,12-dihydro-6H-6,12-epoxydiben-zo[b,f]oxocine-1-carbaldehyde (compound 16, new)

3,4,8,9,10-Pentahydroxy-2,7-dimethyl-11-oxo-11,12-dihydro-6*H*-6,12-epoxydibenzo[*b*,*f*]oxocine-1-carbaldehyde	
Biological Source	*Epicoccum nigrum* (BSL1W)
Sample Code	40E5-41 and BS1-85-1
Sample Amount	16 mg
Molecular Formula	$C_{18}H_{14}O_9$
Molecular Weight	374 g/mol
Solubility	MeOH
Physical Description	Brawn solid
Optical rotation $[\alpha]^{20}_D$	1° (*c* 0.1, MeOH)
HPLC Retention Time	22.14 min (standard gradient)

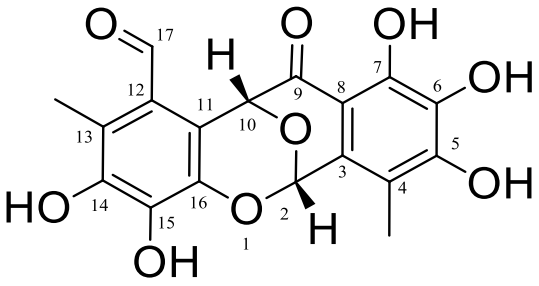

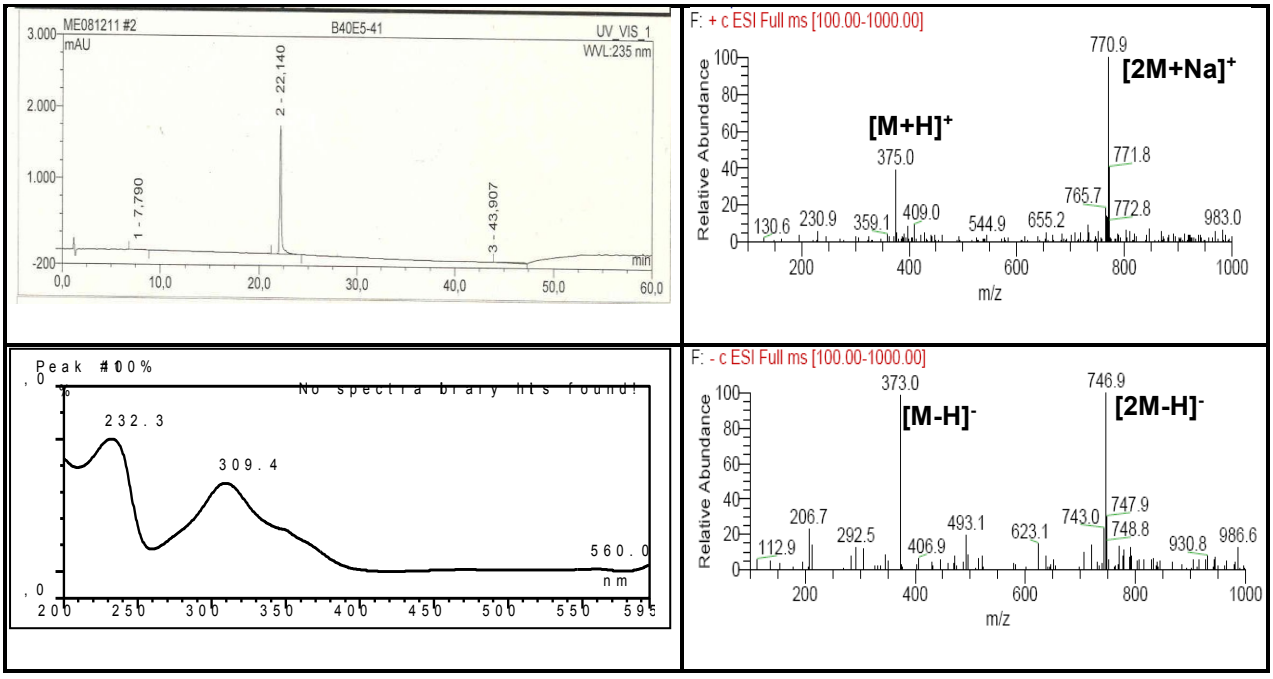

Compound (**16**) was obtained as a brawn amorphous solid. This racemic compound displayed UV absorbances at λ_{max} (MeOH) 232.3 and 309.4 nm. Its ESI mass spectrum exhibited pseudomolecular ion peaks at *m/z* 375.0 $[M+H]^+$ and 770.9 $[2M+Na]^+$ in the positive mode and at *m/z* 370.0 $[M-H]^-$ and 746.9 $[2M-H]^-$ in the negative mode, each in a ratio of 1:1. The molecular formula of **16** was revealed to be $C_{18}H_{14}O_9$ by HRESIMS (*m/z* 375.0707 $[M+H]^+$, Δ +1.0 ppm), which correspond to 12 degrees of unsaturation. Structural elucidation of **16** was based on 1D and 2D NMR spectral analyses including ^{1}H-NMR, ^{1}H-^{1}H COSY and HMBC spectra (Table 3.1.16.1), (Fig. 3.1.16.1). ^{1}H spectrum exhibited five signals belonging to CH_3-4 (δ_H 2.23), CH_3-13 (δ_H 2.30), the oxymethines H-2, H-10, (δ_H 6.34 and 6.79) and the aldehyde proton H-17 (δ_H 10.34). The ^{13}C NMR and DEPT spectra showed two methyl groups (δ_C 10.1 and 11.8), two sp^3-hybridized carbons (δ_C 68.6 and δ_C 89.9) and the aldehyde carbon (δ_C 191.2) as well as thirteen quaternary carbons. NOE correlation from H-17 to H-11 as well as to CH_3-13 and from H-2 to CH_3-4 were observed, which confirm the position of the aldehyde group and both methyl groups.

The structure of **16** was established by HMBC as 3,4,8,9,10-pentahydroxy-2,7-dimethyl-11-oxo-11,12-dihydro-6*H*-6,12-epoxydibenzo [*b*,*f*] oxocine-1-carbaldehyde, which is a dimer of flavipin, a secondary metabolite isolated from *Epicoccum nigrum* (Sekita *et al*. 1982). 2D ROESY correlation between the H-2 and H-11 shows that both protons are located in the same side, the relative stereochemistry in position 2 and 10 is *S* and *R* (or vice versa).

Table 3.16.: NMR data of **16** at 600 MHz (^{1}H) and 150 MHz (^{13}C) in DMSO-d_6.

Position	δ_C	δ_H mult. (*J* Hz)	HMBC (H→C)	ROESY
2	89.9 (CH)	6.34 (s)	4, 8, 9, 10, 11, 15, 16	
3	126.6 (C)			
4	115.5 (C)			10
5	153.0 (C)			
6	132.5 (C)			
7	148.5 (C)			
8	104.0 (C)			
9	196.9 (C)			
10	68.6 (CH)	6.79 (s)	2, 8, 9, 11, 12, 16	4
11	112.9 (C)			
12	121.6 (C)			
13	121.6 (C)			
14	144.2 (C)			
15	138.4 (C)			
16	135.7 (C)			
17	191.2 (CH)	10.34 (s)	11, 12, 13	13
13-Me	11.8 (CH_3)	2.30 (s)	11, 12, 13, 14, 15, 16	17
4-Me	10.1 (CH_3)	2.23 (s)	3, 4, 5, 8	

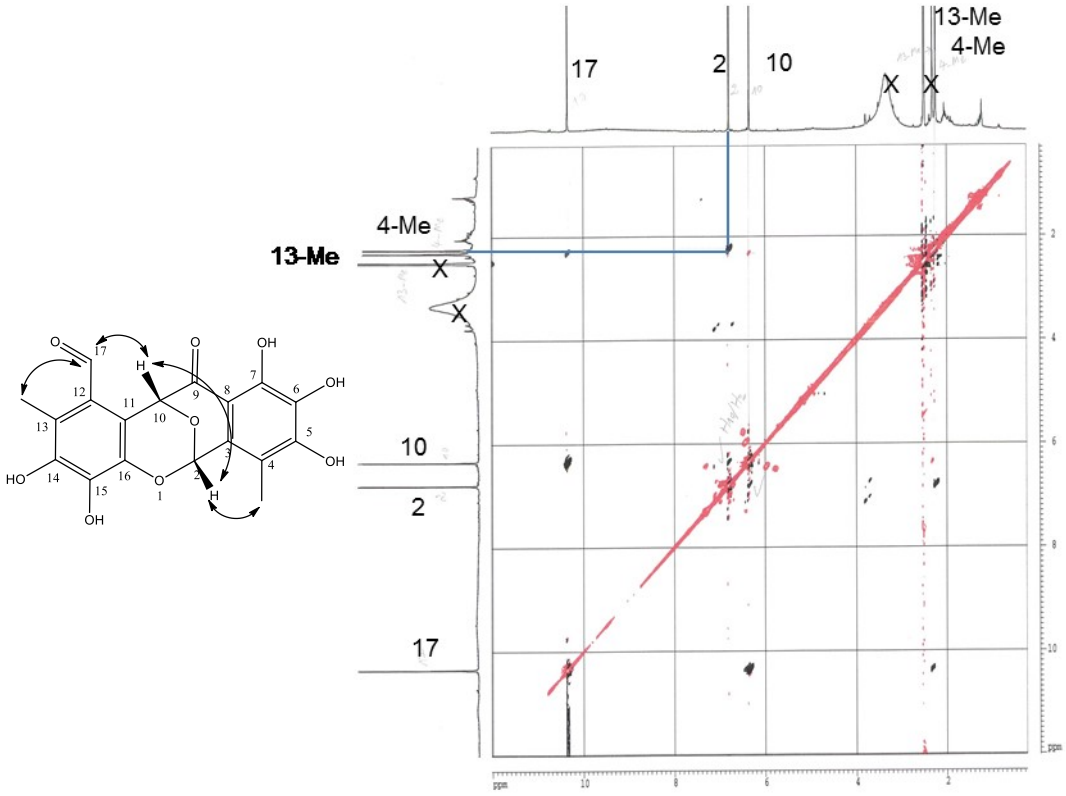

Fig. 3.16.a. Key ROESY correlations and spectrum of **16**.

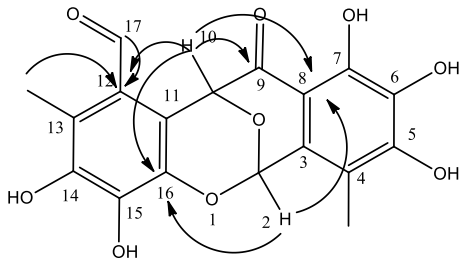

Fig. 3.16.b. Key HMBC correlations of **16**.

3.17. 2-(2-formyl-3,4,5-trihydroxy-6-methylphenyl)-6,7-dihydroxy-5-methylbenzofuran-4-carbaldehyde (compound 17, known)

2-(2-formyl-3,4,5-trihydroxy-6-methylphenyl)-6,7-dihydroxy-5-methylbenzofuran-4-carbaldehyde	
Biological Source	*Epicoccum nigrum* (BSL1W)
Sample Code	40E5-43 and BS1-85-2
Sample Amount	7.8 mg
Molecular Formula	$C_{18}H_{14}NO_8$
Molecular Weight	358 g/mol
Solubility	MeOH
Physical Description	Brawn solid
HPLC Retention Time	23.90 min (standard gradient)

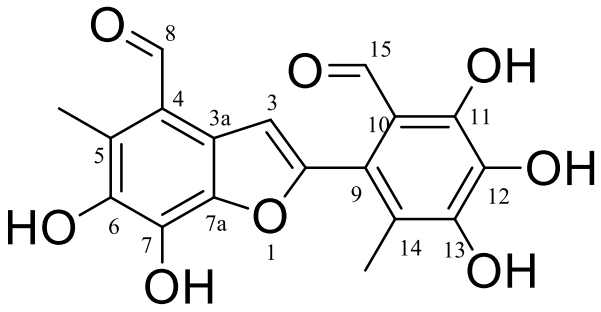

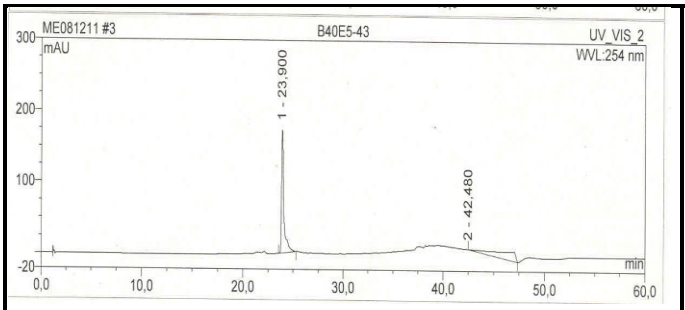

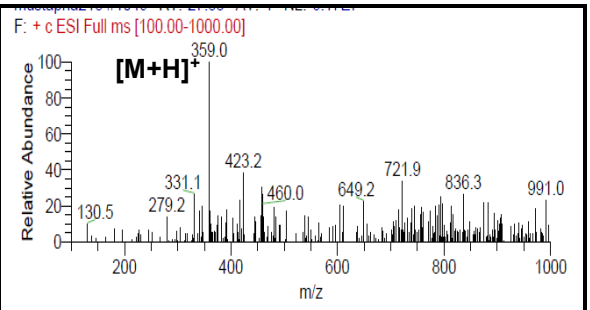

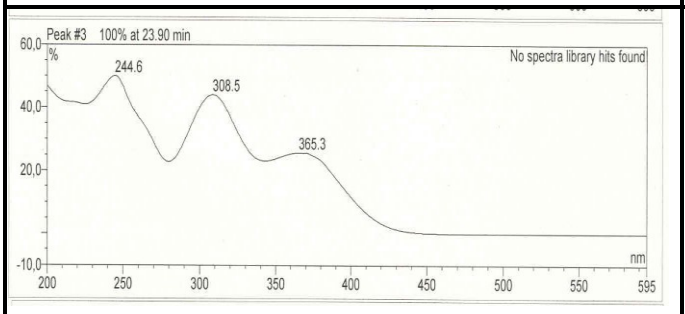

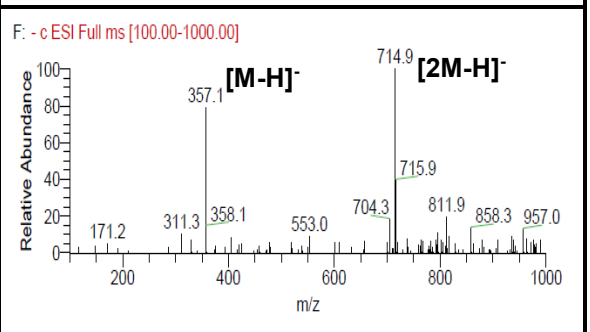

Compound (**17**) was isolated from the EtOAc extract of rice cultures of *Epicoccum nigrum* as a brown solid (7.8 mg). It showed UV absorptions at 244.6, 308.5 and 365.3 nm. Positive and negative ESI-MS showed pseudo molecular ion peaks at *m/z* 359.0 $[M+H]^+$ and at m/z 357.1 $[M-H]^-$ respectively, indicating a molecular weight of 358 g/mol. HRESIMS established a molecular formula of $C_{18}H_{14}O_8$ indicating twelve degrees of unsaturation in the molecule. ^1H NMR (Table 3.17) revealed two signals down field attributed to two aldehyde groups (H-15 and H-8) at δ_H 9.47 and at δ_H 10.41 in addition to two methyl groups (CH_3-14 and CH_3-5) at δ_H 2.01 and δ_H 2.5 as well as an aromatic proton (H-3) at δ_H 7.41. ^1H-^1H COSY spectrum exhibited no correlations. HMBC spectra was extensively studied and the NMR data was compared to the literature to established the structure of **17** as 2-(2-formyl-3,4,5-trihydroxy-6-methylphenyl)-6,7-dihydroxy-5-methylbenzofuran-4-carbaldehyde. This compound was reported as antibacterial bioactive substance isolated from *Aspergillus flavipes* (WO 2005047275).

Table 3.17.: NMR data of **17** at 600 MHz (^1H) and 150 MHz (^{13}C) in Aceton-d_6

Position	17		Literature*	
	δ_H mult. (*J* Hz)	δ_C	δ_H mult. (*J* Hz)	δ_C
2		152.9		151.6
3	7.41	110.5	7.47	108.9
3a		124.0		122.8
4		119.7		117.2
5		128.21		127.5
5-Me	2.58	11.1	2.58	11.0
6		141.9		140.9
7		136.4		136.4
7a		143.54		142.4
8	10.41	190.4	10.42	19.2
9		126.6		124.8
10		114.1		112.6
11		151.7		150.2
12		133.3		132.7
13		152.9		151.5
14		119.7		118.7
14-Me	2.01	12.85	2.01	12.7
15	9.47	196.3	9.48	194.7

*Measured in DMSO-d_6 at 600 MHz (^1H) and 150 MHz (^{13}C) (WO 2005047275)

3.18. Indol-3-carboxylic acid (compound 18, known)

Indol-3-carboxylic acid	
Synonym(s)	1*H*-Indole-3-carboxylic acid
Biological Source	*Aureobasidium pullulans* (MB)
Sample Code	MB60H3-8
Sample Amount	4 mg
Molecular Formula	$C_9H_7NO_2$
Molecular Weight	161 g/mol
Solubility	MeOH
Physical Description	Yellow solid
HPLC Retention Time	19.27 min (standard gradient)

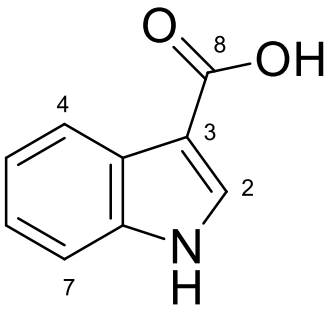

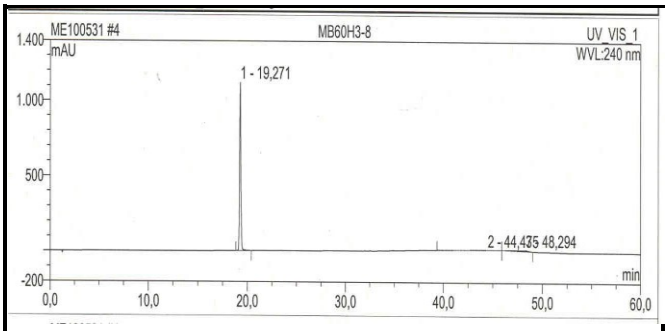

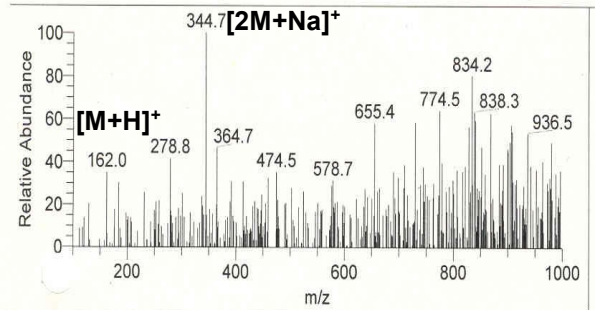

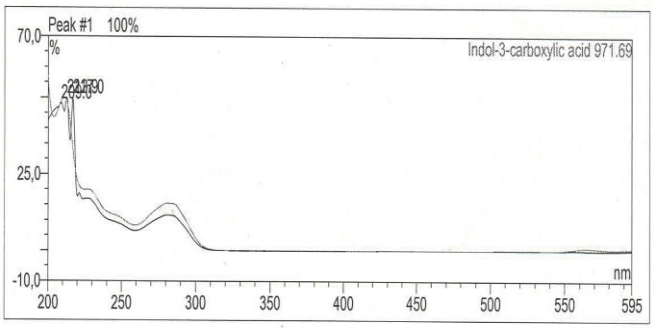

(-)-ESI-MS: no ionization

Indole-3-carboxylic acid (**18**) was isolated from the EtOAc extract of rice cultures of *Aureobasidium pullulans* as yellow amorphous solide (4 mg). The UV absorptions at λ_{max} (MeOH) 209.0 and 211.0 nm, is suggesting an indole chromophore in this compound. Positive ESI-MS showed pseudo molecular ion peak at *m/z* 162.0 $[M+H]^+$ indicating a molecular weight of 161 g/mol , which is in accordance with the molecular formula $C_9H_7NO_2$. The ^1H NMR spectrum (Table 3.18) showed an aromatic ABCD spin system including H-4 at δ_H 8.07 (dd, *J*=6.7, 1.4 Hz,), H-7 at δ_H 7.43 (dd, *J*=7.1, 1.4 Hz,), H-5 and H-6 at δ_H 7.18 (m) as well as a proton resonance at δ_H 7.94 (s). The comparison of the ^1H NMR data with the literature confirmed its identity, which was given by the comparison with the internal HPLC data base and mass spectral data. Thus compound (**18**) was identified as indole-3-carboxylic acid reported by Hiort (2002).

Table 3.18: ^1H NMR data of compound **18** at 500 MHz.

Position	**18**	**Indol-3-carboxylic acid** *
	δ_H (MeOD)	δ_H (DMSO-d_6)
1		11.43, s
2	7.94, s	7.70, s
4	8.07, dd (6.7, 1.4)	8.14, d (7.6)
5	7.18, m	7.02, dt (6.9, 1.3)
6	7.18, m	7.05, dt (6.9, 1.3)
7	7.43, ddd (7.1, 1.4)	7.35, d (7.6)

* Hiort, 2002.

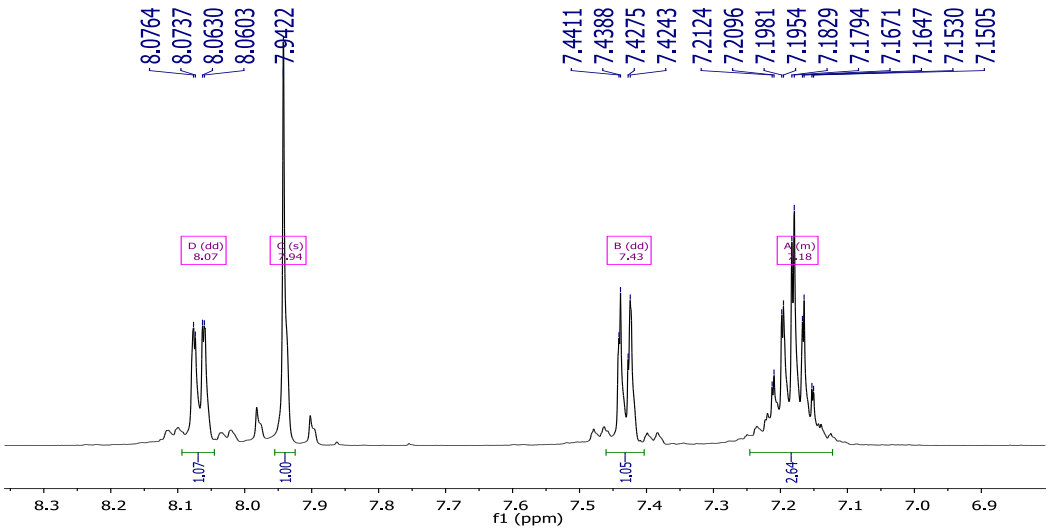

Fig. 3.18. ^{1}H spectrum of compound **18** (in MeOH-d_4 at 500MHz).

3.19. 1H-Indole-3-carbaldehyde (compound 19, known)

1*H*-Indole-3-carbaldehyde	
Biological Source	*Aureobasidium pullulans* (MB)
Sample Code	MB60H3-9
Sample Amount	0.9 mg
Molecular Formula	C_9H_7NO
Molecular Weight	145 g/mol
Solubility	MeOH
Physical Description	Yellow solid
HPLC Retention Time	19.82 min (standard gradient)

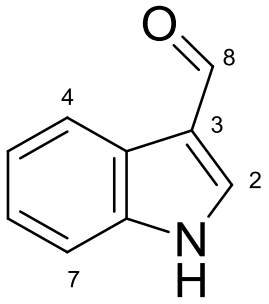

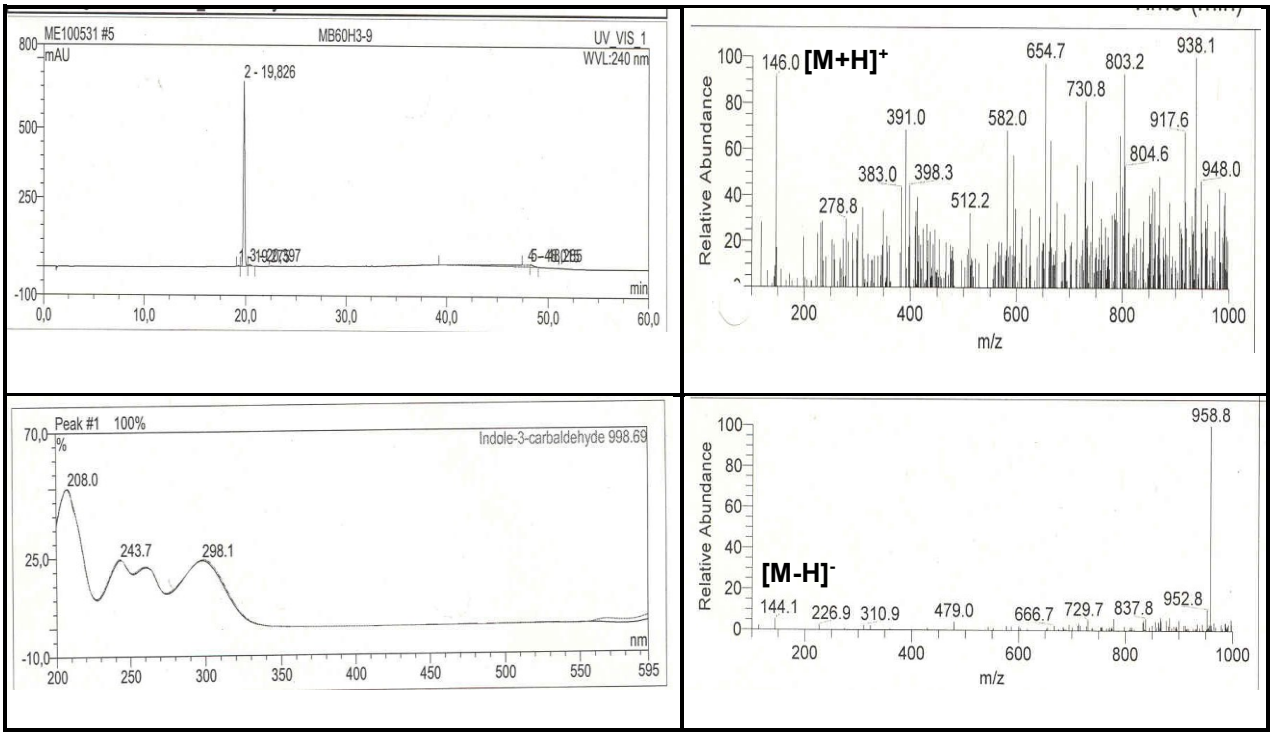

1*H*-indole-3-carbaldehyde (**19**) was isolated from the EtOAc extract of rice culture of *Aureobasidium pullulans* as yellow amorphous solid (0.9 mg). It showed UV absorption at λ_{max} (MeOH) 208.0, 243.7, 260.0 and 298.1 nm. A comparison with the internal HPLC data base suggested its structure to be indole-3-carbaldehyde. Positive ESI-MS showed pseudo molecular ion peaks at *m*/*z* 146.0 $[M+H]^+$ indicating a molecular weight of 145 g/mol , which is in accordance with the molecular formula C_9H_7NO. The ^1H NMR spectrum (Table 3.19) showed four aromatic signals, involved in an ABCD spin system including H-4 at δ_H 8.16 (d, *J*=6.9 Hz), H-7 at δ_H 7.48 (d, *J*=6.9 Hz), H-5 at δ_H 7.24 (td, *J*=1.1, 7.4 Hz) and H-6 at δ_H 7.28 ppm (td, *J*=1.2, 7.8 Hz) as well as a singlet integrated as one proton (H-2) at δ_H 8.11 (s) and an aldehyde proton at δ_H 9.89. Compound (**19**) was identified as 1*H*-indole-3-carbaldehyde (Hiort et al. 2002, Chowdhury et al. 1981).

Table 3.19: ^1H NMR data of **19** (at 500 MHz) and comparison with literature.

Position	**19**	**literature** *
	δ_H (MeOD-d_4)	δ_H (DMSO-d_6)
1		11.43 (s)
2	8.11 (s)	8.27 (s)
4	8.16 (d, 6.9)	8.07, (dd, 7.6, 1.0)
5	7.24 (td, 1.1, 7.4)	7.20 (td, 6.9, 1.3)
6	7.28 (td, 1.2, 7.8)	7.25 (td, 6.9, 1.3)
7	7.48 (d, 6.9)	7.50(dd, 8.2, 1.0)
8	9.89 (s)	9.92 (s)

* Hiort, 2002.

3.20. (Z)-4-(5-Acetoxy-3-methylpent-2-enamido)butanoic acid (compound 20, new)

(*Z*)-4-(5-Acetoxy-3-methylpent-2-enamido)butanoic acid	
Biological Source	*Aureobasidium pullulans* (MB)
Sample Code	MB 15MF5-2
Sample Amount	4 mg
Molecular Formula	$C_{12}H_{19}NO_5$
Molecular Weight	257 g/mol
Solubility	MeOH
Physical Description	Yellow oil
HPLC Retention Time	17.26 min (standard gradient)

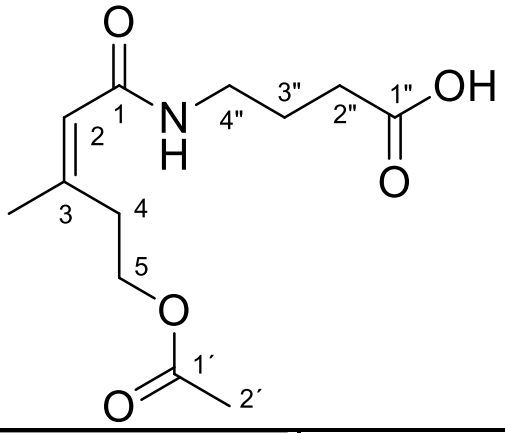

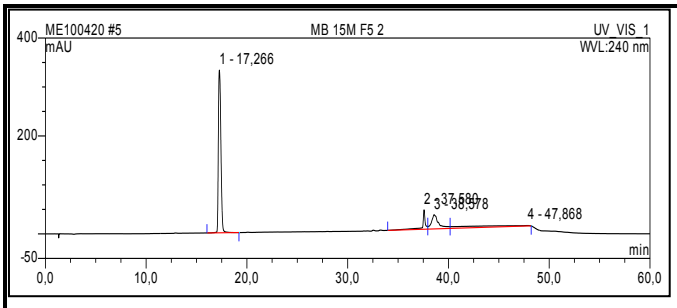

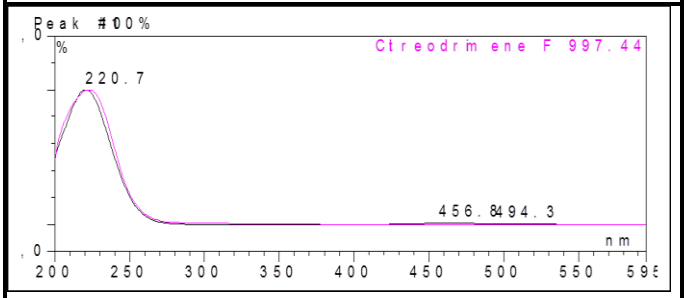

See fig. 3.1.20.1.

Compound **20** was obtained as yellow oil (4.4 mg). It exhibited UV absorption at λ_{max} (MeOH) 220.7 nm and showed pseudo molecular ion peak at *m/z* 257.9 $[M+H]^+$ in the positive ESI-MS, while the negative ionization showed pseudo molecular ion peak at *m/z* 256.0 $[M-H]^-$ indicating a molecular weight of 257 g/mol. The molecular formula of **20** was established as $C_{12}H_{19}NO_5$ from the prominent signal at *m/z* 258.1336, corresponding to $[M+H]^+$ in the HRESIMS (calculated for $C_{12}H_{20}NO_5^+$ *m/z* 258.1336). The ^1H NMR spectrum exhibited eight signals, seven of them are involved in two spin systems as revealed by ^1H-^1H COSY, the first connects H-4" δ_H 3.21 (t, *J*=7.5 Hz, 2H), H-3" δ_H 1.78 (m, 2H) and H-2" δ_H 2.32 (t, *J*=7.5 Hz, 2H), the second includes H-4 δ_H 2.94 (t, *J*=6.75 Hz, 2H) and the oxymethylene H-5 δ_H 4.20 (t, *J*=7.5 Hz, 2H), while in there is a long range correlation between H-2 δ_H 5,76 (s, 1H) and CH_3-3 δ_H 1.89 (d, *J*=1.35 Hz, 3H).

The ^{13}C NMR and DEPT 135 spectra of **20** (Table 3.20) showed big similarity to Pestalotiopamide B (Xu *et al.,* 2011), only the chemical shift of C-4 being an exception (a difference of 7 ppm). NOE correlation (Figure 3.20.b) from CH_3-3 and H-2 showed that **20** has a (*Z*) conformation and not (*E*) like Pestalotiopamide B. Compound **20** was unambiguously identified as (*Z*)-4-(5-acetoxy-3-methylpent-2-enamido)butanoic.

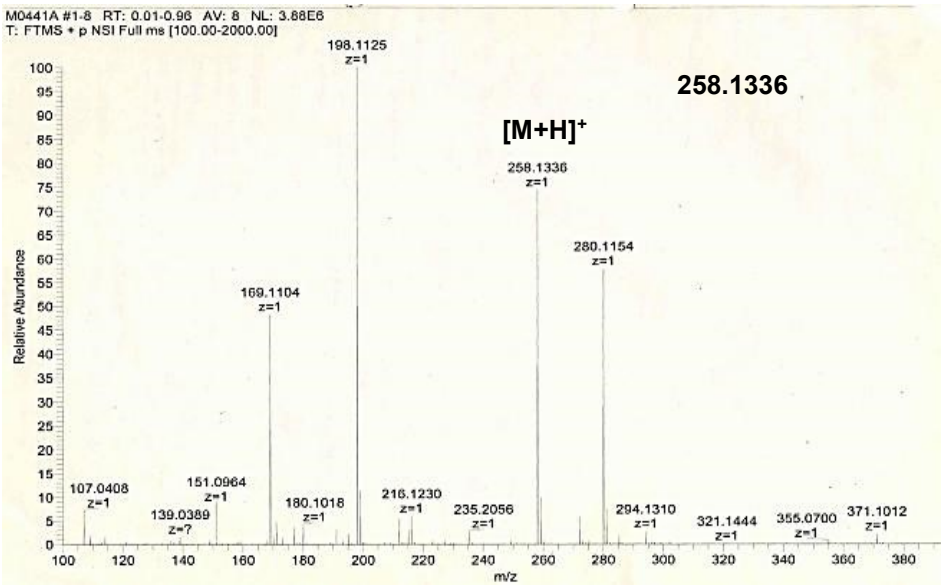

Fig. 3.20. ESI-HRMS of compound **20**

Table 3.20: NMR spectroscopic data of compound **20** and Pestalotiopamide B.

Position	20				Pestalotiopamides B	
	δ_H *mult J* (Hz)	δ_C	COSY	HMBC	δ_H	δ_C
1		169.0				170.2
2	5.76, s	121.8		C1	5.70, d, 0.95	121.1
3		151.3				150.5
4	2.94, t, 6.75	33.3	5	C5, C3	2.42, t, 6.66	40.4
5	4.20, t, 6.75	64.3	4	C2", C3, C1´	4.21, t, 6.66	63.2
1´		173.0				172.8
2´	2.00, s	20.9		C1´	2.01, s	20.7
1"		177.0				176.5
2"	2.32, t, 7.5	32.4	3", 4"	C3", C1"	2.32, t, 7.25	32.6
3"	1.78, m	26.0	2", 4"	C4", C2"	1.89, m	26.2
4"	3.21, t,6.9	39.5	2", 3"	C3", C1	3.23, t, 6.9	39.5
3-CH_3	1.89, d, 1.35	25.5		C4, C2, C3	2.12, d, 0.95	18.4

All measured in MeOH-d_4 at 500 MHz (^{1}H) and 125 MHz (^{13}C)

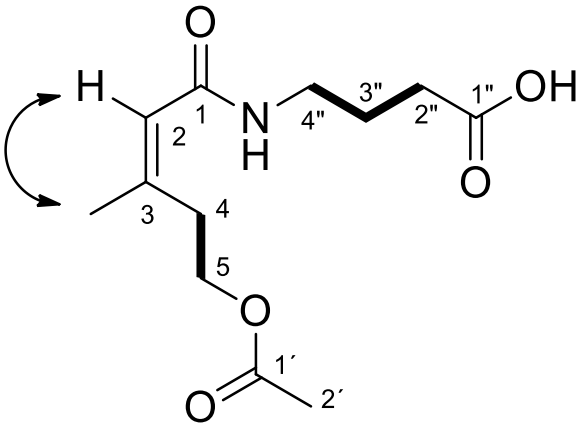

Fig. 3.20.b. ^{1}H-^{1}H-COSY and NOE correlations of **20**.

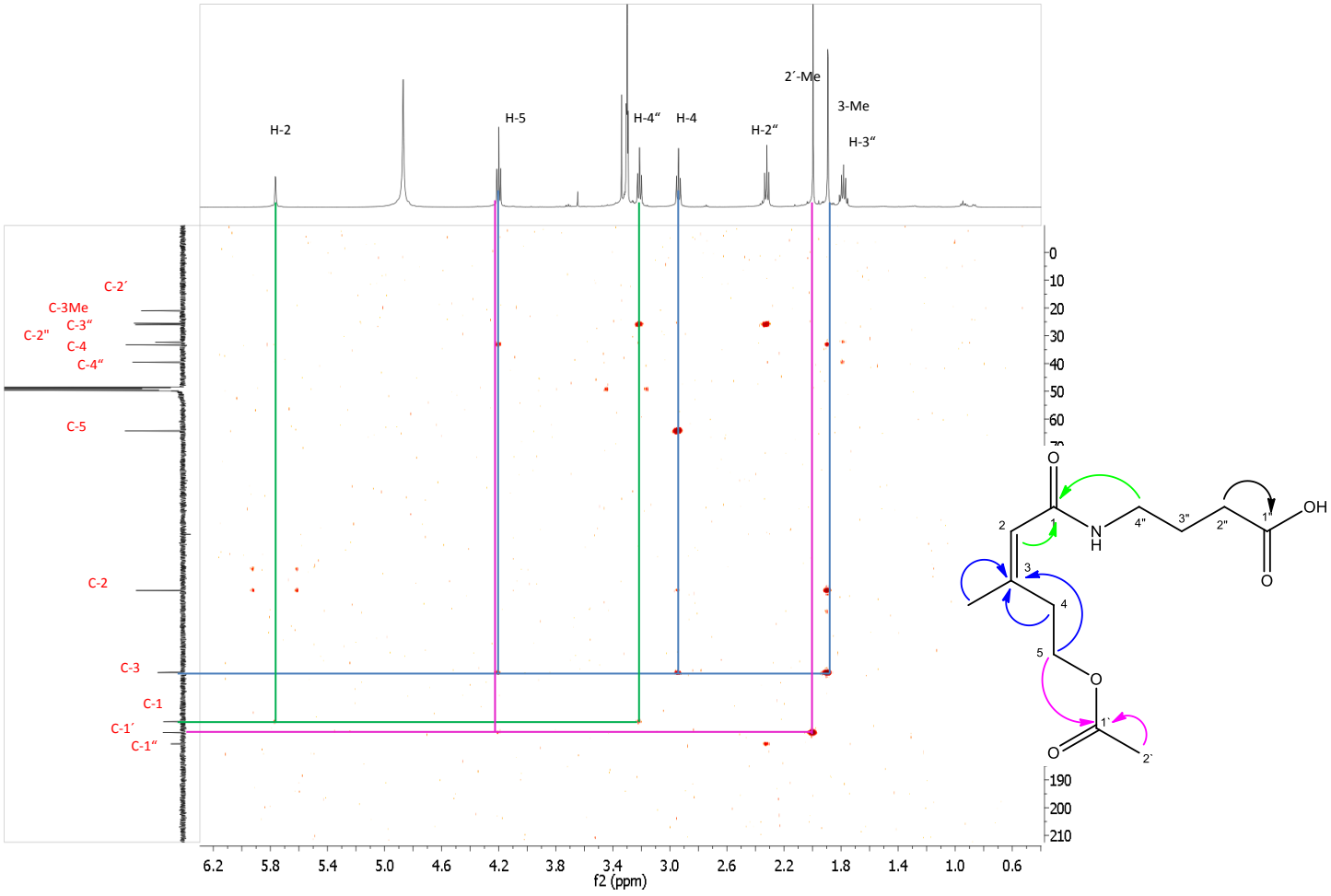

Fig. 3.20.c.: HMBC spectrum showing the key correlations of compound **20**.

3.21. Isoochracinic acid (compound 21, known)

isoochracinic acid	
Synonym(s)	2-(4-hydroxy-3-oxo-1,3-dihydroisobenzofuran-1-yl)acetic acid
Biological Source	*Aureobasidium pullulans* (MB)
Sample Code	MB15MF8-1
Sample Amount	2.1 mg
Molecular Formula	$C_{10}H_8O_5$
Molecular Weight	208 g/mol
Solubility	MeOH
Physical Description	Yellow amorphous solid
$[\alpha]^{20}_D$	− 8.5° (*c* 0.05, MeOH)
HPLC Retention Time	13.48 min (standard gradient)

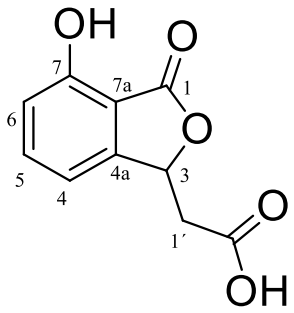

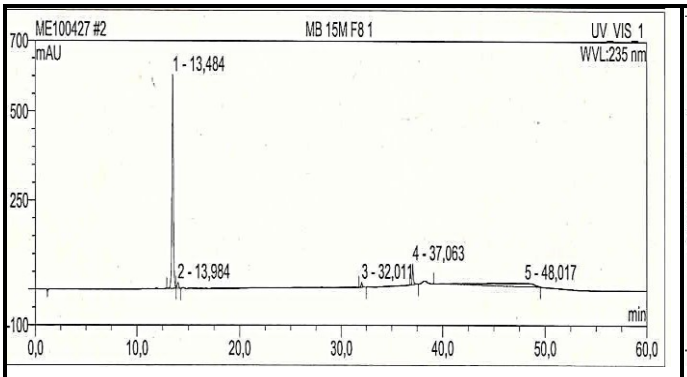

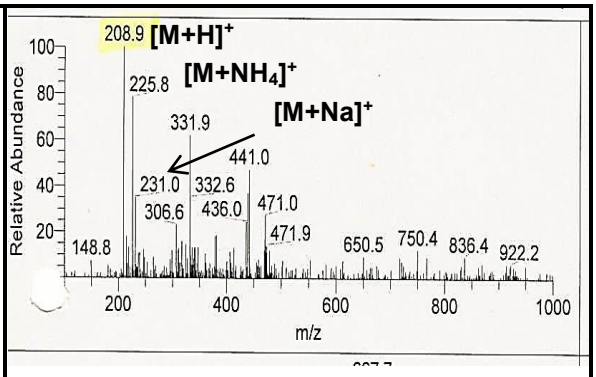

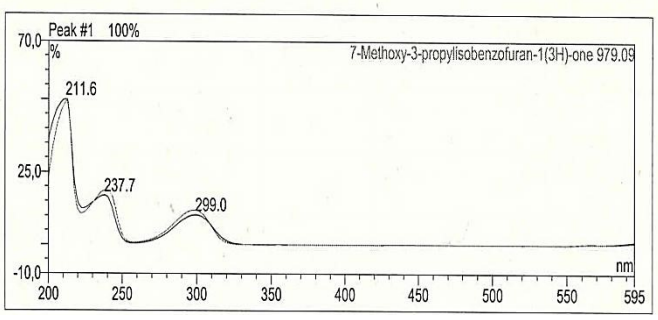

(-)-ESI-MS: no ionization

Isoochracinic acid (**21**) was obtained as a yellow amorphous solid (2.1 mg) with an $[\alpha]^{20}_{D}$ value of -8.5° (*c* 0.05, MeOH). It exhibited UV absorption at λ_{max} (MeOH) 211.6, 237.7 and 299.0 nm and showed pseudo molecular ion peaks at *m/z* 208.9 $[M+H]^+$ (base peack), at *m/z* 225.8 $[M+NH_4]^+$ and *m/z* 231.0 $[M+Na]^+$ in the positive ESI-MS, while no negative ionization was shown. Thus the molecular weight is 257 g/mol, which fit with the molecular formula $C_{12}H_{19}NO_5$. The ^{1}H NMR spectrum (MeOH-d_4) exhibited three aromatic signals corresponding to H-5 at δ_H 7.55 (t, *J* = 7.8 Hz, 1H), to H-4 δ_H 7.03 (d, *J* = 7.5 Hz, 1H) and H-6 at δ_H 6.89 (d, *J* = 8.2 Hz, 1H), and an oxymethine proton H-3 at 5.81 (dd, *J* = 4.9, 7.8 Hz, 1H) and two germinal protons (H-1´a and H-1´b) at 3.00 (dd, *J* = 4.9, 16.6 Hz, 1H) and at 2.76 (dd, *J* = 7.9, 16.6 Hz, 1H). ^{1}H-^{1}H COSY spectrum revealed two spin systems, the first connecting the two protons H-1´with H-3, the second revealing the fragment CH(6)-CH(5)-CH(4).

Comparison of the NMR data, ESI-MS and UV spectrum of **21** with those published for isoochracinic acid (Kameda & Namiki, 1974) revealed a big similarity. Thus **21** was identified as 2-(4-hydroxy-3-oxo-1,3-dihydroisobenzofuran-1-yl)acetic acid which is also known as Isosaccharinic acid. This compound was previously isolated from *Alternaria kikuchiana*, a parasite responsible for the black spot disease on Japanese pears (Kameda & Namiki, 1974).

Table 3.21.: ^{1}H NMR and ^{1}H-^{1}H COSY spectroscopic data of compound **21** and literature data.

Position	21[§]		isoochracinic acid *
	δ_H mult (JHz)	**COSY**	***δ_H mult (JHz)***
1			
2			
3	5.81 (dd, 4.9, 7.8)	1´a, 1´b	5.91 (t, 7.0)
4	7.03 (d, 7.5)	5	7.12 (d, 8.0)
4a			
5	7.55 (t, 7.5)	4, 6	7.60 (t, 8.0)
6	6.89 (d, 8.2)	5	6.97 (d, 8.0)
7			
7a			
1´a	3.00 (dd, 4.9, 16.6)	3	2.95 (d, 7.0)
1´b	2.76 (dd, 7.9, 16.6)	3	2.95 (d, 7.0)

[$] meseaured in MeOH-$d_4$ at 500 MHz (^{1}H)

[*] meseaured in $(CD_3)_2CO$-$CDCl_3$ at 100 MHz (^{1}H)

3.22. 6-Hydroxyisosclerone (compound 22, known)

4,6,8-Trihydroxy-3,4-dihydronaphthalen-1(2*H*)-one	
Synonym(s)	6-Hydroxyisosclerone
Biological Source	*Aureobasidium pullulans* (MB)
Sample Code	MB60H3-4
Sample Amount	1.9 mg
Molecular Formula	$C_{10}H_{10}O_4$
Molecular Weight	194 g/mol
Solubility	MeOH
Physical Description	White amorphous solid
$[\alpha]^{20}_D$	− 50.0° (*c* 0.05, MeOH)
HPLC Retention Time	16.91 min (standard gradient)

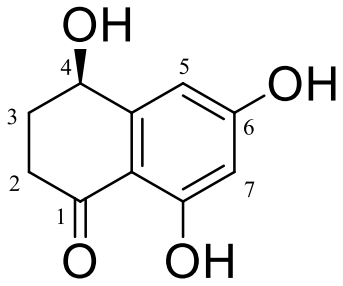

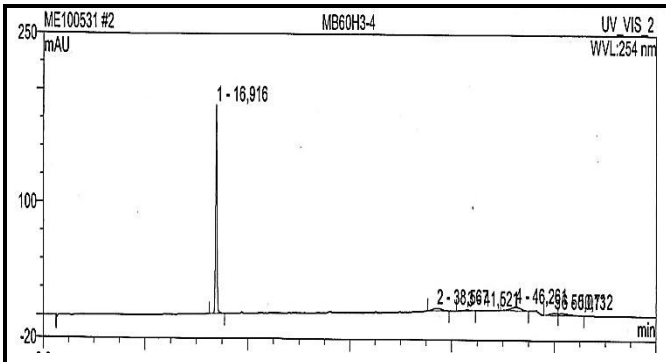

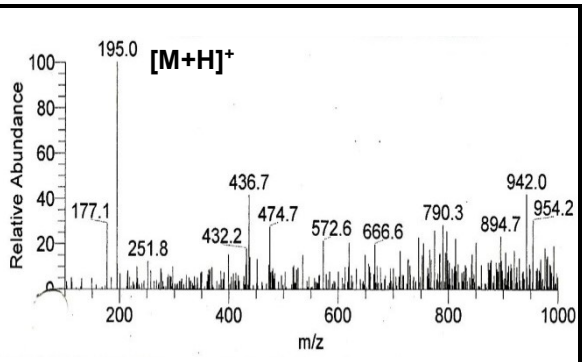

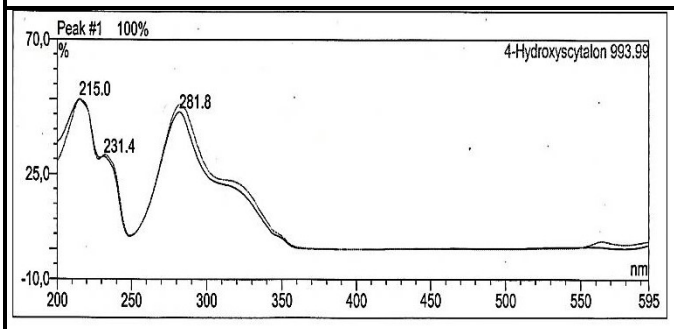

(-)-ESI-MS: no ionization

Compound **22** was obtained as a withe amorphous solid (1.9 mg) with an $[\alpha]^{20}_{D}$ value of -50° (*c* 0.05, MeOH). It exhibited UV absorption at λ_{max} (MeOH) 215.0, 231.4 and 281.8 nm. The molecular weight of 194 g/mol, was established from ESI-MS, where in the positive ionization mode, the molecular ion peak at *m/z* 195.0 $[M+H]^+$ (base peak) was present. This corresponds to the molecular formula $C_{10}H_{10}O_4$. The ^{1}H NMR spectrum (MeOH-d_4) showed two aromatic signals corresponding to H-5 at δ_H 6.54 (dd, *J* = 0.9 and 2.2, 1H) and H-7 δ_H 6.17 (d, *J* = 2.3 Hz, 1H) in addition to a doublet of doublets signal, corresponding to an oxymethine proton (H-4) at δ_H 4.72 (dd, *J* = 3.7 and 8.7 Hz, 1H) and three doublet of doublet of doublet signals (H-2a) at δ_H 2.77 (ddd, *J* = 17.7, 6.6,4.6 Hz), (H-2b) at δ_H 2.60 (ddd, *J* = 17.7, 9.8,4.9 Hz) and (H-3b) at δ_H 2.03 (ddd, *J* =17.6, 11.4, 4.6 Hz). The ^{1}H NMR spectrum showed also a multiplet signal referring to H-3a at δ_H 2.24 (m).

Comparison of the NMR data, ESI-MS and UV spectrum and optical rotation of **22** with those published for 6-hydroxyisosclerone (Dong, 2008; Iwasaki, 1973; Evidente, 2011) lead to the conclusion that **22** is 4-(*S*),6,8-trihydroxy-3,4-dihydronaphthalen-1(2*H*)-one which is known as a phytotoxic substance (Iwasaki, 1973).

Table 3.22.: ^{1}H and ^{1}H-^{1}H COSY spectroscopic data of compound **22** and corresponding literature.

Position	22[§]		Literatur*
	δ_H mult (JHz)	**COSY**	***δ_H mult (JHz)***
1			
2a	2.77 (ddd, 17.7, 6.6,4.6)	2b,3a,3b	2.80 (dt, 18.2, 9.9, 4.8)
2b	2.60 (ddd, 17.7, 9.8,4.9)	2a,3a,3b	2.63 (m)
3a	2.24 (m)	2a,2b,3b,4	2.26 (m)
3b	2.03 (ddd, 17.6, 11.4, 4.6)	2a,2b,3a,4	2.04 (m)
4	4.72 (dd, 3.7, 8.7)	3a,3b	4.73 (w, 10.1)
5	6.54 (dd, 0.9, 2.2)	7	6,54 (s)
6			
7	6.17 (d, 2.3)	5	6.17 (s)
8			

[$] meseaured in MeOH-$d_4$ at 500 MHz (^{1}H)

[*] meseaured in MeOH-d_4 at 400 MHz (^{1}H) (Dong, 2008)

3.23. 3,4,6,8-Tetrahydroxy-3,4-dihydronaphthalen-1(2H)-one (compound 23, known)

3,4,6,8-Tetrahydroxy-3,4-dihydronaphthalen-1(2H)-one	
Biological Source	*Aureobasidium pullulans* (MB)
Sample Code	20-40F6-8, 20-40F8-3
Sample Amount	1.6 mg
Molecular Formula	$C_{10}H_{10}O_4$
Molecular Weight	194 g/mol
Solubility	MeOH
Physical Description	yellow amorphous solid
$[\alpha]^{20}_D$	− 41.0° (*c* 0.05, MeOH)
HPLC Retention Time	13.95 min (standard gradient)

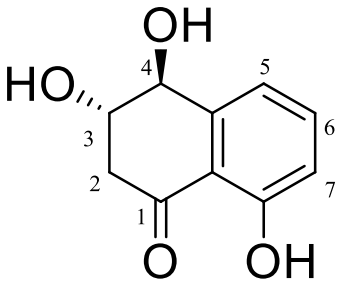

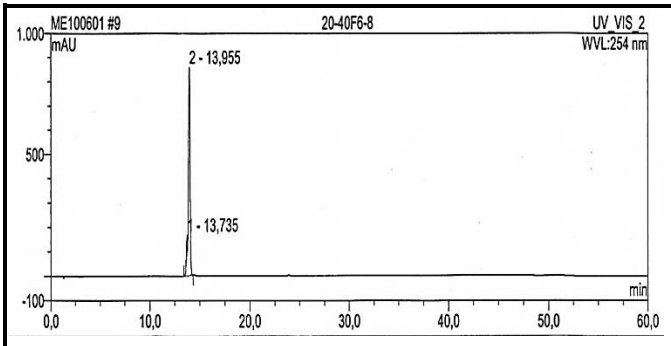

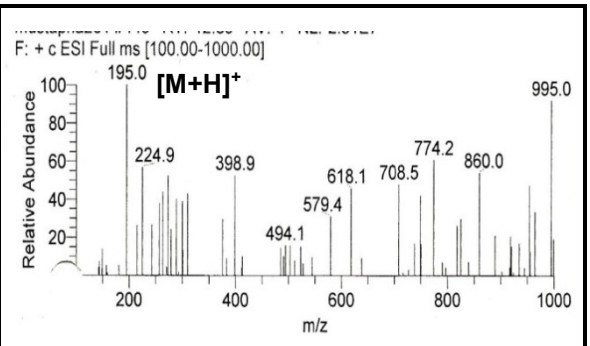

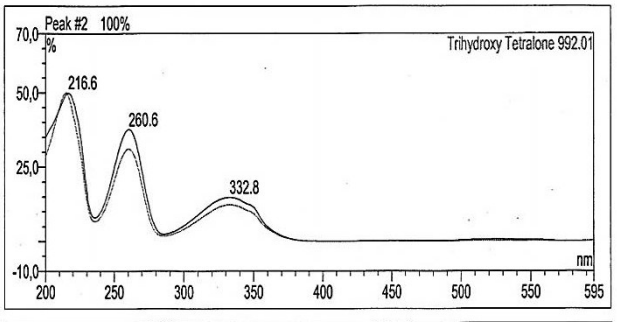

(-)-ESI-MS: no ionization

Compound **23** was obtained from the EtOAc extract of the rice cultures of *Aureobasidium pullulans* as a yellow amorphous solid (1.6 mg) with an $[\alpha]^{20}_{D}$ value of -41.0° (*c* 0.05, MeOH). It showed UV absorption at λ_{max} (MeOH) 216.6, 260.6 and 332.8 nm. The molecular weight of 194 g/mol, was established from ESI-MS, where in the positive ionization, the molecular ion peak at *m/z* 195.0 $[M+H]^+$ (base peak) was present. This corresponds to the molecular formula $C_{10}H_{10}O_4$, similar to compound **22**. The ^{1}H NMR spectrum (MeOH-d_4) showed three aromatic signals building an ABC system, corresponding to H-6 at δ_H 7.56 (t, *J* = 7.6 Hz, 1H), H-5 at δ_H 7.11 (d, *J* = 7.6 Hz, 1H) and H-7 at δ_H 6.86 (d, *J* = 8.4 Hz, 1H), in addition to two doublet of doublet signals, referring to the germinal protons H-2ax at δ_H 2.97 (dd, *J* = 17.3, 7.2 Hz) and H-2eq at δ_H 2.87 (dd, *J* = 17.3, 3.8 Hz), as well as a multiplet, corresponding to H-3 at 4.28 ppm and a doublet H-4 at δ_H 4.84 (d, *J* = 2.7 Hz).

Comparison of the NMR data, ESI-MS and UV spectrum and optical rotation with the published data leads to the conclusion that **23** is 4,6,8-trihydroxy-3,4-dihydronaphthalen-1(2*H*)-one which is known as a phytotoxic substance (Borgschlte *et al.* 1991).

Table 3.23: ^{1}H and ^{1}H-^{1}H COSY spectroscopic data of compound **23** and corresponding literature.

Position	23[§]		Literature*
	δ_H *mult (JHz)*	COSY	δ_H *mult (JHz)*
1			
2a	2.97 (dd, 17.3, 7.2)	2b,3a,3b	2.74 (dd, 17.2, 8.1)
2b	2.87 (dd, 17.3, 3.8)	2a,3a,3b	3.12 (dd, 17.2, 4.0)
3	4.28 (m)	2a,2b,3b,4	4.12 (ddd, 8.1, 6.8, 4.0)
4	4.84 (d, 2.7)	3a,3b	4.65 (d, 6.8)
5	7.11 (d, 7.6)	7	7.17 (d, 7.6)
6	7.56 (dd, 8.4, 7.6)		7.58 (dd, 8.4, 7.6)
7	6.86 (d, 8.4)	5	6.91 (db, 8.4)
8			

[§] meseaured in MeOH-d_4 at 500 MHz (^{1}H)
* meseaured in MeOH-d_4 at 400 MHz (^{1}H) (Borgschlte, 1991)

3.24. Tetrahydroaltersolanol B (compound 24, known)

Tetrahydroaltersolanol B	
Synonym(s)	
Biological Source	*Stemphylium globuliferum*
Sample Code	92%EtOAc 29-34-3
Sample Amount	1.6 mg
Molecular Formula	$C_{16}H_{20}O_6$
Molecular Weight	308 g/mol
Solubility	MeOH
Physical Description	yellow amorphous solid
$[\alpha]^{22}_D$	-17.0° (*c* 0.05, MeOH)
HPLC Retention Time	20.33 min (standard gradient)

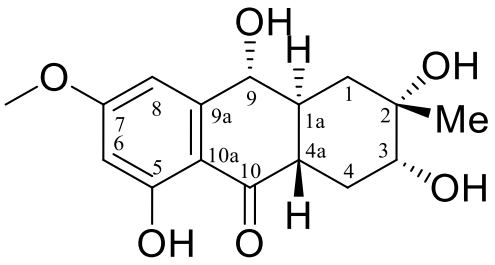

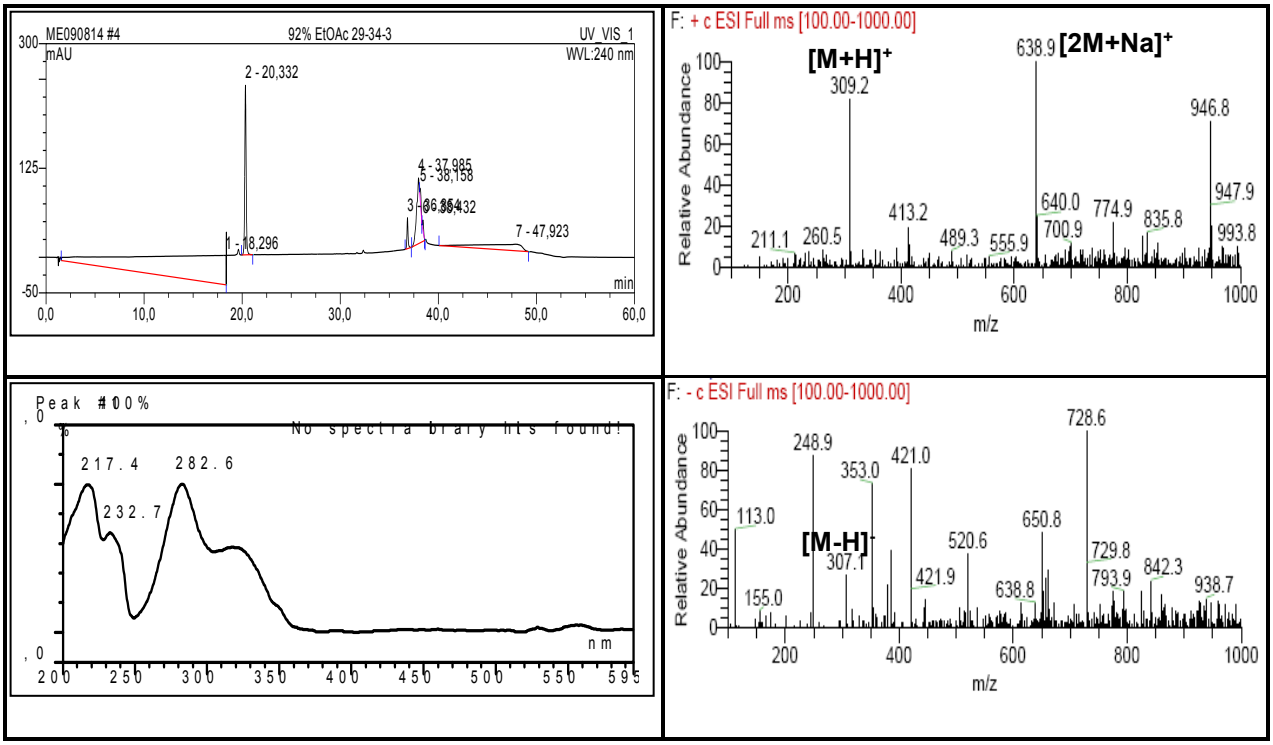

Compound **24** was obtained from the EtOAc extract of the rice cultures of *Stemphylium globuliferum* as a yellow amorphous solid (1.6 mg) with an $[\alpha]^{20}_{D}$ value of -17.0° (*c* 0.05, MeOH). It showed UV absorption at λ_{max} (MeOH) 217.4, 232.7 and 282.6 nm. The molecular weight of 308 g/mol, was established from ESI-MS, based on the pseudo molecular ion peak at *m*/*z* 309.2 $[M+H]^+$ present in the positive ionization. This corresponds to the molecular formula $C_{10}H_{10}O_4$. The ^{1}H NMR spectrum exhibited two *meta*-coupled aromatic protons at δ_H 6.76 (H-8) and 6.31 (H-6), as well as two carbinolic proton at δ_H 4.35 (H-9) and 3.33 (H-3). Two singlets corresponding to the aliphatic methyl group (2-CH_3) detected at δ_H 1.29 and methoxy group (OCH_3-7) at δ_H 3.83 were observed. The proton H-8 which show a *meta*-coupling correlation with H-6, exhibited a second splitting of 1.2 Hz, indicating a long range coupling with the *peri*-proton H-9, which was confirmed by the corresponding correlation observed in the COSY spectrum. Accordingly, the quinone carbonyl present in several anthraquinone (altersolanol A) had been reduced to a hydroxy group. The complete aliphatic spin system in **25** was assembled following the COSY data. In addition, spectroscopical properties analysed during this study proved virtually identical to UV, ^{1}H NMR, mass spectral data, and the $[\alpha]_D$ value published for tetrahydroaltersolanol B (Stoessl and Stothers, 1983), thus confirming the identity of **25** with this compound.

Table 3.24.: ^{1}H and ^{13}C NMR data of compound 24 (^{1}H NMR) and

Position	**25**		Literature *
	δ_H (MeOH-d_4) at 500 MHz	δ_C (DMSO-d_6) at 75 MHz	δ_C (DMSO-d_6) at 50 MHz
1ax	1.34 (dd, 13.2, 12.1)	41.2	41.1
1eq	2.35 (dd, 13.2 ,3.4)		
1a	2.05 (m)	41.6	41.6
2		69.5	69.4
3	Overlapped with water peak	73.5	73.4
4ax	1.61 (q, 12.2)	29.3	29.2
4eq	2.33 (ddd, 12.2, 4.2, 3.7)		
4a	3.45 (m)	41.6	41.6
5		164.4	164.3
6	6.31 (d, 2.2)	99.0	98.9
7		165.7	165.7
8	6.76 (dd, 2.2, 1.2)	104.0	104.0
9	4.35 (d, 10.7)	70.8	70.7
9a		151.6	151.5
10		203.2	203.1
10a		109.2	109.1
2-CH_3	1.29 (s)	26.9	26.9
OCH_3	3.83 (s)	55.6	55.5

* Stoessl and Stothers, 1983.

3.25. Alterporriol O (compound 25, known)

Alterporriol O	
Biological Source	*Stemphylium globuliferum*
Sample Code	92%EtOAc 35-46-1/ F66-70 prep 4-2
Sample Amount	1.6 mg
Molecular Formula	$C_{32}H_{30}O_{14}$
Molecular Weight	194 g/mol
$[\alpha]_D^{20}$ =	- 80.07(*c* = 0.033, MeOH)
Physical Description	yellow amorphous solid
HPLC Retention Time	13.95 min (standard gradient)

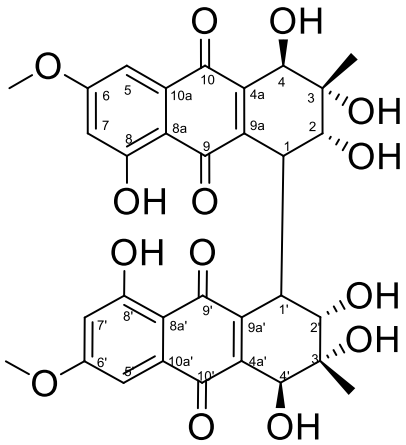

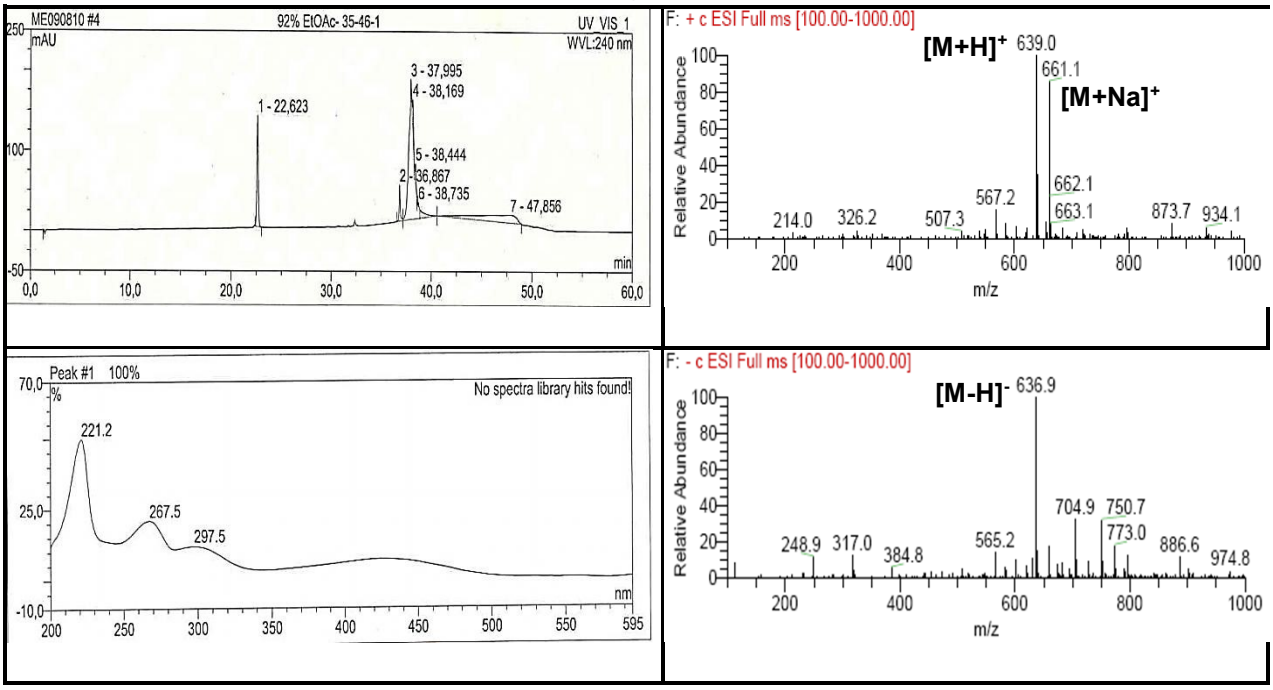

Alterporriol O (**25**) was isolated from the EtOAc fraction of *Stemphylium globuliferum*. It revealed UV absorptions at λmax (MeOH) 221.2, 267.5 and 297.5 nm. Positive and negative ESI-MS showed molecular ion peaks at m/z 639 $[M+H]^+$ and at m/z 637 $[M-H]^-$ respectively, indicating a molecular weight of 638 g/mol. A molecular formula of $C_{32}H_{30}O_{14}$ was established from HRESIMS, which indicates 18 degrees of unsaturation in the molecule. The structure was identified by comparison of its spectroscopic data with those published for Alterporriol O (Zheng *et al.* 2012).

The relative configuration was determined based on ROESY experiment and coupling constants extracted from ^{1}H NMR and the $[\alpha]_D$ value. The equatorial position of the methyl group C-3/3′ was confirmed by their ROE correlations with H-2/2′, H-4/4′, respectively. H-2/2′ showed a large vicinal coupling constant (7.9 Hz) to H-1/1′ and a ROE correlation to OH-4/4′ indicating their axial orientations. Comparison of the NMR data, ESI-MS and UV spectrum and optical rotation with the published data (Zheng *et al.* 2012) leads to the conclusion that **25** is alterporriol O.

Table 3.25.: ^{1}H and ^{13}C spectroscopic data of compound **25** and corresponding literature.

Position	25		Literature*	
	δ_H *mult (JHz)*[a]	δ_C[b]	δ_H *mult (JHz)*[d]	δ_C[d]
1/1′	4.15 (d; 7.4)	44.1	4.07 (d; 6.6)	43.3
2/2′	3.77 (dd; 8.6, 3.8)	73.8	4.12 (d; 6.6)	72.1
3/3′		71.3		70.6
4/4′	4.36 (d; 3.8)	69.6	4. 63 (br s)	68.5
4a/4a′		151.0		149.5
5/5′	7.03 (d; 2.5)	107.3	7.06 (d; 2.4)	105.9
6/6′		167.0		165.5
7/7′	6.78 (d; 2.5)	106.5	6.71 (d; 2.4)	105.5
8/8′		165.4		164.1
8a/8a′		111.6		110.3
9/9′		190.1		189.2
9a/9a′		141.7		141.3
10/10′		184.8		183.3
10a/10a′		135.4		134.1
3/3′-Me	1.11 (s)	22.3	1.29 (s)	21.9
6/6′-OMe	3.90 (s)	56.5	3.95 (s)	55.7

[a]Measured in DMSO-d_6 at 600 (^{1}H), [b]Measured in MeOH-d_4 at 150 (^{13}C) MHz, [d]Measured in Acetone-d_6 at 600 (^{1}H) and at 150 (^{13}C) MHz, *Zheng *et al.* 2012

3.26. Bioactivity test results.

3.26.1 Compounds isolated from AMO 3-2.

We investigated the cytotoxicity of compounds **1**–**7** against the mouse lymphoma cell line L5178Y using the MTT assay (El Amrani *et al.*, 2012). Only compound **2** showed a moderate activity with IC_{50} value of 4.4 µg/mL, while the other compounds were inactive (IC_{50} > 10 µg/mL).

Compounds **1**–**7** were also evaluated for their antimicrobial activities against *Staphylococcus aureus* ATCC 29213, *Streptococcus pneumoniae* ATCC 49619, and *Escherichia coli* ATCC 25922, however, none exhibited any significant activity at a concentration of 64 µg/mL.

3.26.2. Compounds isolated from *Epicoccum nigrum*.

i. MTT Assay:

All isolated compounds isolated from *Epicoccum nigrum* (**8**-**17**) were evaluated for their bioactivity against the murine cancer cell line L5178Y using the MTT assay. The results of the cytotoxicity assay, which are summarized in Table 3.2.1 revealed pronounced to moderate cytotoxicity of compounds **8** and **14** against L5178Y with IC_{50} values of 1.9 and 41.0 µM, respectively. Compound **8** showed also moderate activity against the sensitive and cisplatin-resistant human ovarian cancer cell lines (A2780 sens and A 2780 CisR) with an IC_{50} value of 33.7 µM and 36.5µM, whereas compound **9** exhibited moderate activity against the sensitive human ovarian cancer cell line A2780 sens with an IC_{50} value of 15.8 µM, while the remaining compounds showed a weak or no activity (up to a dose of 10 µg/mL). (Table 3.26.1)

Table 3.26.1 Results of cytotoxicity assay of the compounds isolated from *Epicoccum nigrum* (**8**-**17**)

Compounds	L5178Y growth in % (at 10 µg/mL)	IC_{50} (µM)			
		L5178Y	K562	A2780 sens	A 2780 CisR
8	**-2.0**	**1.9**	86,9	**33,7**	**36,5**
9	77.3		52,8	**15,8**	75,2
11	11.7		87,5	69,4	49,5
14	**3**	**41.0**	n. t.	n. t.	n. t.
15	65.1		n. t.	n. t.	n. t.
16	57.3		n. t.	n. t.	n. t.
17	72		n. t.	n. t.	n. t.

n. t. not tested

ii. **Protein kinase Inhibitory Assay:**

All isolated compounds isolated from *Epicoccum nigrum* (**8**-**17**) were also tested for their activity against 16 protein kinases. Only compounds **12**, **14** and **16** exhibited pronounced activities (Table 3.26.2) Compound **12** showed a selective activity against the protein kinases IGF1-R and AXL with IC_{50} values of 0.44 µM and 1.02 µM, respectively, while compound **16** was found to be active against a panel of protein kinases with IC_{50} values in nM range.

Table 3.26.2. Protein kinase Inhibitory Assay results for compounds 12, 14 and 17. (IC_{50} in µM)

Compounds	IC_{50} in µM															
	AKT1	ALK	ARK5	Aurora-B	AXL	FAK	IGF1-R	MEK1 wt	MET wt	NEK2	NEK6	PIM1	PLK1	PRK1	SRC	VEGF-R2
12	13.8	2,11	14.8	8.61	1.02	6.66	0.440	>100	3.41	11.3	8.26	17.7	12.7	45.4	2.96	1.97
14	>100	31.5	>100	52.0	6.48	64.1	1.45	>100	56.8	>100	>100	>100	>100	>100	44.0	37.1
16	0.0541	0.0137	0.261	0.363	0.0088	0.0288	<0.003	11.9	0.00965	0.790E	0.0463	0.224	0.369	0.232	0.0119	0.0104

- IC_{50} (µM) above 10
- IC_{50} (µM) between 1 and 10
- IC_{50} (µM) between 0.1 and 1
- IC_{50} (µM) below 0.1
- IC_{50} (µM) below 0.003

iii. MIC Test against multidrug resistant bacteria:

The isolated compounds **8**-**12** and **14-15**, all secondary metabolites of *Epicoccum nigrum* were evaluated for their activity against the multidrug resistant bacteria: *Escherichia coli, Enterococcus faecalis,* Methicilin resistant *Staphylococcus aureus* and *Streptococcus pneumonia.* Compounds **10**, **11** and **14** showed a moderate activity against Methicilin resistant *Staphylococcus aureus* with EC_{50} values of 31.25 µg/mL (compounds **10** and **14**) and 15.6 µg/mL for compound **11**.

Table 3.26.3. MIC Test against multidrug resistant bacteria for compounds 8-12 and 14-15.

Compounds	*Escherichia coli*	*Enterococcus faecalis*	Methicilin resistant *Staphylococcus aureus*	*Streptococcus pneumonia*
9	>62,5	n. t.	n. t.	n. t.
10	n. t.	n. t.	***>31,25***	n. t.
11	n. t.	n. t.	**>15,6**	n. t.
12	n. t.	>62,5	>125	>62,5
14	>62,5	n. t.	**>31,25**	>62,5
15	n. t.	n. t.	*>62*	n. t.

Concentrations are listed in μg/mL for active substances (inhibition of more than70%).

n. t. not tested

3.26.3. Compounds isolated from *Aureobasidium pullulans*

The cytotoxicity of compounds **18**–**23** was investigated against the mouse lymphoma cell line L5178Y using the MTT assay, however, none exhibited any significant activity at a concentration of 10 µg/mL.

3.26.4. Compounds isolated from *Stemphylium globuliferum*

Compounds **24**–**25** were evaluated for their activity against the mouse lymphoma cell line L5178Y using the MTT assay, none of this compound showed any significant activity at a concentration of 10 µg/mL.

4. Results of Biodiversity screening of endophytic fungi.

4.1 Biodiversity screening with culture dependent method.

Healthy leaves of *Avicennia marina* were collected from two different geographic regions; namely Hainan in China and Muscat in Oman, with the purpose to compare their fungal endophytic populations. Furthermore, two samples from the same plant collected in Sept 2009 and Aug 2011 at the same region (Hainan in China) were analyzed, with the aim of answering the question "Did the fungal endophytic populations of a certain plant change with time?". The biodiversity results are shown in Table 4.1 The endophytic fungal communities were characterized by polymerase chain reaction (PCR) using ITS1 and ITS4, which allow amplifying a part of the internal transcribed spacer 1, the complete sequence of 5.8S ribosomal RNA gene in addition to a partial sequence of the internal transcribed spacer 2.

To assign the Phylotypes, the closest matches obtained from BLAST were used. A phylogenetic analysis with Neighbor-Joining method was also performed to confirm the assignment of the phylotypes, therefore sequences from GenBank were used as reference (Fig 4.1.).

Table 4.1 Taxonomic position of phylotypes, isolated from *A. marina,* deducted from the comparison to the ITS sequences in GenBank.

Location	Sample	Isolate code	Putative taxon	ITS sequence Lenght	% similarity	Phylum	Class	Order	Closest related from GenBank (Acc. Nr.)
A. marina (Oman)	Petiole + Leaf	AMO 1-1	*Thielavia arenaria*	520	100%	Ascomycota	Sordariomycetes	Sordariales	GU966511.1
		AMO 1-2	*Sordariomycetes* sp.	502	91%	Ascomycota	Sordariomycetes	Sordariales	GQ153124.1
		AMO 1-3	Not identified	122					
		AMO 2-1	*Thielavia microspora*	522	78%	Ascomycota	Sordariomycetes	Sordariales	JF714250.1
		AMO 2-2	Uncultured *Pleosporales*	482	99%	Ascomycota	Dothideomycetes	Pleosporales	GU910945.1
		AMO 3-1	*Alternaria arborescens*	520	99%	Ascomycota	Dothideomycetes	Pleosporales	HQ443201.1
		AMO 3-2	Fungal sp.	506		Ascomycota	Sordariomycetes	Sordariales	JX454777.1

		AMO 4-1	*Alternaria solani*	507	100%	Ascomycota	Dothideomycetes	Pleosporales	HQ270456.1
		AMO 4-2	*Alternaria alternata*	509	100%	Ascomycota	Dothideomycetes	Pleosporales	JQ936166.1
		AMO 5-1	*Thielavia microspora*	528	93%	Ascomycota	Sordariomycetes	Sordariales	GU966510.1
		AMO 6-1	*Thielavia subthermophila*	463	99%	Ascomycota	Sordariomycetes	Sordariales	JN390827.1
		ACL3	*Nigrospora* sp.	498	99%	Ascomycota	Sordariomycetes	Trichosphaeriales	JF694936.1
		ACL 4	*Pestalotiopsis neglecta*	560	99%	Ascomycota	Sordariomycetes	Xylariales	HQ262519.1
	Leaf	ACL 5	*Pestalotiopsis microspora*	503	99%	Ascomycota	Sordariomycetes	Xylariales	HM802304.1
		ACL6	*Pestalotiopsis heterocornis*	544	99%	Ascomycota	Sordariomycetes	Xylariales	JN943628.1
		ACL7	Fungal sp.	506	99%	Ascomycota	Sordariomycetes	Xylariales	JQ692119.1
		ACP 11	*Glomerella acutata*	518	99%	Ascomycota	Sordariomycetes	Glomerellales	GQ924900.1
		ACP 5	*Corynespora cassiicola*	521	99%	Ascomycota	Dothideomycetes	Pleosporales	JX087446.1
A. marina (China 2009)		ACP2	*Phomopsis* sp.	533	99%	Ascomycota	Sordariomycetes	Diaporthales	EU002933.1
		ACP6	*Colletotrichum* sp.	527	97%	Ascomycota	Sordariomycetes	Glomerellales	DQ780412.1
	Petiole	ACP7	*Glomerella acutata*	515	100%	Ascomycota	Sordariomycetes	Glomerellales	GQ924900.1
		AMCL1	*Nigrospora oryzae*	505	98%	Ascomycota	Sordariomycetes	Trichosphaeriales	HQ262527.1
		AMCL2	*Nigrospora oryzae*	494	99%	Ascomycota	Sordariomycetes	Trichosphaeriales	JN662419.1
		AMCL3	Fungal sp.	525	83%	Ascomycota	Sordariomycetes	Trichosphaeriales	JQ410054.1
		AMCL4	*Cladosporium colombiae*	496	100%	Ascomycota	Dothideomycetes	Capnodiales	JQ346204.1
		AMCL7	*Botryosphaeria australis*	530	100%	Ascomycota	Dothideomycetes	Botryosphaeriales	FJ037758.1
		AMCP3	Fungal sp.	485	100%	Ascomycota	Sordariomycetes	Trichosphaeriales	GQ851753.1
		AMCP4	*Nectria mauritiicola*	532	100%	Ascomycota	Sordariomycetes	Hypocreales	HF545314.1
		AMCP5	Fungal sp.	501	100%	Ascomycota	Sordariomycetes	Trichosphaeriales	GQ851753.1
A. marina (China 2011)		AMCP6b	*Cladosporium colombiae*	504	100%	Ascomycota	Dothideomycetes	Capnodiales	JX156363.1
	Petiole	AMCP7	Fungal sp.	492	99%	Ascomycota	Sordariomycetes	Trichosphaeriales	GQ851753.1
		AMCP8	*Daldinia eschscholzii*	527	99%	Ascomycota	Sordariomycetes	Xylariales	GU222391.1
		AMCP10	Fungal sp.	497	99%	Ascomycota	Sordariomycetes	Trichosphaeriales	HM537066.1

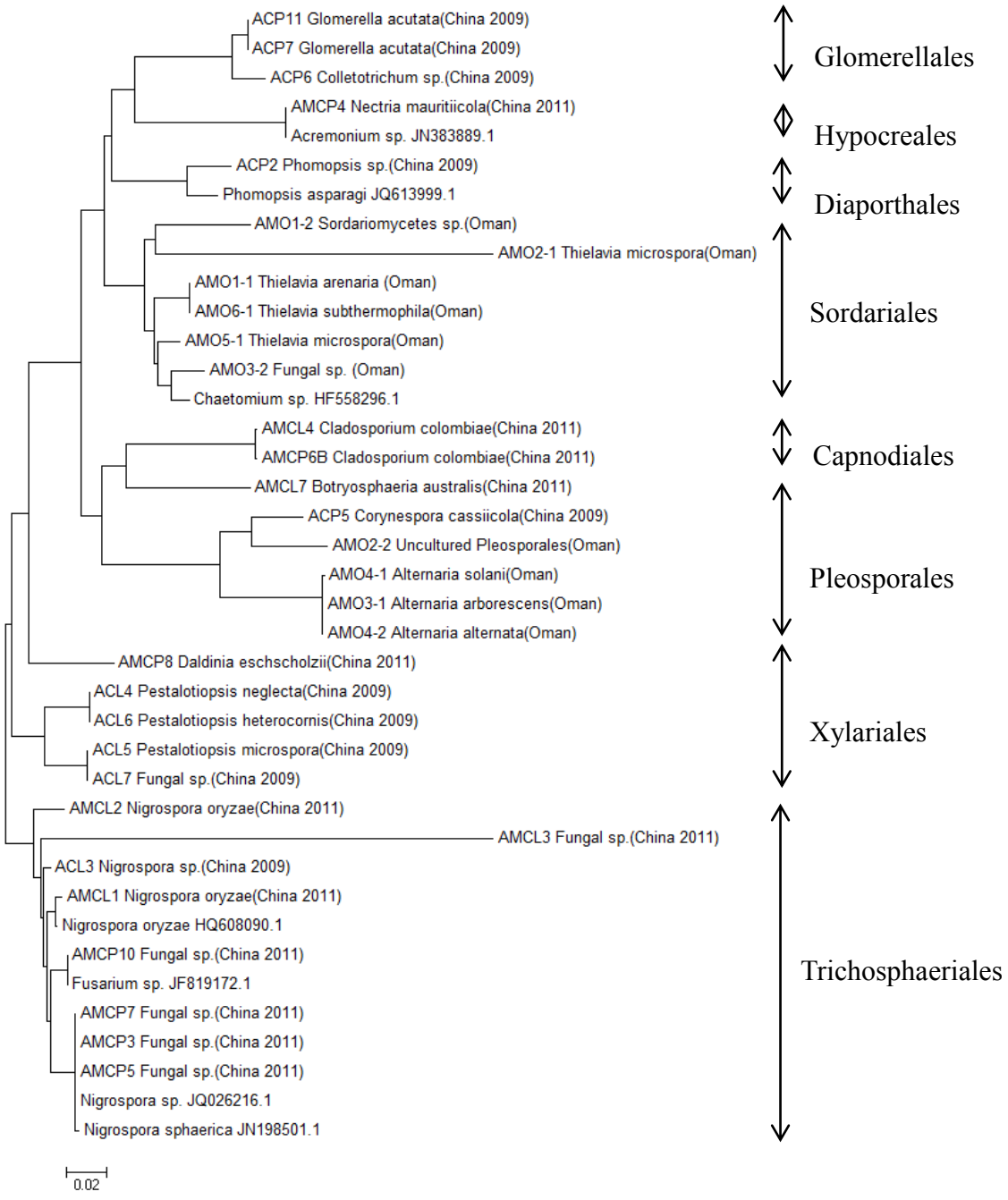

Fig: 4.1: Phylogenetic analysis performed by Neighbor-Joining method.

The fungal population isolated from the leaves of A. marina collected in Oman comprised 10 morphotypes or OTUs (operating taxonomic unites) all belonging to the phylum: Ascomycota and were distributed between two classes, Sordariomycetes and Dothideomycetes. Among these morphotypes, six were members of the order Sordariales (60%) and four were derived from Pleosporales (40%). Moreover, two genera are predominating: *Thielavia* (40%) and *Alternaria* (30%). *Thielavia* fungi were first reported as endophytes by Li *et al*. 2007.

From leaves of the mangrove plant *A. marina* collected in China (2009), 10 morphotypes were also isolated. All isolated and cultured fungi belong to the phylum Ascomycota and 90% are members of Sordariomycetes. Only one member of Dothideomycetes (class Pleosporales). The Sordariomycetes morphotypes are distributed as following: Xylariales (40%), Glomerellales (30%), Diaporthales (10%) and Trichosphaeriales (10%).

All fungi isolated from *A. marina* collected in China (2011) belong to Ascomycota; they are distributed between two classes; namely Sordariomycetes (75%) and Dothideomycetes (25%). Five Orders were represented: Trichosphaeriales (41.7%), Xylariales (25%), Capnodiales (16.7%), Hypocreales (8.3%) and Botryosphaeriales (8.3%).

The structure of the fungal community, characterized in samples collected in Oman, seems to be less diverse (two classes) and different in comparison to the samples collected in China, because of the predominance of the order Sordariales (*A. marina* collected in Oman). However, the fungal populations isolated from the plants growing in China represented four Classes from the samples collected in 2009 and five from the samples collected in 2011. Despite that the two samples do not exhibit the same distribution of endophytic fungi, they have both members from Trichosphaeriales and Xylariales but not with the same ratios.

The fungal endophytic population constitution varied according to the geographic situation and time of sampling, which is in accordance with the results reported. Endophyte diversity depends on geographic situation (Thomas *et al.,* 2008; Herrera *et al.,* 2011). It has been also suggested that the diversity of endophytic fungi may also depend not only from the environmental effects but also from the interaction with other endophytic or pathogenic microorganisms (Anaujo *et al.,* 2002).

4.2 Biodiversity screening with a culture independent method (DGGE).

4.2.1. Optimization of DGGE method.

The application of DGGE to estimate fungal biodiversity is a multi-step procedure which relies on several other methods. DNA must first be extracted from the environmental sample, and amplified by PCR using modified, taxonomically significant primers, containing a GC-clamp. The PCR products obtained can be separated by DGGE.

The DGGE technique enables PCR products which have the same number of nucleotides, but with different internal sequence composition to be separated, in a gradient gel, according to the melting behavior of the DNA.

Optimizing DGGE includes an optimization of total DNA isolation, PCR parameters and primers, in addition to an optimization of the DGGE electrophoresis conditions.

4.2.1.1. Optimization of total DNA isolation.

Different DNA isolation methods and different DNA isolation Kits were tested and compared with the aim of improving the final DGGE results. DNA isolation Kits from QIAGEN (DNeasy® Plant Mini Kit) and Zymo Research Corporation (ZR Fungal/Bacterial DNA Kit™) were compared with the Phenol-Chloroform-Method. DNA amount and purity as well as the final DGGE results were critical for choosing the suitable DNA isolation method.

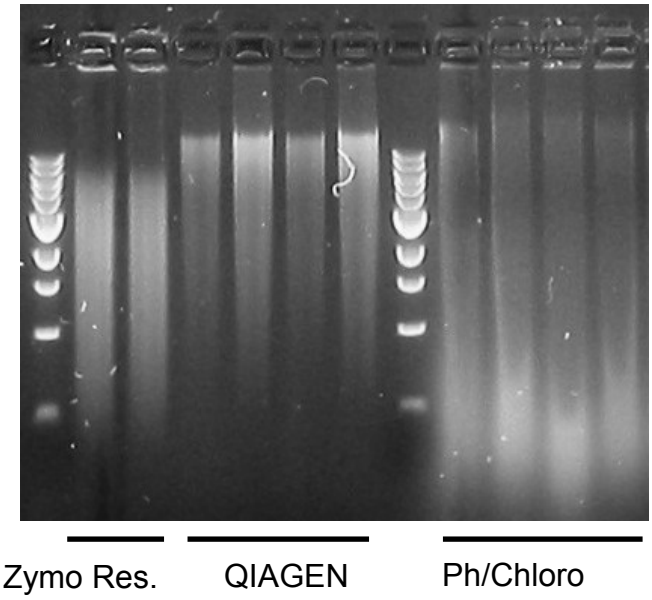

Fig.: 4.2.: Total DNA isolation from leaves of *A. marina* using different methods.

The Kits from QIAGEN (DNeasy® Plant Mini Kit) delivered the best DNA quality, while the Phenol-Chloroform-Method has proved to be in need of improvement, which was done by using polyvinyl pyrrolidone (PVP) or the OneStep™ PCR Inhibitor Removal Kit (Zymo Reaserch) to reduce phenolic impurities.

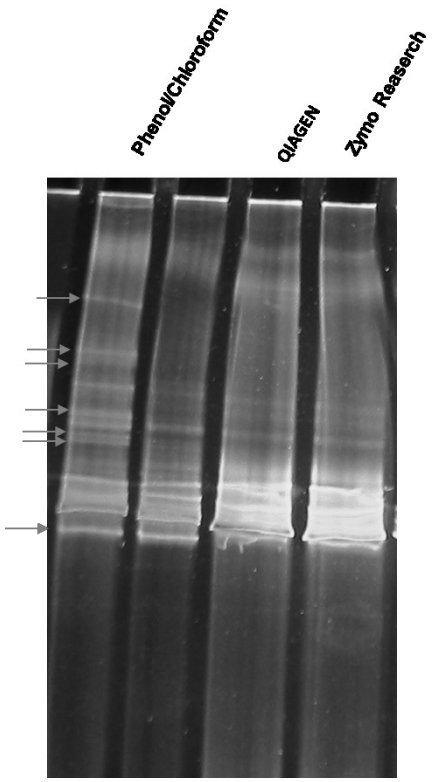

Fig.: 4.3.: DGGE gel with PCR products of DNA isolated from leaves of *A. marina* using different DNA isolation methods.

After performing a DGGE using DNA isolated with three different methods, the Phenol-Chloroform-Method showed more defined bands, which refer to more detected operational taxonomic units (OTUs). Since the aim of DGGE is to detect as many fungi as possible in the analyzed samples, the Phenol-Chloroform-Method proved to be superior compared to the other methodes DGGE using leaf samples of *A. marina*. (Fig.: 4.3.).

4.2.1.2. Optimizing PCR conditions.
Evaluating primers

ITS1/ITS4

The primers ITS1/ITS4 are known from several publications as reliable universal primers for

fungal DNA. They were successfully tested in our group for DGGE analysis (Indriani, 2007). For this purpose, a modified ITS4 primer, including a GC- clamp was used. In our study, DGGE of PCR products, where DNA isolated from leaves of *A. marina,* was amplified*,* the use of these primer failed to produce any bands. The primers ITS1/ITS4 were, therefore found not suitable for DGGE of *A. marina* samples.

NS1/ GC-Fung

The primer pair NS1/GC-fung (May et al. 2001; White et al. 1990), was successfully used for DGGE analysis in many studies. It proved its suitability for fungal diversity screening in plants (Duong et al., 2003 and 2006).

NS1/fung targets a ca. 320 bp sequence from the 18S rDNA. Specific and prominent DGGE bands were observed and used for excision and nucleotide sequence analysis.

Nested PCR

In order to increase the PCR yield, to generate more specific DNA fragments and to still use the primers ITS1/ITS4, we used nested PCR. The latter method requires two successive PCR reactions with different primer pairs. The product resulting from the first amplification with the primers EF4/ITS4 is subjected to a second PCR with the primers ITS1/ITS4, this yield a sequence within the region targeted by the first PCR primers.

Optimization of nested PCR led to an improved yield of DNA, but no bands were observed on the DGGE gel.

4.2.1. Results of estimating fungal diversity in *A. marina* leaves by DGGE

DGGE experiment of the mangrove plant *A. marina* was carried out using an 8% polyacrylamiede gel with gradients ranging from 10% to 50% urea/ formamide (110 Volts, 16 hours). Prominent Bands were cut and incubated in 30µL sterile water (at 4°C), five µL of this water, with the solved DNA, served as template for a PCR with the primer set NS1/Fung. The sequences resulting from this PCR were purified and sequenced. DGGE profiles are shown in Figures 4.4 till 4.6. Not all bands gave useful sequences after sequencing, because the DNA in the bands still contained impurities.

From all DGGE gels of *A. marina* collected in 2011, we just sequenced the DNA isolated from

the bands of the first gel (see Fig.: 4.6. leaf 1 and petiol 1).

The DGGE profile of the sample collected in Oman yielded five different bands, which could be successfully sequenced. From the DGGE profile of *A. marina* (China 2009), fourteen bands were excised and sent for sequencing analysis, while from *A. marina* (China 2011) only six prominent bands were chosen for sequencing.

Table 4.2.1 summaries the putative identities of the different OTUs, after a blast search in GenBank. Out of the 25 OTUs, only 10 (40%) have more than 97% similarity to a sequence in GenBank. The close matches obtained from Blast, were used to assign the phylotypes. A phylogenetic analysis with Neighbor-Joining method was also performed to confirm this assignment; therefore, appropriate sequences from GenBank were used as reference (Fig 4.7.)

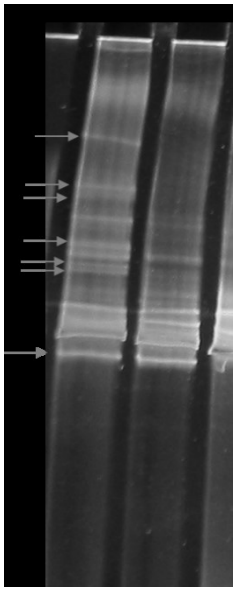

Fig.: 4.4: DGGE profiles of the fungal community in a single leaf of *A. marina* collected in Oman(NS1/GCFung). Two annnealing temperatures were tested: left lane 55°C, right lane 50°C.

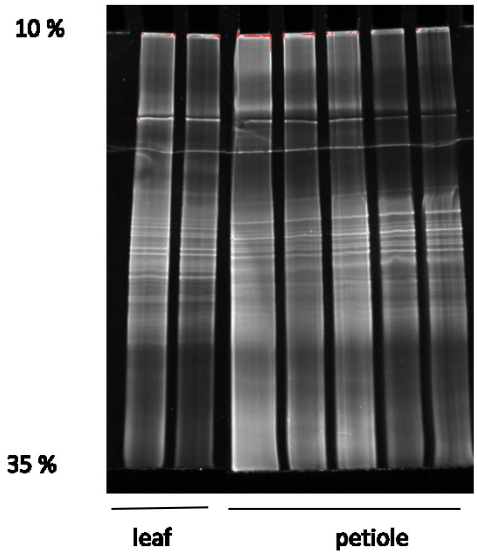

Fig.: 4.5: DGGE profiles of the fungal community in a single leaf and petiole of *A. marina* collected in China (2009).

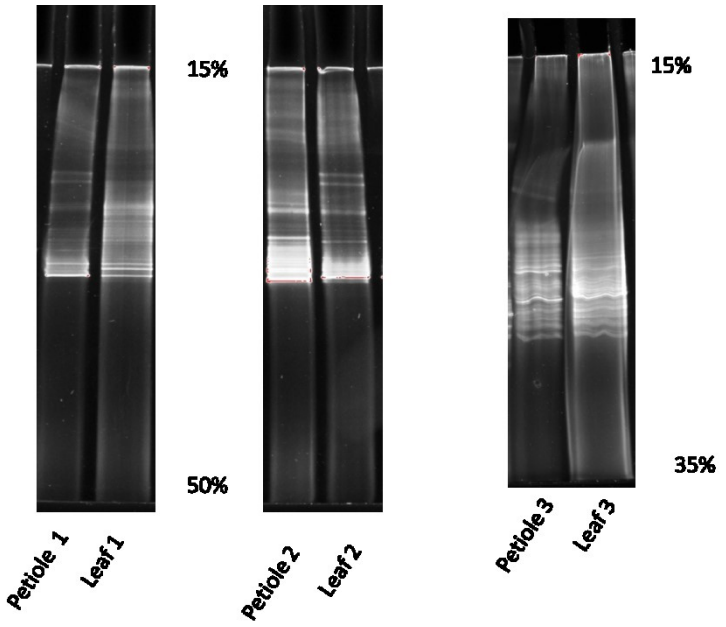

Fig.: 4.6: DGGE profiles of the fungal community in three leaves and petioles of *A. marina* collected in China (2011).

All five morphotypes resulting from DGGE analysis of *A. marina* (Oman), were identified according to the 18S rDNA sequence, they belong all to the phylum: Ascomycota and are members of two orders: Eurotiales (cl. Eurotiomycetes) and Capnodiales (cl.

Dothideomycetes). Out of the DGGE profile of samples collected in China (2009), 14 OTUs were identified. Two of them derive from Basidiomycota (O. Tremellales) and 12 from Ascomycota representing three classes; Dothideomycetes with the orders Capnodiales (3 OTUs) and Pleosporales (7 OTUs), as well as Eurotiomycetes (O. Chaetothyriales) and Sordariomycetes (O. Hypocreales). The five OTUs identified from DGGE profile of the samples collected in China (2011), are all from Ascomycota, one belong to Eutiomycetes (O. Eutiales) and five to Dothideomycetes, the are distributed between Capnodiales (3OTUs), Pleospora and Dothideles.

DGGE was efficient at giving an overall view of the endophytic population in the three samples, the constitution of the endophytic fungal communities is different from those resulting out of the culture depending method, but follow the same tendency, and are different in the two geographic sites and time of collection.

Table 4.2.1. Taxonomic position of uncultered phylotypes from *A. marina,* deducted from the comparison to the ITS sequences in GenBank.

	Organ	Band/ Isolate Code	Putative taxon	18S rDNA sequence lenght	Phylum	Class	Order	% sim.	Closest related from GenBank (Acc. Nr.)
A. marina (Oman)	**Leaf**	B10	*Penicillium* sp.	272	Ascomycota	Eurotiomycetes	Eurotiales	97	JX192598
		B12	*Cladosporium oxysporum*	274	Ascomycota	Dothideomycetes	Capnodiales	99	JQ966538
		B1a	*Cladosporium* sp.	264	Ascomycota	Dothideomycetes	Capnodiales	98	JX273051
		B9	*Penicillium* sp.	273	Ascomycota	Eurotiomycetes	Eurotiales	93	JX192598
		C1	*Aspergillus fumigatus*	275	Ascomycota	Eurotiomycetes	Eurotiales	97	GU980961
A. marina (China 2009)	**Leaf**	CH1	Fungal sp.	273	Ascomycota	Sordariomycetes	Hypocreales	88	FJ490408
		CH2	*Cryptococcus* sp.	273	Basidiomycota	Tremellomycetes	Tremellales	98	FJ153090
		CH3	Fungal sp.	273	Ascomycota	Dothideomycetes	Pleosporales	95	JQ345729
		CH6	*Phaeosphaeria avenaria*	273	Ascomycota	Dothideomycetes	Pleosporales	99	EU189209
		O1	*Ophiosphaerella* sp.	276	Ascomycota	Dothideomycetes	Pleosporales	97	JX273052
		O11	Ophiosphaerella sp.	276	Ascomycota	Dothideomycetes	Pleosporales	99	JX273052
		O4	*Berkleasmium* sp.	276	Ascomycota	Dothideomycetes	Pleosporales	99	DQ280267
		O5	*Boeremia exigua*	276	Ascomycota	Dothideomycetes	Pleosporales	97	DQ359219
		O7	*Didymella* sp.	276	Ascomycota	Dothideomycetes	Pleosporales	97	HQ696086
		O8	*Cryptococcus* sp.	276	Basidiomycota	Tremellomycetes	Tremellales	97	JN656545
	Petiole	CH9	Uncultured ascomycete	273	Ascomycota	Eurotiomycetes	Chaetothyriales	99	EU333020
		M1	*Septoria pachyspora*	276	Ascomycota	Dothideomycetes	Capnodiales	96	JN940650

		M2	*Cercospora acaciae-mangii*	276	Ascomycota	Dothideomycetes	Capnodiales	97	JN938698
		M8	*Septoria pachyspora*	276	Ascomycota	Dothideomycetes	Capnodiales	95	JN940650
A. marina (China 2011)	**Leaf**	L1	*Capnodium dermatum*	284	Ascomycota	Dothideomycetes	Capnodiales	89	AF006724
		L2	*Passalora eucalypti*	290	Ascomycota	Dothideomycetes	Capnodiales	93	GU214558
		L4	Fungal sp.	288				86	JF497107
		L5	Uncultured fungus	299	Ascomycota	Dothideomycetes	Pleosporales	84	FJ490404
		L6	*Aspergillus fumigatus*	286	Ascomycota	Eurotiomycetes	Eurotiales	98	JQ665711
		L7	*Hortaea werneckii*	273	Ascomycota	Dothideomycetes	Dothideales	94	JN546122

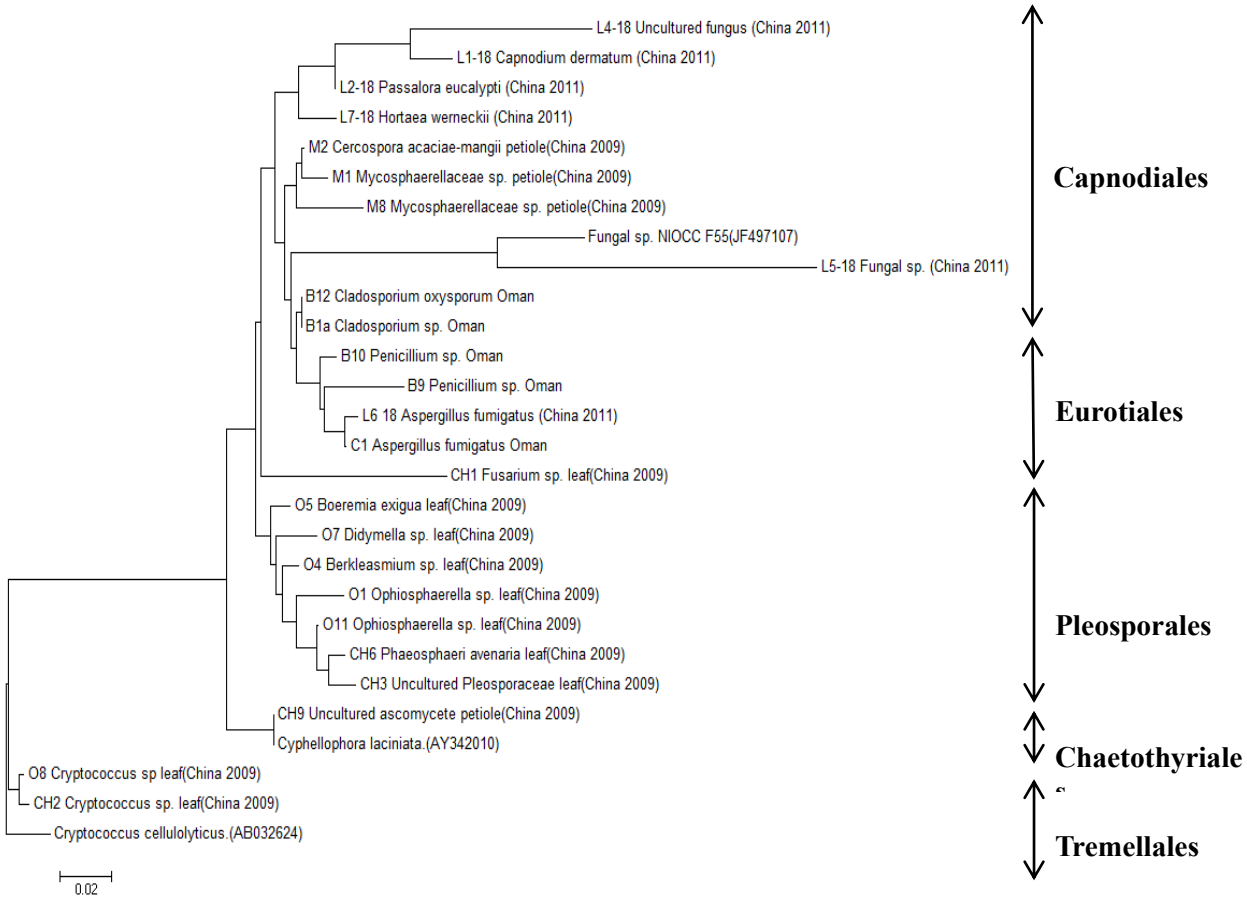

Fig.: 4.7: Phylogenetic analysis performed by Neighbor-Joining method.

The tree was rooted with *Cryptococcus cellulolyticu*

5. Discussion

5.1. Fungal secondary metabolite investigation

Fungi have an enormous contribution to our life. Not only, because of the production of alcohol and bread, which is well known or the role of yeast in the food industry, but also because of consumption of edible mushrooms and cheese, which get their flavors and aroma from the presence of fungi. Fungi have been used for the production of recombinant proteins with great therapeutic potential (Owen *et al.,* 2012), but they are also known for degrading biological matter (Casieri *et al.,* 2010). Hawksworth estimated the number of fungi at 1.5 million species; while other authors see this number ranging from 0.5–9.9 million. Since only 5% of fungal species are currently known and because Fungi are potent producers of a wide range of chemically diverse and biologically important small molecules, millions of potentially bioactive natural products of fungal origin remain to be discovered (Hawksworth, 2001).

When using traditional methods of natural products investigation, it occurs frequently, that after a long purification process, the result is only a re-isolation of known and trivial natural products. Improving the efficiency of isolation and structural elucidation processes as well as the selection, screening, dereplication methods, more extensive collections of fungal species, and further improvements of culturing methods are necessary to improve the discovery of novel natural product templates, which are still a viable source of new drug candidates over the last 20 years (Butler, 2004; 2008; Aly *et al.*, 2011).

In the present study, an advanced HPLC systems with an internal library, which is extremely valuable for dereplication of compounds previously isolated, as well as HPLC/ESI-MS, which is known to be a sensitive ionization technique suitable for small and large molecular-weight natural products were used. All of these techniques coupled with chromatographic techniques and guided with different bioassays led to the isolation of 11 new natural products: four farinomaleins (**2-5**), an isoindoline (**6**), five flavipin derivatives (**12-16**) and an isomer of pestalotiopamide B (**20**).

5.2. Farinomalein derivatives from AMO 3-2

The isolate AMO 3-2 is an endophytic fungus obtained from the mangrove plant *Avicennia*

marina growing in Oman. It proved to be unamenable to taxonomic identification either by morphological characteristics or by molecular methods (ITS sequence). When cultured on rice, most of its secondary metabolites extracted with EtOAc and screened with HPLC-UV demonstrated a UV spectrum known to be characteristic for maleimide derivatives. They are all farinomalein derivatives. To the best of our knowledge, only two farinomalein derivatives have been isolated so far, farinomalein A (Putri *et al.,* 2009) and its derivative pestalotiopsoid A (Xu *et al.,* 2009). The first compound was obtained from the entomopathogenic fungus *Paecilomyces farinosus* isolated from a lepidopteran larval cadaver and the second from *Pestalotiopsis* sp. isolated from the Chinese mangrove plant *Rhizophora mucronata.*

Chemical investigation of AMO 3-2 yielded the known compound farinomalein (**1**) and its methyl ester (**2**), which is isolated for the first time as a natural product, together with three other new farinomalein derivatives (**3**-**5**).

A plausible biogenetic pathway of farinomalein is proposed (Fig. 5.1.). The deamination of valine and subsequent oxidation would give rise to 3-methyl-2-oxobutanoic acid, which then could condense with acetyl-CoA to yield the intermediate molecule, 2-isopropylfumaric acid. This dicarboxylic acid may react with 3-aminopropanoic acid to form farinomalein.

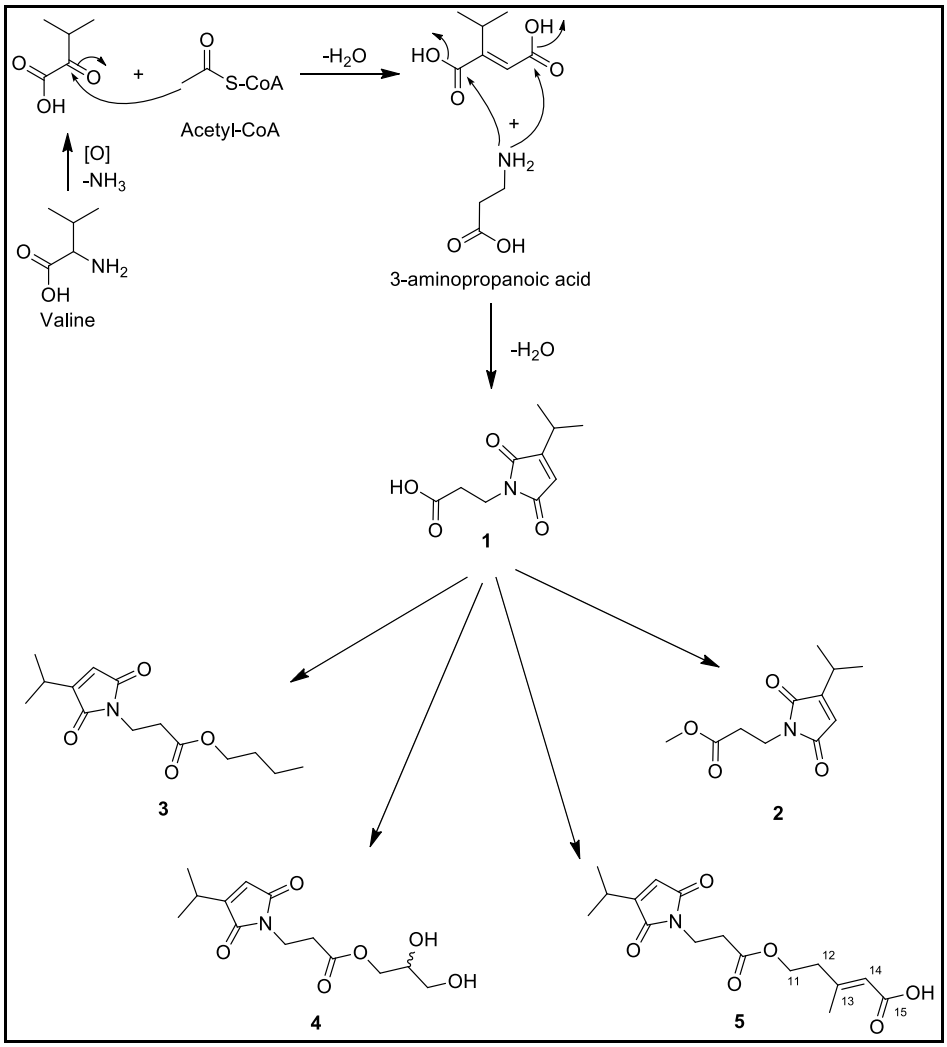

Fig. 5.1. Proposed biogenetic pathway of farinomalein.

Since maleimide derivatives such as *N*-methylmaleimide, *N*-ethylmaleimide, and phenylmaleimide PM-20 have been found to be cytotoxic toward different human tumor cell lines through the inhibition of topoisomerase II (Jensen *et al*., 2002), we tested the farinomaleins for their cytotoxicity (MTT-assay) against the mouse lymphoma cell line L5178Y, but only compound **2** showed a moderate activity with a IC_{50} value of 4.4 μg/mL. Farinomaleins have a maleimide ring, with isopropyl substitution; this may explain the differences in the activity.

When evaluated for their antimicrobial activities against *Staphylococcus aureus* ATCC 29213, *Streptococcus pneumoniae* ATCC 49619, *Escherichia coli* ATCC 25922, none of the

farinomaleins exhibited any significant activity at a concentration of 64 µg/mL. Farinomalein A (**1**) was reported to have a potent activity against the plant pathogen *Phytophthora sojae,* with an MIC value of 5 µg/disk, when compared with the antifungal agent amphotericin B, which showed a MIC value of 10 µg/disk (Putri *et al.,* 2009). Our tests against different plant or human pathogen fungi like *Alternaria solani*, *Candida albicans*, *Candida krusei*, *Aspergillus fumigatus* and *Aspergillus faecius* could not show the same trend.

5.3. Other secondary metabolites from AMO 3-2

Beside the farinomalein derivatives, two other compounds were also isolated from the EtOAc- extract of the marine derived AMO 3-2, namely (*R*)-5,7-dihydroxy-3-methylisoindolin-1-one (**6**) and *p*-hydroxyphenylacetic acid (**7**).

p-Hydroxyphenylacetic acid was reported to enhance the growth of red alga *Porphyra tenera conchocelis* (Fries & Iwasaki 1977). Papadopoulos and co-workers found that *p*-hydroxyphenylacetic is a potent antioxidant. The latter was isolated as a mixture with (*R*)-5,7-dihydroxy-3-methylisoindolin-1-one, which was also obtained in pure form (**6**). Both compounds didn't show any activity when evaluated for their cytotoxic or antimicrobial activities.

5.4. Flavipin derivatives from *Epicoccum nigrum*

In this study, the fungal strain *Epicoccum nigrum* was isolated from flowers of *Mentha suaveolens Ehr.* growing wild in Morocco. It was cultured on rice medium and extracted with EtOAc to yield five known natural products (**8**-**9** & **17**) and five new secondary metabolites (**12-16**).

The ascomycete *E. nigrum* is distributed worldwide and has been frequently isolated as an endophyte (Hilair *et al*., 2008; Abdel-Lateff *et al*., 2003; Favaro *et al.,* 2012). More than 70 species in the *Epicoccum* genus have been described but latter classified as one variable species, *E. nigrum* Link. (Schol-Schwarz, 1959).

E. nigrum has been used as a biological control agent for plant pathogens (Hashem *et al.*, 2004), it is known to produce a variety of bioactive secondary metabolites such as flavipin

(Bamford *et al*., 1961), epicorazins A-B (Baute *et al.,* 1978), epirodin (Ikawa *et al.,* 1978), epicocconone (Bell *et al.,* 2003) and other compounds with various activities ranging from antioxidant activity (Abdel-Lateff *et al*., 2003) to inhibition of HIV-1 replication (Shu *et al*., 1997).

The compounds isolated in this study exhibited a variety of activities. MTT test revealed pronounced cytotoxicity of epicoccine (**8**) against L5178Y with IC_{50} values of 1.9 µM. 5-methoxy-7-methyl-1,3-dihydroisobenzofuran-4,6-diol (**9**) was found to be active against the sensitive human ovarian cancer cell line A2780 sens with an IC_{50} value of 15.8 µM, while compounds **12**, **14** and **16** displayed a pronounced activity against a panel of protein kinases (Table 3.2.2) though compound **14** seemed to be selective for protein kinases IGF1-R and AXL with IC_{50} values of 0.44 µM and 1.02 µM, respectively, while compounds **12** and **16** (which was active in nM range against several protein kinases (IC_{50})), seems to be multikinase inhibitors. Compounds **10**, **11** and **14** showed a moderate activity against methicilin resistant *Staphylococcus aureus* (MRSA) with EC_{50} values of 31.25 µg/mL (compounds **10** and **14**) and 15.6 µg/mL for compound **11**. Compound **17** was reported as antibacterial and antifungal agent isolated from *Aspergillus flavipes* (DSM 15290) (WO 2005/047275).

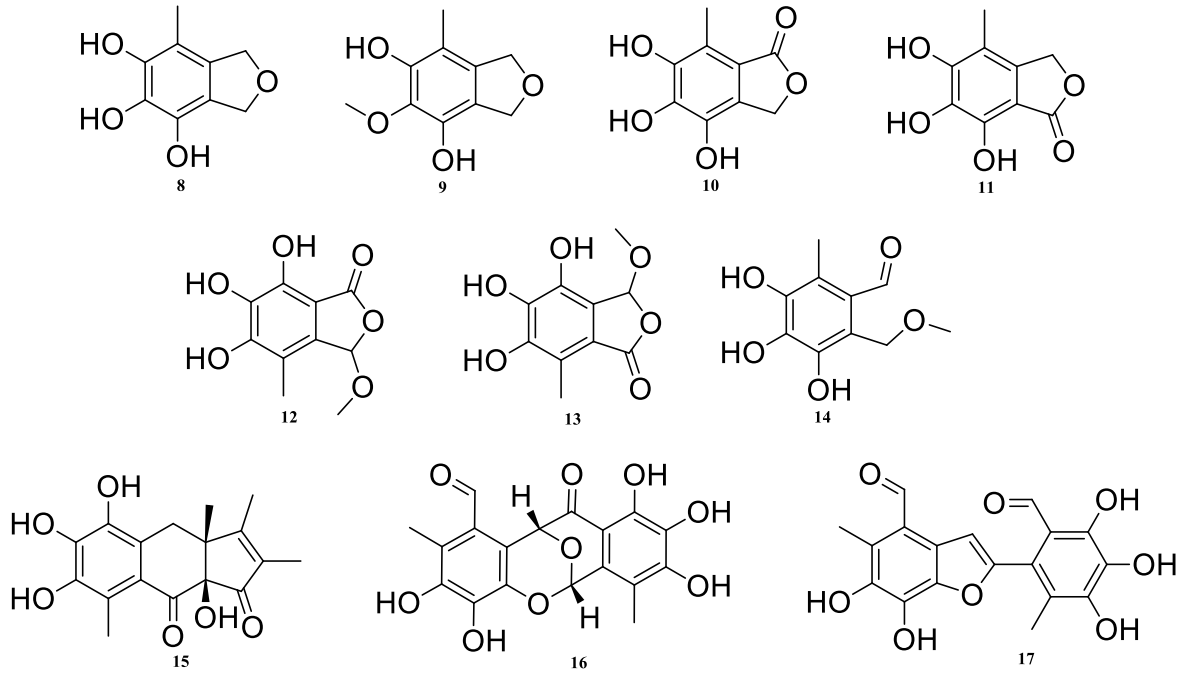

Fig. 5.2. Compounds isolated from *Epicoccum nigrum*

All compounds seem to have the same biosynthetic origin, they all have the same arrangement of the benzene ring of flavipin, which is a fully substituted benzene ring. Beside two aldehyde groups and three adjacent hydroxyl groups, flavipin has also a methyl group functionality in the aromatic ring. A methylation of an aldehyde group of flavipin could yield **14**, while **16** is a product of a condensation of two flavipin moieties. Petterson (1965) used ^{14}C to determine the biosynthesis steps of flavipin to illustrate that the latter is built following polyketide pathway with orsellinic acid and 2,4-dihydroxy-5,6-dimethylbenzoic acid as possible intermediates.

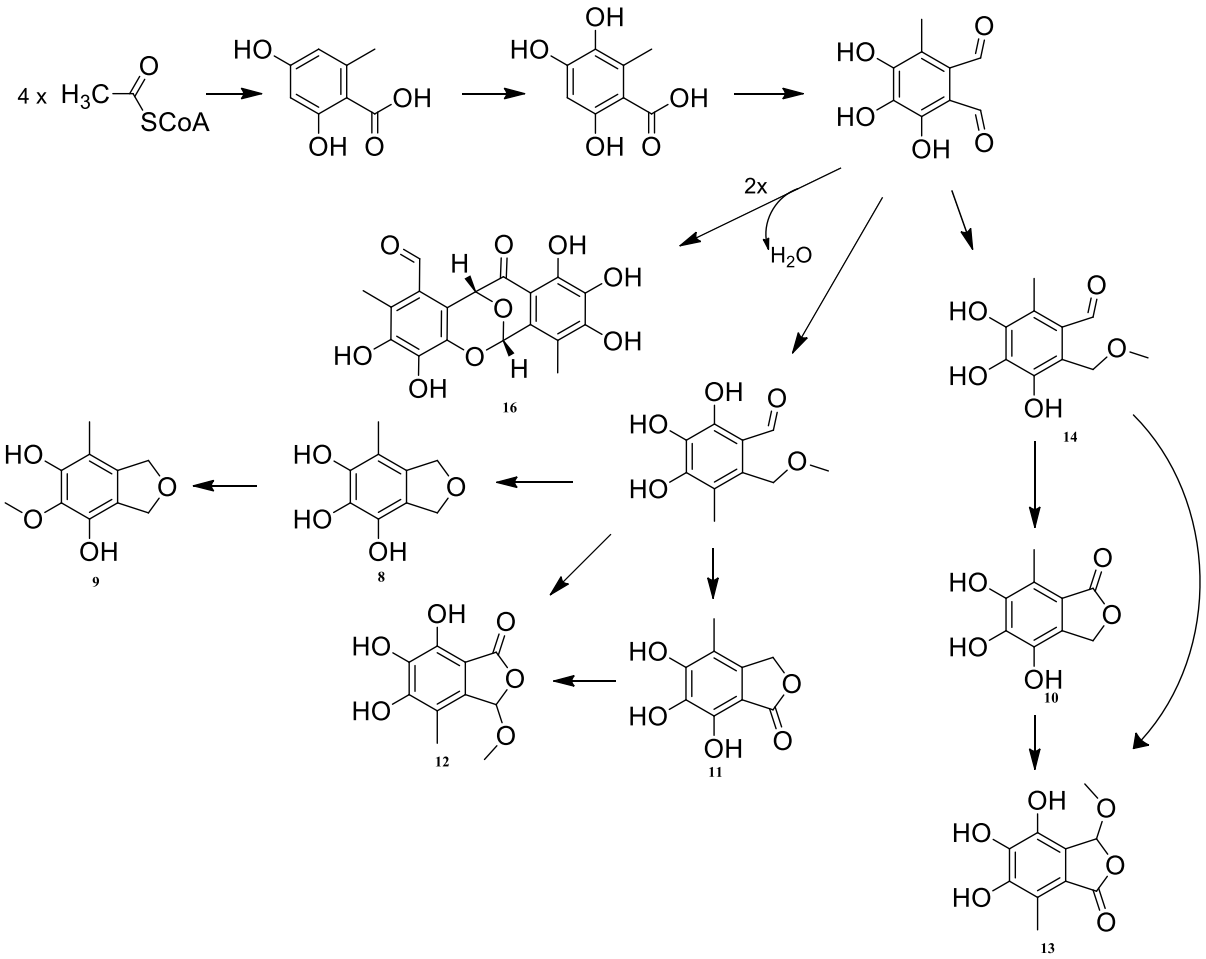

Fig. 5.3. Proposed biogenetic pathway of *Epicoccum nigrum* compounds. Flavipin biosynthesis pathway was suggested and partially confirmed by Petterson (1965).

5.5. Secondary metabolites from *Aureobasidium pullulans*

The isolate *Aureobasidium pullulans* was obtained from leaves of *Aloe vera* collected in Morocco. The EtOAc extract of rice culture showed cytotoxic activity against the mouse lymphoma cell line L5178Y in contrast to the pure compounds **18–23**, which did not exhibit any significant activity at a concentration of 10 µg/mL.

Six compounds were isolated from the solid rice cultures; namely indole-3-carboxylic acid (**18**), 1*H*-indole-3-carbaldehyde (**19**), the new secondary metabolite (*Z*)-4-(5-acetoxy-3-methylpent-2-enamido)butanoic (**20**), isoochrascinic acid (**21**), 6-hydroxyisosclerone (**22**) and 3,4,6,8-tetrahydroxy-3,4-dihydronaphthalen-1(2*H*)-one (**23**).

The (*E*)-isomer of compound **20** was reported as natural product of *Pestalotiopsis* sp. isolated from the plant *Rhizophora mucronata* collected in south China (Xu *et al*., 2011). The fungal strain *Aureobasidium pullulans* is a yeast-like fungus in the Ascomycota class Dothideomycetes (Schoch *et al.,* 2006). This ubiquitous fungus is widespread and can be found in oligotrophe environments. It can also be found in stressed environments, such as in hypersaline waters (Gunde-Cimerman *et al*., 2000), but also as an endophyte of plants such as grapevine **(**Martini *et al.,* 2009). *A. pullulans* isolates exhibit antagonistic activity against a number of phytopathogenic fungi (Schena *et al*., 1999; 2003). The adaptation of *A. pullulans* to different environmental conditions could be the result of its richness in genes capable to synthetize different secondary metabolites, which support the survival and proliferation of the fungus.

5.6. Compounds isolated from *Stemphylium globuliferum*

Leaf tissues of the traditional medicinal plant *Mentha pulegium* (Lamiaceae) growing in Morocco were the source, from which *Stemphylium globuliferum* was isolated. The leaves of *M. pulegium* are used in traditional medicine to treat common colds and disorders of the liver and gall-bladder, as a carminative, as a diuretic, and to stimulate digestive action (Stahl-Biskup and Schultz, 2006).

Two compounds were isolated from the EtOAc extract of the solid rice cultures, tetrahydroaltersolanol B (**24**), and alterporriol O (**25**).

When evaluating the cytotoxic activity of the isolated compounds from the fungus *Stemphylium globuliferum* toward L5178Y cell line using the MTT assay, no significant activity of these compounds at a concentration up to 10 µg/mL was found.

The biosynthesis of anthraquinones in fungi is not well known, but it is confirmed, that fungi build anthraquinones by condensation of acetate and malonate to an octaketide chain (Stoessl *et al*., 1983; Suemitsu *et al*., 1989; Ohnishi *et al*., 1992). A fungal polyketide synthase catalyzes this reaction, it follows the loss of carboxylic acid carbon from the terminal unit at C-3, any other details about dehydration and hydroxylation steps are not well known (Fig. 4.4).

It is possible that the anthraquinones that are formed from altersolanol share a common biogenetic origin whith it (Stoessl, 1969). Indeed, altersolanol A was previously isolated from the same extract of *Stemphylium globuliferum*. It is obvious, that compound (**24**) is related to altersolanol A, because they all share the same substitution in the aromatic ring and a methyl group in their aliphatic ring.

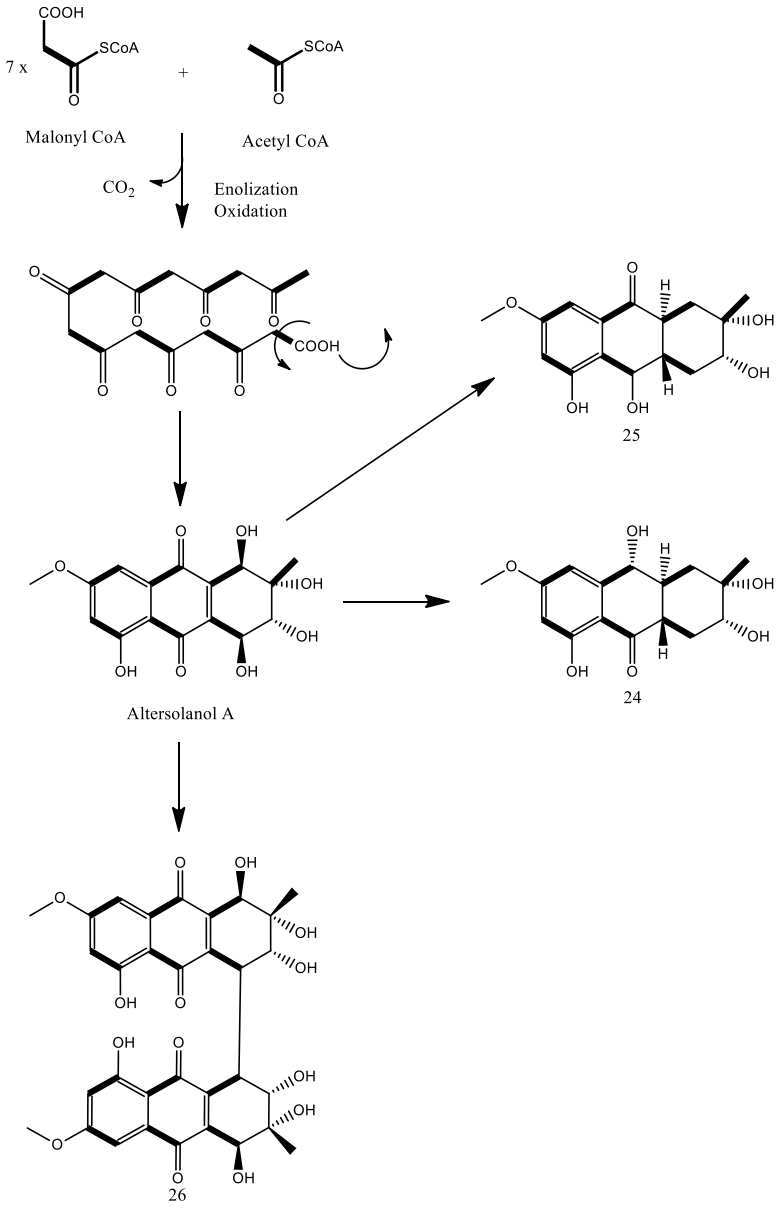

Fig. 5.4: Biosynthesis of altersolanol and modified anthraquinones (Stoessl *et al*., 1983; Suemitsu *et al*., 1989; Ohnishi *et al*., 1991; 1992).

5.7. Biodiversity screening of endophytic fungi

5.7.1. Molecular identification method

Precise identification and classification of fungi to the species level (if possible) is critical to the study of natural products. Without proper identification, chemical investigations of fungi become more difficult to reproduce (Bugni *et al.,* 2004).

When morphological characters are inadequate, convergent, reduced, missing or overlapping, establishing taxonomic relationships become difficult. The traditional morphological approaches to fungal systematics are problematic and frequently fail to provide a solid evolutionary framework, particularly at the species level. It is not only because of the lack of characters useful for grouping species but also because some fungi (*Mycelia sterilia*) do not produce any known spores, either sexual or asexual, which make their identification with morphological methods impossible (Geiser, 2004).

Many taxonomists have combined available morphological characters with biochemical or molecular characters to clarify taxonomic relationships, as well as to infer phylogenies among fungal species.

The absence of a universally accepted “DNA barcode” for fungi is a serious limitation for multitaxon ecological and biodiversity studies (Schoch *et al.,* 2012). Hebert and his research group (Hebert *et al.,* 2003) imagine the ideal DNA barcode as standardized 500- to 800-bp sequences to identify species of all eukaryotic kingdoms using primers that are applicable for the broadest possible taxonomic group. Reference barcodes must be derived from expertly identified vouchers deposited in biological collections with online metadata and validated by available online sequence chromatograms. Interspecific variation should exceed intraspecific variation (the barcode gap), and barcoding is optimal when a sequence is constant and unique to one species. Ideally, the barcode locus would be the same for all kingdoms. In the absence of universal barcodes, the gene of choice to assess phylogenetic relationships and resolve taxonomic questions at different taxonomic levels has been the ribosomal DNA (rDNA) gene (Jeewon *et al.,* 2003; Duong *et al.,* 2006).

5.7.2. Identification using rDNA

Studying the phylogeny and ecology of these organisms is depending on a growing database of DNA sequence, offering information about a wide spectrum of microbial eukaryotes. Aiming at improve our understanding of the evolutionary relationships among the taxa was one of the initial impulse for the acquisition of rDNA gene sequence information for microbial eukaryotes, which arose in the 1980s and 1990s (Schlegel, 2003). These researches provided precious support for understanding the evolution of eukaryotic organisms and continue to facilitate the generation, testing, and modification of numerous hypotheses related to this topic (Adl *et al.,* 2005; Baldauf, 2003).

The ribosomal DNA genes (rDNA) are suitable for identification of fungi due to many reasons. These genes (Fig.: 5.7.1.) occur in multiple copies with up to 200 copies per haploid genome arranged in tandem repeat or clusters (Karp *et al*., 1999; Hibbet, 1992). They are relatively small, highly stable and contain a mosaic of conserved and diverse regions. The ribosomal gene cluster includes three regions coding for the small subunit ribosome genes (SSU or 18S) and long subunit ribosome genes (LSU or 28S) which are separated by two intergenic transcribed spacers (ITS1 and ITS2) region Surrounding from both sides the 5.8S rRNA gene. Each cluster is separated from the next cluster by intergenic spacer (IGS) region which comprises two spacers, non-transcribed spacer (NTS) and external transcribed spacer (ETS) that serves to separate the repeats or clusters from one another on the chromosomes (Guarro *et al*., 1999). Although these rDNA genes are present as tandem repeats, they evolve as a single unit even though the rate of evolution may vary within individual regions of the ribosomal DNA cluster. Therefore, they can be used to compare organisms at several levels (Dixon and Hillis, 1991).

The ITS regions and the nuclear small subunit ribosomal DNA (18S rDNA) were selected for identification in this study for several reasons. First, many established universal fungal primers are based on the conserved regions of sequences, making it possible to obtain the PCR products from most of the fungi for sequencing (White *et al.,* 1990; Smit *et al.,* 1999). Second, the large number of sequences in GenBank makes similarity searches convenient, though the most frequently sequenced region for such purposes is the ~550 base-pair (bp) long internal transcribed spacer (ITS) region of the nuclear ribosomal DNA (Hibbett *et al.,*

2005).

Finally, the repetitive nature of rDNA, over 100 copies of which usually exist per fungal genome, makes it relatively straightforward to amplify even from scanty input material.

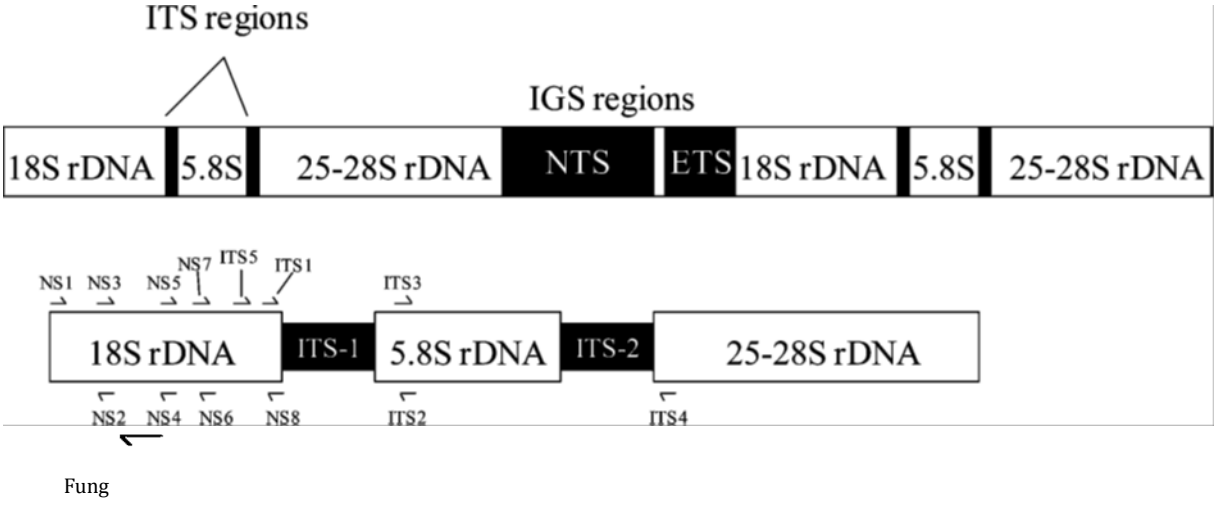

Fig.: 5.7.1. Fungal rDNA gene cluster with an expansion showing common primer sites (modified after Bugni and Ireland, 2004)

5.7.3. Primer choice

ITS 1 and ITS 4 are known as universal primers which allow the amplification of both ITS regions and the 5.8S gene. They can be used to amplify the DNA of most fungi, from the phyla Oomycotina, Ascomycotina until Basidiomycotina, which was confirmed in this study, many fungi could be identified down to the species level, including members of the genera *Thielavia*, *Corynespora*, *Cladosporium*, *Pestalotiopsis*, *Glomerella*, as well as some species from the genus *Alternaria* (*A. solani, A. alternate* and *A. arborescens*).

Many fungi from the genus *Aspergillus* cannot be identified based on the DNA sequences of ITS region down to the species level, because the low variation between members of this genus. However, based on ITS sequences, it is usually possible to assign a given strain to section or subgenus level (within the genus *Aspergillus*), especially in the sections Flavi and Nigri (Magnani *et al.,* 2005; Glass *et al.,* 2005).

For DGGE Analysis, the Primer set NS1/GCfung was used. Since all assays conducted using the primer pair ITS1/ITS4 did not give any results, we chose the set NS1/GCfung, reported

successfully from other groups (Duong *et al.,* 2004; 2006). This primer pair targets a ~320 bp sequence located on the 18S rDNA.

5.7.4. Biodiversity screening with culture dependent method.

Schmit and Mueller (2007) estimate the number of endophyte species detected in plant between 500,000 and 600,000 worldwide; this number is increasing every year, but approximately 465,000 of them are not described yet (Sieber, 2007). The identification of this large number of species is coupled with many problems, like the high genetic variability of endophytic fungi (Arnold *et al*. 2000) or the large number of host species. Frequently, endophytic isolates do not sporulate in culture media so morphological description turns into an insufficient method for fungi classification (Fröhlich *et al*., 2000; Baayen *et al.,* 2002; Lacap *et al.,* 2003). In average up to 20% of the population of fungal endophytes can be *Mycelia sterilia*. However, this can increase up to 54% of the population (Fisher *et al.,* 1994). The definition of the concept "morphotype" as a "group of morphologically differentiated individuals of a species of unknown or of no taxonomic significance" (Hawksworth *et al*. 1995), makes cultural characteristics of fungi more helpful as complementary data for the molecular identification (Guo *et al.,* 2003; Lacap *et al.,* 2003). The use of phylogenetic analysis in combination with this concept (morphotype or morphospecies) in the identification for endophytic fungi increased rapidly (Botella *et al*., 2011; Albrectsen *et al*., 2010; Sánchez Márquez *et al.,* 2010), however there are also problems with this methodology. Due to the lack of similar sequences can be blasted in GenBank, many taxa cannot be identified to the species level (Pinruan *et al.,* 2010; Botella *et al.,* 2011). Other problems are ascribable to big number of wrong identified species in GenBank, it has been shown that 96% of names under *Colletotrichum gloeosporioides* have been wrongly applied (Cai *et al.,* 2009).

By using sequencing of the ITS rDNA region as a useful and quick method of endophyte identification in combination with phylogenetic analysis we aimed at minimizing those problems. Only 12% of the isolated fungal endophytes couldn't be identified to the species level and showed a similarity rate inferior to 97% with the sequences available in GenBank. From the thirtythree different morphotypes, *Nigrospora oryzae, Cladosporium colombiae, Glomerella acutata* and *Thielavia microspora* ocured twice, respectively, which reduce the

number of different genotypes to 29. To assign the unidentified sequences (fungal endophytic isolates), a phylogenitc analysis was performed by adding some reference sequences from GenBank, and this served as confirmation of the blast results. The fungal endophytic populations were totally different between all three samples. While in the sample collected in Oman, the genra *Thielavia* and *Alternaria* were dominating, they were not even represented in the fungal communities in both samples collected in China. *Thielavia* fungi as endophytes were first reported by Li *et al.* (2007).

The groups of endophytic fungi isolated from the samples collected in China in 2009 and 2011 share only a common genus (*Nigrospora*), but when considering the order level, they have 3-4 members from Xylariales, which belong to the class of Sordariomycetes commonly found in family Fagaceae (Arnold, 2007). Xylariales which is known to mostly have foliar endophytes, was the most abundant in *A. marina* (China 2009), but represented mostly with the very common genus *Pestalotiopsis* (especially: *Pestalotiopsis neglecta* and *Pestalotiopsis heterocornis*). Strobel *et al*. (2000) obtained four endophytic *Pestalotiopsis* species in bark of *Fragraea bodenii* in Papua New Guinea. Hyde (2000) found 14 endophytic *Pestalotiopsis* species in three plants, belonging to *Goodeniaceae*, *Aizoaceae* and *Chenopodiaceae*.

5.7.5. Biodiversity screening with a culture independent method (DGGE).

DGGE was performed in combination PCR using NS1/GCfung as primer set, which allow amplifying a ~320 bp sequence from the SSU (18S rDNA). Twenty-five OTUs were characterized, about 40 % showed a similarity ratio less than 97 % when compared with sequences from GenBank, due to the lack of published sequences but may be also, because the sequence used is too small.

A phylogenetic analysis was performed by Neighbor-Joining method, reference sequences available in the GenBank were added as reference. The results show two Basidiomycetous OTUs not identified with culture method. Arnold and co-workers (2007) reported a fourfold increase in the number of Basidiomycetous species recovered from leaves of *Pinus taeda* when endophyte communities were assessed using culture-free methods (environmental PCR of surface-sterilized foliage).

The dominating orders are Pleosporales (7 OTUs in *A. marina* China, 2009 and 1 OUT from *A. marina* China, 2011) and Capnodiales (3 OTUs in *A. marina* - China, 2009; 2 OUT from *A.*

marina-China, 2011 and 2 OTUs from *A. marina*-Oman), both belongs to the class Dothideomycetes. Eurotiales was the abundant order in the fungal endophytic population of *A. marina* (Oman), with two different *Penicillum sp.* and *Aspergillus fumigatus*, the latter was also detected by *A. marina* (China, 2009) as the only member of Eurotiales.

Endophyte diversity depends on host identity (Higgins *et al.,* 2007) and on geographic situation (Thomas *et al.,* 2008; Herrera *et al.,* 2011).

DGGE was efficient at giving an overall view of the endophytic population in the three different samples; the number of characterized OTUs was comparable with the cultured isolates. On DGGE gels, the sequencing of DNA isolated from some bands located close to each other revealed identical DNA sequences. As we know from previous studies, a single species can show more than one band in DGGE due to multiple copies of the same DNA with slight genetic variations (Nübel *et al.,* 1996).

Both the results of DGGE or the culture dependent method follow the same tendency and confirm that the fungal endophytic population varies according to the geographic site and/or time period.

6. Conclusion

Endophytic fungi, isolated from terrestrial or mangrove plants, produce natural products with a large chemical and structural diversity. Some of them might be suitable for specific medicinal applications, especially those showing biological activities in pharmaceutically relevant bioassay systems. The latter represent potential lead structures and could be optimized to yield effective therapeutic and bioactive agents.

Four endophytic fungi were investigated as biological sources for the study, namely *Epicoccum nigrum*, *Stemphylium globuliferum*, *Aureobasidium pullulans* and the unidentified isolate AMO 3-2 with the aim of isolating secondary metabolites from endophytic fungi, followed by structural elucidation and examination of their pharmacological potential. The fungi were grown in solid rice medium for a period of three to four weeks. The extracts obtained were then subjected to different chromatographic separation techniques till secondary metabolites were isolate in pure form.

Structural elucidation of the isolated secondary metabolites was performed using state-of-the-art analytical techniques, including mass spectrometry (MS) and nuclear magnetic resonance (NMR) experiments. Finally, the isolated compounds were subjected to various bioassays to examine their anti-microbial, antifungal and cytotoxic activities as well as inhibitory profiles towards selected protein kinases.

1. AMO 3-2.

Five farinomalein derivatives including four new compounds, farinomaleins B-E, and one new isoindoline congener ((*R*)-5,7-dihydroxy-3-methylisoindolin-1-one) as well as the known secondary metabolite *p*-hydroxyphenylacetic acid were isolated from the unidentified endophytic fungus AMO 3-2, obtained from the inner tissues of healthy leaves of the mangrove plant *Avicennia marina* from Oman. The structures of the new compounds were unambiguously elucidated on the basis of their mass, as well as one and two dimensional NMR spectroscopic data. When evaluated for their cytotoxicity against the mouse lymphoma cell line L5178Y, only farinomalein B showed a moderate activity.

2. *Epicoccum nigrum.*

The fungal strain *Epicoccum nigrum* was isolated from *Mentha suaveolens* growing in

Morocco. Five new compounds were obtained from this fungal strain, namely epicoccone C, epicoccone D, 2,3,4-trihydroxy-6-(methoxymethyl)-5-methylbenzaldehyde, 5,6,7,9a-tetrahydroxy-2,3,3a,8-tetramethyl-3a,4-dihydro-1*H*-cyclo-penta[b]naphthalene-1,9(9a*H*)-dione and 3,4,8,9,10-pentahydroxy-2,7-dimethyl-11-oxo-11,12-dihydro-6*H*-6,12-epoxydibenzo[*b,f*]-oxocine-1-carbaldehyde and five known compounds including epicoccine, 5-methoxy-7-methyl-1,3-dihydroisobenzofuran-4,6-diol, epicoccone A, epicoccone B and 2-(2-formyl-3,4,5-trihydroxy-6-methylphenyl)-6,7-dihydroxy-5-methylbenzofuran-4-carbaldehyde.

These compounds showed different activities, starting from cytotoxic activity against L5178Y cells or against the sensitive human ovarian cancer cell line A2780 sens and against methicilin resistant *Staphylococcus aureus* (MRSA) as well as against several protein kinases.

3. *Aureobasidium pullulans.*

Aureobasidium pullulans was isolated from *Aloe vera*. From this fungus, two indole derivatives, isoochracinic acid, 6-hydroxyisosclerone and its derivative as well as the new natural product (*Z*)-4-(5-acetoxy-3-methylpent-2-enamido)butanoic acid. None of this compounds revealed significant activity in the cytotoxicity (MTT) assay against L5178Y cell line.

4. *Stemphylium globuliferum*.

The extract of the fungal strain *Stemphylium globuliferum*, isolated from *Mentha pullegium*, yielded two known anthrachinone derivatives, namely tetrahydroaltersolanol B and alterporriol O. These compounds did not show activity in cytotoxicity assay or against multiresistant bacteria.

A total of twentyfive compounds were isolated in this study, eleven of which were identified as new natural products. Both known and new compounds were tested for their biological activities using different bioassay systems.

Fungal diversity in the mangrove plant *Avicenna marina* was assessed with culture independent method using polymerase chain reaction (PCR) coupled with denaturing gradient gel electrophoresis (DGGE) as well as a culture based method, which consist of isolating the endophytic fungi and identifying them separately. Both a small sequence from

the SSU and form ITS regions were used to identify the isolates,

A phylogenetic analysis was performed and reference sequences from GenBank served as reference to classify OTUs, which could not be identified by blast comparison with GenBank sequences.

While both methods delivered different fungal communities, the results of DGGE or the culture dependent method followed the same tendency and confirmed that the fungal endophytic population varies following the geographic situation and time period.

7. References

Ainsworth GC, Bisby GR (1983) Ainsworth & Bisby's dictionary of the fungi. Commonwealth Agricultural Bureaux [for the] Commonwealth Mycological Institute.

Ayer WA, Browne LM, Lin G (1989) Metabolites of Leptographium wageneri, the causative agent of black stain root disease of conifers. Journal of natural products 52:119–129.

Bacon, C. W., and White, J. F. (2000). Microbial Endophytes, Marcel Dekker inc. New York, pp 341-388.

Bamford PC, Norris GLF, Ward G (1961) Flavipin production by Epicoccum spp. Transactions of the British Mycological Society 44:354–356.

Banerji J, Rusconi S, Schaffner W (1981) Expression of a beta-globin gene is enhanced by remote SV40 DNA sequences. Cell 27:1483–1495.

Bell PJL, Karuso P (2003) Epicocconone, A Novel Fluorescent Compound from the Fungus Epicoccum nigrum. J Am Chem Soc 125:9304–9305.

Bergmann S, Schümann J, Scherlach K, Lange C, Brakhage AA, Hertweck C (2007) Genomics-driven discovery of PKS-NRPS hybrid metabolites from Aspergillus nidulans. Nat Chem Biol 3:213–217.

Bhagobaty RK, Joshi SR (2011) Multi-loci molecular characterisation of endophytic fungi isolated from five medicinal plants of Meghalaya, India. Mycobiology 39:71–78.

Borgschulte K, Rebuffat S, Trowitzsch-Kienast W, Schomburg D, Pinon J, Bodo B (1991) Isolation and structure elucidation of hymatoxins B-E and other phytotoxins from Hypoxylon mammatum fungal pathogen of Leuce poplars. Tetrahedron 3:8351–8360.

Brands M, Endermann R, Gahlmann R, Krüger J, Raddatz S (2003) Dihydropyrimidinones—a

new class of anti-staphylococcal antibiotics. Bioorganic & medicinal chemistry letters 13:241–245.

Bringmann, G., Lang G., Steffens, S., and Schaumann, K. (2004). Petrosifungins A and B, novel cyclodepsipeptides from a sponge-derived strain of *Penicillium brevico- mpactum*. *J*. *Nat*. *Prod*., **67**, 311–315.

Butler, M. S. (2005). Natural products to drugs: natural product derived compounds in clinical trials. *Nat*. *Prod*. *Rep*., **22**, 162-195.

Butler, M. S. (2008). Natural products to drugs: natural product-derived compounds in clinical trials. *Nat*. *Prod*. *Rep*., **25**, 475-516.

Caron DA, Countway PD, Savai P, Gast RJ, Schnetzer A, Moorthi SD, Dennett MR, Moran DM, Jones AC (2009) Defining DNA-Based Operational Taxonomic Units for Microbial-Eukaryote Ecology. Applied and Environmental Microbiology 75:5797–5808.

Chandra S (2012) Endophytic fungi: novel sources of anticancer lead molecules. Appl Microbiol Biotechnol 95:47–59.

Chen M-D, Zhou X, He M-Z, Ruan Y-P, Huang P-Q (2004) A Versatile Approach for the Asymmetric Synthesis of 3-Alkyl-2,3-dihydro-1H-isoindolin-1-ones. ChemInform 35:DOI: 10.1002/chin.200422132.

Cragg, G. M., and Newman, D. J. (2001). Natural product drug discovery in the next millennium. *Pharmaceut*. *Biol*., **39** (Suppl.), 8-17.

Cragg, G. M., Newman, D. J., and Snader, K. M (1997). Natural products in drug discovery and development. *J*. *Nat*. *Prod*., **60**, 52-60.

De Souza JJ, Vieira IJC, Rodrigues-Filho E, Braz-Filho R (2011) Terpenoids from endophytic fungi. Molecules 16:10604–10618.

Debbab, A., Aly, A. H., Lin, W. H., and Proksch, P. (2010). Bioactive compounds from marine

bacteria and fungi. *Micob*. *Biotechnol*., **3**, 544-563.

Ebada SS, Proksch P (2011) Chemical and pharmacological significance of natural guanidines from marine invertebrates. Mini Rev Med Chem 11:225–246.

El Amrani M, Debbab A, Aly AH, Wray V, Dobretsov S, Müller WEG, Lin W, Lai D, Proksch P (2012) Farinomalein derivatives from an unidentified endophytic fungus isolated from the mangrove plant Avicennia marina. Tetrahedron Letters 53:6721–6724.

Evidente A, Superchi S, Cimmino A, Mazzeo G, Mugnai L, Rubiales D, Andolfi A, Villegas-Fernández AM (2011) Regiolone and Isosclerone, Two Enantiomeric Phytotoxic Naphthalenone Pentaketides: Computational Assignment of Absolute Configuration and Its Relationship with Phytotoxic Activity. European Journal of Organic Chemistry 2011:5564–5570.

Fináková S, Proksa B, Sturdíkova M (2007) Biosynthesis and biological activity of enniatins. Pharmazie 62:563–568.

Frederick CB, Bentley MD, Shive W (1981) Structure of triornicin, a new siderophore. Biochemistry 20:2436–2438.

Gilbert ND (2010) The 10 × ’20 Initiative: Pursuing a Global Commitment to Develop 10 New Antibacterial Drugs by 2020. Clin Infect Dis 50:1081–1083.

Grove, J.F., MacMilan, J., Mulholland, T.P.C., and Rogers, M. (1952). Griseofulvin. Part IV. The structures. J. Chem. Soc., 3977-3987.

Guo B, Dai JR, Ng S, Huang Y, Leong C, Ong W, Carté BK (2000) Cytonic acids A and B: novel tridepside inhibitors of hCMV protease from the endophytic fungus Cytonaema species. J Nat Prod 63:602–604.

Guo B, Wang Y, Sun X, Tang K (2011) Bioactive natural products from endophytes: A review. Applied Biochemistry and Microbiology 44:136–142.

Hartley SE, Gange AC (2009) Impacts of Plant Symbiotic Fungi on Insect Herbivores: Mutualism in a Multitrophic Context. Annual Review of Entomology 54:323–342.

Harvey A (2000) Strategies for discovering drugs from previously unexplored natural products. Drug Discovery Today 5:294–300.

Hawkesworth, D. L., Sotton, B. C., and Ainsworth, G. C. (1983). Ainsworth & Bisby's Dictionary of the Fungi, Commonwealth Mycological Institute, Kew, UK.

Hebert PDN, Cywinska A, Ball SL, deWaard JR (2003) Biological identifications through DNA barcodes. Proc Biol Sci 270:313–321.

Höller U, Gloer JB, Wicklow DT (2002) Biologically Active Polyketide Metabolites from an Undetermined Fungicolous Hyphomycete Resembling Cladosporium. J Nat Prod 65:876–882.

Hyde KD, Soytong K (2008) The fungal endophyte dilemma. Fungal Diversity 3:163–173.

Kameda K, Namiki M (1974) A New Phthalide from a Fungus, alternaria Kikuchiana. Chemistry Letters 3:1491–1492.

Kemami Wangun HV, Ishida K, Hertweck C (2008) Epicoccalone, a Coumarin-Type Chymotrypsin Inhibitor, and Isobenzofuran Congeners from an Epicoccum sp. Associated with a Tree Fungus. European Journal of Organic Chemistry 2008:3781–3784.

Kingston DGI (2011) Modern Natural Products Drug Discovery and its Relevance to Biodiversity Conservation. J Nat Prod 74:496–511.

Koehn FE (2008) High impact technologies for natural products screening. Prog Drug Res 65:175, 177–210.

Koehn FE, Carter GT (2005) The evolving role of natural products in drug discovery. Nature

Reviews Drug Discovery 4:206–220.

Kumar DS., Hyde KD (2004) Biodiversity and tissue-recurrence of endophytic fungi in Tripterygium wilfordii. Fungal Diversity 17:69–90.

Lacap DC, Hyde KD, Liew ECY (2003) An evaluation of the fungal "morphotype" concept based on ribosomal DNA sequences. Fungal Diversity 12:53–66.

Lam KS (2007) New aspects of natural products in drug discovery. Trends Microbiol 15:279–289.

Limsuwan S, Trip EN, Kouwen TRHM, Piersma S, Hiranrat A, Mahabusarakam W, Voravuthikunchai SP, van Dijl JM, Kayser O (2009) Rhodomyrtone: a new candidate as natural antibacterial drug from Rhodomyrtus tomentosa. Phytomedicine 16:645–651.

Martini M, Musetti R, Grisan S, Polizzotto R, Borselli S, Pavan F, Osler R (2009) DNA-Dependent Detection of the Grapevine Fungal Endophytes Aureobasidium pullulans and Epicoccum nigrum. Plant Disease 93:993–998.

McChesney JD, Venkataraman SK, Henri JT (2007) Plant natural products: Back to the future or into extinction? Phytochemistry 68:2015–2022.

Mejia LC, Maynard Z, Arnold AE, Hebbar P, Samuels GJ, Robbins N, Herre EA (2008) Endophytic fungi as biocontrol agents of Theobroma cacao pathogens. Biological Control 46:4–14.

Newman DJ, Cragg GM (2007) Natural products as sources of new drugs over the last 25 years. J Nat Prod 70:461–477.

Newman DJ, Cragg GM, Snader KM (2003) Natural products as sources of new drugs over the period 1981-2002. J Nat Prod 66:1022–1037.

Newman, D. J. (2008). Natural products as lead to potential drugs: an old process or the new hope for drug discovery. *J*. *Med*. *Chem*., **51**, 2589-2599.

Newman, D. J., and Cragg, G.. M. (2007). Natural products as sources of new drugs over the last 25 years. *J*. *Nat*. *Prod*., **70**, 461-477.

Newman, D. J., Cragg, G. M., and Snader, K. M. (2000). The influence of natural products upon drug discovery. *Nat*. *Prod*. *Rep*., **17**, 215-234.

Pancher M, Ceol M, Corneo PE, Longa CM., Yousaf S, Pertot I, Campisano A (2012) Fungal endophytic communities in grapevines (Vitis vinifera L.) respond to crop management. Applied and environmental microbiology 78:4308–4317.

Parkinson JS, Blair DF (1993) Does E. coli have a nose? Science 259:1701–1702.

Pettersson G (1965) The Biosynthesis of Flavipin. I. Incorporation of Acetate and Methionine. Acta Chem Scand 19:35–40.

Putri SP, Kinoshita H, Ihara F, Igarashi Y, Nihira T (2009) Farinomalein, a maleimide-bearing compound from the entomopathogenic fungus Paecilomyces farinosus. J Nat Prod 72:1544–1546.

Qiu M, Xie R-sheng, Shi Y, Zhang H, Chen H-min (2010) Isolation and identification of two flavonoid-producing endophytic fungi from *Ginkgo biloba* L. Ann Microbiol 60:143–150.

Rodriguez RJ, White Jr JF, Arnold AE, Redman RS (2009) Fungal endophytes: diversity and functional roles. New Phytologist 182:314–330.

Rollinger, J. M., Langer, T., and Stuppner, H. (2006). Strategies for efficient lead structure discovery from natural products. *Curr*. *Med*. *Chem*., 13, 1491-1507.

Schena L., Ippolito A., Zahavi T., Cohen L., Nigro F., Droby S. (1999) Genetic diversity and biocontrol activity of Aureobasidium pullulans isolates against postharvest rots.

Postharvest Biology and Technology 17:189–199.

Schlegel M (2003) Phylogeny of eukaryotes recovered with molecular data: highlights and pitfalls. European journal of protistology 39:113–122.

Schoch CL et al. (2012) From the Cover: Nuclear ribosomal internal transcribed spacer (ITS) region as a universal DNA barcode marker for Fungi. Proceedings of the National Academy of Sciences 109:6241–6246.

Schol-Schwarz MB (1959) The genus Epicoccum Link. Transactions of the British Mycological Society 42:149–IN3.

Shu Y-Z, Ye Q, Li H, Kadow KF, Hussain RA, Huang S, Gustavson DR, Lowe SE, Chang L-P, Pirnik DM, Kodukula K (1997) Orevactaene,1 a novel binding inhibitor of HIV-1 rev protein to Rev response element (RRE) from Epicoccum nigrum WC47880. Bioorganic & Medicinal Chemistry Letters 7:2295–2298.

Skropeta D, Pastro N, Zivanovic A (2011) Kinase Inhibitors from Marine Sponges. Marine Drugs 9:2131–2154.

Strobel, G. A. (2002). Rainforest endophytes and bioactive products. Critical reviews in biotechnology. *Crit*. *Rew*. *Biotechnol*., **22**, 315-333.

Strobel, G., and Daisy, B. (2003). Bioprospecting for microbial endophytes and their natural products. *Microbiol*. *Mol*. *Biol*. *Rev*., **67**, 491-502.

Strobel, G., Daisy, B., Castillo, U., and Harper, J. (2004). Natural products from endophytic microorganisms. *J*. *Nat*. *Prod*., **67**, 257-268.

Strobel, G.A., Yang, X. Sears, J. Kramer, R. Sidhu, R.S., and Hess, W.M. (1996). Taxol from Pestaliopsis microspora, an endophytic fungus of Taxus wallichiana. Microbiology 142, 435-440.

Strobel. G.A., Stierle, A., Stierle, D., and Hess, W.M. (1993). Taxomyces andreanae a proposed

new taxon for bulbiliferous hypomycete associated with pasific yew. Mycotaxon, 47, 71-78.

Sun L, Pei K, Wang F, Ding Q, Bing Y, Gao B, Zheng Y, Liang Y, Ma K (2012) Different Distribution Patterns between Putative Ercoid Mycorrhizal and Other Fungal Assemblages in Roots of Rhododendron decorum in the Southwest of China. PLoS ONE 7:e49867.

Tamura K, Peterson D, Peterson N, Stecher G, Nei M, Kumar S (2011) MEGA5: Molecular Evolutionary Genetics Analysis Using Maximum Likelihood, Evolutionary Distance, and Maximum Parsimony Methods. Molecular Biology and Evolution 28:2731–2739.

Thirunavukkarasu N, Suryanarayanan TS, Girivasan KP, Venkatachalam A, Geetha V, Ravishankar JP, Doble M (2011) Fungal symbionts of marine sponges from Rameswaram, southern India: species composition and bioactive metabolites. Fungal Diversity 55:37–46.

Traber, R., Hofmann, H., Kuhn, M., and von Wartburg, A. (1982). Isolierung und strukturermittlung der neuen cyclosporin E, F, G, H und I. Helv. Chim. Acta 65, 1655-1677.

Vajkoczy P, Knyazev P, Kunkel A, Capelle H-H, Behrndt S, von Tengg-Kobligk H, Kiessling F, Eichelsbacher U, Essig M, Read T-A, Erber R, Ullrich A (2006) Dominant-negative inhibition of the Axl receptor tyrosine kinase suppresses brain tumor cell growth and invasion and prolongs survival. Proc Natl Acad Sci USA 103:5799–5804.

Vandenkoornhuyse P, Mahé S, Ineson P, Staddon P, Ostle N, Cliquet JB, Francez AJ, Fitter AH, Young JP. (2007) Active root-inhabiting microbes identified by rapid incorporation of plant-derived carbon into RNA. Proceedings of the National Academy of Sciences 104:16970–16975.

Wang JM, Ding GZ, Fang L, Dai JG, Yu SS, Wang YH, Chen XG, Ma SG, Qu J, Xu S (2010) Thiodiketopiperazines Produced by the Endophytic Fungus Epicoccum nigrum.

Journal of natural products 73:1240–1249.

Wang L-W, Xu B-G, Wang J-Y, Su Z-Z, Lin F-C, Zhang C-L, Kubicek CP (2012) Bioactive metabolites from Phoma species, an endophytic fungus from the Chinese medicinal plant Arisaema erubescens. Appl Microbiol Biotechnol 93:1231–1239.

Wang L-W, Xu B-G, Wang J-Y, Su Z-Z, Lin F-C, Zhang C-L, Kubicek CP (2012b) Bioactive metabolites from Phoma species, an endophytic fungus from the Chinese medicinal plant Arisaema erubescens. Appl Microbiol Biotechnol 93:1231–1239.

Wangun HVK, Dahse H-M, Hertweck C (2007) Epicoccamides B–D, Glycosylated Tetramic Acid Derivatives from an Epicoccum sp. Associated with the Tree Fungus Pholiota squarrosa. Journal of Natural Products 70:1800–1803.

Wani, M. C., Taylor, H. L., Wall, M. E., Goggon, P., McPhail, A. T. (1971). Plant antitumor agents. VI. Isolation and structure of taxol, a novel antileukemic and antitumor agent from Taxus brevifolia. J. Am. Chem. Soc., 93, 2325-2327.

Watermann F, Hillebrand H, Gerdes G, Krumbein W, Sommer U (1999) Competition between benthic cyanobacteria and diatoms as influenced by different grain sizes and temperatures. Marine Ecology Progress Series 187:77–87.

White, TJ., Bruns, T., Lee, S. and Taylor, J.W. (1990). 38. Amplification and direct sequencing of fungal ribosomal RNA genes for phylogenetics. PCR Protocols a guide for methods and application, 315-322.

Wu Z, Tsumura Y, Blomquist G, Wang X-R (2003) 18S rRNA Gene Variation among Common Airborne Fungi, and Development of Specific Oligonucleotide Probes for the Detection of Fungal Isolates. Appl Environ Microbiol 69:5389–5397.

Xu J, Aly AH, Wray V, Proksch P (2011) Polyketide derivatives of endophytic fungus Pestalotiopsis sp. isolated from the Chinese mangrove plant Rhizophora mucronata. Tetrahedron Letters 52:21–25.

Xu J, Ebada S, Proksch P (2010) Pestalotiopsis a highly creative genus: chemistry and bioactivity of secondary metabolites. Fungal Diversity 44:15–31.

Zalar P, Gostinčar C, de Hoog GS, Uršič V, Sudhadham M, Gunde-Cimerman N (2008) Redefinition of Aureobasidium pullulans and its varieties. Stud Mycol 61:21–38.

Zhang W, Draeger S, Schulz B, Krohn K (2009) Ring B aromatic steroids from an endophytic fungus, Colletotrichum sp. Nat Prod Commun 4:1449–1454.

Zhang, H., Zhang, J., Hu, S., Zhang, Z., Zhu, C., Ng, S. W., and Tan, R. (2010). Ardeemins and cytochalasins from *Aspergillus terreus* residing in *Artemisia annua*. *Planta Med*., **76**, 1616-1621.

Zheng C-J, Shao C-L, Guo Z-Y, Chen J-F, Deng D-S, Yang K-L, Chen Y-Y, Fu X-M, She Z-G, Lin Y-C, Wang C-Y (2012) Bioactive hydroanthraquinones and anthraquinone dimers from a soft coral-derived Alternaria sp. fungus. J Nat Prod 75:189–197.

8. List of abbreviations

$[\alpha]^{20}_{D}$	Specific rotation at the sodium D-line
amu	Atomic mass unit
Approx.	Approximately
br	Broad signal
CC	Column chromatography
$CDCl_3$	Deuterated chloroform
$CHCl_3$	Chloroform
CI	Chemical ionization
COSY	Correlation spectroscopy
d	Doublet
DAD-HPLC	HPLC with diodenarray detector
dd	Doublet of doublet signal
DEPT	Distortionless enhancement by polarization transfer
DMSO	Dimethyl sulfoxide
e.g.	*exempli gratia* (for the sake of example)
EI	Electron impact ionizarion
ESI	Electron spray ionization
et al.	et altera (and others)
EtOAc	Ethyl acetate
eV	Electron Volt
FAB	Fast atom bomhardment
g	Gram
HMBC	Heteronuclear multiple bond connectivity
HMQC	Heteronuclear multiple quantum coherence
H_2O	Water
HPLC	High performance liquid chromatography
HR-MS	High resolution-mass spectrometry
Hz	Hertz
IC_{50}	Half maximal inhibitory concentration
L	Liter
LC	Liquid chromatography
LC-MS	Liquid chromatography-mass spectrometry
m	Multiplet signal
MeOD	Deuterated methanol
MeOH	Methanol
mg	Milligram
MHz	Mega Hertz
min	Minute

mL	Milliliter
MS	Mass spectrometry
MTT	3-(4,5-Dimethylthiazol-2-yl)-2,5-diphenyltetrazolium bromide
m/z	Mass per charge
μg	Microgram
μL	Microliter
μM	Micromolar
MW	Molecular weight
ng	Nanogram
n-BuOH	*n*-Butanol
NMR	Nuclear magnetic resonance
NOE	Nuclear Overhauser effect
NOESY	Nuclear Overhauser and exchange spectroscopy
ppm	Part per million
q	Quartet signal
ROESY	Rotating frame Overhauser enhancement spectroscopy
RP-18	Reversed phase C 18
s	Singlet signal
SAM	*S*-adenosyl methionine
Si	Silica
t	Triplet signal
TFA	Trifluoroacetic acid
TLC	Thin layer chromatography
UV	Ultra-violet
VLC	Vaccum liquid chromatography

9. Attachments

Attachment 1: The ^{1}H NMR spectrum of Farinomalein A (**1**)

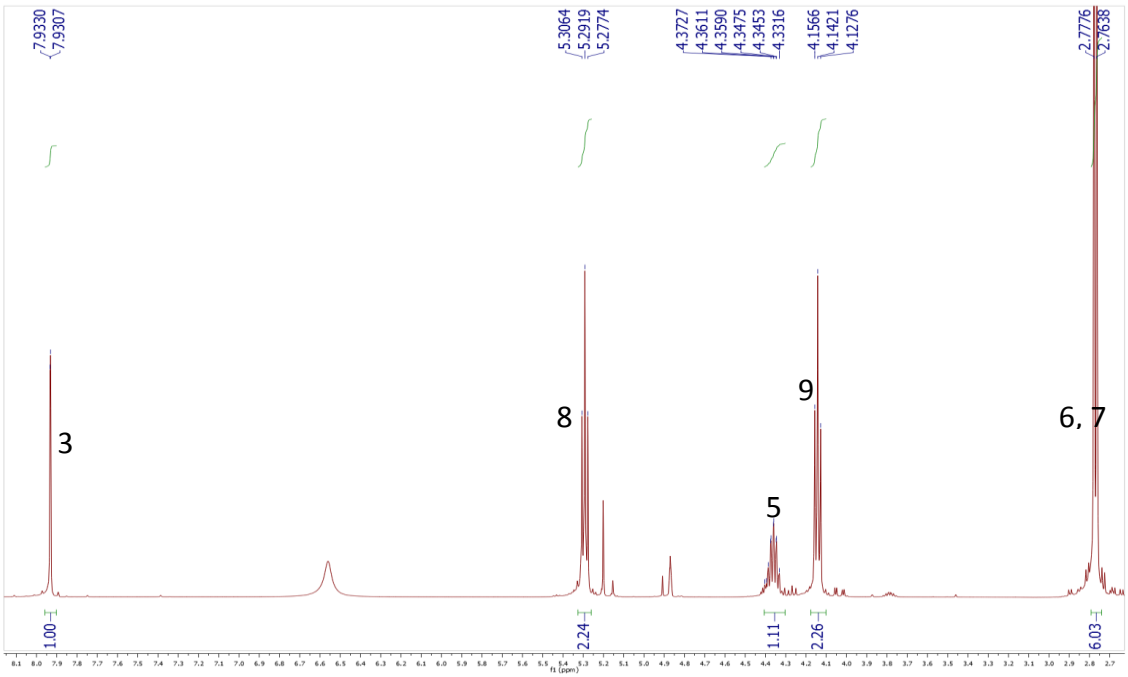

Attachment 2: The ^{1}H NMR spectrum of Farinomalein B (**2**)

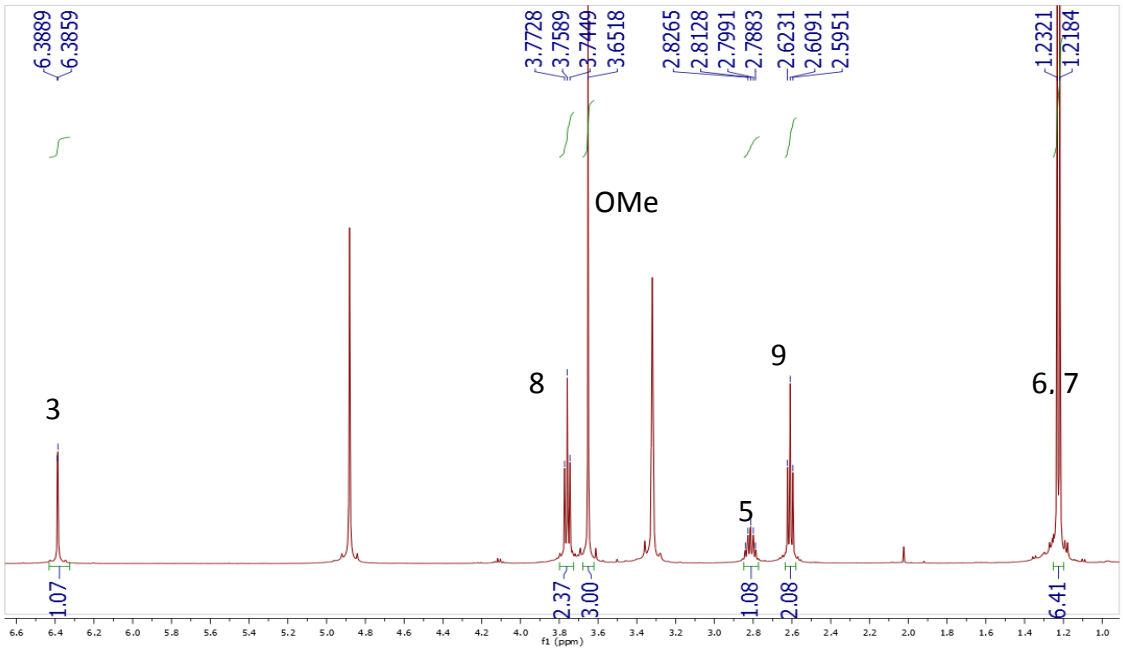

Attachment 3: The ^{1}H NMR spectrum of Farinomalein C (**3**)

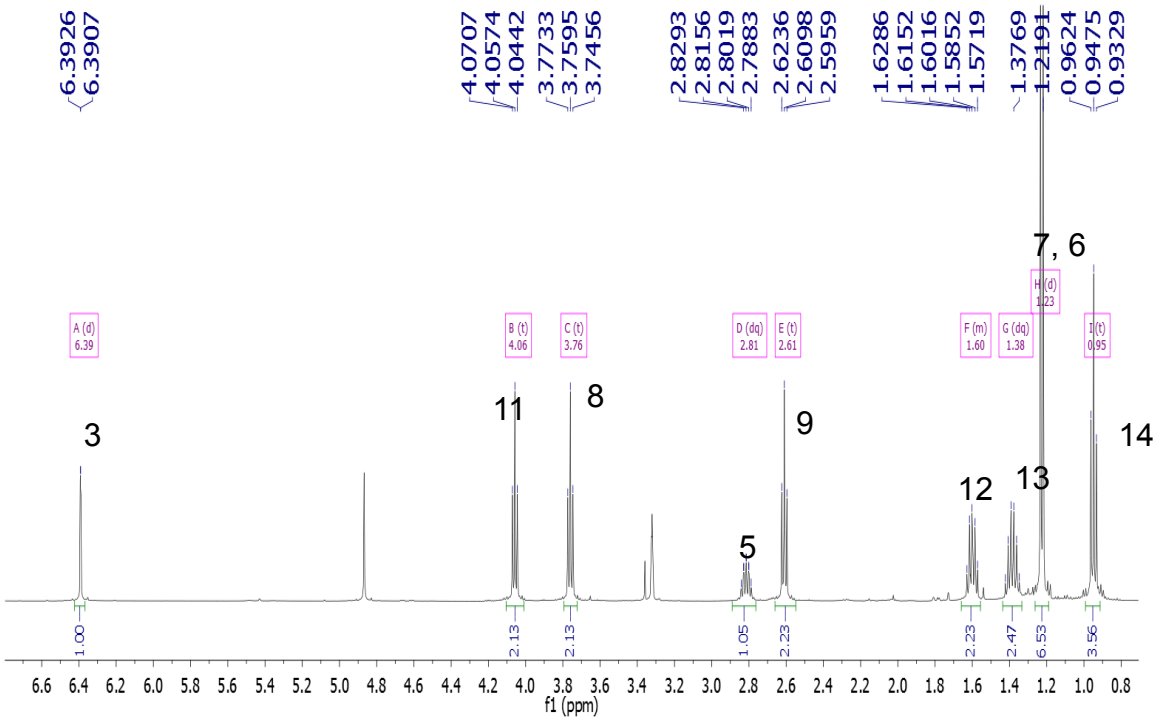

Attachment 4: The ^{1}H NMR spectrum of Farinomalein D (**4**)

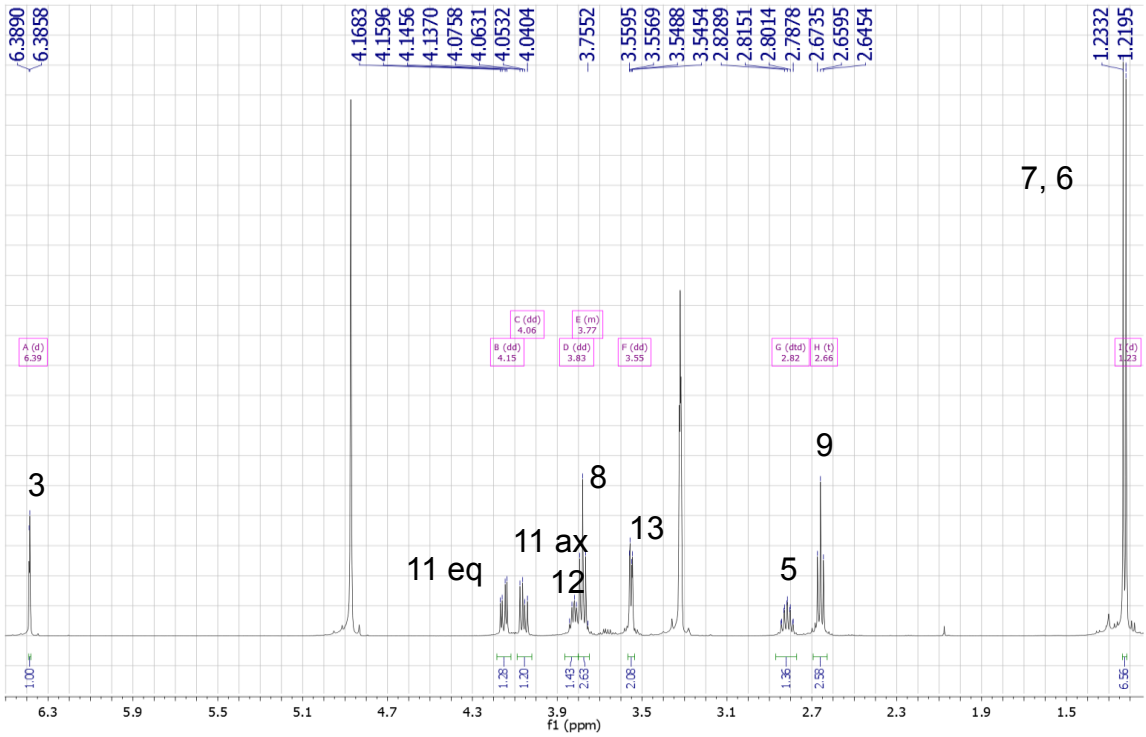

Attachment 3: The ^{1}H NMR spectrum of Farinomalein D (**5**)

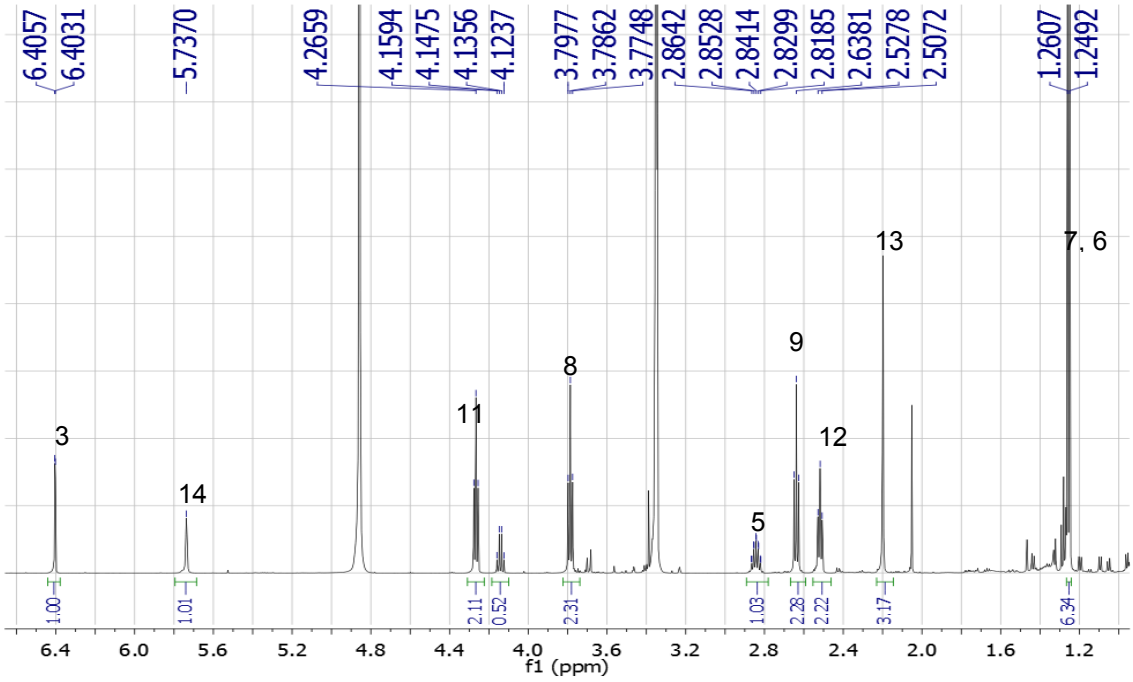

Attachment 4: The ^{1}H NMR spectrum of (*R)*-5,7-Dihydroxy-3-methylisoindolin-1-one (**6**)

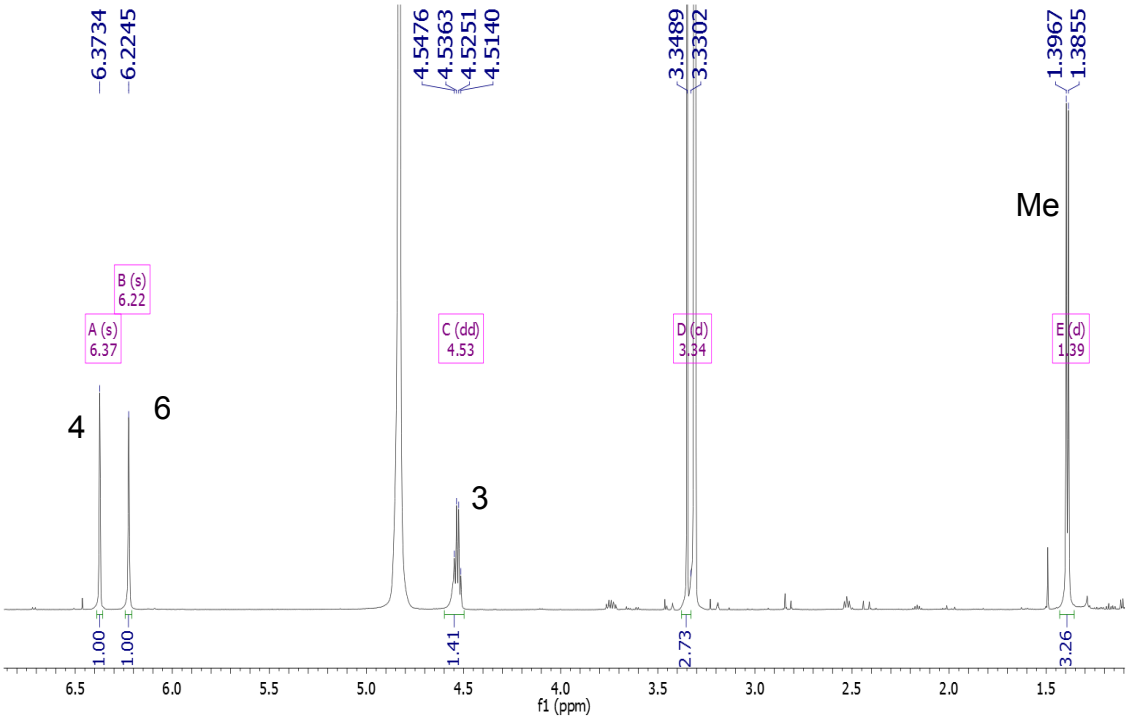

Attachment 5: The ^{1}H NMR spectrum of *p*-hydroxyphenylacetic acid (**7**)

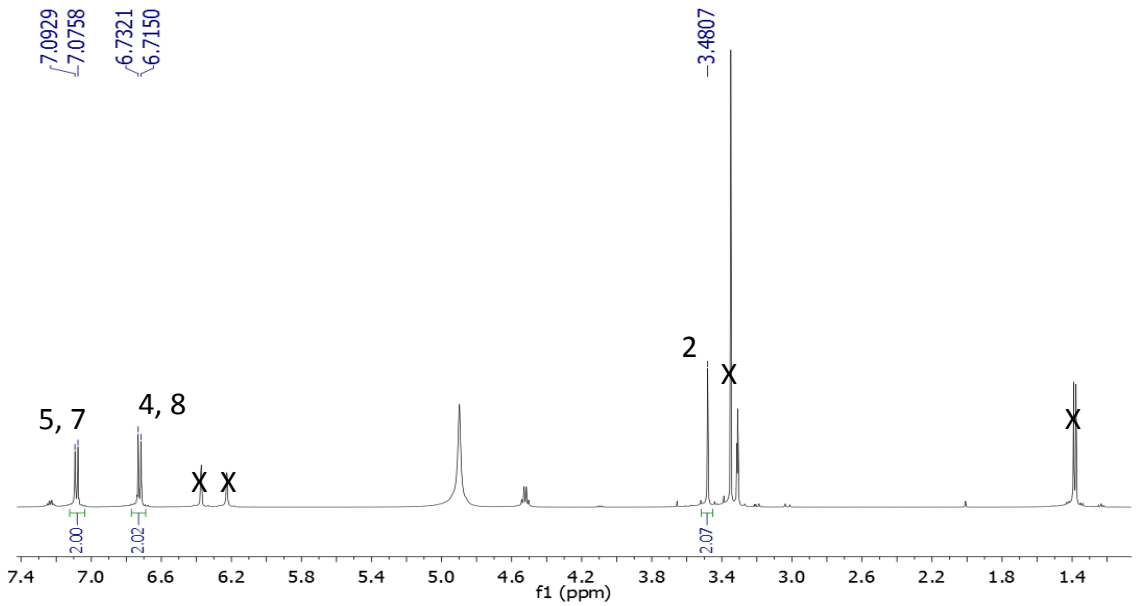

Attachment 6: The ^{1}H NMR spectrum of epicoccine (**8**)

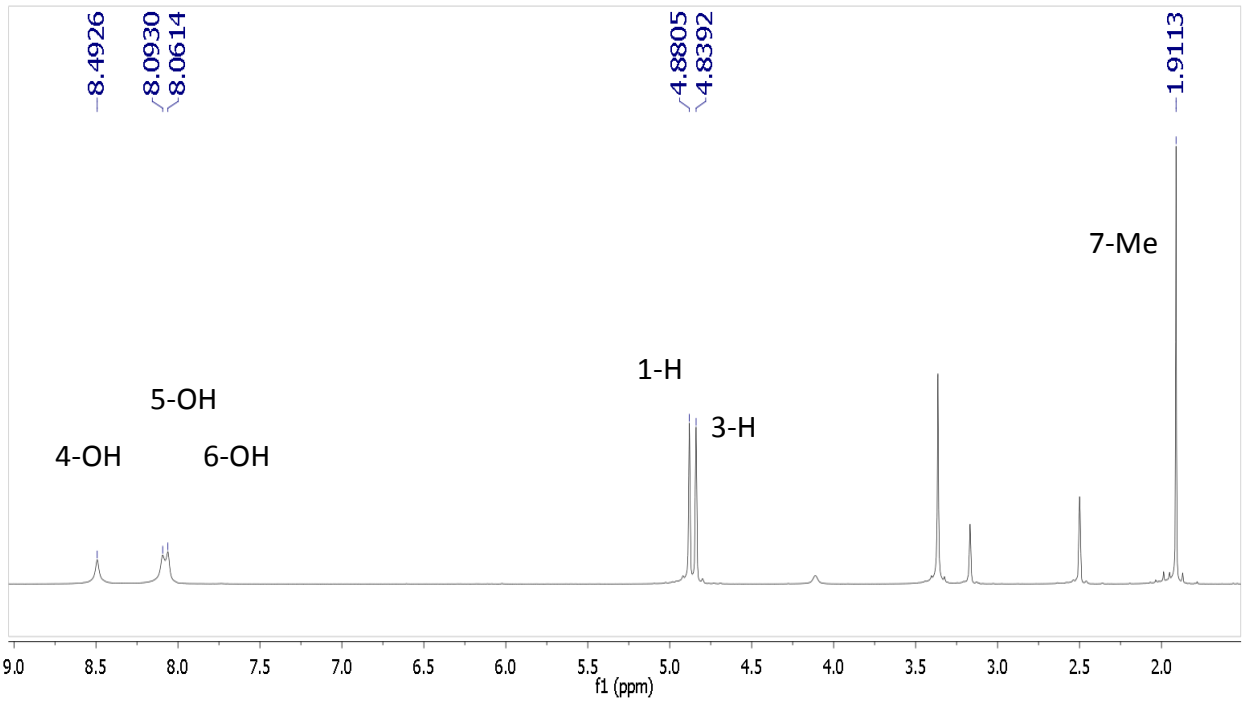

Attachment 7: The ^{1}H NMR spectrum of 5-methoxy-7-methyl-1,3-dihydroisobenzofuran-4,6-diol (9)

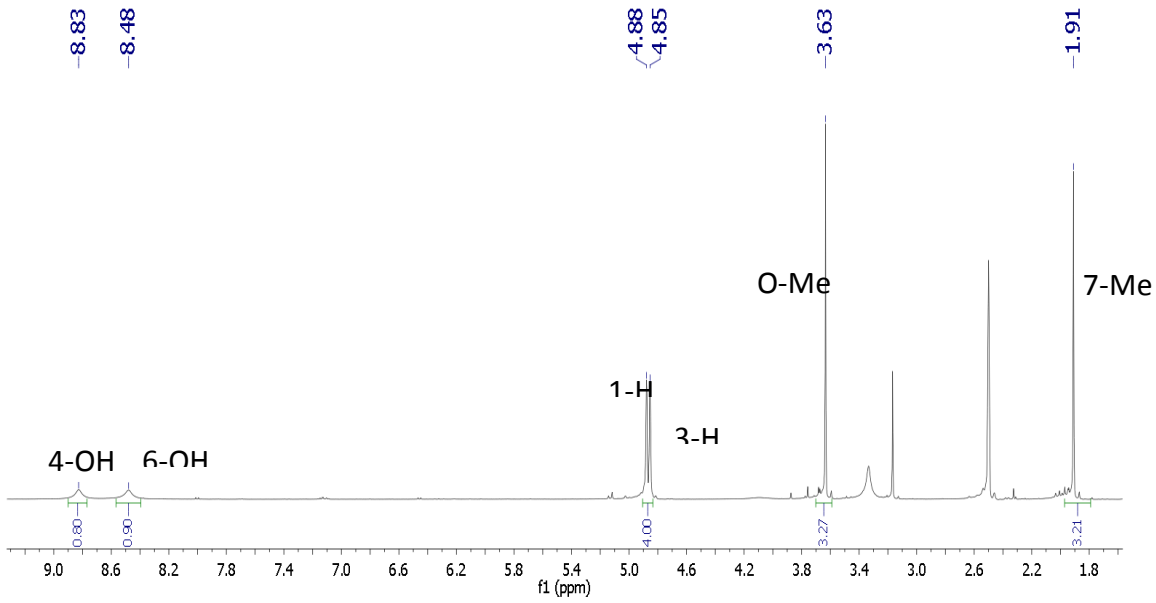

Attachment 8: The 1H NMR spectrum of epicoccone A (**10**)

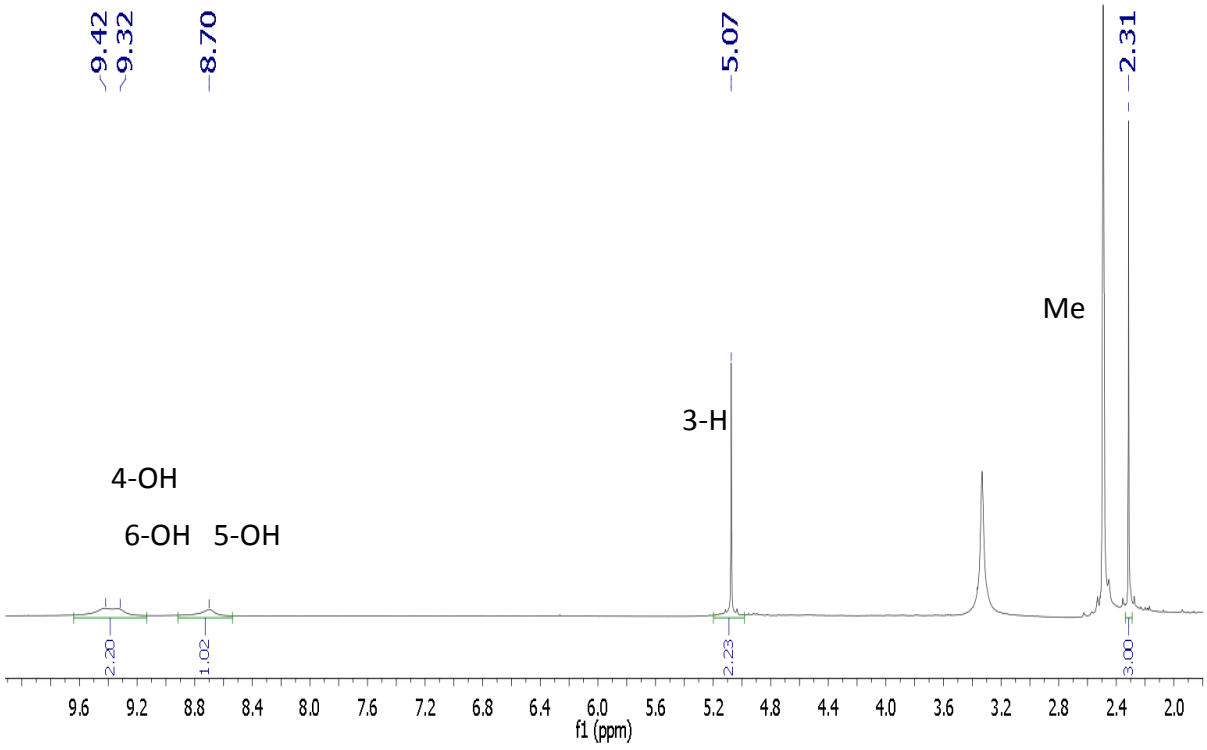

Attachment 9: The ^{1}H NMR spectrum of epicoccone B (**11**)

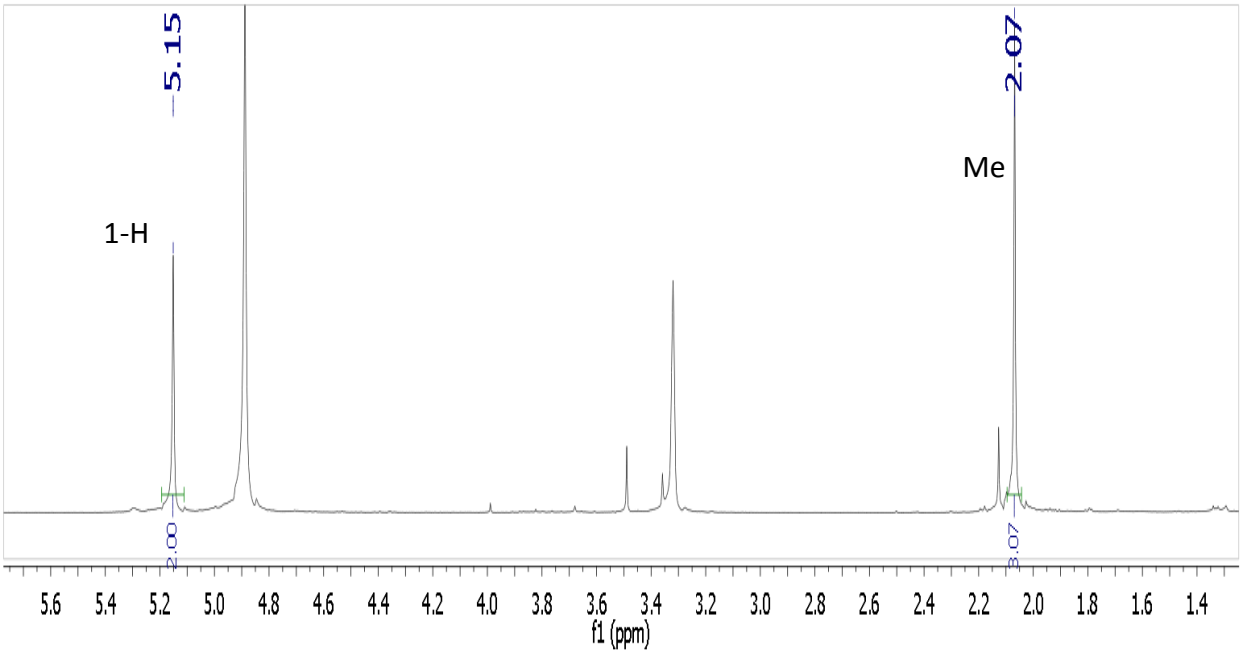

Attachment 12: The ^{1}H NMR spectrum of Epicoccone C (**12**)

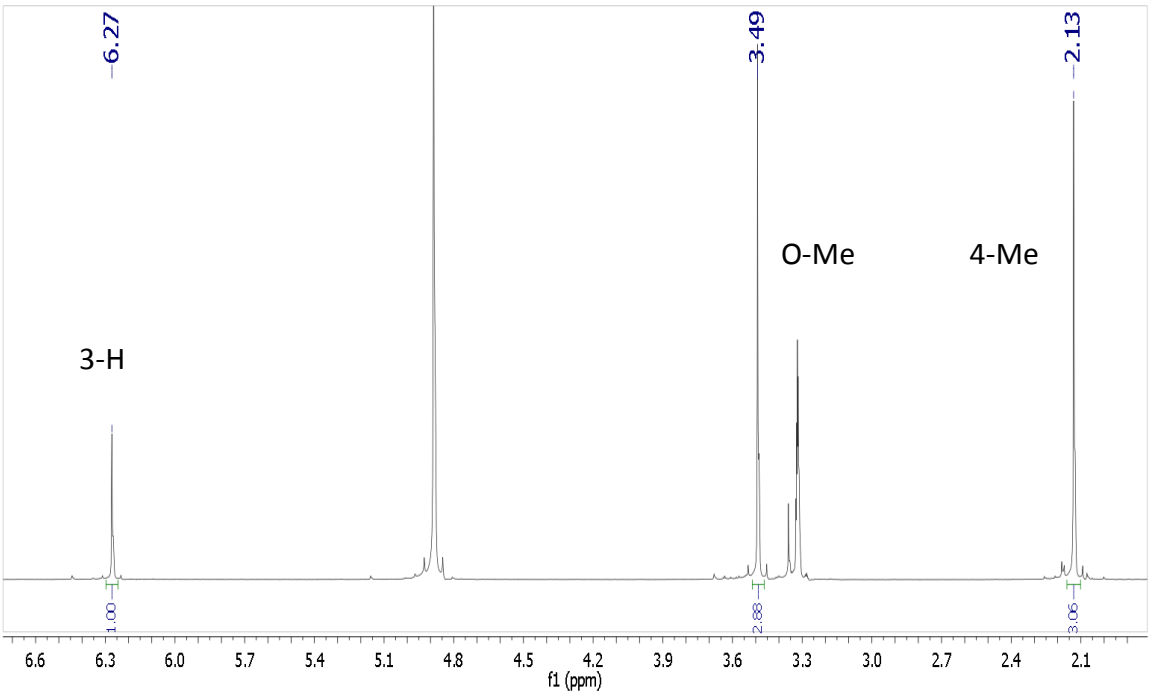

Attachment 13: The ^{1}H NMR spectrum of The epicoccone D (**13**)

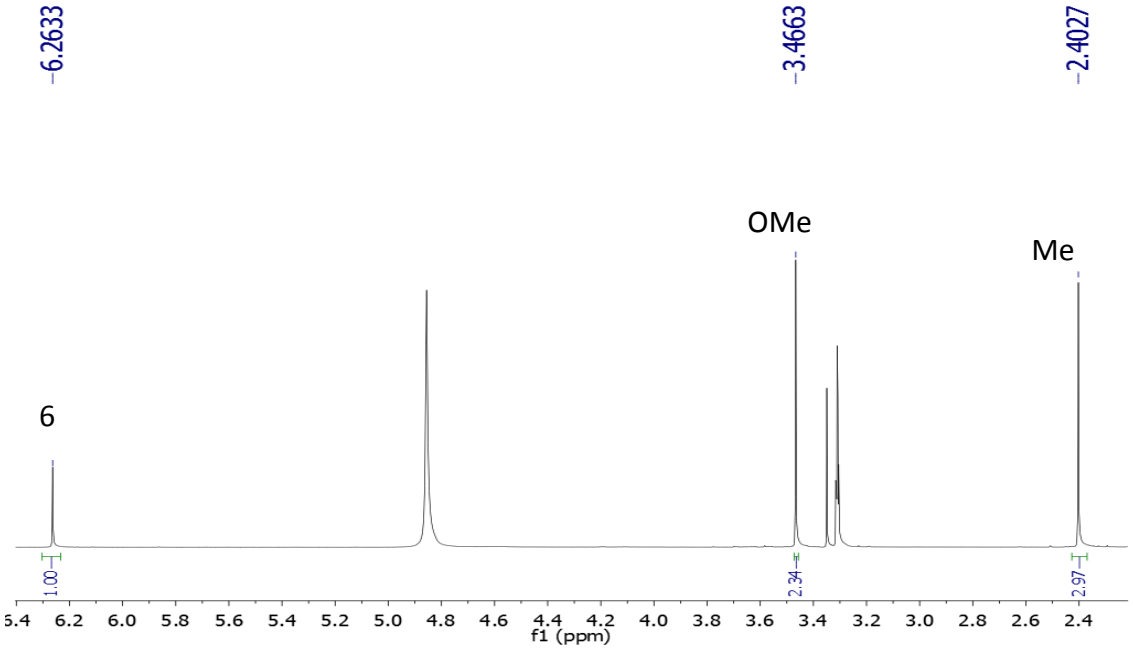

Attachment 14: 2,3,4-trihydroxy-6-(methoxymethyl)-5-methylbenzaldehyde (**14**)

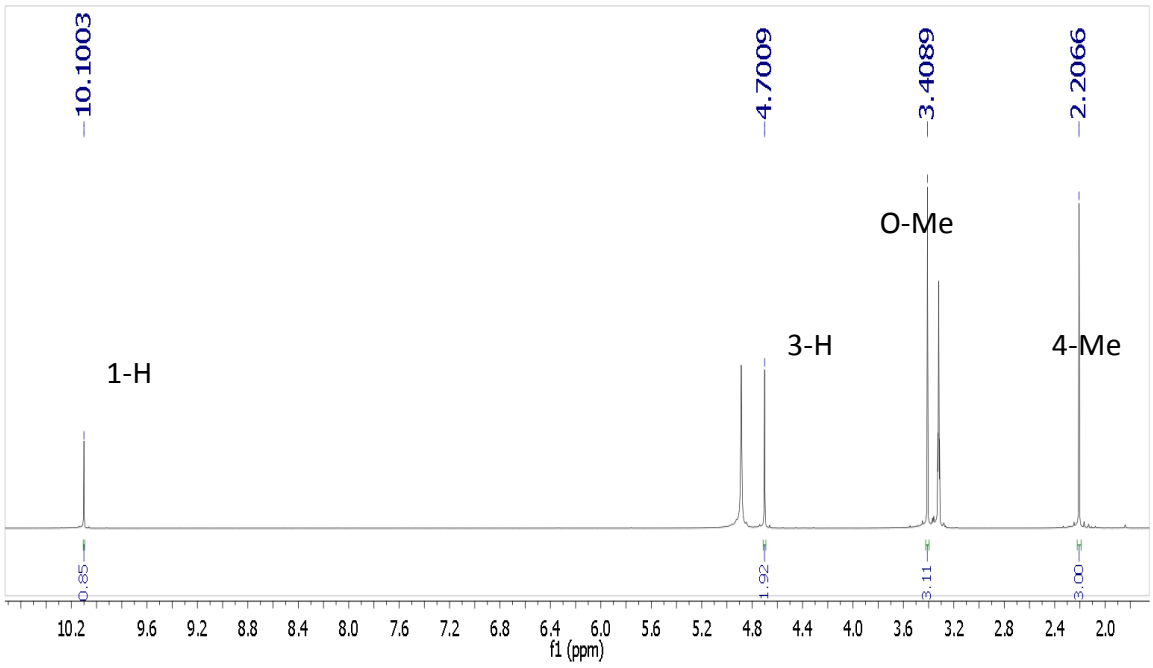

Attachment 15: The [1]H NMR spectrum of 5,6,7,9a-Tetrahydroxy-2,3,3a,8-tetramethyl-3a,4-dihydro-1*H*-cyclopenta[*b*]naphthalene-1,9(9a*H*)-dione (**15**)

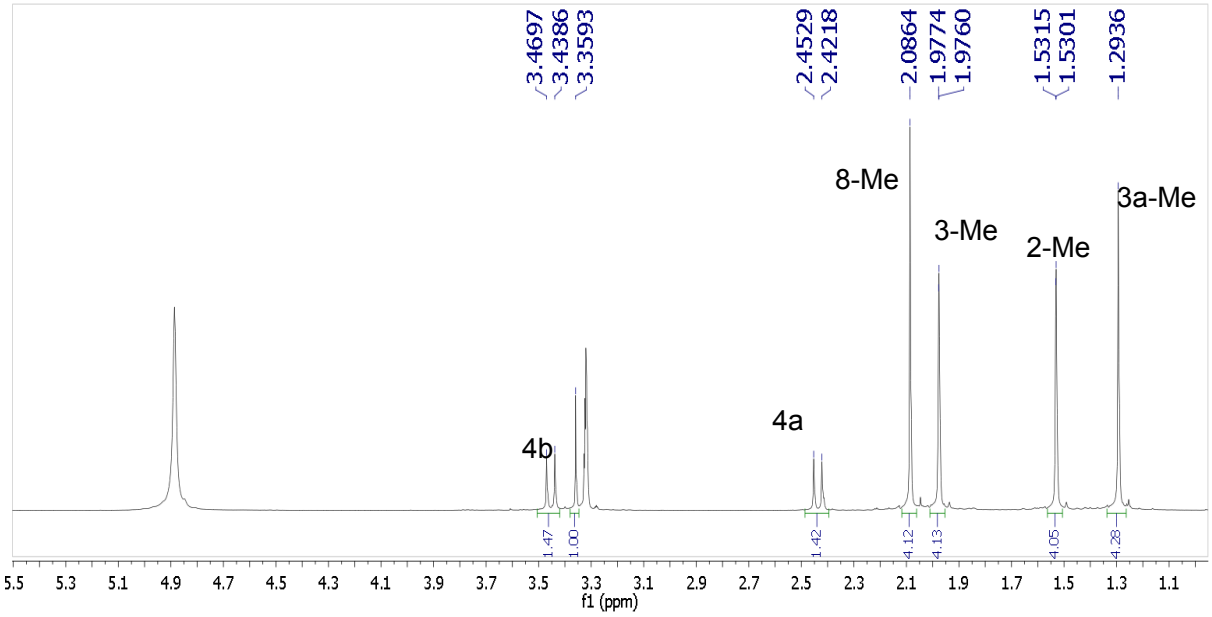

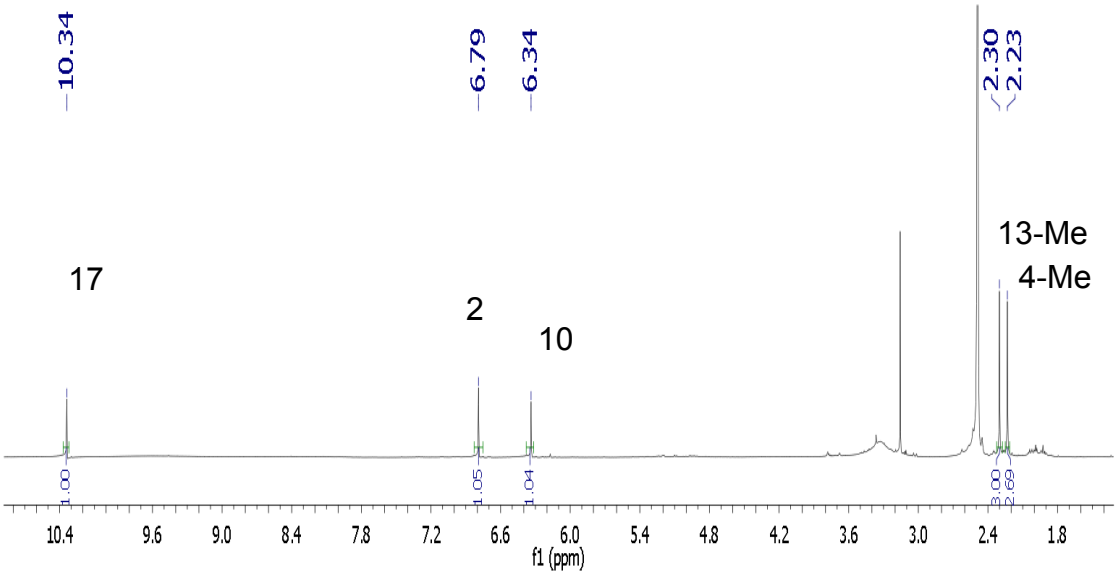

Attachment 16: The [1]H NMR spectrum of 3,4,8,9,10-Pentahydroxy-2,7-dimethyl-11-oxo-11,12-dihydro-6*H*-6,12-epoxydiben-zo[*b*,*f*]oxocine-1-carbaldehyde (**16)**

Attachment 17: The ^{1}H NMR spectrum of 2-(2-formyl-3,4,5-trihydroxy-6-methylphenyl)-6,7-dihydroxy-5-methylbenzofuran-4-carbaldehyde (**17**)

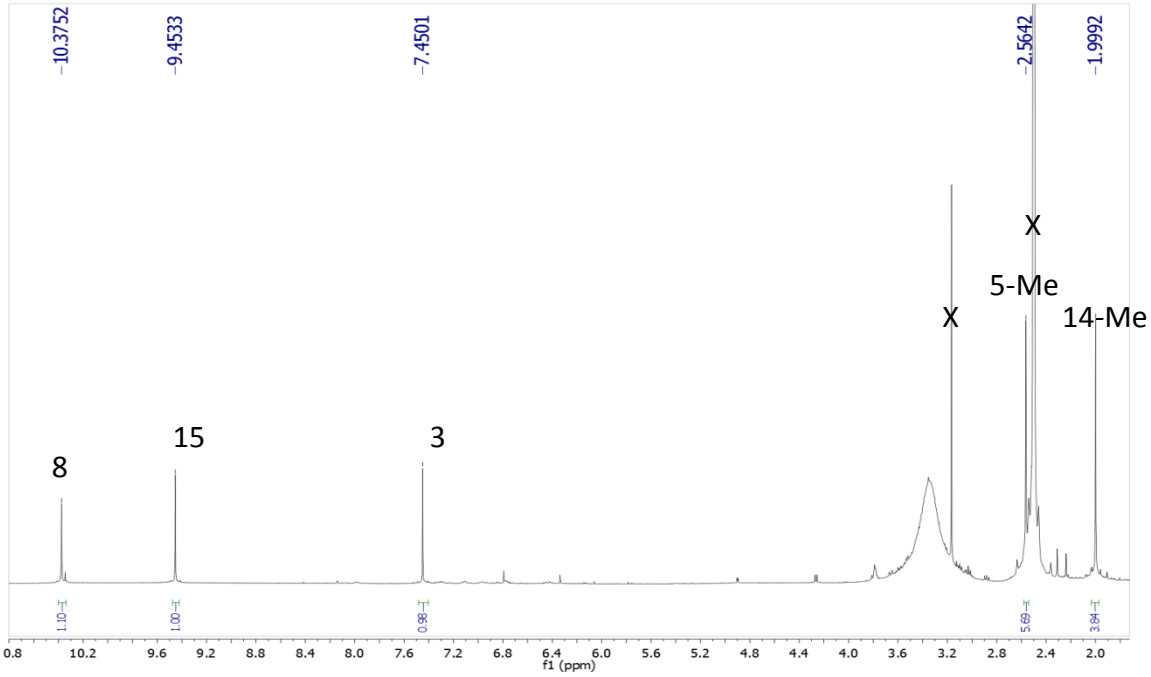

Attachment 18: The ^{1}H NMR spectrum of indol-3-carboxylic acid (**18**)

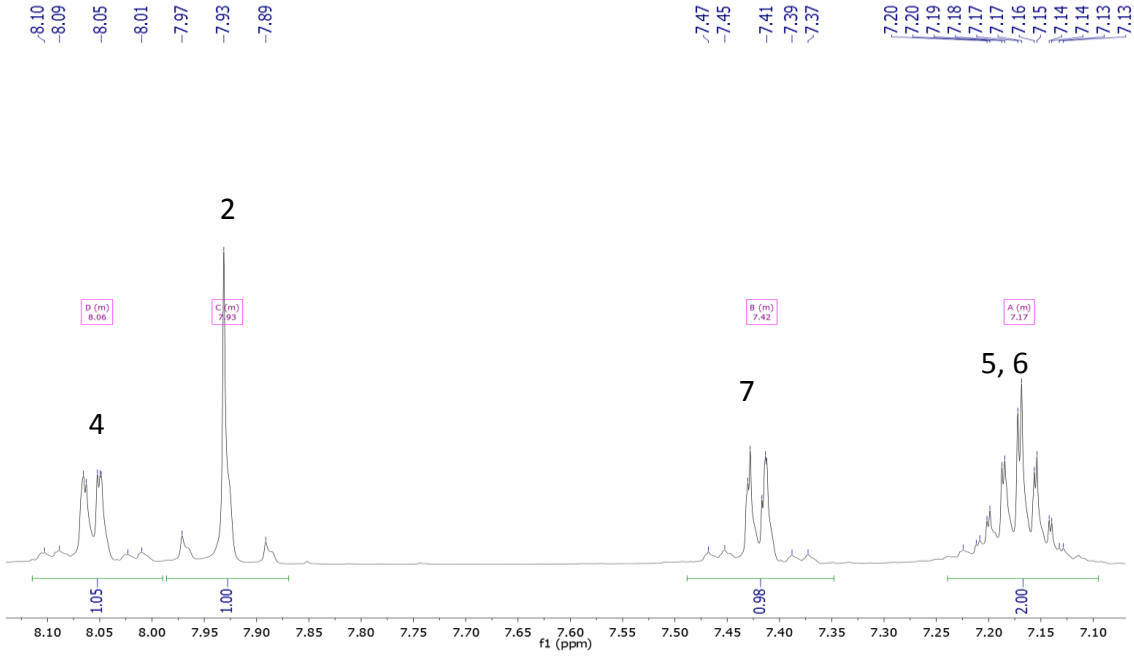

Attachment 19: The ^{1}H NMR spectrum of 1*H*-Indole-3-carbaldehyde (**19**)

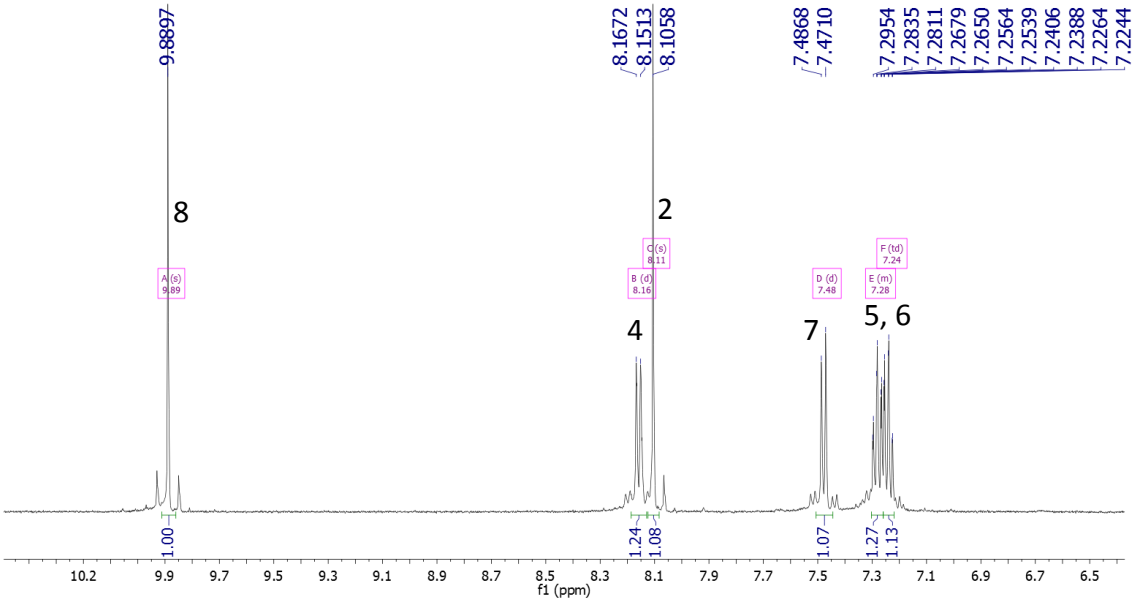

Attachment 20: The ^{1}H NMR spectrum of (*Z*)-4-(5-acetoxy-3-methylpent-2-enamido)butanoic acid (**20**)

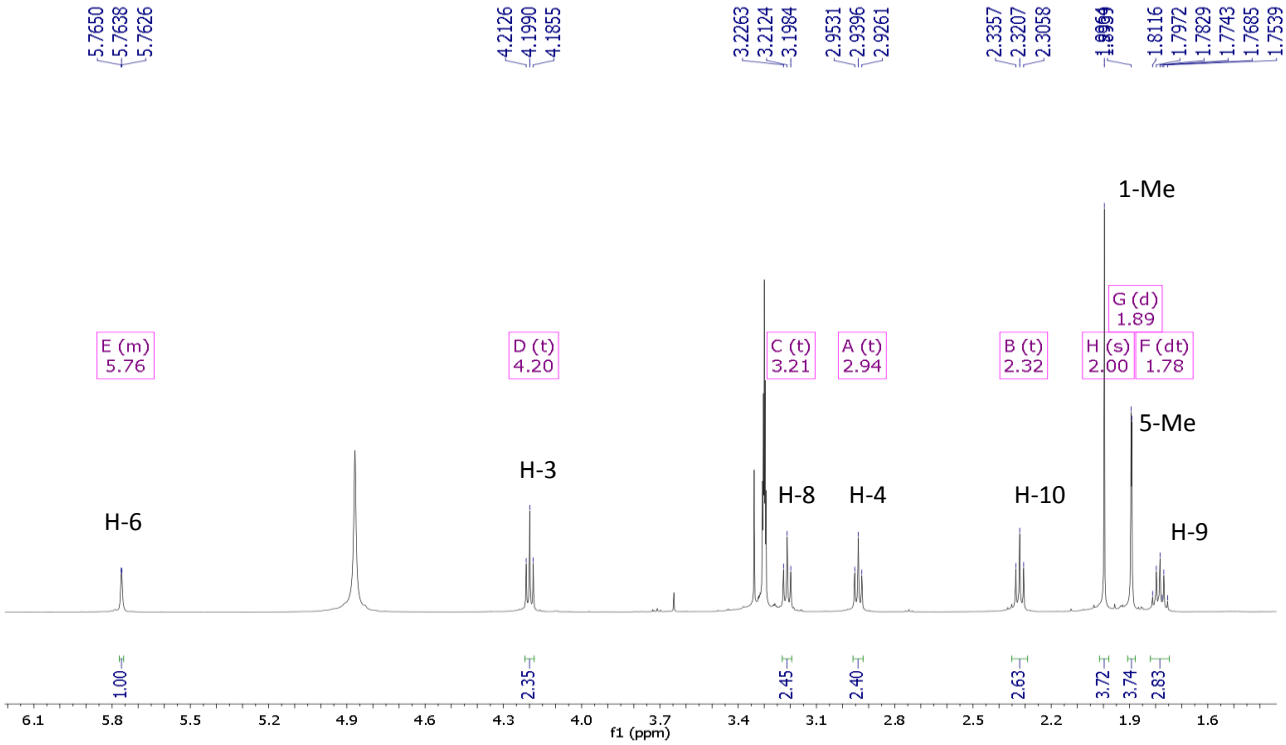

Attachment 210: The ^{1}H NMR spectrum of Isoochracinic acid (**21**)

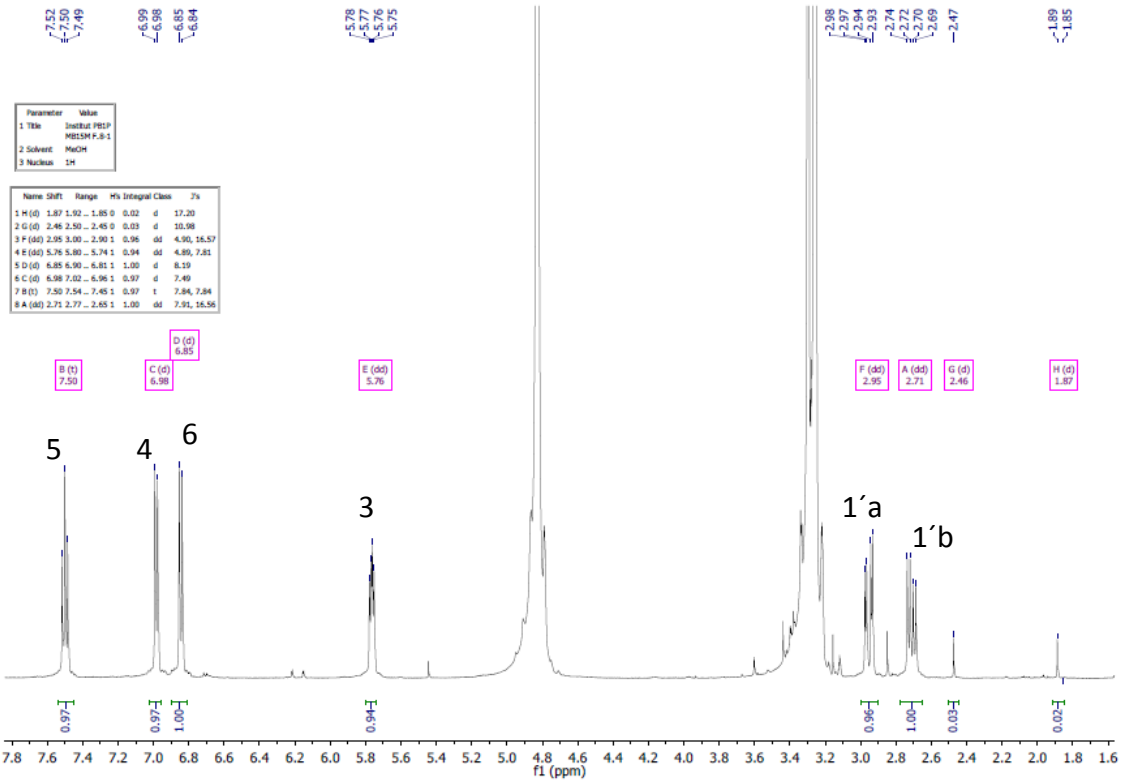

Attachment 22: The ^{1}H NMR spectrum of 6-Hydroxyisosclerone (**22**)

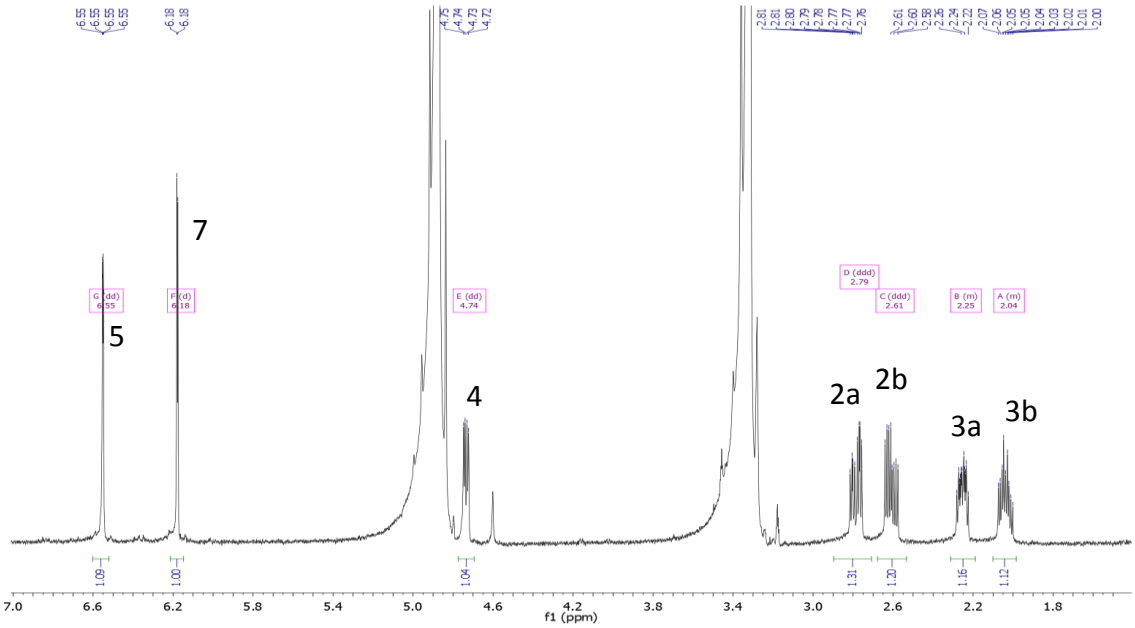

Attachment 23: The ^{1}H NMR spectrum of 3,4,6,8-tetrahydroxy-3,4-dihydronaphthalen-1(2H)-one (**23**)

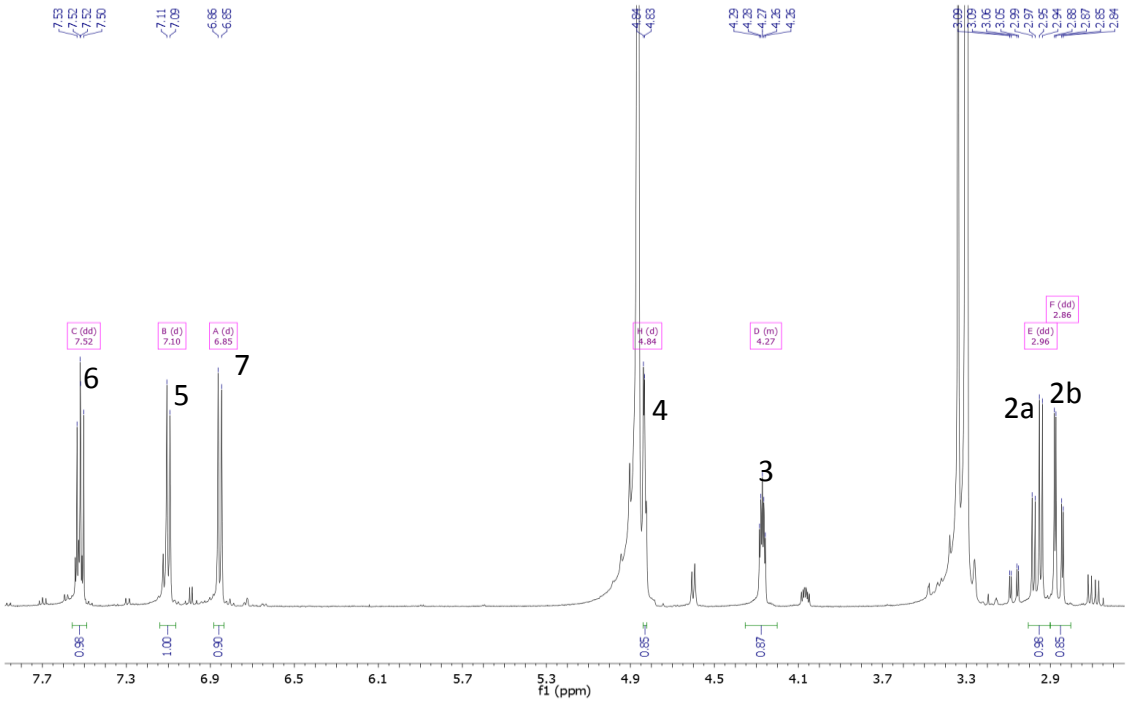

Attachment 24: The ^{1}H NMR spectrum of Tetrahydroaltersolanol B (**24**)

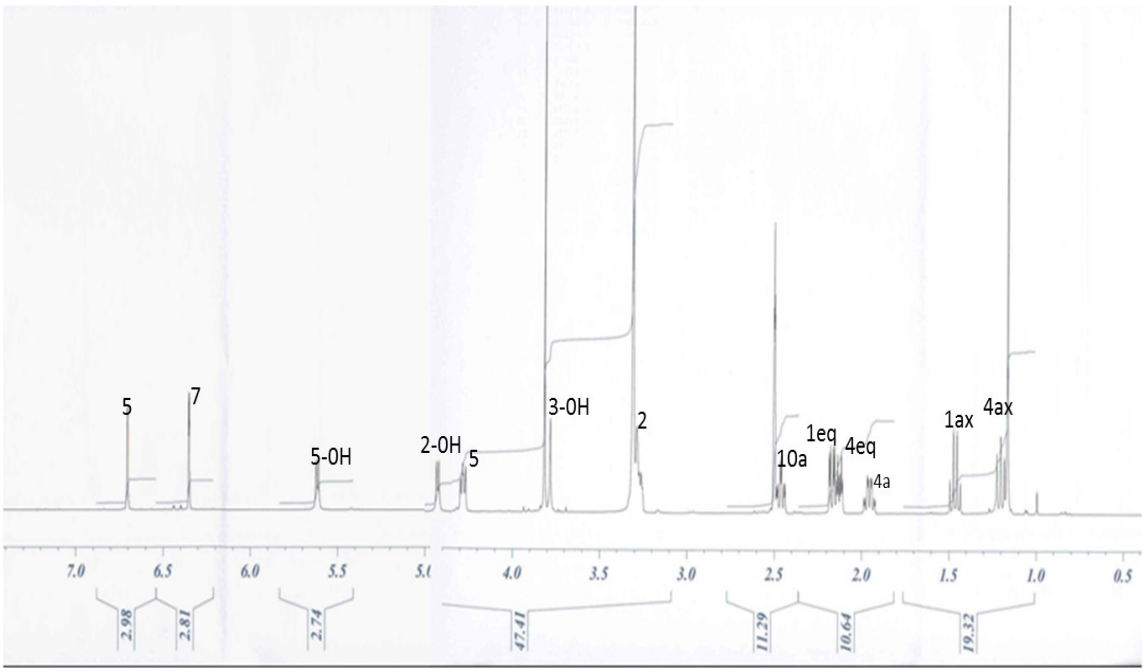

Attachment 25: The ^{1}H NMR spectrum of Alterporriol O (**25**)

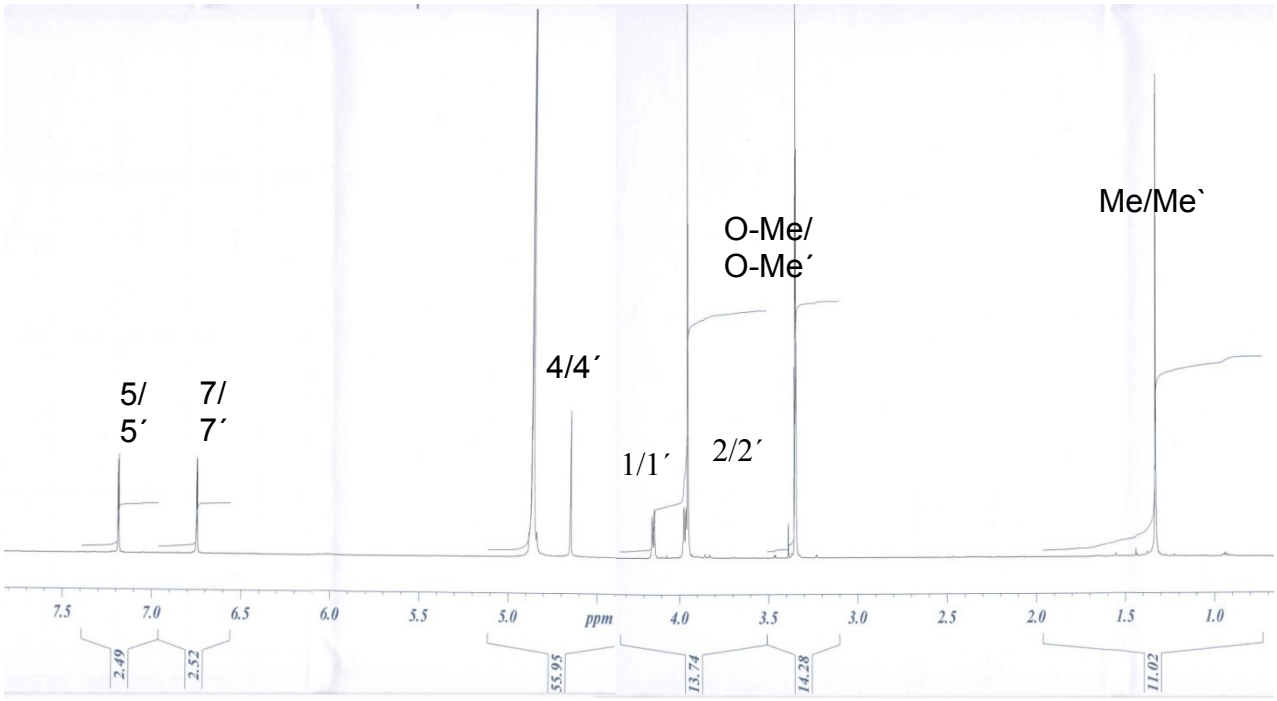

Curriculum Vitae

Persönliche Daten:

Name:	El Amrani
Nachname:	Mustapha
Geburtsdatum:	19.06.1976
Geboren in:	Boudnib-Marokko
Staatsangehörigkeit:	Marokkanisch/Deutsch

Berufliche Erfahrungen:

07/2009 – 12/2012	Heinrich-Heine-Universität Düsseldorf, **Wissenschaftlicher Mitarbeiter/ Doktorand**

Ausbildung:

10/2004 – 06/2009	Heinrich-Heine Universität Düsseldorf **Diplom Biologie**
02/2003 – 09/2004	Heinrich-Heine Universität Düsseldorf, **Deutsche Sprachprüfung für den Hochschulzugang (DSH)**
01/2001 – 07/2001	Goethe-Institut, **Zertifikat Deutsch**
09/1995 – 01/2000	Universität Cadi Ayyad Marrakesch, **Maîtrise** (**Magister**) in Biotechnologie und Pflanzen Genetik
06/1995	Lycée Hassan II, Marrakesch, **Abitur**

Tagungen:

1. 58th International Congress and Annual Meeting of the Society for Medicinal Plant and Natural Products Research and the 7th Tannin Conference, Berlin, 29th August-2nd September 2010. [Poster]
2. 4th Asia-Link Meeting & 10th Anniversary of Proksch Group at HHU, September 20-22nd, 2010, Dusseldorf. [Poster]
3. 6th Polish-German Symposium on Pharmaceutical science. May 2011 [Poster]
4. Young Researcher Meeting (Oral Presentation)-Münster, 2nd and 3rd March 2012. [Vortrag]

Veröffentlichungen:

Pullularins E and F, Two New Depsipeptides from the Endophytic Fungus *Bionectria ochroleuca* Isolated from the Mangrove Plant *Sonneratia caseolaris*, Weaam Ebrahim, Julia Kjer, **Mustapha El Amrani**, Victor Wray, Wenhan Lin, Rainer Ebel, Daowan Lai, Peter Proksch. *Marin Drugs* ***2012***

Farinomalein Derivatives from an Unidentified Endophytic Fungus Isolated from the Mangrove Plant *Avicennia marina,* Mustapha El Amrani, Abdessamad Debbab, Amal H. Aly, Victor Wray, Sergey Dobretsov, Werner E. G. Müller, Wenhan Lin, Daowan Lai, Peter Proksch. *Tetrahedron Letters* ***2012***